

**Cyclase associated protein CAP in the regulation
of the actin cytoskeleton and cell polarity in
*Dictyostelium discoideum***

INAUGURAL-DISSERTATION

zur

Erlangung des Doktorgrades

der Mathematisch-Naturwissenschaftlichen Fakultät

der Universität zu Köln



vorgelegt von

Hameeda Sultana

aus Bangalore, Indien

2004

Referees/Berichterstatter : Prof. Dr. Angelika A. Noegel
Prof. Dr. Siegfried Roth

Date of oral examination : 06.07.2004
Tag der mündlichen Prüfung

The present research work was carried out under the supervision and the direction of Prof. Dr. Angelika A. Noegel in the Institute of Biochemistry I, Medical Faculty, University of Cologne, Cologne, Germany, from June 2001 to July 2004.

Diese Arbeit wurde von Juni 2001 bis Juli 2004 am Biochemischen Institut I der Medizinischen Fakultät der Universität zu Köln unter der Leitung und der Betreuung von Prof. Dr. Angelika A. Noegel durchgeführt.

*To my everloving Ammi-Abba
& family...*

ACKNOWLEDGEMENTS

This thesis is not only the result of three years of bench work, data processing, reading and writing but it is also the result of the knowledge and the help of others. First and foremost I would like to express my sincere gratitude to my esteemed advisor, Prof. Dr. Angelika A. Noegel, Institute of Biochemistry I, Medical Faculty, University of Cologne, Germany. I am deeply grateful to her for the enormous freedom given to me to pursue my own interests while at the same time providing excellent guidance to ensure that my efforts contribute to the cytoskeletal research. Her creative suggestions, constructive criticism and steadfast encouragement is praiseworthy and unforgettable. Her analytical perusal of the manuscript is highly acknowledged. I would like to thank in perpetuity for all her help and superb guidance.

I acknowledge my special thanks to Dr. Francisco Rivero for his instant cooperation and help as and when required. His constructive suggestion during the course of my study is highly appreciable. I also thank him for providing RacA strains and GFP-VatB plasmid. I sincerely thank Dr. Ludwig Eichinger for providing me the lab facilities to carry out the microarray analysis and for his necessary suggestions. I owe special thanks to Patrick Farbrother for his help through out the microarray analysis. I also thank Dr. Akis Karakesisoglou for his friendly nature and laughs. A special note of thank to Dr. Christoph Clemen for his friendly gesture and support.

I owe a special gratitude to Bettina Lauss, who made all the necessary official things easy and fast. Her encouragement and friendly support is admirable and unforgettable. My special thanks are due to Dr. Budi Tunggal for his valuable suggestions and wonderful company in our office. I thank Rolf for his necessary technical assistance, Berthold, Maria, Rosi, Bärbel and Roberto for their necessary help. I thank all my colleagues for providing a friendly atmosphere and a special one to Thorsten Olski. I record my special thanks to Inge Götz-Krichi for her friendly support and constant help.

I sincerely thank Dr. Salvatore Bozzaro (University of Torino), Dr. Kees Weijer (University of Dundee), Dr. Edward Cox (Princeton University) and Dr. Richard A. Firtel (University of California) for providing the mutant strains.

My everloving and wonderful parents Ammi-Abba were the source of inspiration and motivation throughout my life. I am deeply indebted for their love and affection, which stood by me as a strong support and without their blessings it would have been a difficult task to complete this work.

I owe a huge indebtedness to my everloving and affectionated Pops-deed for their constant encouragement and incredible love which bolstered my days to reach my goals and I thank them for their wonderful everlasting support throughout my studies. My everloving little sister lubu was my biggest inspiration and emotional support during all my studies. I thank her for her loving and caring nature. I express my heartiest gratitude to my everloving brother lulu for all his inspiration and constant support. I thank all my family members and beloved children abrar-pinky, shazu-nazu, wasimu-saleemu, faizu, kola and little adiyana for their affection.

I am greatly indebted to my wonderful husband and a word of appreciation is not at all sufficient to express my gratitude for all his great inspiration, understanding and heartfelt cooperation throughout this study.

Finally, the financial assistance received by me from the DFG is highly acknowledged.

Cologne
03/05/2004

Hameeda Sultana

Table of Contents

Chapter	Description	Page(s)
ABBREVIATIONS		
I.	INTRODUCTION	1-10
1.0	<i>Dictyostelium discoideum</i> : a model system in motion	1
2.0	CAP is a highly conserved protein	2
3.0	Organization of CAP structure	3
4.0	Model of CAP function	5
5.0	The interaction of CAP with actin is PIP ₂ regulated	6
6.0	CAP is a multifunctional protein	7
7.0	Cell polarity and cAMP signalling in <i>Dictyostelium</i>	7
8.0	Overview	10
II.	MATERIALS AND METHODS	11-51
1.0	Materials	11
1.1.	Laboratory materials	11
1.1.1	Instruments and equipments	11
1.2.	Kits	13
1.2.1	Enzymes, antibodies, substrates, inhibitors and antibiotics	13
1.3.	Chemicals and reagents	14
1.4.	Media and buffers	15
1.4.1.	Media and buffers for <i>Dictyostelium</i> culture	15
1.4.2.	Media for <i>E. coli</i> culture	16
1.4.3.	Media and buffers for yeast culture	17
1.4.4.	Buffers and other solutions	18
1.5.	Biological materials	19
1.6.	Plasmids	20
1.7.	Synthetic Oligonucleotides	21
2.0	Cell biological methods	21
2.1	Growth of <i>Dictyostelium</i>	21
2.1.1	Growth in liquid nutrient medium	21
2.1.2	Growth on SM agar plates	22
2.2	Development of <i>Dictyostelium</i>	22
2.3	Preservation of <i>Dictyostelium</i> cells	22
2.4	Transformation of <i>Dictyostelium</i> cells	23
2.4.1	Transformation of <i>Dictyostelium</i> cells by CaCl ₂	23
2.4.2	Transformation of <i>Dictyostelium</i> cells by electroporation	24

Chapter	Description	Page(s)
2.5	Analysis of agglutination	24
2.6	Endocytosis assay	25
3.0	Molecular biological methods	25
3.1	Purification of plasmid DNA	25
3.2	Digestion with restriction enzymes	26
3.3	Generation of blunt ends in linearised plasmid DNA	26
3.4	Dephosphorylation of DNA fragments	27
3.5	Setting up of ligation reaction	27
3.6	Isolation of <i>Dictyostelium</i> genomic DNA	27
3.7	DNA agarose gel electrophoresis	28
3.8	Recovery of DNA fragments from agarose gel	28
3.9	Isolation of total RNA from <i>Dictyostelium</i> cells	29
3.10	RNA formaldehyde-agarose gel electrophoresis	29
3.11	Northern blotting	30
3.12	Radiolabelling of DNA	30
3.12.1	Chromatography through Sephadex G-50 spin column	31
3.12.2	Hybridisation of Southern- or northern-blot with radiolabelled DNA probe	31
3.13	Transformation of <i>E. coli</i>	32
3.13.1	Transformation of <i>E. coli</i> cells by the CaCl ₂ method	32
3.13.2	Transformation of <i>E. coli</i> cells by electroporation	32
3.14	Glycerol stock of bacterial culture	33
3.15	DNA colony blot for screening of <i>E. coli</i> transformants	33
3.16	Construction of vectors	34
3.16.1	Vectors for expression of GFP-fusion proteins of CAP and its domains (Noegel et al., 1999)	34
3.16.2	Vectors for expression of binding partner studies of CAP	35
3.16.3	Vectors for expression of GST fusions of sGC, ARPE and Vacuolar ATPases d subunit	35
3.17	DNA sequencing	35
3.18	Computer analyses	36
4.0	Methods for the Yeast Two Hybrid System	36
4.1	Transformation of Yeast by Lithium Acetate Method	36
4.2	DNA isolation from Yeast	36
4.3	β-galactosidase colony lift assay	37
4.4	Yeast strain maintenance	38
5.0	Biochemical methods	38
5.1	Preparation of total protein from <i>Dictyostelium</i>	38
5.2	Isolation of phagosomes	38

Chapter	Description	Page(s)
5.3	Cell fractionation studies to determine the subcellular localization of CAP	39
5.4	Immunoprecipitation from <i>Dictyostelium</i> cell lysate	39
5.5	SDS-polyacrylamide gel electrophoresis	40
5.5.1	Coomassie blue staining of SDS-polyacrylamide gels	41
5.5.2	Silver staining of polyacrylamide gels	41
5.5.3	Drying of SDS-polyacrylamide gels	41
5.6	Western blotting using the semi-dry method	42
5.6.1	Ponceau S staining of western blots	42
5.7	Immunodetection of membrane-bound proteins	42
5.7.1	Enzymatic chemi-luminescence (ECL) detection system	43
5.8	Expression and purification of GST fusions of sGC, ARPE and VD	43
5.8.1	Small-scale protein expression	43
6.0	Immunological methods	44
6.1	Indirect immunofluorescence of <i>Dictyostelium</i> cells	44
6.1.1	Preparation of <i>Dictyostelium</i> cells	44
6.1.2	Methanol fixation	44
6.1.3	Picric acid-paraformaldehyde fixation	45
6.2	Immunolabelling of fixed cells	45
6.2.1	Mounting of coverslips	46
6.3	Phalloidin staining of fixed cells	46
6.4	Immunolabelling of <i>Dictyostelium</i> cells expressing GFP-CAP and its domains fixing during phagocytosis and pinocytosis	46
7.0	Microscopy	47
7.1	Live cell imaging of <i>Dictyostelium</i> cells expressing GFP-CAP	48
7.2	Imaging distribution and live dynamics of GFP-CAP during pinocytosis	48
7.3	Imaging the distribution of GFP-CAP during phagocytosis	48
7.4	Imaging the distribution and dynamics of GFP-CAP in aggregation competent cells	49
7.5	Microscopy of agar plates	49
8.0	Microarray analysis	49
8.1	RNA preparation	49
8.2	Spiking of internal mRNA controls	50
8.3	Quantitation, normalization and data analysis	51
8.4	Signal Quantification	51

Chapter	Description	Page(s)
III.	RESULTS	52-117
1.0	Localization and dynamics of CAP in the signalling mutants	52
1.1	Expression levels of the endogenous CAP in the <i>aca</i> ⁻ , <i>pia</i> ⁻ , <i>pia</i> ⁻ .2 <i>ac</i> ⁻ , <i>gα2</i> ⁻ and <i>gβ</i> ⁻ , <i>car1</i> ^{1/3} ⁻ , <i>pik</i> 1 ^{/2} ⁻ and <i>pka</i> ⁻ cells	52
1.1.1	Localization of CAP in the signal transduction mutants	53
1.1.2	Localization of CAP in <i>pka</i> ⁻ cells	54
1.2	Expression of GFP-CAP fusion protein in the <i>aca</i> ⁻ , <i>pia</i> ⁻ , <i>gα2</i> ⁻ and <i>gβ</i> ⁻ and <i>pik</i> 1 ^{/2} ⁻ cells	56
1.2.1	Localization of GFP-CAP in signalling mutants	56
1.3	Re-localization of CAP in <i>aca</i> ⁻ , <i>pia</i> ⁻ , HSB101, <i>gα2</i> ⁻ , <i>gβ</i> ⁻ , <i>cAR1</i> ^{1/3} ⁻ , <i>pik</i> 1 ^{/2} ⁻ , and <i>PKA</i> ⁻ during phagocytosis	57
1.3.1	Determination of the presence of CAP in phagosomes	59
1.3.2	Association of CAP with membrane fractions	59
1.4	Analysis of CAP and CAP-GFP in the <i>pia</i> ⁻ , <i>gα2</i> ⁻ , <i>gβ</i> ⁻ , and <i>pik</i> 1 ^{/2} ⁻ cells during phagocytosis	60
1.4.1	Redistribution of GFP fusion proteins of CAP and its domains in <i>aca</i> ⁻ cells during phagocytosis	61
1.4.2	Live imaging visualizing the dynamics of GFP-CAP in <i>aca</i> ⁻ , <i>pia</i> ⁻ , <i>gα2</i> ⁻ , <i>gβ</i> ⁻ , and <i>pik</i> 1 ^{/2} ⁻ cells	62
1.4.3	Quantitative analysis of phagocytosis in the <i>aca</i> ⁻ , <i>pia</i> ⁻ , <i>gα2</i> ⁻ and <i>gβ</i> ⁻ and <i>pik</i> 1 ^{/2} ⁻ cells	65
1.5	Re-localization of CAP during pinocytosis in the <i>aca</i> ⁻ , <i>pia</i> ⁻ , <i>gα2</i> ⁻ , <i>gβ</i> ⁻ and <i>pik</i> 1 ^{/2} ⁻ cells	68
1.5.1	Live dynamics of GFP-CAP in the <i>aca</i> ⁻ , <i>pia</i> ⁻ , <i>gα2</i> ⁻ and <i>gβ</i> ⁻ cells during pinocytosis	69
1.6	Dynamics of CAP-GFP in the <i>pik</i> 1 ^{/2} ⁻ cells during pinocytosis	71
1.6.1	Quantitative analysis of pinocytosis in <i>pik</i> 1 ^{/2} ⁻ cells and cells expressing GFP-CAP	72
1.6.2	Distribution of F-actin in the <i>pik</i> 1 ^{/2} ⁻ cells expressing GFP-CAP	73
1.7	Role of CAP in the aggregation of <i>pik</i> 1 ^{/2} ⁻ cells expressing GFP-CAP	75
1.8	Role of CAP during aggregation competence in the <i>pik</i> 1 ^{/2} ⁻ cells expressing GFP-CAP	75
1.9	Role of CAP in the growth and development of <i>pik</i> 1 ^{/2} ⁻ cells expressing GFP-CAP	77
2.0	Role of CAP in the aggregation and development of aggregation deficient <i>aca</i> null cells	78
2.1	Expression of GFP fusions of CAP and its domains in <i>aca</i> ⁻ cells	78

Chapter	Description	Page(s)
2.2	Localization of GFP fusions of CAP and its domains in <i>aca</i> ⁻ cells	79
2.3	Moderate overexpression of CAP rescues the aggregation defect of <i>aca</i> ⁻ cells	80
2.3.1	Role of CAP-GFP fusions in the <i>aca</i> ⁻ cells during aggregation	82
2.4	Agglutination of the <i>aca</i> ⁻ cells expressing CAP-GFP and N-CAP-Pro-GFP	82
2.5	Developmental phenotypes of <i>aca</i> ⁻ cells expressing CAP-GFP	84
2.6	Cell adhesion mechanism in the <i>aca</i> ⁻ cells expressing CAP-GFP and N-CAP-Pro-GFP	85
2.7	Time course and quantification of cell-cell adhesion in the <i>aca</i> ⁻ cells expressing CAP-GFP and N-CAP-Pro-GFP	86
2.8	Expression of cAR1 receptor in the agglutinating <i>aca</i> ⁻ cells expressing CAP-GFP and N-CAP-Pro-GFP	88
2.9	Expression of cell adhesion molecules in the <i>aca</i> ⁻ cells expressing CAP-GFP and N-CAP-Pro-GFP	88
2.10	Distribution of polarity markers in the <i>aca</i> ⁻ cells and <i>aca</i> ⁻ cells expressing CAP-GFP and the N-CAP-Pro-GFP	91
3.0	Role of CAP in <i>LimD</i>⁻ and AX2 cells expressing constitutively active and dominant negative RacA	94
3.1	Localization of CAP in AX2 cells expressing constitutively active and dominant negative RacA	94
3.2	Localization of CAP in <i>LimD</i> ⁻ cells	95
3.3	Complementation analysis of CAP bsr by GFP-LimD	96
3.4	Dynamics of GFP-LimD in CAP bsr during endocytosis	96
3.5	Expression of GFP-LimD restores pinocytosis of CAP bsr cells	98
3.4	Role of CAP in cAMP signalling	98
4.0	Identification of binding partners for <i>Dictyostelium</i> CAP	100
4.1	Does CAP physically interact with aggregation specific adenylyl cyclase (ACA)?	100
4.2	Does CAP interact with guanylyl cyclase?	102
4.3	Interaction of CAP with ARP2/3 complex subunits	103
4.4	Interaction of CAP with Vacuolar H ⁺ -ATPases (V-ATPases) complex	104
4.5	The vacuolar network is disturbed in the absence of CAP	106
4.6	Expression of CAP GFP fusion protein restores the disturbed vacuolar system in CAP bsr	108
5.0	Transcriptional analysis of CAP bsr using DNA microarrays	109

Chapter	Description	Page(s)
IV.	DISCUSSION	114-131
1.	Localization and dynamics of CAP in signalling mutants	114
2.0	CAP is a general regulator of phagocytosis	116
3.0	Dynamics of CAP during pinocytosis	117
3.1	CAP rescues the impaired pinocytosis of pik ^{1/2} ⁻ cells	117
3.2	CAP restores the altered distribution of actin and filamentous actin in pik ^{1/2} ⁻ cells	118
4.0	Developmental regulation of CAP in pik^{1/2}⁻ cells	119
5.0	Role of CAP in aggregation and early development of aca⁻ cells	119
5.1	Moderate CAP overexpression improves the development of aca ⁻ cells but does not allow complete restoration	120
6.0	An overview of the significance of CAP in the signalling mutants	121
7.0	Localization of CAP depends on LimD and is modulated by RacA	121
8.0	LimD expression restores the defect in endocytosis of CAP bsr	122
9.0	CAP is required for cAMP signalling	122
10.0	Does CAP interact with cyclases?	123
11.0	Does CAP interact with the Arp2/3 complex?	124
12.0	Interaction of CAP with the Vacuolar H⁺ ATPases complex	124
13.0	Microarray analysis signifies CAP as a regulator of signal transduction, multi-cellular development and cytoskeleton	127
14.0	Outlook	130
V.	SUMMARY/ZUSAMMENFASSUNG	132-133
	BIBLIOGRAPHY	
	Erklärung	
	Curriculum Vitae/Lebenslauf	

Abbreviations

AP	alkaline phosphatase
APS	ammonium persulphate
ATP	adenosine 5'-triphosphate
bp	base pair(s)
BSA	bovine serum albumin
Bsr	blasticidin resistance cassette
cAMP	cyclic adenosine monophosphate
CAP	cyclase associated protein
CCD	cooled charge-coupled device
cDNA	complementary DNA
CIAP	calf intestinal alkaline phosphatase
dNTP	deoxyribonucleotide triphosphate
DABCO	diazobicyclooctane
DEPC	diethylpyrocarbonate
DMSO	dimethylsulphoxide
DNA	deoxyribonucleic acid
DNase	deoxyribonuclease
DTT	1, 4-dithiothreitol
ECL	enzymatic chemiluminescence
EDTA	ethylenediaminetetraacetic acid
EGTA	ethyleneglycol-bis (2-amino-ethylene) N, N, N, N-tetraacetic acid
G418	geneticin
GFP	green fluorescent protein
GST	glutathione S-transferase
HEPES	N-[2-Hydroxyethyl] piperazine-N'-2-ethanesulphonic acid
HRP	horse radish peroxidase
IgG	immunoglobulin G
IPTG	isopropyl- β -D-thiogalactopyranoside
kb	kilo base pairs
kDa	kilodalton
β -ME	beta-mercaptoethanol
MOPS	Morpholinopropanesulphonic acid
Mw	molecular weight
NP-40	nonylphenylpolyethyleneglycol
OD	optical density
ORF	open reading frame
PAGE	polyacrylamide gel electrophoresis
PCR	polymerase chain reaction
PEG	polyethylenglycol
PIPES	piperazine-N, N'-bis [2-ethanesulphonic acid]
PMSF	phenylmethylsulphonylfluoride
RNA	ribonucleic acid
RNase	ribonuclease
rpm	rotations per minute

Abbreviations

SDS	sodium dodecyl sulphate
TEMED	N,N, N',N'-tetramethyl-ethylendiamine
TRITC	tetramethylrhodamine isothiocyanate
U	unit
UV	ultra violet
vol.	volume
v/v	volume by volume
w/v	weight by volume
X-gal	5-bromo-4-chloro-3-indolyl- β -D-galactopyranoside

Units of Measure and Prefixes

<u>Unit</u>	<u>Name</u>
Ci	curie
°C	degree Celsius
D	Dalton
g	gram
h	hour
L	litre
m	meter
min	minute
s	sec
V	volt

<u>Symbol</u>	<u>Prefix (Factor)</u>
k	kilo (10^3)
c	centi (10^{-2})
m	milli (10^{-3})
μ	micro (10^{-6})
n	nano (10^{-9})
p	pico (10^{-12})
α	alpha
β	beta
γ	gamma

Introduction

1.0 *Dictyostelium discoideum*: a model system in motion

Movement is a manifestation of mechanical work, which requires a fuel (ATP) and proteins that convert the energy stored in ATP into motion. Also, all movements involve the cytoskeleton, a cytoplasmic system of fibres. The machinery that powers these movements is built from the actin cytoskeleton. The actin cytoskeleton is huge, larger than any organelle, filling the cytosol with actin filaments. The actin cytoskeleton of a cell is required for cell shape changes, cell motility and chemotaxis, as well as for cytokinesis, intracellular transport processes, development and signal transduction. The multiplicity of these actin related processes require the existence of actin in a variety of complex, dynamic structures, which are regulated by actin-binding proteins. Actin-binding proteins are particularly complex in their relationship with actin in its various forms where they can stimulate polymerisation and depolymerisation depending on the conditions. They are characterized by their ability and mode of interactions with G- or F-actin. The large number of F-actin binding proteins identified in various cells contrasts with very few G-actin binding proteins (Kreis and Vale, 1993).

Dictyostelium discoideum is a eukaryote that is related to animals and fungi, a position it shares with *Acanthamoebae* and the acellular slime moulds (Baldauf et al., 2000). The *Dictyostelium discoideum* genome (34 Mb) shows a high degree of sequence similarity to homologs, orthologs, and paralogs in other eukaryotic organisms including protozoan parasites and vertebrates; among them are the numerous genes interacting with G- and F- actin. *Dictyostelium* amoebae have a complex cytoskeleton whose dynamics is actively studied using the genetic approaches. The *Dictyostelium* undergoes a development, which is relatively simple and can be easily investigated with all the experimental techniques that are commonly used in developmental biology. *Dictyostelium* cells have adopted a strategy for multicellular development that differs from that of metazoa. In their vegetative stage, *Dictyostelium* cells are single-celled amoebae that feed on bacteria and multiply by binary fission. The striking feature of *Dictyostelium* is that, when their food source is depleted, they undergo a switch in behaviour and the individual cells come together and form a fruiting body (Figure 1). This is a highly differentiated multicellular structure composed of spore cells supported by stalk cells that are arranged as a stalk and a basal disc, which anchors to the substratum. *Dictyostelium* is therefore a valuable and convenient experimental system for studies of the role of the actin cytoskeleton, cell motility, phagocytosis, macropinocytosis, chemotaxis, signal transduction, development and differentiation.

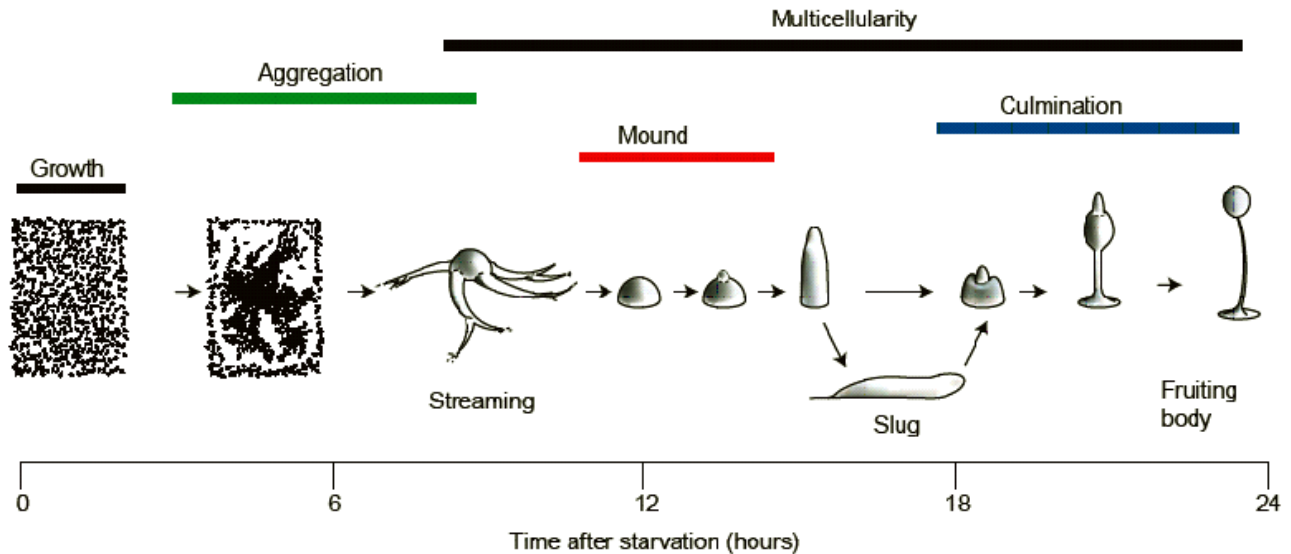


Figure 1: *Dictyostelium* development. Amoebae proliferate as single cells during the growth phase. Upon starvation, amoebae undergo chemotaxis towards a pulsatile cAMP source. During aggregation, cells coalesce into adherent cell 'streams' that eventually come together to form the mound, the first stage of multicellular development. The mound compacts to form a tight aggregate and then develops a 'tip', which coordinates further development. After extension to form the first finger, the developing structure either immediately forms a fruiting body, the process of culmination or forms a motile slug that migrates to seek conditions favourable for culmination. Scale shows relative timing of development (taken from Coates and Harwood, 2001).

2.0 CAP is a highly conserved protein

Cyclase associated protein (CAP) is an evolutionarily conserved regulator of the G-actin/F-actin ratio and has been identified in a wide range of species (Figure 2). CAP, was first isolated as a 70 kDa component of the *Saccharomyces cerevisiae* adenylyl cyclase complex that serves as an effector of Ras during nutritional signalling, which is involved in Ras/cAMP-dependent signal transduction and serve as an adapter protein translocating the adenylyl cyclase complex to the actin cytoskeleton (Field et al., 1988). CAP and CAP-homologues have two domains, an N-terminal and a C-terminal domain separated by one (*D. discoideum*) or two (yeast, human) proline rich stretches, and distinct functions have been attributed to the domains as well as to the proline rich region. Genetic and biochemical studies in yeast have demonstrated that a major target of Ras is adenylyl cyclase, and it has been shown that the N-domain of CAP is responsible for mediating the Ras sensitivity of adenylyl cyclase, whereas the C-domain is responsible for binding to monomeric actin and is required for regulating cellular morphology (Nishida et al., 1998, Gerst et al., 1991). Proline rich sequences often function as SH3 domain binding sites, which are thought to mediate formation of specific protein complexes, and the proline rich region 2 (P2) of yeast CAP was identified as an SH3 domain binding site and is known to interact with the SH3 domain of yeast actin binding protein Abp1p (Freeman et al., 1996). Furthermore, genetic studies in yeast have recently

implicated CAPs in vesicle trafficking and endocytosis (Hubberstey and Mottillo, 2002). In a screen to identify genes required for *Drosophila* oocyte polarity, the *Drosophila* homolog of yeast CAP was isolated. CAP preferentially accumulated in the oocyte where it inhibited actin polymerization resulting in a loss of asymmetric distribution of mRNA determinants within the oocyte (Baum et al., 2000). Benlali et al., 2000, identified CAP in a screen for mutations that disrupted eye development by increasing the F-actin levels and inducing premature photoreceptor differentiation. ASP56, the mammalian homologue of CAP, was isolated from pig platelets on the basis of its actin sequestering activity and shown to be a G-actin binding protein (Gieselmann et al., 1992). Taken together these studies suggest that CAP is a multifunctional protein with roles in signalling and regulation of the cytoskeleton that have been attributed to individual domains of the protein.

Protein	Organism	GenBank accession No.	Reference	Similarity† with yeast CAP (M58284) (%)	Similarity† with human CAP (NM_006367) (%)
CAP	<i>Homo sapiens</i>	NM_006367, M98474, L12168	Matviw <i>et al.</i> (1992)	46	—
CAP2	<i>H. sapiens</i>	NM_006366	Yu <i>et al.</i> (1994)	48	73
CAP1	<i>Mus musculus</i>	NM_007598, L12367	Vojtek <i>et al.</i> (1993)	46	97
MCH1	<i>Rattus norvegicus</i>	NM_022383, L11930	Zelicof <i>et al.</i> (1993)	46	97
CAP	<i>S. cerevisiae</i>	M58284	Field <i>et al.</i> (1988)	—	46
Srv2	<i>S. cerevisiae</i>	M32663	Fedor-Chaiken <i>et al.</i> (1990)		
CAP	<i>S. pombe</i>	L16577	Kawamukai <i>et al.</i> (1992)	49	48
CAP homolog	<i>Chlorohydra viridissima</i>	X79567	Fenger <i>et al.</i> (1994)	44	52
CAP	<i>D. discoideum</i>	U43027	Gottwald <i>et al.</i> (1996)	50	53
CAP	<i>Lentinus edodes</i>	AB001578	Zhou <i>et al.</i> (1998)	50	49

Figure 2: Comparison of CAP gene products. Similarity shows the degree of homology based on similar (not necessarily identical) amino acids (Taken from Hofmann et al., 2002).

3.0 Organization of CAP structure

In a search for novel actin binding proteins in *Dictyostelium discoideum*, a cDNA clone coding for a protein of approximately 50 kDa was isolated (Gottwald et al., 1996) that was found to be highly homologous to the class of adenyl cyclase-associated proteins (CAP). *Dictyostelium* CAP shares approximately 40% identity and 60 % similarity to the other members of this protein family. It is composed of two domains separated by a proline rich stretch. *Dictyostelium* CAP homologue has a single proline rich region that can be aligned with the proline rich region P1 of the yeast protein. The CAP homologue of *Dictyostelium discoideum* is a phosphatidylinositol 4, 5-bi phosphate (PIP₂) regulated G-actin sequestering protein, which is present in the cytosol and shows enrichments at the

plasma membrane regions. The G-actin binding activity has been localized to the carboxyl-terminal domain of the protein residues (306-464), which is separated by a proline rich linker region of 39 residues from the N-terminal domain encompassing residues 1-226 (Figure 3).

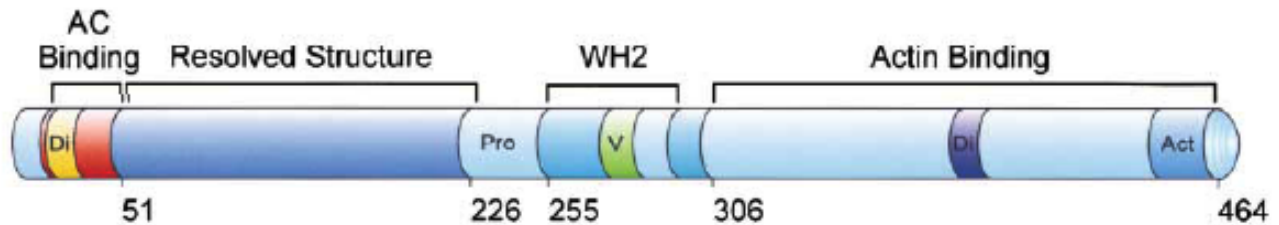


Figure 3: Domain organisation of *Dictyostelium* CAP. *Dictyostelium discoideum* CAP has a highly conserved domain structure (Gottwald et al., 1996; Hubberstey and Mottillo, 2002; Paunola et al., 2002). An adenylate cyclase binding domain (AC) and a dimerization domain (Di) are located at the amino terminus and are followed by the proline-rich region (Pro) and the WH2 domain (which includes a highly conserved verprolin homology region (V)). At the carboxyl terminus is an actin binding domain (Act) and a second dimerization site (Di). The N-terminal domain consists of residues 51–226, the Proline rich region extends from 226-255 and the C-terminal domain constitutes 306-464 residues (taken from Ksiazek et al., 2003).

The N-terminal domain of CAP localizes the protein to the membrane (Noegel et al., 1999). A comparison of the amino-terminal domain of CAP proteins of 14 organisms revealed a conserved RLEXAXXRLE motif (Hubberstey and Mottillo, 2002). This highly conserved motif interacts with adenylyl cyclase in yeast and has been termed the ‘CAP signature’ motif. In the *D. discoideum* CAP this motif has been replaced by a RLD-RLE motif. It is yet unclear if this conservative change of one amino acid could affect the adenylyl cyclase binding activity of the *D. discoideum* CAP.

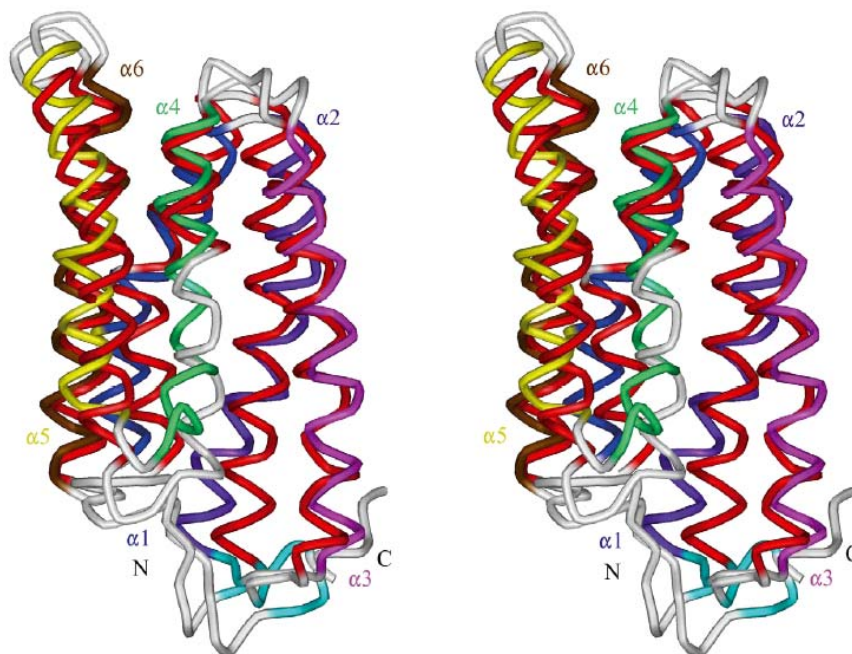


Figure 4: The overall folds of the structures solved by NMR and X-ray crystallography of CAP-N are very similar. Stereoview of the C α -backbone of the X-ray structure (helices in red) superimposed on the minimized averaged NMR structure (the six helices are shown each in different colours) (taken from Mavoungou et al., 2004).

The structure of the N-terminal domain of CAP (residues 51-226) was solved by X-ray diffraction (Ksiazek et al., 2003). Recently the NMR characterization of the amino-terminal domain of CAP from *D. discoideum* CAP (1-226) and the determination of the 3D structure of the stable folded core of this domain has been solved. The three-dimensional structure of CAP-N indeed consists of six antiparallel helices, (Figure 4), each of them containing at least 10 to 20 amino acids. The helices are arranged into a six-helix bundle, which is connected in the complete protein to the C-terminal domain through a proline rich linker (Mavoungou et al., 2004). The structure of the C-terminal domain of *S. cerevisiae* CAP has been solved recently (Roswarski et al., to be published) (PDB ID: 1K4Z). In contrast to our N-terminal domain structure, the C-terminus of yeast CAP is built solely by parallel β -strands that form a right-handed β -helix of six turns. The β -helix itself forms a homodimer with two β -structures are arranged antiparallel to each other. It is interesting to note that the cyclase and actin binding sites are located in the whole protein on positions that are structurally independent from each other.

4.0 Model of CAP function

It is clear from the NMR, gel filtration, and structural data for CAP (1–226) and the C-terminal domain that CAP domains oligomerize and that this feature may be important for the biological activities of CAP. Oligomerization most probably is mediated by the first 50 N-terminal residues of CAP and/or by the β -helical C-terminal domain of CAP in its native form (Ksiazek et al., 2003).

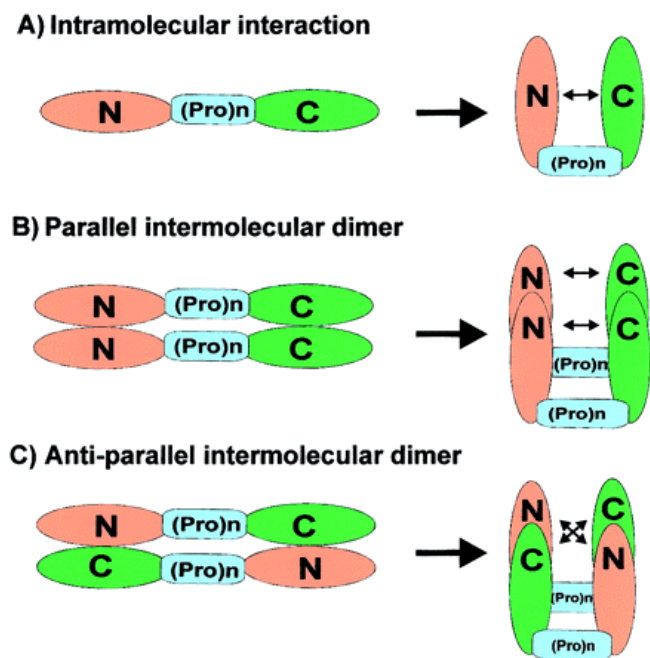


Figure 5: Model for CAP multimerization: a schematic representation of CAP consisting of the amino-terminal domain (orange), poly-proline region (blue), and carboxyl-terminal actin binding domain (green). Several studies have demonstrated that CAP molecules strongly interact. Based on available evidence, several potential interaction models exist. A) The N- and C-terminal domains interact, as revealed by two-hybrid and immunoprecipitation analysis. CAP molecules may simply interact through intramolecular associations between the N- and C-terminal domains. Since CAP has been found in large protein complexes *in vivo*, it potentially forms dimers or higher order intermolecular structures (B, C). That the N-terminal domain can interact with itself and the C terminus presents the possibility that either parallel (B) or antiparallel dimers (C) may form. These dimers may subsequently form intramolecular interactions (B) or create further intermolecular bonds between the N- and C-terminal domains (C) (taken from Hubberstey and Mottillo, 2002).

CAP proteins bind monomeric actin and can form oligomeric structures, probably dimers, although higher order structures have not been excluded. The amino terminus and carboxyl terminus can interact with each other as well as with themselves suggesting that CAP may form a parallel dimer in which the amino terminus interacts with the carboxyl terminus to potentially block actin binding. Alternatively, antiparallel dimers that interact between the amino and carboxyl termini, which then fold over to interact with themselves, may exist (Figure 5). Since the poly-proline domain resides essentially in the middle of the protein, both models allow for the poly-proline SH3 interacting domain to be free to bind target proteins (e.g., ABP1) and render proper localization to the CAP molecule, though other domains may be involved (Hubberstey and Mottillo, 2002).

5.0 The interaction of CAP with actin is PIP₂ regulated

CAP interaction with actin may be controlled through phospholipid binding (i.e., PIP₂) in a similar fashion as profilins, and phospholipid interactions may regulate the interaction between the amino- and carboxyl-terminal domains. However, the possibility that actin binding may involve interaction between the amino and carboxyl termini cannot be excluded (Hubberstey and Mottillo, 2002).

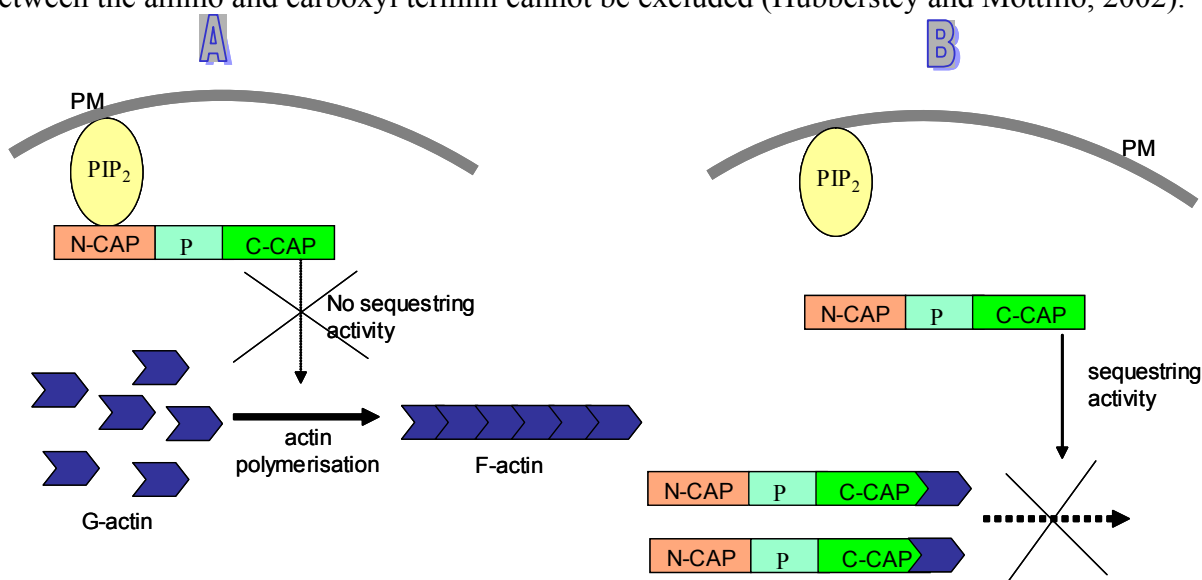


Figure 6: PIP₂ regulation and actin sequestering activity of CAP. Two possible scenarios could lead the PIP₂ regulation of CAP. (A) Binding of the N-terminus of CAP to the PIP₂ molecule prevents the actin sequestering activity of CAP by inhibiting the C-terminus of CAP to sequester the G-actin monomers. (B) The C-terminus of CAP allows the sequestering activity and inhibits the F-actin polymerization if there is no binding of the N-terminus of CAP to the PIP₂ molecule.

It has been reported that PIP₂ can regulate the binding of the *Dictyostelium* CAP to G-actin and it has been suggested that the PIP₂ binding site is located to the N-terminal half of the protein. PIP₂ may act in an inhibitory way, and increased PIP₂ concentrations in the cell could transiently

stimulate actin polymerization predominantly near the plasma membrane by preventing the action of actin sequestering proteins (Figure 6). The regulation of CAP by PIP₂ would fit into the cooperative mechanism of regulating the dynamics of the actin cytoskeleton (Gottwald et al., 1996).

6.0 CAP is a multifunctional protein

Different functions have been attributed to the different domains of CAP. The N-terminal domain seems to be required for ACA regulation, PIP₂-regulation, cell polarity and development and for the correct localization of the CAP. The protein is present throughout the cytoplasm and shows enrichment near the plasma membrane especially at the rear and front ends. Furthermore, it undergoes rapid rearrangements in moving cells. The actin binding activity is assigned to the C-terminal domain and is involved in cytokinesis, cell polarity and development (Noegel et al., 2004). Proline rich sequences often function as SH3 domain binding sites which are thought to mediate formation of specific protein complexes and possess the sequence APASSAPAAPV (position 228-238) resembling the SH3 consensus binding sequence XPXXPPPYXPX (Y indicates a hydrophobic residue; prolines 2, 7 and 10 are essential) as analyzed for the SH3 domain of Abl (Freeman et al., 1996; Ren et al., 1993). Recently we also reported that the proline rich region is essential for phototaxis and cell size maintenance (Noegel et al., 2004). CAP bsr, a *Dictyostelium* mutant in which the CAP gene has been inactivated by homologous recombination in such a way that the expression of the full-length protein was reduced to <5% of the protein concentration in wild-type AX2, revealed changes during growth and development. Growing cells were heterogeneous with regard to cell size and were often multinucleated. The mutant had an endocytosis and a chemotaxis defect. When chemotactic motility was assayed by applying a cAMP gradient, the cells did not properly orientate in the direction of the chemotactic agent. Development was significantly delayed and developmentally regulated genes such as contact site A (csA) and cAMP receptor I were expressed significantly later than in wild type. However, the mutant was able to complete the developmental cycle and to form fruiting bodies containing viable spores (Noegel *et al.*, 1999) implying that CAP a multifunctional protein.

7.0 Cell polarity and cAMP signalling in *Dictyostelium*

Cell polarity is defined as an asymmetry of cell shape and cellular functions that is stable for some time and requires localized assembly of signalling complexes, directed cytoskeletal rearrangements, and distinct recruitments of proteins (Nelson, 2003). During growth *Dictyostelium* cells do not

display a fixed polarity. They constantly change their shape and form new ends in response to environmental signals, which target them towards a food source. However, after the onset of starvation periodic signals of the chemoattractant cAMP lead to polarization of the cells and initiate the development into a multicellular organism.

cAMP signalling is essential for the chemotactic aggregation of individual *Dictyostelium* cells into multicellular aggregates and for progression through late development (Firtel and Meili, 2000). The aggregation centers produce cAMP pulses, which are detected, amplified, and relayed to the surrounding cells. The cAMP is sensed by a cAMP receptor on the cell surface, which couples to a heterotrimeric G protein. *Dictyostelium* harbours four cAR receptors whose expression levels are tightly regulated throughout development (Firtel and Chung, 2000). G-protein-mediated signal transduction pathways play an essential role in the developmental programme and are involved in regulating the actin cytoskeleton. Nine G α subunits (G α 1-G α 9), and one G $\beta\gamma$ subunits have been identified (Devreotes, 1994). G α 2 is a key player, as the null cells of G α 2 do not aggregate and are unable to activate the adenylyl or guanylyl cyclases and Akt/PKB. They show no chemotaxis and do not respond to extracellular cAMP suggesting that G α 2 is the only G α -subunit that interacts with any of the cAMP receptors (Wu et al., 1995). The G α subunits are transiently expressed at specific stages while the single G $\beta\gamma$ subunits are expressed throughout growth and development. Deletion of the gene encoding the G β subunit results in the inability of the cells to chemotax to chemoattractants and to activate the cyclases, and abrogates all signal transduction via G-proteins. It has been known that G α 2 mediates cAMP-induced activation of adenylyl or guanylyl cyclase and phospholipase C (Okaichi et al., 1992; Bominaar et al., 1994). The G $\beta\gamma$ complex is set free and, together with CRAC, it activates the adenylyl cyclase (ACA) and leads to synthesis of cAMP (cAMP relay) (Firtel and Chung, 2000).

The receptor mediated G-protein linked adenylyl cyclase systems are universal signal transducers and play a significant role in signalling leading to directed cell migration as well as in growth and development. *Dictyostelium* harbors three adenylyl cyclases: an aggregation specific adenylyl cyclase (ACA) is homologous to the G-protein regulated mammalian adenylyl cyclase, a germination-specific adenylyl cyclase (ACG) is expressed in prespore cells and spores and adenylyl cyclase B (ACB) is optimally expressed during culmination and is essential for the maturation of the spores and terminal differentiation (Pitt et al., 1992; Kim et al., 1998; Soderbom et al., 1999). ACB (*acrA*) has recently been identified as functioning in a cell autonomous fashion during late development. ACA is expressed at high levels during aggregation and reduced levels during

multicellular development (Pitt et al., 1992), and *acrA* is expressed at low levels in growing cells and at more than 25 fold higher levels during development. Cells lacking ACA are capable of moving up the chemoattractant gradient, but are unable to stream. Although, ACA is not required for chemotaxis, it is essential for the cells to align in a head to tail fashion and stream into aggregates. ACA is highly enriched at the uropod of chemotaxing cells to align in a head to tail fashion and stream into aggregates and the asymmetric distribution of ACA-YFP is dependent on the actin cytoskeleton and on the acquisition of cellular polarity. Thus *aca*⁻ cells have polarity defects and do not stream (Kriebel et al., 2003).

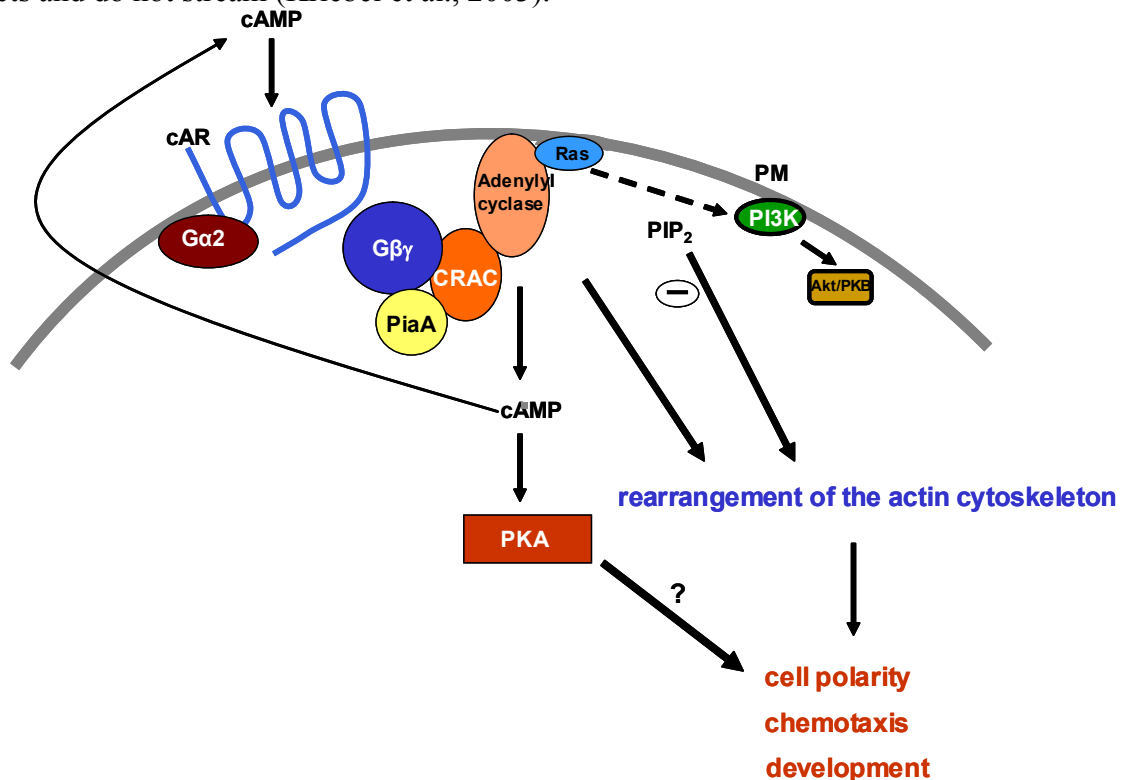


Figure 7: Schematic representation of cAMP signalling pathways in *Dictyostelium*. Chemoattractant binding to a seven transmembrane receptor belonging to the group of G-protein-coupled receptors (GPCR) leads to the activation of Gα₂, releasing the βγ subunit. The ACA, Gβγ subunits together with CRAC and PIA form a complex and activate adenylyl cyclase ACA. ACA activates further downstream effectors initiating a signalling cascade which activates pathways involving PI3-kinase and further downstream molecules, involved in the remodeling of the actin cytoskeleton.

In a genetic analysis to identify novel genes involved in G protein-linked pathways controlling development, a new gene Pianissimo (*piaA*) has been identified which is a novel cytosolic regulator required for chemo-attractant receptor and G protein mediated activation of the 12 transmembrane domain adenylyl cyclase in *Dictyostelium* (Chen et al., 1997). PIA and CRAC, the previously identified cytosolic regulator of adenylyl cyclase have several common features and both are essential for activation of adenylyl cyclase and are involved in cAMP signalling. It is probable that the CRAC PH domain interacts with PIP₃ and/or PIP₂ producing the expected activation of PI3-

kinases in response to chemoattractants (Firtel and Chung 2000). Four PI3K genes have been identified in *Dictyostelium*: *DdPIK5*, which encodes a member of the PI3K-I subfamily and *DdPIK1*, 2 and 3, which encode members of the PI3K-2 subfamily, and *DdPIK4* encodes a PI-4 kinase. The PI3K pathway has been implicated in the regulation of a multitude of intracellular events including mitogenesis (Carraway et al., 1995), membrane ruffling (Kotani et al., 1994), chemotaxis (Wennstrom et al., 1994), apoptosis (Yao et al., 1990), activation of neutrophils and oxygen radical formation (Ding et al., 1995; Traynor-Kaplan et al., 1989), receptor internalization (Joly et al., 1994; Kapeller et al., 1993), pinocytosis (Kotani et al., 1995) and neurite outgrowth (Kimura et al., 1994).

cAMP and cAMP-dependent protein kinase (PKA) are regulators of development in many organisms. All intracellular cAMP signalling is affected through PKA. PKA, the major downstream effector of the cAMP-ACA signalling pathway inside the cell, is activated when its regulatory subunit (PKA-R) binds cAMP and dissociates from the catalytic subunit (PKA-C). Therefore, PKA is essential in controlling aggregation and postaggregative development in *Dictyostelium* (Mann et al., 1997). cAMP also initiates a network of signalling pathways such as cGMP signalling, which is responsible for changes in the cytoskeleton (Liu and Newell, 1988).

8.0 Overview

The process of cAMP signalling involves the signalling molecules, the chemotactic machinery as well as components of the cytoskeleton such as CAP, which in *Dictyostelium* is involved in actin cytoskeleton rearrangements. To decipher the multifunctional role of CAP in diverse cellular events will, undoubtedly, help in elucidating new and exciting biological mechanisms. As part of this approach we investigated the role of CAP in the mutants of cAMP signalling pathway, with the aim of understanding its cellular functions by investigating its localization and involvement in cytoskeleton-dependent processes using a green fluorescent protein (GFP)-tagged version of CAP, identifying its interacting partners, and its involvement in global regulation.

Materials and Methods

1.0 Materials

1.1 Laboratory materials

Cellophane sheet (Dry ease)	Novex
Centrifuge tubes, 15 ml, 50 ml	Greiner
Coverslips (glass), Ø 12 mm, Ø 18 mm, Ø 55 mm	Assistent
Corex tube, 15 ml, 50 ml	Corex
Cryo tube, 1 ml	Nunc
Electroporation cuvette, 2 mm electrode gap	Bio-Rad
Gel-drying frames	Novex
Hybridisation bag	Life technologies
Microcentrifuge tube, 1.5 ml, 2.2 ml	Sarstedt
Micropipette, 1-20 µl, 10-200 µl, 100-1,000 µl	Gilson
Micropipette tips	Greiner
Needles (sterile), 18G–27G	Terumo, Microlance
Nitrocellulose membrane, BA85	Schleicher and Schuell
Nitrocellulose-round filter, BA85, Ø 82 mm	Schleicher and Schuell
Nylon membrane,	Biodyne B Pall
Nucleopore® membrane filters	Nucleopore
Parafilm	American National Can
Pasteur pipette, 145 mm, 230 mm	Volac
PCR softtubes, 0.2 ml	Biozym
Petri dish (35 mm, 60 mm, 100 mm)	Falcon
Petri dish (90 mm)	Greiner
Plastic cuvette, semi-micro	Greiner
Plastic pipettes (sterile), 1 ml, 2 ml, 5 ml, 10 ml, 25 ml	Greiner
Quartz cuvette, Infrasil	Hellma
Quartz cuvette, semi-micro	Perkin Elmer
Saran wrap	Dow
Scalpels (disposable), Nr. 10, 11, 15, 21	Feather
Slides, 76 x 26 mm	Menzel
Syringes (sterile), 1 ml, 5 ml, 10 ml, 20 ml	Amefa, Omnifix
Syringe filters (Acrodisc), 0.2 µm, 0.45 µm	Gelman Sciences
Tissue culture flasks, 25 cm ² , 75 cm ² , 175 cm ²	Nunc
Tissue culture dishes, 6 wells, 24 wells, 96 wells	Nunc
Whatman 3MM filter paper	Whatman
X-ray film, X-omat AR-5, 18 x 24 mm, 535 x 43 mm	Kodak

1.1.1 Instruments and equipments

Centrifuges (microcentrifuges):

Centrifuge 5417 C

Centrifuge Sigma

Cold centrifuge Biofuge fresco

Centrifuges (table-top, cooling, low speed):

Centrifuge CS-6R

Centrifuge RT7

Centrifuge Allegra 21R

Centrifuges (cooling, high speed):

Eppendorf

B. Braun Biotech Instruments

Heraeus Instruments

Beckman

Sorvall

Beckman

Beckman Avanti J25	Beckman
Sorvall RC 5C plus	Sorvall
Centrifuge-rotors:	
JA-10	Beckman
JA-25.50	Beckman
SLA-1500	Sorvall
SLA-3000	Sorvall
SS-34	Sorvall
Electrophoresis power supply, Power-pac-200-300	Bio-Rad
Electroporation unit, Gene-Pulser	Bio-Rad
Freezer (-80°C)	Nunc
Freezer (-20°C)	Siemens, Liebherr
Fluorimeter	PTI
Gel-documentation unit	MWG-Biotech
Heating block, DIGI-Block JR	neoLab
Heating block, Dry-Block DB x 20	Techne
Hybridising oven	Hybaid
Ice machine	Ziegra
Incubators: Incubator, microbiological	Heraeus
Incubator with shaker, Lab-Therm	Kuehner
Laminar flow, Hera Safe (HS 12)	Heraeus
Magnetic stirrer, MR 3001 K	Heidolph
Microscopes:	
Light microscope, CH30	Olympus
Light microscope, DMIL	Leica
Light microscope, CK2	Olympus
Fluorescence microscope, DMR	Leica
Fluorescence microscope, 1X70	Olympus
Confocal laser scan microscope, DM/IRBE	Leica
Stereomicroscope, MZFLIII	Leica
Stereomicroscope, SZ4045TR	Olympus
Oven, conventional	Heraeus
PCR machine, PCR-DNA Engine PTC-2000	MJ Research
pH-Meter	Knick
Refrigerator	Liebherr
Semi-dry blot apparatus, Trans-Blot SD	Bio-Rad
Shakers	GFL, Kuehner
Sonicator, Ultra turrax T25 basic	IKA Labortechnik
Speed-vac concentrator, DNA 110	Savant
Spectrophotometer, Ultraspec 2000, UV/visible	Pharmacia Biotech
Ultracentrifuges:	
Optima TLX	Beckman
Optima L-70K	Beckman
Ultracentrifuge-rotors:	
TLA 45	Beckman
TLA 100.3	Beckman
SW 41	Beckman
UV-crosslinker, UVC 500	Hofer
UV- transilluminator, TFS-35 M	Faust

Vortex, REAX top	Heidolph
Video camaras	
JAI CV-M10 CCD Camera	Stemmer Imaging
SensiCam	PCO Imaging
Waterbath	GFL
X-ray-film developing machine, FPM-100A	Fujifilm

1.2 Kits

Fairplay™ Microarray labelling kit	stratagene
Nucleobond AX	Macherey-Nagel
NucleoSpin Extract 2 in 1	Macherey-Nagel
Nucleotrap	Macherey-Nagel
Original TA Cloning	Invitrogen
pGEM-T Easy	Promega
Qiagen Midi- and Maxi-prep	Qiagen
Qiagen RNAeasy Midi/Mini kit	Qiagen
Stratagene Prime It II	Stratagene

1.2.1 Enzymes, antibodies, substrates, inhibitors and antibiotics

Enzymes used in the molecularbiology experiments:

Calf Intestinal Alkaline Phosphatase (CIAP)	Boehringer
Deoxyribonuclease I (DNase I)	Boehringer
Klenow fragment	Boehringer
Lysozyme	Sigma
Protein A Sepharose CL-4B	Amersham
Restriction endonucleases	Amersham, Life technologies, New England Biolabs
Reverse transcriptase, Superscript II	Life technologies
Ribonuclease H (RNase H)	Boehringer
Ribonuclease A (RNase A)	Sigma
T ₄ DNA ligase	Boehringer
Taq-polymerase	Life technologies/Boehringer

Primary antibodies:

Mouse anti-CAP monoclonal antibody, 230-18-8	Gottwald et al., 1996
Mouse anti-CAP monoclonal antibody, 223-445-1	Gottwald et al., 1996
Mouse anti-actin monoclonal antibody, Act 1-7	Simpson et al., 1984
Mouse anti-GFP monoclonal antibody, K3-184-2	Gloss et al., 2003
Mouse anti-csA monoclonal antibody, 33-294-17	Bertholdt et al., 1985
Mouse anti- α -actinin monoclonal antibody, 47-62-17	Schleicher et al., 1984
Mouse anti-filamin- monoclonal antibody, 82-454-12	Brink et al., 1989
Mouse anti-myosin-monoclonal antibody, 56-395-2	Pagh and Gerisch, 1986
Mouse anti-comitin monoclonal antibody 190-340-2	Weiner et al., 1993
Mouse anti-vacuolin monoclonal antibody, 221-1-1	Rauchenberger et al., 1997
Mouse anti-V/H+ ATPase monoclonal antibody, 221-35-2	Jenne et al., 1998
Mouse anti-Rab5-monoclonal antibody	Sigma
Goat anti-GST antibody	Amersham
Mouse anti-profilin I -monoclonal antibody, 153-246-10	Haugwitz et al., 1991
Mouse anti-profilin II -monoclonal antibody, 174-336-12	Haugwitz et al., 1991

Secondary antibodies:

Goat anti-mouse IgG, peroxidase conjugated	Sigma
Goat anti-rabbit IgG, peroxidase conjugated	Sigma
Mouse anti-goat IgG, peroxidase conjugated	Sigma
Sheep anti-mouse IgG, Cy3 conjugated	Sigma

Substrates:

Hydrogen peroxide (H ₂ O ₂)	Sigma
--	-------

Inhibitors:

Benzamidin	Sigma
Complete Mini®, Protease inhibitor cocktail tablets	Roche
Diethylpyrocarbonate (DEPC)	Sigma
Leupeptin	Sigma
Pepstatin	Sigma
Phenylmethylsulphonylfluoride (PMSF)	Sigma

Antibiotics:

Ampicillin	Gruenenthal
Blasticidin S	ICN Biomedicals
Chloramphenicol	Sigma
Dihydrostreptomycinsulphate	Sigma
Geneticin (G418)	Life technologies
Kanamycin	Sigma, Biochrom
Tetracyclin	Sigma

1.3 Chemicals and reagents

Most of the chemicals and reagents were obtained either from Sigma, Fluka, Difco, Merck, Roche, Roth or Serva. Those chemicals or reagents that were obtained from companies other than those mentioned here are listed below:

Acetic acid (98-100%)	Riedel-de-Haen
Acrylamide (Protogel: 30:0,8 AA/Bis-AA)	National Diagnostics
Agar-Agar (BRC-RG)	Biomatic
Agarose (Electrophoresis Grade)	Life technologies
Amino acids	sigma
Bacto agar	Difco
Bacto-peptone	Difco
Bacto-Trypton	Difco
5-Bromo-4-chloro-3-indolyl-β-D-galactopyranosid (X-gal)	Roth
Bromophenol blue (Na-Salt)	serva
BSA (Bovine serum albumin)	Roth
Chloroform	Riedel-de-Haen
Calciumchlorid-Dihydrat	Merck
Chloroform	Riedel-de-Haen
Coomassie-Brilliant-Blue G 250	Roche
Coomassie-Brilliant-Blue R 250	Serva
p-Cumaric acid	Fluka
Cyclohexamide	Sigma

1,4-Dithiothreitol (DTT)	Gerbu
Dimethylformamide (DMF)	Riedel-de-Haen
Ethanol	Riedel-de-Haen
Ethylen diamine tetraacetic acid (EDTA)	Merck
Glycerine	Riedel-de-Haen
Glycine	Riedel-de-Haen
Isopropyl- β -D-thiogalactopyranoside (IPTG)	Loewe Biochemica
Methanol	Riedel-de-Haen
Morpholino propane sulphonic acid (MOPS)	Gerbu
N- [2-Hydroxyethyl] piperazine-N'-2-ethanesulfonic acid (HEPES)	Biomol
Nonidet P40	Fluka
Peptone	Oxoid
Sodium dodecyl sulphate (SDS)	Serva
Sodium hydroxide	Riedel-de-Haen
Triton X-100	Merck
TRIzol	Gibco BRL
Tween 20	Roth
Yeast Nitrogen Base	Difco
Yeast extract	Oxoid
<u>Radiolabelled nucleotide:</u>	
α - ³² P-deoxyadenosine triphosphate, (10 mCi/ml)	Amersham

1.4 Media and buffers

All media and buffers were prepared with deionised water filtered through an ion-exchange unit (Membra Pure). The media and buffers were sterilized by autoclaving at 120°C and antibiotics were added to the media after cooling to approx. 50°C. For making agar plates, a semi-automatic plate-pouring machine (Technomat) was used.

1.4.1 Media and buffers for *Dictyostelium* culture

AX2-medium (Claviez *et al.*, 1982), pH 6.7:

7.15 g yeast extract
 14.3 g peptone (proteose)
 18.0 g maltose
 0.486 g KH₂PO₄
 0.616 g Na₂HPO₄.2H₂O
 add H₂O to make 1 litre

Soerensen phosphate buffer (Malchow, 1972), pH 6.0:

2 mM Na₂HPO₄
 14.6 mM KH₂PO₄

Phosphate agar plates, pH 6.0:

9 g agar
 add Soerensen phosphate buffer, pH 6.0 to make 1 litre

Salt solution (Bonner, 1947):

10 mM NaCl
10 mM KCl
2.7 mM CaCl₂

Starvation buffer, (Shaulsky *et al.*, 1998) pH 6.5:

10 mM MES, pH 6.5
10 mM NaCl
10 mM KCl
1 mM CaCl₂
1 mM MgSO₄

SM agar plates, (Sussman, 1951)pH 6.5:

9 g agar
10 g peptone
10 g glucose
1 g yeast extract
1 g MgSO₄.7H₂O
2.2 g KH₂PO₄
1 g K₂HPO₄
add H₂O to make 1 litre

1.4.2 Media for *E. coli* cultureLB medium, pH 7.4:(Sambrook *et al.*, 1989)

10 g bacto-tryptone
5 g yeast extract
10 g NaCl
adjust to pH 7.4 with 1 N NaOH
add H₂O to make 1 litre

For LB agar plates, 0.9% (w/v) agar was added to the LB medium and the medium was then autoclaved. For antibiotic selection of *E. coli* transformants, 50 mg/l ampicillin, kanamycin or chloramphenicol was added to the autoclaved medium after cooling it to approx. 50°C. For blue/white selection of *E. coli* transformants, 10 µl 0.1 M IPTG and 30 µl X-gal solution (2% in dimethylformamide) was plated per 90 mm plate and the plate was incubated at 37°C for at least 30 min before using.

SOC medium (Sambrook *et al.*, 1989), pH 7.0:

20 g bacto-tryptone
5 g yeast extract
10 mM NaCl
2.5 mM KCl
dissolve in 900 ml deionised H₂O
adjust to pH 7.0 with 1 N NaOH

The medium was autoclaved, cooled to approx. 50°C and then the following solutions, which were

separately sterilized by filtration (glucose) or autoclaving, were added:
 10 mM MgCl₂·6H₂O
 10 mM MgSO₄·7H₂O
 20 mM Glucose
 add H₂O to make 1 litre

1.4.3 Media and buffers for *Yeast* culture

YEPD-Medium:

20 g/l Difco Pepton
 10 g/l Yeast extract

YEPD-Agar plates:

20 g/l Difco Pepton
 10 g/l Yeast extract
 18 g/l Agar agar

100 x Adenine solution:

200 mg (1,1 mmol) Adenine in 100 ml water dissolve with addition of little amounts of HCl and filter sterilize.

100 x Tyrosine solution:

300 mg (1,7 mmol) Tyrosin in 100 ml dissolve with addition of NaOH solution and filter sterilize.

100 x Histidine solution:

200 mg (1 mmol) Histidine in 100 ml Water and filter sterilize.

100 x Leucine solution:

1000 mg (7,6 mmol) Leucin in 100 ml Water and filter sterilize.

100 x Tryptophan solution:

200 mg (1 mmol) Tryptophan in 100 ml Water filter sterilize.

100 x Uracil solution:

200 mg (1,8 mmol) Uracil in 100 ml Water dissolve by warming in water bath and filter sterilize.

1 M 3-Amino-1,2,4-triazol solution:

8,4 g 3-Amino-1,2,4-triazol in 100 ml Water, filter once and filter sterilize.

100 x Cycloheximide solution:

1 mg/ml Cycloheximid in Water solution filter sterilize.

The composition of the selection media and agar plates is indicated in the following table. Agar agar and Yeast extract without nitrogen base was dissolved in water and autoclaved. The glucose solution was prepared in water and filter sterilised. The remaining stock solutions were added after cooling to 55 °C.

Reagents	Selection plates				
	SD/-Trp	SD/-Leu	SD/-Leu/-Trp	SD/-Leu/-His/-Trp/+3-AT	SD/-Leu/-His/-Trp/-Ade
Yeast Nitrogen Base [g]	6,7	6,7	6,7	6,7	6,7
Agar agar [g]	20	20	20	20	20
Water [ml]	750	750	770	745	780
20% Glucose [ml]	100	100	100	100	100
10X Amino acid solution [ml]	100	100	100	100	100
100X Tyrosine [ml]	10	10	10	10	10
100X Uracile [ml]	10	10	10	10	10
100X Histidine [ml]	10	10	10	-	-
100X Leucine [ml]	10	-	-	-	-
100X Tryptophane [ml]	-	10	-	-	-
100X Adenine [ml]	10	10	10	10	-
3-AT-solution [ml]	-	-	-	25	-

- indicates omission of the reagent

10 x Amino acid solutions:

300 mg (2, 3 mmol) Isoleucine
1500 mg (1, 1 mmol) Valine
200 mg (0, 9 mmol) Arginine
300 mg (1, 6 mmol) Lysine
200 mg (1, 34 mmol) Methionine
500 mg (3 mmol) Phenylalanine
2000 mg (16, 8 mmol) Threonine,
adjust final volume to 1l and filter sterilize.

1.4.4 Buffers and other solutions

The buffers and solutions that were commonly used during the course of this study are mentioned below.

10x MOPS (pH 7.0/ pH 8.0):

41.9 g MOPS
16.7 ml 3 M sodium acetate
20 ml 0.5 M EDTA
add H₂O to make 1 litre

20x SSC (pH 7.0):

3 M NaCl
0.3 M sodium citrate

Hybridisation solution (50 µl):

Hybridisation buffer 48 µl
Fish sperm DNA [10 mg/ml] 1µl
Oligo dA (18 mer, 100 µM) 1µl
mix well

Hybridisation buffer:

1.2M Phosphate buffer, pH 6.8
2mM EDTA
50 % Formamide
1% Na-Laurylsarcosinate
0.2 % SDS
4 xDenhardt's Reagent

100 x Denhardt's reagent:

2 % Ficoll 400
2 % Polyvinylpyrrolidone
2 % bovine serum albumin

Blocking Solution (282 ml):

270 ml 1-Methy-2-pyrrolidinone (solution should be colourless)
0.4 g Succinic anhydride (store desiccated)
12.1 ml 1M Sodium borate, pH 8.0 (42mM)

10x NCP-Puffer (pH 8.0):

12.1 g Tris/HCl
87.0 g NaCl
5.0 ml Tween 20
2.0 g sodium azide
add H₂O to make 1 litre

<u>PBG (pH 7.4):</u>	0.5 % bovine serum albumin 0.1 % gelatin (cold-water fish skin) in 1x PBS, pH 7.4
<u>1x PBS (pH 7.4):</u>	8.0 g NaCl 0.2 g KH ₂ PO ₄ 1.15 g Na ₂ HPO ₄ 0.2 g KCl dissolve in 900 ml deionised H ₂ O adjust to pH 7.4 add H ₂ O to make 1 litre, autoclave
<u>Homogenisation buffer, pH 7.4:</u>	30 mM Tris/HCl, pH 7,4 2 mM DTT 2 mM EDTA 4 mM EGTA 5 mM Benzamidin 0,5 mM PMSF 1 Tablet complete® mini Protease Inhibitor Mix (Roche) per 10 ml buffer add 30 % sucrose, prepared freshly before use.
<u>5X Immunoprecipitation Buffer:</u>	0.5 m Potassium phosphate buffer 0.375 M NaCl 25 mM EDTA 5 mM Benzamidine 2.5 mM PMSF Adjust the pH to 7.9, prepare fresh.
<u>1.2 M Phosphate buffer (pH 6.8):</u>	1.2 M Na ₂ HPO ₄ , pH 9.1 was mixed with 1.2 M NaH ₂ PO ₄ , pH 4.02 in the ratio of 2:1.
<u>TE buffer (pH 8.0):</u>	10 mM Tris/HCl, pH 8.0 1 mM EDTA
<u>10X TAE buffer (pH 8.3):</u>	27.22 g Tris 13.6 g sodium acetate 3.72 g EDTA add H ₂ O to make 1 litre

1.5 Biological materials

Bacterial strains:

Strain name	Reference
<i>E. coli</i> DH5 α	Hanahan, 1983
<i>E. coli</i> XL1 blue	Bullock <i>et al.</i> , 1987
<i>E. coli</i> JM 38	Vieira and Messing, 1982
<i>Klebsiella aeorgenes</i>	Williams and Newell, 1976

Dictyostelium discoideum strains:

Strain name	description	Reference
AX2-214	axenically growing derivative of wild strain, NC-4 (commonly referred to as AX2)	Raper, 1935
CAP bsr	CAP mutant	Noegel et al., 1999
Car 1 ⁻ /3 ⁻	Mutants of cAR1 and cAR 3 receptor	Kim et al., 1997
Aca ⁻	aggregation stage adenyl cyclase ACA mutant	Pitt et al., 1992
Pia ⁻	Pianissimo, PIA mutant	Chen et al., 1997
HSB101	HSB1 mutant defective for PIA, ACA and ACR	Pergolizzi et al., 2002
Gα2 ⁻	G-protein α2 subunit mutant	Devreotes, 1994
Gβ ⁻	G-protein β subunit mutant	Lilly et al., 1993, Wu et al., 1995
pik 1 ⁻ /2 ⁻	PI3-kinase 1 and 2 mutants	Zhou et al., 1995
pkaC	Protein Kinase A catalytic subunit mutant	Mann and Firtel, 1991
pkaR	Protein kinase A regulatory subunit mutant	Harwood et al., 1992
limD ⁻	LIMD, a polarity gene mutant	Khurana et al., 2002
AX2 (RacA-V12)	Ax2 strain with constitutively active Rac GTPase	F. Rivero, unpublished
AX2 (RacA-N17)	AX2 strain with dominant negative Rac GTPase	F. Rivero, unpublished

Most of these mutants were generated by homologous recombination and were kind gifts of Salvatore Bozzaro (University of Torino, Italy), Richard A. Firtel (University of California, USA), Kees Weijer (University of Dundee, Scotland), Edward Cox (University of Princeton, USA) and Francisco Rivero (University of Cologne, Germany).

Yeast Strains:

Strain name	Reference
Y187	Harper et al., 1993
Y190	Flick et al., 1990, Harper et al., 1993
PJ69-4A	James et al., 1996
AH109 ^t	James et al., 1996

1.6 Plasmids

Plasmid name	Reference
pDEXRH	Westphal <i>et al.</i> , 1997
pDdA15gfp	Neujahr <i>et al.</i> , 1997
pGEM-T Easy	Kit: Promega
pUC bsr	Sutoh, 1993
pGADT7	Clontech
pGBKT7	Clontech
pCL1	Clontech
pAS2-1	Clontech
pACT2	Clontech
pGEX-4T-1	Amersham
pGEX-4T-2	Amersham

1.7 Synthetic oligonucleotides

The oligonucleotides were designed on the basis of sequence information available and ordered for synthesis from Sigma. Following is a list of the primers used for PCR or sequence analysis or both during the course of the present investigation. The position and orientation of the primers are indicated in the text when discussed.

Name	Sequence ^a	description ^b
C-ACA1	<i>GTTGCAATTTCAAGAGTAGT</i>	acaA: 4394-4413
C-ACA2	<i>TTCTTAACCTGAAAGATGGA</i>	acaA: 4813-4794
CAP1	<u>CGGGATCCCGATGTCAGAAGCAACTATTGT</u>	cap: 1-20
CAP2	<u>CGGGATCCCGTTAAATATGTGAAGTTGATTCA</u>	cap: 1395-1374
C-sGC1	<u>CGGGATCCCGATGGATTCAAATAATTCAAATTT</u>	sgcA: 6214-6236
C-sGC2	<u>CGGGATCCCGTTATCTTTCCAAAATTTAATAC</u>	sgcA: 8532-8510
C-sGC3	<i>GCTACAAAATCTTTTCTTGT</i>	sgcA: 6721-6741
C-sGC4	<i>GGTGATTGAGGTGATTGTT</i>	sgcA: 8381-8363
C-sGC5	<i>ATGTCTGGTTTAGGTAGATGG</i>	sgcA: 7213-7233
AD1	<u>GGAATTC</u> CCCATGTTATTATTAGAAACAC	ARPE: 40-60
AD2	<u>CGGGATCCCGTCTGATTTAATTTTGTTAAAGA</u>	ARPE: 929-907
VD1	<u>GGATCCCGATGGGTTTATTTGGTGGTAGAAAACATGGTG</u>	VATD: 1-31
VD2	<u>CTCGAGTTAAAAGATTGGAATTATTGATTCTTTTTG</u>	VATD: 1071-1039
VD3	<i>ACCCATTAGGTTTATTCAAGT</i>	VATD: 407-427
DdCAD1	<u>CGGAATTC</u> CGATGTCTGTTGATGCAAATAA	cadA: 1-20
DdCAD2	<u>CGGAATTC</u> CGTTATTTTCAGAGTTTAAGTTA	cadA: 642-621
M13 reverse	CAGGAAACAGCTATGAC	Sequencing primer
SP6 universal	ATTTAGGTGACACTATAG	Sequencing primer
T7 universal	TAATACGACTCACTATAGGG	Sequencing primer

a: Sequence is shown from 5' to 3' end. Restriction enzyme sites are underline, the *Dictyostelium* sequences are in italics.

b: Positions are with respect to the published sequences-Aggregation stage adenylyl cyclase (acaA) (Pitt et al., 1992), cyclase associated protein (CAP) (Gottwald et al., 1996), soluble guanylyl cyclase (sgcA) (Roelofs et al., 2001), Vacuolar ATP synthase subunit d (VATD) (Temesvari et al., 1994), ARP2/3 complex 34kDa subunit, (ARPE) (Insall et al., 2001), cell adhesion molecule DdCAD1 (cadA) (Wong et al., 1996).

2.0 Cell biological methods

2.1 Growth of *Dictyostelium*

2.1.1 Growth in liquid nutrient medium (Claviez et al., 1982)

Dictyostelium discoideum AX2 and the derived transformants were grown in liquid AX2 medium containing dihydrostreptomycin (40 µg/ml) and other appropriate selective antibiotic (depending upon the mutant) at 21°C either in a shaking-suspension in Erlenmeyer flask with shaking at 160 rpm

or the cells were grown on petri dish. For all the cell biological works, cultures were harvested at a concentration of $3\text{-}5 \times 10^6$ cells/ml.

2.1.2 Growth on SM agar plates

In general, *Dictyostelium* cells were plated onto SM agar plates overlaid with *Klebsiella aerogenes* and incubated at 21°C for 3-4 days until *Dictyostelium* plaques appeared on the bacterial lawns. To obtain single clones of *Dictyostelium*, 50-200 cells were suspended in 100 μ l Soerensen phosphate buffer and plated onto *Klebsiella*-overlaid SM agar plates. Single plaques obtained after incubation at 21°C for 3-4 days were picked up with sterile tooth-picks, transferred either to new *Klebsiella*-overlaid SM agar plates or to separate petri dishes in AX2 medium supplemented with dihydrostreptomycin (40 μ g/ml) and ampicillin (50 μ g/ml) to get rid of the bacteria and any other appropriate selective antibiotic (depending upon mutant).

2.2 Development of *Dictyostelium*

Multicellular development in *Dictyostelium* is induced by starvation. Cells grown to a density of $2\text{-}3 \times 10^6$ cells/ml were pelleted by centrifugation at 2,000 rpm (Sorvall RT7 centrifuge) for 2 min at 4°C and were washed two times in an equal volume of cold Soerensen phosphate buffer in order to remove all the nutrients present in the culture medium. For development analysis in suspension culture, the cells were resuspended in Soerensen phosphate buffer at a density of 1×10^7 cells/ml and were shaken at 160 rpm and 21 °C for desired time periods.

For development on phosphate agar plates, 1×10^7 cells were resuspended in 3 ml Soerensen phosphate buffer and evenly distributed onto phosphate-buffered agar plates (90 mm) or water agar plates (90 mm). The plates were air-dried and any excess liquid was carefully aspirated without disturbing the cell layer. The plates were then incubated at 21°C and developmental phenotypes were observed and the desired images were captured at indicated time points.

2.3 Preservation of *Dictyostelium* cells

Dictyostelium cells were allowed to grow densely in AX2 medium to a concentration of $4\text{-}5 \times 10^6$ cells/ml. 9 ml of the densely grown culture was collected in a 15 ml Falcon tube on ice and supplemented with 1 ml Horse serum and 1 ml DMSO. The contents were mixed by gentle pipetting, followed by preparing aliquots of 1 ml in cryotubes (1.8 ml, Nunc). The aliquots were incubated on ice for 60 min, followed by incubation at -20°C for at least 2 h. Finally the aliquots were transferred to -80°C for long term storage.

For reviving the frozen *Dictyostelium* cells, the aliquot was taken out from -80°C and thawed immediately at 37°C in a waterbath. In order to remove DMSO, the cells were transferred to a Falcon tube containing 30 ml AX2 medium and centrifuged at 2,000 rpm (Sorvall RT7 centrifuge) for 2 min at 4°C . The cell pellet was resuspended in 10 ml of AX2 medium and 200 μl of the cell suspension was plated onto SM agar plates overlaid with *Klebsiella*, while the remaining cell suspension was transferred into a 100-mm petri dish (Falcon) and antibiotics were added when appropriate. Cells in the petri dish were allowed to recover overnight at 21°C and the medium was changed the next day to remove the dead cells and the traces of DMSO, whereas, the SM agar plates coated with cell suspension and bacteria were incubated at 21°C until plaques of *Dictyostelium* cells started to appear.

2.4 Transformation of *Dictyostelium* cells

2.4.1 Transformation of *Dictyostelium* cells by CaCl_2

The cells were grown in culture medium at shaking to a density of $1-2 \times 10^6$ cells, pipetted 10-12 ml of cells on a petri dish and led them adhered to the surface at 21°C . The medium was replaced with 10 ml MOPS-HL5 buffer, and incubated for another one hour. In the mean time the DNA mix was prepared, 15-30 μg DNA in 0.6 ml 1X HBS and placed in a sterile glass tube. Then, 125mM CaCl_2 was added with vortexing briefly and the mixture was incubated at room temperature for 25 minutes. The MOPS-HL5 buffer was then removed completely without losing the cells and the above DNA precipitate was added drop wise to the cells and incubated for 25 minutes. Without removing DNA 10 ml of MOPS- HL5 buffer was added to the cells, and incubated for 3-4 hrs. The buffer was removed, and 36% glycerol in 1X HBS was carefully added and incubated for 5 minutes and glycerol was removed without losing cells. 10 ml of fresh axenic medium was added and the cells were incubated at 21°C overnight, and drug was added the next day.

MOPS-HL5-buffer:

5 g yeast extracts
10 g glucose
10 g protease peptone (Oxoid)
1.3 g MOPS
 H_2O pH 7.1-7.2
autoclave

HBS (Hepes buffered saline)-buffer:

4 g NaCl
0.18 g KCl
0.05 g Na_2HPO_4 or 0.062 g $\text{Na}_2\text{HPO}_4 \cdot \text{H}_2\text{O}$
2.5 g Hepes
0.5 g glucose
pH 7.05 (with NaOH)
250 ml for 2x HBS
filter sterilize

Healing-solution:

2M CaCl_2 , filter sterilize

2.4.2 Transformation of *Dictyostelium* cells by electroporation

The electroporation method for transformation of *Dictyostelium* cells described by de Hostos *et al.* (1993) was followed with little modifications. *Dictyostelium discoideum* AX2 cells were grown axenically in suspension culture to a density of $2-3 \times 10^6$ cells/ml. Cell suspension was incubated on ice for 20 min and centrifuged at 2,000 rpm (Sorvall RT7 centrifuge) for 2 min at 4°C to collect the cells. The cells were then washed with an equal volume of ice-cold Soerensen phosphate buffer followed by an equal volume of ice-cold Electroporation-buffer. After washings, the cells were resuspended in Electroporation-buffer at a density of 1×10^8 cells/ml. For electroporation, 20-25 µg of the plasmid DNA was added to 500 µl (5×10^7 cells) of the above cell suspension and the cell-DNA mixture was transferred to a pre-chilled electroporation cuvette (2 mm electrode gap, Bio-Rad). Electroporation was performed with an electroporation unit (Gene Pulser, Bio-Rad) set at 0.9 kV and 3 µF without the pulse controller. After electroporation, the cells were immediately spread onto a 100-mm petri dish (Falcon) and were allowed to sit for 10 min at 21°C. Thereafter, 1 ml of Healing-solution was added dropwise onto the cells and the petri dish was incubated at 21°C on a shaking platform at 50 rpm for 15 min. 10 ml of AX2 medium was added into the petri dish and the cells were allowed to recover overnight. The next day, the medium was changed to the selection medium containing appropriate antibiotic. To select stable transformants, selection medium was replaced after every 24-48 h until the control plate (containing cells electroporated without any DNA) was clear of live cells.

Electroporation-buffer:

100 ml 0.1 M potassium phosphate buffer
17.12 g sucrose
add distilled H₂O to make 1 litre
autoclaved

0.1 M Potassium phosphate buffer:

170 ml 0.1 M KH₂PO₄
30 ml 0.1 M K₂HPO₄
adjust to pH 6.1

Healing-solution:

150 µl 0.1 M CaCl₂
150 µl 0.1 M MgCl₂
10 ml electroporation-buffer

2.5 Analysis of agglutination (Rivero *et al.*, 1999)

Axenically growing *Dictyostelium* AX2 cells and derived mutants were harvested, washed twice with equal volumes of Soerensen phosphate buffer and resuspended in Soerensen phosphate buffer to a density of 1×10^7 cells/ml. For strains with different cell size, cells were adjusted to the same total cell volume by resuspending them at an OD₆₀₀ of 0.9 in 10 ml Soerensen phosphate buffer. The cell suspension was then transferred to an Erlenmeyer flask and incubated on a shaker at 160 rpm and

21°C. Samples were taken at the indicated time points and the decrease in light scattering was measured at 600 nm. Cell-to-cell adhesions of wild type and mutant cells were done as follows. Briefly, the cells were grown to $2-6 \times 10^6$ cells/ml, washed twice with cold Soerensen phosphate buffer and resuspended in the same buffer to a cell density of 1×10^7 cells/ml and then proceeded as before. At desired times the samples were drawn and shaken in the presence or absence of 10 mM EDTA in Nunc well plates and the decrease in light scattering was measured at 600 nm.

2.6 Endocytosis assays

Phagocytosis assays was performed according to Maniak et al., 1995. Briefly, *Dictyostelium* cells were grown to $< 5 \times 10^6$ /ml over 5 generations in axenic medium. Cells were centrifuged and resuspended at 2×10^6 cells/ml in fresh axenic medium at 21 °C. TRITC-labeled yeast cells prepared (according to Material and Methods 6.4) were added in 5-fold excess (10^9 yeast cells/ml stock). Cells were incubated on a rotary shaker at 160 rpm. Samples were taken at different intervals and the fluorescence of non-internalized yeasts was quenched by incubating for 3 min with 100 µl of trypan blue (2 mg/ml). Cells were centrifuged again, resuspended in phosphate buffer and the fluorescence was measured using a fluorimeter (544nm excitation / 574nm emission). Fluid-phase endocytosis assays were performed according to the methods of Aubry et al. (1994). Briefly, *Dictyostelium* cells were grown to $< 5 \times 10^6$ cell/ml, the cells were centrifuged and resuspended at 5×10^6 /ml in fresh axenic medium at 21°C and incubated for 15 min on a shaker to allow cells to recuperate. Then TRITC-dextran was added to a final concentration of 2 mg/ml. Samples were withdrawn at different time intervals and the cells were pelleted after incubating for 3 min with 100 µl of trypan blue (2 mg/ml) to remove non-specifically bound marker. The pellet was resuspended in phosphate buffer and the fluorescence was measured using a fluorimeter (544 nm excitation/574 nm emission).

3.0 Molecular biological methods

3.1 Purification of plasmid DNA

In general, for small cultures (1 ml) of *E. coli* transformants, the alkaline lysis method of Holmes and Quigley (1981) was used to extract plasmid DNA. This method is good for screening a large number of clones simultaneously for the desired recombinant plasmid. Briefly, single transformants were picked up from the culture plate and were grown overnight in 1 ml of LB media containing suitable antibiotic. Next day, the *E. coli* cells were pelleted by centrifugation at 6,000 rpm in a microcentrifuge for 3-5 min. The pellet was then resuspended completely in 250 µl of STET/lysozyme buffer and the suspension was incubated at the room temperature for 10 min to lyse

the bacterial cells. The bacterial lysate was boiled at 100°C for 1 min and was then centrifuged in an eppendorf centrifuge at maximum rpm for 15 min at room temperature. The plasmid DNA present in the supernatant was precipitated by adding equal volume of isopropanol and incubating at room temperature for 10 min. The precipitated DNA was pelleted in the eppendorf centrifuge at 12,000 rpm for 15 min and the DNA pellet was washed with 70% ethanol, dried in the speed-vac concentrator and finally resuspended in 40 µl TE, pH 8.0 containing RNase A at 1 µg/ml.

STET/lysozyme buffer (pH 8.0):

50 mM Tris/HCl, pH 8.0

50 mM EDTA

0.5% Triton-X-100

8.0% Sucrose

Add lysozyme at 1 mg/ml at the time of use

Alternatively, for pure plasmid preparations in small and large scales, kits provided either by Macherey-Nagel (Nucleobond AX kit for small scale plasmid preparations) or by Qiagen (Qiagen Midi- and Maxi-Prep kit for large scale plasmid preparations). These kits were used when the pure plasmid DNA was required for sequencing, PCR or transformation. These kits follow basically the same approach: first, an overnight culture of bacteria containing the plasmid is pelleted and the cells are lysed by alkaline lysis. The freed plasmid DNA is then adsorbed on a silica matrix, washed with ethanol, and then eluted into TE, pH 8.0. This method avoids the requirement of caesium chloride or phenol-chloroform steps during purification.

3.2 Digestion with restriction enzymes

All restriction enzymes were obtained from NEB, Amersham or Life technologies and the digestions were performed in the buffer systems and temperature conditions as suggested by the manufacturers. The plasmid DNA was digested for 1-2 h and the chromosomal DNA for 12-16 h.

3.3 Generation of blunt ends in linearised plasmid DNA

For many cloning experiments, it was necessary to convert the 5' or 3' extensions generated by restriction endonucleases into blunt ends. Repair of 5' extensions was carried out by the polymerase activity of the Klenow fragment, whereas repair of 3' extensions was carried out by the 3' to 5' exonuclease activity of the Klenow fragment.

Reaction-mix for 5' extensions:

1-4 µg linearised DNA

5 µl 10x High salt buffer

1 µl 50x dNTP-mix (each 4 mM)

2 U Klenow fragment

add H₂O to make 50 µl

Reaction-mix for 3' extensions:

1-4 µg linearised DNA

5 µl 10x High salt buffer

2 U Klenow fragment

add H₂O to make 50 µl

10x High salt buffer:

500 mM Tris/HCl, pH 7.5
1 M NaCl
100 mM MgCl₂
10 mM DTT

The reaction was carried out at 37°C for 25-30 min. After incubation, the reaction was immediately stopped by inactivating the enzyme at 75°C for 10 min or by adding 1 µl 0.5 M EDTA. This was followed by phenol/chloroform extraction and precipitation of DNA with 2 vols of ethanol.

3.4 Dephosphorylation of DNA fragments

To avoid self-ligation of the vector having blunt ends or that has been digested with a single restriction enzyme, 5' ends of the linearised plasmids were dephosphorylated by calf-intestinal alkaline phosphatase (CIAP, Boehringer). Briefly, in a 50 µl of reaction volume, 1-5 µg of the linearised vector-DNA was incubated with 1 U calf-intestinal alkaline phosphatase (CIAP) in CIAP-buffer (provided by the manufacturer) at 37°C for 30 min. The reaction was stopped by inactivating the enzyme by heating the reaction-mixture at 65°C for 10 min. The dephosphorylated DNA was extracted once with phenol-chloroform and precipitated with 2 vol. ethanol and 1/10 vol. 2 M sodium acetate, pH 5.2.

3.5 Setting up of ligation reaction

DNA fragment and the appropriate linearised plasmid were mixed in approximately equimolar amounts. T4 DNA ligase (Life technologies/Boehringer) and ATP were added as indicated below and the ligation reaction was left overnight at 10-12°C.

Ligation reaction:

Linearised vector DNA (200-400 ng)
DNA-fragment
4 µl 5x Ligation buffer
1 µl 0.1 M ATP
1.5 U T4 ligase
add H₂O to make 20 µl

5x Ligation buffer:

supplied along with the T4 ligase
enzyme by the manufacturer

3.6 Isolation of *Dictyostelium* genomic DNA

Genomic DNA from *Dictyostelium* was prepared according to the method described by Nellen *et al.* (1987), with slight modifications. *Dictyostelium* cells were allowed to grow on *Klebsiella*-covered SM plates at 21°C. After 2-3 days, when the plates were covered with densely grown *Dictyostelium*, cells were collected in 15 ml ice-cold water, pelleted and washed twice with ice-cold water to get rid of *Klebsiella*. Alternatively, the pellet of 1 x 10⁸ *Dictyostelium* cells grown in shaking suspension was

washed twice with ice-cold Soerensen phosphate buffer. The pellet of *Dictyostelium* cells was finally resuspended in 5 ml cold Nucleolysis buffer. The nuclei fraction was obtained by centrifugation at 3,000 rpm (Sorvall RT7 centrifuge) for 10 min. The nuclear pellet obtained was carefully resuspended in 1 ml TE, pH 8.0, with 0.5% SDS and 0.1 mg/ml proteinase K and incubated at 37°C for 3-5 h. The genomic DNA was extracted twice with phenol/chloroform (1:1 v/v), precipitated by adding 2.5 vol. 96% ethanol and 1/10 vol. 3 M sodium acetate, pH 5.2. The DNA precipitate was carefully spooled with a Pasteur pipette, washed with 96% ethanol, air-dried and dissolved in the desired volume of TE, pH 8.0.

Nucleolysis buffer:

10 mM magnesium acetate
10 mM NaCl
30 mM HEPES, pH 7.5
10% sucrose
2% Nonidet P40

Estimation of DNA concentration:

1 O.D at 260 nm = 50 µg DNA

3.7 DNA agarose gel electrophoresis

Agarose gel electrophoresis was performed according to the method described by Sambrook *et al.* (1989) to resolve and purify the DNA fragments. Electrophoresis was typically performed with 0.7% (w/v) agarose gels in 1x TAE buffer submerged in a horizontal electrophoresis tank containing 1x TAE buffer at 1-5 V/cm. Only for resolving fragments less than 1,000 bp, 1% (w/v) agarose gels in 1x TAE buffer were used. DNA-size marker (Life technologies) was always loaded along with the DNA samples in order to estimate the size of the resolved DNA fragments in the samples. The gel was run until the bromophenol blue dye present in the DNA-loading buffer had migrated the appropriate distance through the gel. The gel was examined under UV light at 302 nm and was photographed using a gel-documentation system (MWG-Biotech)

DNA-size marker:

1 kb DNA Ladder (Life technologies): 12,216; 11,198; 10,180; 9,162; 8,144; 7,126; 6,108; 5,090; 4,072; 3,054; 2,036; 1,636; 1,018; 506; 396; 344; 298; 220; 201; 154; 134; 75 bp

3.8 Recovery of DNA fragments from agarose gel

DNA fragments from restriction enzyme digests or from PCR reactions were separated by agarose gel electrophoresis and the gel piece containing the desired DNA fragment was carefully and quickly excised while observing the ethidium bromide stained gel under a UV transilluminator. The DNA

fragment was then purified from the excised gel piece using the Macherey-Nagel gel elution kit (NucleoSpin Extract 2 in 1), following the method described by the manufacturers.

3.9 Isolation of total RNA from *Dictyostelium* cells

The pellet of 1×10^8 cells (harvested at growth or different stages of development) was washed with ice-cold DEPC-H₂O (0.1% DEPC, mixed by stirring for 5-6 h, autoclaved) and lysed in 1 ml of guanidine isothiocyanate (TRI reagent). Centrifuged at 13K rpm/4°C/10 min to pellet the insoluble materials, the supernatant was transferred to a fresh eppendorf tube and allowed to stand at room temperature for 5 min. Followed by immediately adding 1 vol. of chloroform (Tris or water saturated) to separate the aqueous and organic phase and allowed to stand at room temperature for 5 min. Centrifuged at 13K rpm/4°C/15 min and the upper aqueous phase was collected carefully and was extracted with an equal volume of phenol/chloroform (1:1 v/v), till no interphase was visible. This was followed by an extraction with an equal volume of chloroform and finally the RNA present in the upper aqueous phase was precipitated by adding equal volume of isopropanol and incubated the samples overnight at -80°C. Next day, the RNA was pelleted and washed with 70% ethanol, air-dried and dissolved in the desired volume of DEPC-H₂O. Otherwise the RNA was mostly extracted from the Qiagen RNAeasy kits following the kit manual. The concentration of RNA was determined by measuring the O.D₂₆₀ of the RNA solution using a spectrophotometer. The RNA samples were stored at -80°C.

DEPC-H₂O:

0.1% DEPC in H₂O
mixed by stirring for 5-6 h
autoclaved

Estimation of RNA concentration:

1 O.D at 260 nm = 40 µg RNA

3.10 RNA formaldehyde-agarose gel electrophoresis

The formaldehyde-agarose denaturing electrophoresis (Lehrach *et al.*, 1977) is used for separation and resolution of single stranded RNA.

Sample preparation for electrophoresis:

In general, 30 µg of purified total RNA was mixed with an equal volume of RNA-sample buffer and denatured by heating at 65°C for 10 min. After denaturation, the sample was immediately transferred to ice and 1/10 vol. of RNA-loading buffer was added. Thereafter, the RNA samples were loaded onto a denaturing formaldehyde-agarose gel.

Formaldehyde-agarose gel preparation:

For a total gel volume of 150 ml, 1.8 g agarose (final concentration 1.2%) was initially boiled with 111 ml DEPC-H₂O in an Erlenmeyer flask, cooled to 60°C and then 15 ml of RNA-gel-casting buffer, pH 8.0 and 24 ml of 36% formaldehyde solution were added. The agarose solution was mixed by swirling and poured into a sealed gel-casting chamber of the desired size. After the gel was completely set, denatured RNA samples were loaded and the gel was run in 1x RNA-gel-running buffer, pH 7.0, at 100 V until the bromophenol blue dye had migrated the appropriate distance through the gel. A test gel was sometimes run with 5 µg of total RNA to check the quality of the RNA samples. In such a case, 10 µg/ml ethidium bromide was added to the RNA-sample buffer during sample preparation and after electrophoresis the gel was examined under UV light at 302 nm and was photographed using the gel-documentation system.

10x RNA-gel-casting buffer (pH 8.0):

200 mM MOPS
50 mM sodium acetate
10 mM EDTA
adjust pH 8.0 with NaOH
autoclaved

10x RNA-gel-running buffer (pH 7.0):

200 mM MOPS
50 mM sodium acetate
10 mM EDTA
adjust pH 7.0 with NaOH
autoclaved

RNA-sample buffer:

50% formamide
6% formaldehyde
in 1x RNA-gel-casting buffer, pH 8.0

RNA-loading buffer:

50% sucrose, RNase free
0.25% bromophenol blue
in DEPC-H₂O

Internal RNA-size standard:

26S rRNA (4.1 kb)
17S rRNA (1.9 kb)

3.11 Northern blotting

After electrophoresis, the RNA formaldehyde agarose gel was rinsed in sufficient amount of deionised H₂O for 5 min and then equilibrated in 10x SSC for 25 min. The resolved RNA was then transferred from the gel to the nylon membrane (Biodyne B membrane, Pall) using the transfer setup as described for Southern blotting (see Materials and Methods 3.9.). After overnight transfer with 20x SSC, the transferred RNA was immobilised by baking the membrane in an oven at 80°C for 1 h.

3.12 Radiolabelling of DNA

The Prime-it kit (Stratagene) was used for radiolabelling of DNA fragments following the method suggested by the manufacturer. Briefly, 0.1-0.3 µg DNA sample was suspended in 24 µl ddH₂O (final volume). Then 10 µl of random-oligonucleotide-primer (supplied along with the kit) was added and the DNA template was denatured at 95°C for 5 min. After denaturation, 10 µl of 5x dATP-primer

buffer (supplied along with the kit), 5 μ l of α -³²P-ATP (Amersham) and 1 μ l Klenow enzyme (5 U/ μ l, supplied along with the kit) was added and the reaction-mixture was incubated at 37°C for 10 min. After 10 min the reaction was immediately stopped by adding 2 μ l stop-mix (supplied along with the kit). Now the reaction-mixture was diluted with 100 μ l TE, pH 8.0 to increase the reaction volume and the reaction-mixture was overlaid on a 0.9 ml Sephadex G-50 spin column (see Materials and Methods 3.13.1.). The free nucleotides present in the reaction-mixture were separated by centrifugation at 3,000 rpm (Sorvall RT7 centrifuge) for 2 min through the Sephadex G-50 spin column and the radiolabelled DNA probe was collected in a 1.5 ml eppendorf tube. The purified radiolabelled DNA probe was denatured by heating at 100°C for 10 min, cooled on ice and used for hybridisation of Southern- or northern-blot.

3.12.1 Chromatography through Sephadex G-50 spin column

This technique (Sambrook *et al.*, 1989), which employs gel filtration to separate high-molecular weight DNA from smaller molecules, was used to segregate radiolabelled DNA from unincorporated α -³²P-ATP. 30 g of Sephadex G-50 (Pharmacia) was slowly added to 250 ml of TE, pH 8.0, in a 500-ml bottle and the beads were allowed to swell overnight at room temperature. Next day, the supernatant was decanted and was replaced with an equal volume of TE, pH 8.0. The beads were autoclaved and stored in a screw-capped bottle at 4°C. For preparation of Sephadex G-50 spin column, the swollen Sephadex G-50 beads were packed in a disposable 1-ml syringe plugged with sterile glass wool and the column was spun at 3,000 rpm (Sorvall RT7 centrifuge) for 2 min. Sephadex G-50 was added until the packed column volume was 0.9 ml. The column was then used for separation of the radiolabelled DNA probe.

3.12.2 Hybridisation of Northern blots with a radiolabelled DNA probe

Northern-blot were rinsed briefly with 2X SSC and incubated in a heat-sealable hybridisation-bag (Life technologies) in 15-20 ml of pre-hybridisation buffer for 1h at 37°C on a shaking platform. After pre-hybridisation, the denatured radiolabelled DNA probe was added directly to the pre-hybridisation-buffer in the hybridisation-bag and the hybridisation was performed by incubating the blot overnight at 37°C. After hybridisation, the blot was washed twice with 2x SSC/0.1% SDS for 10 min each at room temperature with gentle shaking followed by two washings with wash buffer for 30 min each at 37°C with gentle shaking. The blot was then wrapped in a plastic wrap and autoradiography was performed by exposing the blot to X-ray film at -70°C for the desired time.

Pre-hybridisation/Hybridisation buffer:

50% formamide
1% sodium lauryl sarcosinate

Wash buffer:

same contents as Pre-hybridisation/
hybridisation buffer except without

0.2% SDS	4x Denhardt's reagent
2 mM EDTA, pH 7.2	
0.12 M phosphate buffer, pH 6.8	<u>100x Denhardt's reagent:</u>
2x SSC	2% ficoll 400
4x Denhardt's reagent	2% polyvinylpyrrolidone
	2% bovine serum albumin

3.13 Transformation of *E. coli*

3.13.1 Transformation of *E. coli* cells by the CaCl₂ method

Preparation of CaCl₂-competent *E. coli* cells:

An overnight grown culture of *E. coli* (0.5 ml) was inoculated into 50 ml LB medium and incubated at 37°C, 250 rpm until an OD₆₀₀ of 0.4-0.6 was obtained. The bacteria were then pelleted at 4°C for 10 min at 4,000 rpm (Beckman Avanti J25, rotor JA-25.50) and the bacterial pellet was resuspended in 20 ml of ice-cold 0.1 M CaCl₂ and incubated on ice for 15 min. The bacterial cells were again pelleted and resuspended in 2 ml of ice-cold 0.1 M CaCl₂. These CaCl₂-competent cells were stored at 4°C for up to 1 week. Alternatively, the pellet of CaCl₂-competent *E. coli* cells was resuspended in 0.1 M CaCl₂/20% glycerol and then aliquoted (200 µl/tube). The aliquots were then quickly frozen in a dry ice/ethanol bath and immediately stored at -80°C.

Transformation of CaCl₂-competent *E. coli* cells:

Plasmid DNA (~50-100 ng of a ligase reaction or ~10 ng of a supercoiled plasmid) was mixed with 100-200 µl of CaCl₂-competent *E. coli* cells and incubated on ice for 30 min. The cells were then heat-shocked at 42°C for 45 s and immediately transferred to ice to cool for 2 minutes. The cells were then mixed with 1 ml of pre-warmed (at 37°C) SOC medium and incubated at 37°C with shaking at ~150 rpm for 45 min. Finally, 100-200 µl of the transformation mix, or an appropriate dilution, was plated onto selection plates and the transformants were allowed to grow overnight at 37°C.

3.13.2 Transformation of *E. coli* cells by electroporation

Preparation of electroporation-competent *E. coli* cells

An overnight grown culture (5 ml) was inoculated into 1,000 ml of LB medium and incubated at 37°C with proper aeration and shaking at 250 rpm until an OD₆₀₀ of 0.4-0.6 was obtained. The culture was then incubated on ice for 15-20 min. Thereafter the culture was transferred to pre-chilled 500-ml centrifuge bottles (Beckman) and the cells were pelleted by centrifugation at 4,200 rpm (Beckman Avanti J25, rotor JA-10) for 20 min at 4°C. The bacterial pellet was washed twice with an equal volume of ice-cold water and the cells were resuspended in 40 ml of ice-cold 10% glycerol,

transferred to a pre-chilled 50-ml centrifuge tube and centrifuged at 4,200 rpm (Beckman Avanti J25, rotor JA-25.50) for 10 min at 4°C. Finally, the cells were resuspended in equal volume of 10% chilled glycerol and aliquoted (50-100 µl) in 1.5-ml eppendorf tubes that have been placed in a dry ice/ethanol bath. The frozen aliquots were immediately transferred to –80°C for long-term storage.

Transformation of electroporation-competent *E. coli* cells

Plasmid DNA (~20 ng dissolved in 5-10 µl ddH₂O, no salts) was mixed with 50-100 µl electroporation-competent *E. coli* cells. The transformation mix was transferred to a 2 mm BioRad electroporation cuvette (pre-chilled) and the cuvette was incubated on ice for 10 min. The DNA was then electroporated into competent *E. coli* cells using an electroporation unit (Gene Pulser, BioRad) set at 2.5 kV, 25 µF, 200 Ω. Immediately after electroporation, 1 ml of pre-warmed (37°C) SOC medium was added onto the transformed cells and the cells were incubated at 37°C with shaking at ~150 rpm for 45 min. Finally, 100-200 µl of the transformation mix, or an appropriate dilution, was plated onto selection plates and the transformants were allowed to grow overnight at 37°C.

3.14 Glycerol stock of bacterial culture

Glycerol stocks of all the bacterial strains/transformants were prepared for long-term storage. The culture was grown overnight in LB medium with or without the selective antibiotic (depending upon the bacterial transformant). 850 µl of the overnight grown culture was added to 150 µl of sterilized glycerol in a 1.5 ml microcentrifuge tube, mixed well by vortexing and the tube was frozen on dry ice and stored at –80°C.

3.15 DNA colony blot for screening of *E. coli* transformants

The method of Sambrook *et al.* (1989) was used to screen many bacterial colonies simultaneously. After the bacterial colonies had grown to a diameter of 0.1-0.2 mm, the plates were removed from the 37°C incubator and stored at 4°C for 1-2 h in an inverted position. Thereafter a dry nitrocellulose filter (BA85, Ø82 mm, Schleicher and Schuell) was labelled with a ballpoint pen and placed with the numbered side down, on the surface of the agar medium in contact with the bacterial colonies until the filter was completely wet. The filter and underlying agar were then marked in three or more asymmetric locations by stabbing through it with a 18-gauge needle. The filter was then carefully peeled off and the plates were incubated at 37°C for 4-8 h until the colonies had regenerated. The bacteria adhering to the filter were immediately lysed by placing the filter, colony side up, for 5 min on a sheet of 3MM Whatman paper that had been saturated with denaturing solution. The filter was then transferred to a second sheet of 3MM Whatman paper that had been saturated with neutralizing solution. After 5 min, the filter was transferred to a third sheet of 3MM Whatman paper that had been

saturated with 2x SSC and placed for 5 min. While transferring filters from one sheet to another, care was taken to remove as much fluid as possible from the underside of the filter by briefly placing the filter on a dry paper towel. Now the filter was laid, colony side up, on a sheet of dry 3MM Whatman paper and was allowed to dry at room temperature for 30-60 min. Thereafter, the liberated DNA was immobilised onto the filter by baking the filter for 2 h at 80°C in an oven. After baking, the filter was floated and submerged for 5 min in 2x SSC, followed by incubation in pre-wash solution at 50°C for 30 min. Loose bacterial debris or any fragments of agarose were removed during incubation in the pre-wash solution by gently scraping on the colony surface. Thereafter, the filter was transferred to pre-hybridisation solution with 50% formamide and incubated at 42°C for 1-2 h with gentle shaking, followed by hybridisation with the denatured radiolabelled probe as described above (Materials and Methods 3.13.2.). After hybridisation, the filter was washed twice with 2x SSC/0.1% SDS for 5-10 min each at room temperature with gentle shaking followed by two washings with 1x SSC/0.1% SDS for 30 min each at 37°C with gentle shaking. The filter was then wrapped in a saran wrap and autoradiography was performed by exposing the filter to a X-ray film for the desired time at -70°C. The individual colonies giving positive hybridisation signals were picked and grown.

Denaturing solution:

0.5 M NaOH
1.5 M NaCl

Pre-wash solution:

5x SSC
0.5% SDS
1 mM EDTA

Neutralizing solution:

1.5 M NaCl
0.5 M Tris/HCl, pH 8.0

Pre-hybridisation solution:

same as described in Materials and Methods (3.12.2.)

3.16 Construction of vectors

3.16.1 Vectors for expression of GFP-fusion proteins of CAP and its domains (Noegel et al., 1999)

Full length CAP was cloned into pDEX-T65S-GFP (Westphal et al., 1997) in which CAP protein is N-terminally fused to GFP and transcription of the fusion protein is under the control of the actin 15 promoter allowing the expression during growth and development. Full length GFP-CAP carries the gene encoding red shifted GFP carrying the T65S mutation (Westphal et al., 1997). The stable transformants in the various signalling mutants were selected for growth in the presence of 20 µg/ml G418 (Geneticin) or 10 µg/ml Blasticidin S (Bsr) or both in the case of the co-transformants. Since most of the mutants were G418 resistant, co-transformants were achieved by also transforming the empty Blasticidin vector with Bsr selection along with the plasmid of interest. The expression plasmids coding for fusions of GFP-CAP and the N- and C-terminal domain with N-terminally fused

GFP, that either contained or lacked the proline rich region (CAP-GFP, N-CAP-Pro-GFP, N-CAP-GFP, Pro-C-CAP-GFP, C-CAP-GFP (Noegel et al., 1999). The various GFP-CAP fusion constructs were transformed into the signal transduction mutants by either CaCl_2 transformation or electroporation. The transformants were inspected for the GFP expression under the fluorescence microscope (Olympus) and by immunoblots.

3.16.2 Vectors for expression of binding partner studies of CAP

Construction of Yeast two hybrid expression vectors	
pGBKT7-CAP	Vector: pGBKT7, <i>Bam</i> HI digested, 7.3 kb, CIP treated, gel purified Insert: PCR, CAP1/CAP2 oligos, 1.5 Kb, <i>Bam</i> HI digested, gel purified.
pAS2-CAP	Vector: pAS2, <i>Bam</i> HI digested, CIP treated, gel purified Insert: PCR, <i>Bam</i> HI digested,
pACT2-ACA	Vector: pACT2, <i>Eco</i> RI digested, CIP treated, gel purified Insert: PCR, C-ACA1/C-ACA2 oligos, 419 bp, <i>Eco</i> RI digested, gel purified
pGADT7-sGC	Vector: pGADT7, <i>Bam</i> HI digested, 8 kb, CIP treated, gel purified Insert: PCR, C-sGC1/C-sGC2 oligos, 2.4 kb, <i>Bam</i> HI digested, gel purified
pGADT7-AD	Vector: pGADT7, <i>Eco</i> RI- <i>Bam</i> HI digested, 8 kb, gel purified Insert: PCR, AD1/AD2 oligos, 956 bp, <i>Eco</i> RI- <i>Bam</i> HI digested, gel purified
pGADT7-VD	Vector: pGADT7, <i>Bam</i> HI- <i>Xho</i> I digested, 8 kb, gel purified Insert: PCR, VD1/VD2 oligos, 1071 bp, <i>Bam</i> HI- <i>Xho</i> I digested, gel purified

Inserts were generated by PCR amplifications from wild type AX2 genomic/cDNA. PCR products were pre-ligated into pGEM-T Easy vectors for further sub-cloning after sequence determination.

3.16.3 Vectors for expression of GST fusions of sGC, ARPE and Vacuolar ATPase d subunit

Construction of GST-fusion vectors	
pGEX-4T-2-sGC	Vector: pGEX-4T-2, <i>Not</i> I digested, 4.9 kb, CIP treated, gel purified Insert: pGEM-T Easy-sGC, <i>Not</i> I digested, 2.4 kb, gel purified
pGEX-4T-1-AD	Vector: pGEX-4T-1, <i>Eco</i> RI- <i>Xho</i> I digested, 4.9 kb, gel purified Insert: pGADT7-AD, <i>Eco</i> RI- <i>Xho</i> I, 1kb, gel purified
pGEX-4T-1-VD	Vector: pGEX-4T-1, <i>Not</i> I digested, 4.9 kb, CIP treated, gel purified Insert: pGEM-T Easy-VD, <i>Not</i> I digested, 1.1 kb, gel purified

3.17 DNA sequencing

Sequencing of the PCR-amplified product or plasmid DNA was performed at the sequencing facility of the Centre for Molecular Medicine, University of Cologne, Cologne, by modified dideoxy nucleotide termination method using a Perkin Elmer ABI prism 377 DNA sequencer.

3.18 Computer analysis

Sequencing analysis, homology searches, structural predictions and multiple alignments of protein sequences were performed using the University of Wisconsin GCG software package (Hiroak *et al.* 1990) and Expsy Tools software, accessible on the World Wide Web.

4.0 Methods for the ‘Yeast Two Hybrid System’

4.1 Transformation of yeast by LiOAc method

The lithium acetate transformation method (Geitz, 1996) was used for the high efficiency yeast transformations. 2-3 medium sized (3 mm) yeast colonies from a plate were inoculated into YEPD medium and grown at 30 °C and 200 rpm till 0.8 OD₆₀₀. For yeast strains grown on YEPD plates, YEPD medium was used and yeast strains containing pACT2/pGADT7 vectors grown on SD-Leu plate, or yeast strains containing pAS2/pGBKT7 vectors grown on SD-Trp plates, the corresponding SD medium was used. The cultures were harvested in a sterile 50ml falcon tube and centrifuged at 3000 x g for 5 min the cells were resuspended in 25 ml of sterile water and centrifuged again. Cells were suspended in 1ml of 100 mM LiAc and transferred to an eppendorf tube, centrifuged again and resuspended to a final volume of 500 µl with 100 mM LiAc and vortexed to mix well. The cells were pelleted and LiAc was removed. The transformation mix was added, vortexed for 1 min and incubated at 30 °C for 30 min. A heat shock at 42 °C for 15 min was performed. Centrifugation was at 8000 rpm for 1 min to remove the liquid. The cells were resuspended in 1ml of sterile water and plated on the desired omission plates and incubated for 2-5 days to recover transformants.

Transformation mix:

45 % PEG 9.0 ml
1M LiOac 1.0 ml
2mg/ml SS-DNA
0.1-1 µg plasmid DNA
1M Tri-Cl (pH 7.5) 100 µl
0,5M EDTA 20 µl

4.2 DNA Isolation from yeast:

Hoffman’s method (Hoffmann and Winston, 1987) was used for the isolation of plasmid DNA from yeast with little modifications. A saturated yeast culture was prepared by inoculating up to 2-3 medium sized colonies (3 mm in diameter) into YEPD or selective medium. Cells were pelleted from a 5.0 ml culture by centrifuging at 4,000 rpm for 5 min. The pellet was resuspended in 200 µl STET buffer by vortexing briefly and cells were placed into a 1.5 ml tube. About 100 mg 0.45 mm glass

beads were added to the cells and vortexed for 5 min. Then the tube was incubated at 100 °C in a heating block for 3 min, cooled briefly on ice and centrifuged at 13,000 rpm for 10 min at 4 °C. 100 µl supernatant was transferred into a fresh tube. To this 500 µl of 7.5 M ammonium acetate was added and mixed by inverting the tube. The mixture was then incubated at –20 °C for 1 h, centrifuged at 13,000 rpm for 10 min at 4 °C. 100 µl supernatant was transferred to a fresh tube containing 200 µl of 96% cold ethanol, mixed well and allowed to stand at room temperature for 5 min followed by centrifugation at 13,000 rpm for 10 min at room temperature. The supernatant was discarded and the pellet was washed with 70% ethanol. Ethanol was removed carefully without disturbing the pellet. The pellet was air dried and resuspended in 20 µl of TE buffer, 10 µl of which was used for transformation of bacteria.

STET buffer :

7.5M ammonium acetate

8% sucrose in 50 mM Tris/HCl, pH 8.0, 28.9 g/50 ml

5 % TritonX-100

50 mM EDTA

4.3 β-galactosidase colony lift assay

Yeast colonies were assayed qualitatively for blue/white selection according to the method described by Schneider *et al.* 1996. Colonies on transformation plates were grown at 30 °C for 2-4 days on (SD/-Trp, -Leu) or (SD/-Trp, -Leu, -His +3AT) agar plates. Few colonies from these plates were streaked on an appropriate master replica plate and grown for 1-2 additional days. A clean dry nitrocellulose filter was kept on the surface of the plate containing colonies to be assayed. The filter was marked for orientation by punching holes asymmetrically through the filter into the agar. The filter was lifted carefully and transferred to liquid nitrogen using forceps and completely submerged for 10 sec keeping the colony side up. The completely frozen filter was removed and allowed to thaw at room temperature and carefully placed on sterile filters pre-soaked in Z-buffer X-gal solution facing the colony side up without trapping air bubbles under or between the filters. The filters were incubated at room temperature or at 30 °C and checked periodically for the appearance of blue color. A corresponding blue colony was selected and picked from the plate.

Z-Buffer, pH 7,0: Z-Buffer/X-gal-Solution:

10,69 g (0,04 mol) Na₂HPO₄ x 7 H₂O 100 ml Z-Buffer, pH 7,0

5,5 g (0,04 mol) NaH₂PO₄ x H₂O 0,27 ml 14,4 M beta-Mercaptoethanol

0,75 g (0,01 mol) KCl 1,67 ml X-gal-solution (20 mg/ml DMF)

0,246 g (0,01 mol) MgSO₄ x 7 H₂O

adjusted volume to 1l with distilled water

4.4 Yeast Strain Maintenance

Yeast grown to saturation in shaking culture in the corresponding medium was mixed with glycerol to the final concentration of 25 % and stored at -70°C . Alternatively, an isolated colony was picked from the plate by using a sterile loop and thoroughly resuspended in 200-500 μl of YEPD medium (or appropriate SD dropout medium.). Sterile glycerol was added to a final concentration of 25 %, mixed thoroughly and immediately stored at -70°C .

5.0 Biochemical methods

5.1 Preparation of total protein from *Dictyostelium*

1×10^7 to 5×10^8 *Dictyostelium* cells obtained from growth as well as different stages of development were washed once in Soerensen phosphate buffer. Total protein was prepared by lysing the pellet of cells in 500 μl 1x SDS sample buffer. For detection of the protein expression in different cell lines, equal amount of protein (equivalent to 2×10^5 cells/lane to 1×10^7 cells/lane) was loaded onto discontinuous SDS-polyacrylamide gels.

5.2 Isolation of phagosomes

Phagosomes from AX2 cells were prepared as described (Maniak *et al.*, 1995) with some modifications. Cells were washed twice in Soerensen phosphate buffer, resuspended at 4×10^6 cells/ml in nutrient medium and allowed to recover for 30 minutes at 21°C . Carboxylated para magnetic beads of 1-2 μm in diameter (Polysciences Europe GmbH, Eppelheim, FRG) were added in a ratio of 100 beads per cell. The suspension was shaken for 10 minutes and phagocytosis was stopped by centrifugation at $720 \times g$ at 4°C and by washing three times with ice-cold Soerensen phosphate buffer. The pellet was resuspended to a cell density of 5×10^7 /ml in homogenization buffer. Cells were opened by three cycles of freezing in liquid nitrogen and thawing on ice. Phagosomes were separated from the lysate by magnetic extraction and washed three times in homogenization buffer. For determination of the protein content, phagosomes were lysed at 95°C for 5 minutes in lysis buffer and the beads were removed by centrifugation. 2X SDS sample buffer was added prior to SDS-PAGE and immunoblotting.

Homogenisation buffer / Lysis buffer:

30 mM Tris-HCl, pH 8.0 / 20 mM Tris-HCl, pH 8.0

30 % sucrose / 0.1 % SDS

3 mM DTT / 1 mM DTT

3 mM benzamidine / 10 mM EDTA

0.5 mM PMSF / 0.5 mM PMSF

5.3 Cell fractionation studies to determine the subcellular localization of CAP

Dictyostelium cells were collected by centrifugation (1000 x g for 5 min), washed twice with Soerenson phosphate buffer and resuspended in homogenization buffer supplemented with a protease inhibitor mixture. Cells were lysed on ice using a sonicator, and light microscopy was performed to ensure that the majority of the cells were broken. The membrane and cytosol fractions were separated by centrifugation (100,000 x g for 1hr), to detect the presence of CAP in these fractions. The fractionation studies were done repeatedly. 9×10^8 cells of AX2 wild type cells and AX2 transformants stably expressing the GFP-CAP fusion were lysed with the homogenisation buffer and were sonicated for complete lysis. The supernatant fraction was separated and the pellet was washed twice by centrifugation (100,000 x g for 15 min) resuspended in 1 ml of homogenisation buffer and finally 100 μ l of supernatant and pellet fractions were suspended in 2X SDS sample buffer (Laemmli, 1970) and resolved on 12 % SDS-PAGE gels.

5.4 Immunoprecipitation from *Dictyostelium* cell lysate

Dictyostelium cells grown axenially were harvested and washed twice with Soerensen phosphate buffer and resuspended in immunoprecipitation (IP) buffer. The volume of the buffer depended on the obtained amount of cells (for 1g of the cell pellet 2 ml of the buffer was used) that is the cells were suspended in twice the volume of the IP buffer. The cells were then opened by sonication. The complete lysis of the cell was confirmed by visual inspection of a drop of lysate under the light microscope. The cell lysate prior to immunoprecipitation was pre-cleared with Protein A sepharose beads for 30 min and the cell debris and proteins non specifically bound to the beads were removed by centrifugation (2,000 x g for 3 min, at 4 °C). 600 μ l of cleared supernatent were incubated with 100-800 μ l of GFP mAb, 325 μ l of immunoprecipitation buffer, 0.1 % Triton X-100/NP-40 and protein A sepharose beads at 4 °C for 3 h to complete the immunoprecipitation. After incubation the samples were centrifuged for 3 min at 2,000-x g and the beads were washed several times in the IP buffer. Washed beads were then incubated with 2X SDS-sample buffer for 5 min at 95 °C. The released proteins were resolved on 10-15 % SDS-PAGE gels. The size fractioned proteins were stained with comassie blue or silver staining. The bands appearing in AX2 cells expressing GFP-CAP or CAP bsr expressing GFP-CAP or its domains with or without proline rich regions cells in comparison to AX2 and CAP bsr were analysed by MALDI-MS.

Immunoprecipitation buffer:

0.33 x PBS, pH 7.4
2 mM benzamidine
4 mM DTT

2mM EDTA
 0.5 mM PMSF
 (Triton X-100 was added after the sonication to a final concentration of 0.5 %)

5.5 SDS-polyacrylamide gel electrophoresis

SDS-polyacrylamide gel electrophoresis was performed using the discontinuous buffer system of Laemmli (1970). Discontinuous polyacrylamide gels (10-15 % resolving gel, 5 % stacking gel) were prepared using glass-plates of 10 cm x 7.5 cm dimensions and spacers of 0.5 cm thickness. A 12-well comb was generally used for formation of the wells in the stacking gel. The composition of 12 resolving and 12 stacking gels is given in the table below:

Components	Resolving gel			Stacking gel
	10 %	12 %	15 %	5%
Acrylamide/Bisacrylamide (30:0.8) [ml]:	19.7	23.6	30	4.08
1.5 M Tris/HCl, pH 8.8 [ml]:	16	16	16	-
0.5 M Tris/HCl, pH 6.8 [ml]:	-	-	-	2.4
10 % SDS [μ l]:	590	590	590	240
TEMED [μ l]:	23	23	23	20
10 % APS [μ l]:	240	240	240	360
Deionised H ₂ O [ml]:	23.5	19.6	13.2	17.16

Samples were mixed with suitable volumes of 2x SDS sample buffer, whereas protein pellets were resuspended in a suitable volume of 1x SDS sample buffer. The samples were denatured by heating at 95°C for 5 min and loaded into the wells in the stacking gel. A molecular weight marker, which was run simultaneously on the same gel in an adjacent well, was used as a standard to establish the apparent molecular weights of proteins resolved on SDS-polyacrylamide gels. The molecular weight markers were prepared according to the manufacturer's specifications. After loading the samples onto the gel, electrophoresis was performed in 1x gel-running buffer at a constant voltage of 100-150 V until the bromophenol blue dye front had reached the bottom edge of the gel or had just run out of the gel. After the electrophoresis, the resolved proteins in the gel were either observed by Coomassie blue staining or transferred onto a nitrocellulose membrane.

SDS-sample buffer:

<u>1x</u>	<u>2x</u>	
50	100	(mM) Tris/HCl, pH 6.8
2	4	(% v/v) SDS
10	20	(% v/v) glycerine
0.1	0.2	(% v/v) bromophenol blue
2	4	(% v/v) β -mercaptoethanol

10x Gel-running buffer:

1.9 M glycine
0.25 M Tris/HCl, pH 8.8
1 % SDS

Molecular weight markers:

LMW-Marker (Pharmacia)-
94, 67, 43, 30, 20.1, 14.4 kD

Pre-stained marker (Bio-Rad)-
208, 115, 79.5, 49.5, 34.8, 28.3, 20.4, 7.2 kD

5.5.1 Coomassie blue staining of SDS-polyacrylamide gels

After electrophoresis, the resolved proteins were visualised by staining the gel with Coomassie blue staining solution. The gel to be stained was placed in the Coomassie blue staining solution immediately after electrophoresis and the gel was allowed to stain at room temperature with gentle agitation for at least 30 min. After staining, the staining solution was poured off and destaining solution was added. The gel was then destained at room temperature with gentle agitation. For best results, the destaining solution was changed with fresh destaining solution several times until protein bands were clearly visible.

Coomassie blue staining solution:

0.1 % Coomassie blue R250
50 % ethanol
10 % acetic acid
filter the solution before use

Destaining solution:

7 % acetic acid
20 % ethanol

5.5.2 Silver staining of polyacrylamide gels

Size fractionated proteins on polyacrylamide gels were fixed with 30 % ethanol-10% acetic acid solution for one hour. The gel was rinsed with 20% ethanol before sensitizing with 0.02 % sodium thiosulphate for 1 min. After three washings (20 sec each) with MilliQ water, the gel was stained with a 0.2 % silver nitrate solution for 45 minutes. The excess of silver nitrate was removed by washing of the gel three times with MilliQ water. The protein bands were developed with developer solution until they were suitably visible. The reaction was stopped by soaking the gel in stop solution for 5 min.

Developer: 0.3 % Sodium carbonate

Stop solution: 50 g Tris base, 0.025 % Formaldehyde, 25 ml glacial acetic acid, 10 mg/ml sodium thiosulphate, water to 1000 ml.

5.5.3 Drying of SDS-polyacrylamide gels

After destaining, the gel was immersed in gel-dry buffer for 10-15 min at room temperature. Two sheets of cellophane (Novex), slightly bigger than the size of the gel, were also immersed in gel-dry buffer. The gel was then carefully placed between two moistened sheets of cellophane avoiding

trapping of air-bubbles, clamped between the gel-drying frames (Novex) and dried overnight at room temperature.

Gel-drying buffer:

25 % ethanol
5 % glycerine

5.6 Western blotting using the semi-dry method

The proteins resolved by SDS-polyacrylamide gel electrophoresis (SDS-PAGE) were electrophoretically transferred from the gel to a nitrocellulose membrane by using the method described by Towbin *et al.* (1979) with little modifications. The transfer was performed using Towbin's buffer in a semi-dry blot apparatus (Bio-Rad) at a constant voltage of 10 V for 35-45 min. The instructions provided along with the semi-dry apparatus were followed in order to set up the transfer.

Towbin's buffer (transfer buffer):

39 mM glycine
48 mM Tris/HCl, pH 8.3
0.0375 % SDS
20 % methanol or ethanol

5.6.1 Ponceau S staining of western blots

To check for the transfer of proteins onto the nitrocellulose membrane, the membrane was stained in 10-15 ml of Ponceau S solution for 2-5 min at room temperature. After staining, the membrane was removed from the Ponceau S solution and rinsed with deionised water to destain until bands of proteins were visible and the background was clear. The position of the constituent proteins of the molecular weight marker and/or the protein of interest was marked and the membrane was again washed with several changes of deionised water to completely remove the stain. Now the membrane carrying the transferred proteins was used for immunodetection (see Materials & Methods, 5.7) of specific proteins.

Ponceau S solution:

1 ml Ponceau S concentrate (Sigma)
19 ml distilled H₂O

Ponceau S concentrate (Sigma):

2 % w/v Ponceau S in 30 % w/v TCA
and 30 % w/v sulfosalicylic acid

5.7 Immunodetection of membrane-bound proteins

The western blot was immersed in blocking buffer (1x NCP) and the blocking was performed with gentle agitation either overnight at room temperature or for 2-3 h at room temperature with several changes of 1x NCP. After blocking, the blot was incubated at room temperature with gentle agitation

with either commercially available primary antibodies at a proper dilution (in 1x NCP) for 1-2 h, or hybridoma-supernatant for overnight. After incubation with primary antibody, the blot was washed 5-6 times with 1x NCP at room temperature for 5 min each with repeated agitation. Following washings, the blot was incubated for 1 h at room temperature with a proper dilution (in 1x NCP) of enzyme conjugated secondary antibody directed against the primary antibody. The secondary antibody was conjugated with either Horseradish peroxidase (HRP) or alkaline phosphatase (AP). After incubation with secondary antibody, the blot was washed as described above. After washings, substrate reaction was carried out depending upon the enzyme coupled to the secondary antibody. An enzymatic chemi-luminescence (ECL) detection system (see Materials & Methods 5.7.1) was used for blots incubated with HRP-conjugated secondary antibody.

5.7.1 Enzymatic chemi-luminescence (ECL) detection system

The blot was incubated in ECL-detection-solution for 1-2 min and then wrapped in a saran wrap after removing the excess ECL-detection-solution. Now an X-ray film was exposed to the wrapped membrane for 1-30 min and the film was developed to observe the immunolabelled protein.

ECL-detection-solution:

2 ml 1 M Tris/HCl, pH 8.0
200 μ l 250 mM 3-aminonaphthylhydrazide in DMSO
89 μ l 90 mM p-Coumaric acid in DMSO
18 ml deionised H₂O
6.1 μ l 30 % H₂O₂ (added just before using)

5.8 Expression and purification of GST- fusion protein of sGC, ARPE, and V-ATPases d subunit

E.coli strain DH5 α cells were transformed with expression vector pGEX-sGC, VD and AD for expression of glutathione S-transferase (GST)-fusion proteins under the control of lac promoter.

5.8.1 Small-scale protein expression

Small-scale expression of GST-sGC, AD, and VD fusion protein was performed to check the efficiency of expression of various recombinant clones as well as to standardise the conditions of expression before proceeding for the large-scale expression and purification of the above GST fusion proteins. Single colonies of recombinant cells were picked and grown overnight in 10 ml of LB medium containing ampicillin (100 μ g/ml) at 37°C or room temperature and 250 rpm. 5 ml of the overnight grown culture was inoculated into 45 ml of fresh LB medium containing ampicillin. The

culture was then allowed to grow at 37°C till an OD₆₀₀ of 0.5-0.6 was obtained. Now the induction of expression was initiated by adding IPTG. In order to standardise the conditions of maximum expression of the fusion protein, induction was performed with varying concentrations of IPTG (0.1 mM, 0.5 mM and 1.0 mM final concentration) at two different temperature conditions (22°C and 37°C). Samples of 1 ml were withdrawn at different times after induction (0 h, 2 h, 4 h and overnight) the cells were pelleted and resuspended in 100 µl of 1x SDS sample buffer. The samples were denatured at 95 °C for 5 min and 10 µl of each sample were checked on a 10% SDS-polyacrylamide gel. Expression of the GST fusion proteins was analysed by Coomassie staining of the SDS-polyacrylamide gel as well as by western blotting using anti-GST antibody. The standardised small-scale expressions will be preceded for the large-scale expression and purifications and further followed by GST pull down assays.

6.0 Immunological methods

6.1 Indirect immunofluorescence of *Dictyostelium* cells

6.1.1 Preparation of *Dictyostelium* cells

Dictyostelium cells were grown in shaking culture to a density of 2-4 x 10⁶ cells/ml. The desired amount of cells were collected in a centrifuge tube, washed once with Soerensen phosphate buffer and finally resuspended in Soerensen phosphate buffer at 1 x 10⁶ cells/ml. 400 µl of the cell suspension was then pipetted onto a 18 mm acid-washed glass coverslip lying on a parafilm-covered glass-plate resting in a dark humid-box. Cells were allowed to attach to the glass coverslip for 15 min. Thereafter, cells attached onto the coverslip were fixed immediately by one of the fixation techniques described below that work well for preserving cytoskeletal elements in *Dictyostelium*.

6.1.2 Methanol fixation

After the cells have attached to the coverslip, the supernatant was aspirated and the coverslip was dipped instantaneously into the pre-chilled (-20°C) methanol in a petri dish and incubated at -20°C for 10 min. The coverslip was then taken out from methanol and placed on the parafilm covered glass plate resting in a humid-box with the cell-surface facing upwards, followed by 3 washings (each with 500 µl of PBG, pH 7.4, for 5 min at room temperature) and immunolabelling as described in Materials and Methods (6.3.2).

PBG (pH 7.4):

0.5 % bovine serum albumin

0.1 % gelatin (cold-water fish skin) in 1x PBS, pH 7.4

6.1.3 Picric acid-paraformaldehyde fixation

After the cells have attached to the glass coverslips, the supernatant was gently aspirated from the edge of the coverslip and 200 μ l of freshly prepared picric acid-paraformaldehyde solution was directly added onto the cell-surface of the coverslip and incubated at room temperature for 30 min. After incubation, the picric acid-paraformaldehyde solution was aspirated and the coverslip was then picked up with a fine forceps and swirled in 10 mM PIPES buffer, pH 6.0, followed by blotting off the excess solution from the coverslip with a tissue paper. Now the coverslip was swirled in PBS/glycine and placed in a moist chamber with the cell-surface facing upwards. The coverslip was then washed with 500 μ l PBS/ glycine for 5 min to block free reactive groups followed by post-fixation with 500 μ l of 70% ethanol for 10 min. This was followed by 2 washings with 500 μ l PBS/glycine for 5 min each followed by 2 washings with 500 μ l of PBG for 15 min each. After washings, the cells were immunolabelled as discussed in Materials and Methods (6.3.2).

Picric acid-paraformaldehyde solution:

0.4 g paraformaldehyde was dissolved in 5 ml ddH₂O by stirring at 40°C and adding 3-4 drops of 2M NaOH. After dissolving, the volume was adjusted to 7 ml with ddH₂O. To this paraformaldehyde solution, 10 ml of 20 mM PIPES buffer, pH 6.0, and 3 ml of saturated picric acid was added and the pH was finally adjusted to 6.5.

PBS/glycine:

500 ml PBS
3.75 g glycine
filter sterilized
store at -20°C

20 mM PIPES buffer, pH 6.0:

0.605 g PIPES
in 100 ml distilled H₂O
adjust to pH 6.0
filter sterilized

6.2 Immunolabelling of fixed cells

Coverslips containing the fixed cells were incubated with 300 μ l of the desired dilution (in PBG) of primary antibody for 1-2 h in the humid-box at room temperature or overnight at 4 °C. After incubation, the excess unattached antibody was removed by washing the coverslip 6 times with PBG for 5 min each. Now the coverslip was incubated for 1 h with 300 μ l of a proper dilution (in PBG) of Cy3-conjugated secondary antibody. Following this incubation, two washings with PBG for 5 min each followed by three washings with PBS for 5 min each were performed. After washings, the coverslip was mounted onto a glass slide (see Materials and Methods, 6.3.3.).

6.2.1 Mounting of coverslips

After immunolabelling of the fixed cells, the coverslip was swirled once in deionised water and the extra water was soaked off on a soft tissue paper. Now a drop of gelvatol was placed to the middle of a clean glass slide and the coverslip was mounted (with the cell-surface facing downwards) onto the drop of gelvatol taking care not to trap any air-bubble between the coverslip and the glass slide. Mounted slides were then stored in the dark at 4°C for overnight. Thereafter, the mounted slides were observed under a fluorescence microscope or confocal laser-scanning microscope.

Gelvatol:

2.4 g of polyvinyl alcohol (Mw 30,000-70,000; Sigma) was added to 6 g of glycerol in a 50 ml centrifuge tube and mixed by stirring. To the mixture, 6 ml of distilled H₂O was added and the mixture was incubated at room temperature. After several hours of incubation at room temperature, 12 ml of 0.2 M Tris/HCl, pH 8.5, was added and the mixture was heated to 50°C for 10 min with occasional mixing to completely dissolve polyvinyl alcohol. The solution was centrifuged at 5,100 rpm for 15 min. After centrifugation, 2.5 % of diazobicyclo octane (DABCO), an anti-oxidant agent, was added to reduce the bleaching of the fluorescence. The solution was aliquoted in small volumes in 1.5 ml microcentrifuge tubes and stored at -20°C.

6.3 Phalloidin staining of fixed cells

Phalloidin staining of *Dictyostelium* F-actin was performed as follows. Cells were harvested and the coverslips coated with cells were prepared as explained in Materials and Methods (6.3.1.). Cells were then fixed onto the coverslip by the picric acid-paraformaldehyde fixation method as discussed in Materials and Methods (6.3.1.2). After fixation and usual washings, coverslips were incubated for 30 min with 300 µl of PBG TRITC-phalloidin (1:200 dilution). Thereafter, the coverslips were washed twice with 300 µl of PBG for 5 min each followed by three washings with 300 µl of PBS for 5 min each. After the washing steps the coverslips were mounted onto glass slides (see Materials and Methods, 6.3.3) for observation under a fluorescence microscope or capturing images in the confocal laser-scanning microscope.

6.4 Immunolabelling of *Dictyostelium* cells expressing GFP-CAP and its domains during phagocytosis and pinocytosis

To correlate the localization of GFP-CAP and its domains in the various signalling mutants with the organization of the actin cytoskeleton during the process of phagocytosis, cells expressing GFP-

fusions of CAP and its domains were fixed during phagocytosis and pinocytosis and immunolabelled with CAP monoclonal antibody 230-18-8. Briefly, cells were prepared as above, and, after the cells had adhered to the glass coverslip, the Soerensen phosphate buffer on the coverslip was replaced with 300 μ l of the solution containing heat-killed unlabelled yeast cells diluted 1:10 in Soerensen phosphate buffer or with TRITC-dextran for pinocytosis. Cells were incubated with yeast or TRITC dextran for different time intervals (5 min, 10 min, 15 min and 20 min). Thereafter, the solution on the coverslips was carefully aspirated and the cells were immediately fixed onto the coverslip by methanol fixation method (see Materials and Methods, 6.3.1.1) in case of phagocytosis or with picric acid-paraformaldehyde fixing (see Materials and Methods, 6.3.1.2) for pinocytosis. After fixation and usual washings, the coverslip was first immunolabelled with mAb 230-18-8 for CAP detection followed by Cy3 conjugated secondary antibody as described above and mounted onto a glass slide (see Materials and Methods 6.3.2 and 6.3.3). The images were obtained using a Leica confocal microscope.

Preparation of heat-killed yeast cells:

Five grams of dry yeast *Saccharomyces cerevisiae* (Sigma) were suspended in 50 ml of PBS in a 100 ml Erlenmeyer flask and incubated for 30 min in a boiling waterbath with stirring. After boiling, the yeast cells were washed five times with PBS, followed by two washings with Soerensen phosphate buffer. The yeast cells were then finally resuspended in Soerensen phosphate buffer at a concentration of 1×10^9 yeast cells/ml. Aliquots of 1 ml and 20 ml were made and stored at -20°C .

Heat-killed, TRITC-labelled yeast cells :

For labelling, the pellet of 2×10^{10} heat-killed unlabelled yeast cells (Materials and Methods, 5.4.) was resuspended in 20 ml of 50 mM Na_2HPO_4 , pH 9.2, containing 2 mg of TRITC (Sigma) and incubated for 30 min at 37°C on a rotary shaker. After washing twice with 50 mM Na_2HPO_4 , pH 9.2, and four times with Soerensen phosphate buffer, aliquots of 1×10^9 yeast cells/ml were frozen at -20°C .

7.0 Microscopy

Visual inspection of *Dictyostelium* cells expressing CAP-GFP fusion protein was performed using an inverted fluorescence microscope (Olympus IX70). For studying the localization of GFP-CAP fusion protein in live cells during cell locomotion, phagocytosis and endocytosis, an inverted confocal laser scanning microscope (Leica DM/IRBE) equipped with a 40x PL Fluotar 1.25 oil immersion objective

or a 63x PL Fluotar 1.32 oil immersion objective was used. The 488-nm band of an argon-ion laser was used for excitation, and a 510-525-nm band-pass filter was used for emission. Confocal images of immunolabelled specimens were obtained with a confocal laser-scanning microscope (Leica TCS-SP) equipped with a 63x PL Fluotar 1.32 oil immersion objective. A 488-nm argon-ion laser for excitation of GFP fluorescence and a 568-nm krypton-ion laser for excitation of Cy3 or TRITC fluorescence were used. For simultaneous acquisition of GFP and Cy3 fluorescence, the green and red contributions to the emission signal were acquired separately using the appropriate wavelength settings for each photomultiplier. The images from the green and red channels were independently attributed with colour codes and then superimposed using the accompanying software.

7.1 Live cell imaging of GFP-CAP expressing *Dictyostelium* cells

To record the distribution of GFP-CAP in live dynamics, GFP-CAP expressing cells were grown to a density of $2\text{-}3 \times 10^6$ cells/ml and washed in Soerensen phosphate buffer and resuspended at a density of 1×10^7 cells/ml. The cells were then starved for about 1 h with shaking. Starvation facilitated observation as it allowed the cells to digest endocytosed nutrient medium, which is autofluorescent. For observation, cells were initially diluted in Soerensen phosphate buffer at 1×10^6 cells/ml and then 500 μ l of the cell suspension (5×10^5 cells) were transferred onto a 18 mm glass coverslip glued to a plastic rim of the same size. Cells were allowed to adhere to the glass coverslip for 10-15 min and confocal images were obtained and processed as described above.

7.2 Imaging the distribution and live dynamics of GFP-CAP during pinocytosis

For analysis of the dynamics of GFP-CAP during fluid phase endocytosis, coverslips containing GFP-CAP expressing cells were prepared as described. After the cells had attached to the glass coverslip, the buffer was carefully aspirated and was replaced with Soerensen phosphate buffer containing 1 mg/ml TRITC-dextran (Mw 70,000; Sigma). Confocal sections were obtained by scanning at different intervals in one plane using a 488-nm argon-ion laser for GFP fluorescence and a 568-nm krypton-ion laser for TRITC fluorescence. Details of imaging and image processing have been discussed.

7.3 Imaging distribution of GFP-CAP during phagocytosis

For analysis of the dynamics of GFP-CAP during phagocytosis, coverslips containing GFP-CAP expressing cells were prepared. After the cells had adhered to the glass coverslips, 5-10 μ l of the heat-

killed, TRITC-labelled yeast cells (1×10^9 yeast cells/ml) was carefully added from one edge of the coverslip. Immediately after the yeast cells had settled (in 2-5 min), confocal images were obtained.

7.4 Imaging the distribution and dynamics of GFP-CAP in aggregation-competent cells

GFP-CAP expressing cells grown to a density of $2-3 \times 10^6$ cells/ml were washed twice in an equal volume of Soerensen phosphate buffer and resuspended at a density of 1×10^7 cells/ml. The cells were then starved for 6 h with shaking at 250 rpm in order to make them aggregation-competent. Aggregation-competent cells have a typical elongated shape with a well-defined front and tail. After starvation for 6 h, 50 μ l of the cell-suspension (5×10^5 cells) was transferred onto a 18 mm glass coverslip (glued to a plastic rim of the same size) that had been pre-loaded with 200-300 μ l Soerensen phosphate buffer. Cells were allowed to adhere to the glass coverslip for 10-15 min. After the cells had elongated, a single cAMP pulse (10^{-5} μ M) was given and confocal images were obtained.

7.5 Microscopy of agar plates

Various stages of development of *Dictyostelium* cells were also visualized using the fluorescence microscope (Leica DNR) equipped with a 2.5x or 5.0x objective and images were captured by a cooled CCD camera (SensiCam, PCO). To determine development of *Dictyostelium* on phosphate agar plates an Olympus SZ-4045TR stereomicroscope was used or a Leica MZFIII stereomicroscope. Images were captured with a JAI CV-M10 or Hitachi HV-C20A CCD video camera and for processing images Adobe Photoshop was used.

8.0 Microarray analysis

Array targets: The 34 Mb genome of *Dictyostelium discoideum* carries about 12,000 genes. A collection of a total of 6,000 genes used as the array targets carries partial sequences of 450 known genes (PCR amplified sequences of an average length of 500 bp) and approximately 5,400 non-redundant ESTs from the cDNA project of *Dictyostelium discoideum* (Morio *et al.* 1998) (<http://www.csm.biol.tsukuba.ac.jp/cDNAproject.html>) and appropriate positive (partial genes from *D. discoideum* genomic DNA), negative controls (fish sperm DNA, human Cot-1) and internal controls (Sport report Poly A).

8.1 RNA preparation

Wild-type AX2 and CAP bsr cells grown axenically to $2-3 \times 10^6$ cells/ml were washed twice with Soerensen phosphate buffer and suspended to a final concentration of 1×10^7 cells per ml in

Soerensen phosphate buffer. They were used for extraction of total RNA. The total RNA was extracted from the vegetative cells with the Qiagen RNeasy Midi/Mini Kit according to the “Protocol for Isolation of total RNA from Animal Cells” with the modification of washing the cells twice with water after harvesting to remove medium. After extraction the RNA concentration is determined by measuring the OD₂₆₀ (should be > 500 µg/ml). The quality of RNA was examined on a test gel, which should give two bands of 4.1 and 1.9 kb for rRNA without degradation.

Array	Reaction	CAP-RNA	Conc ⁿ 20 µg	spike	Dye	Reaction	AX2-RNA	spike	Dye	Conc ⁿ 20 µg
12649635	185	Batch I a	10 µl	4A	Cy3	193	Batch I a	4B	Cy5	22.5 µl
12649529	186	Batch I b	11 µl	4A	Cy5	194	Batch I b	4B	Cy3	8.5 µl
12649632	187	Batch II a	11 µl	4A	Cy3	195	Batch II a	4B	Cy5	17 µl
12649533	188	Batch II b	9.5 µl	4A	Cy5	196	Batch II b	4B	Cy3	8.5 µl
12649532	189	Batch III a	8.5 µl	4A	Cy3	197	Batch III a	4B	Cy5	9 µl
12649531	190	Batch III b	11.5 µl	4A	Cy5	198	Batch III b	4B	Cy3	10 µl
12649530	191	Batch IV a	10 µl	4A	Cy3	199	Batch IV a	4B	Cy5	10 µl
12649633	192	Batch IV b	9.5 µl	4A	Cy5	200	Batch IV b	4B	Cy5	14 µl

8.2 Spiking of internal mRNA controls

Quality control is an important issue of DNA microarray analysis. Therefore we used ten internal mRNA controls from *Arabidopsis thaliana* genes that are added (spiked) to the *D. discoideum* RNA prior to cDNA generation and labelling. These mRNAs are provided in a Spikemix with different known amounts of each mRNA. Two different mixes are used for the two labelling reactions (Cy3 and Cy5) of one microarray experiment and the spiking was done as follows. The spiking of the RNA was done by mixing equal quantities of Spikemix and *D. discoideum* total RNA. The RNA mixture was precipitated by adding 0.1 volume of 3 M sodium acetate, pH 4.8, and 2.5 volume of 100 % ethanol and kept at -20 °C for 2 h. The RNA was precipitated by centrifuging in a tabletop centrifuge at 10,000g for 30 min. Ethanol was removed by aspiration and the pellet was washed with 70 % ethanol, centrifuged for 15 min at 10,000g, aspirated and dried. The RNA was dissolved in 12 µl of RNase-free water.

cDNA generation and fluorescent labelling: The reverse transcription of mRNA to cDNA was done with the protocol from the Stratagene Fair Play Kit with some modifications.

8.3 Quantitation, normalization and data analysis

The fluorescently labelled cDNA target bound to the spot was detected with the Scan Array 4000XL confocal laser scanner. The microarray is scanned for Cy3 and Cy5 successively with a resolution of 10µm/pixel. The fluorescent dyes were excited by laser-light of pertinent wavelength and emission was detected by a photo-multiplier. To obtain images well suited for signal quantification, image brightness was adjusted by setting the laser power (photo-multiplier power should always be set at 70 to 80 %). Signals should be as bright as possible, but spots must not be saturated (indicated by white colouring). It might be necessary to scan at two different laser-power settings. One setting where most spots give bright signals, but few of the positive controls are saturated, and another setting where no saturation is seen, but most spots give weak signals.

8.4 Signal Quantification

The spot and background intensities of the scanned images were quantified by using Quant Array. The two images for the Cy3 and Cy5 scan were aligned first and then an array pattern was laid over the images to support spot detection. In this step the spot identities were also assigned. The signal intensities were then measured and written into an export file, which was used for data analysis.

For the detailed procedure please see <http://www.uni-koeln.de/med-fak/biochemie/transcriptomics/>

Results

1.0 Localization and dynamics of CAP in the signalling mutants

Many extracellular signals elicit changes in the actin cytoskeleton, which are mediated through an array of signalling proteins and pathways. This array of signalling pathways leads to the rearrangement of the actin cytoskeleton, which is an important factor for a cell to polarize and migrate. Some of the components which play a characteristic role in this array of signalling pathways are the G-protein coupled cell surface receptors (cAR), heterotrimeric guanine nucleotide G-proteins ($\alpha 2$ and β subunit), adenylyl cyclase (ACA), the regulators of adenylyl cyclase like CRAC and Pianisimo (PIA/HSB1), the HSB1 mutant defective for PIA, ACA and ACR (HSB101), PI3-kinases and cAMP dependent protein kinase A (PKA). As CAP appears to be an important regulator of the actin cytoskeleton and cAMP signalling pathways, the localization of CAP was analysed in mutants affected in these signalling components. CAP (cyclase associated protein) is a PIP₂ regulated G-actin sequestering protein which is present in the cytosol and shows enrichments in plasma membrane near regions (Noegel et al., 1999). The question why the protein is found in the cell cortex near the membrane and which molecules and signals could be responsible for this kind of localization of CAP initiated these studies. The CAP protein possesses no signal sequence or the transmembrane domain nor does it have extended basis regions to show such localization. Hence there could be some molecules, which could be responsible for targeting CAP to the cell cortex for its functioning at the membrane.

1.1 Expression levels of the endogenous CAP in the *aca*⁻, *pia*⁻, HSB101, *g α 2*⁻ and *g β* ⁻, *car1/3*⁻, *pik 1/2*⁻ and *pka*⁻ cells

To understand the role of CAP in the signal transduction mutants, we first, estimated the amounts of endogenous CAP. The protein levels were detected by probing the blot with CAP specific monoclonal antibody 230-18-8 detecting the endogenous protein.

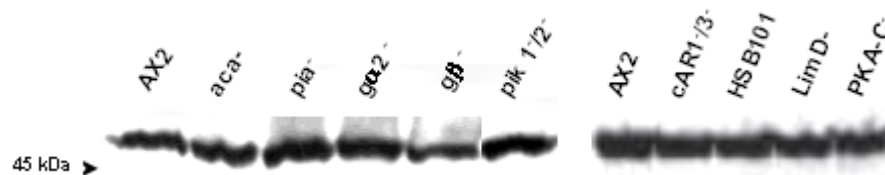


Figure 8: Expression levels of the endogenous CAP protein in mutants affecting the cAMP signalling system. 3×10^5 cells were lysed in the SDS sample buffer and the protein was resolved on SDS PAGE (12% acrylamide), the protein was blotted onto a nitrocellulose membrane using a semi-dry blotter and probed with the mAb 230-18-8, which recognises the endogenous protein (50 kDa). The CAP amounts are unaffected in all mutants.

We found that the expression levels of CAP were unaltered in these mutants and the protein amounts were comparable to the wild type AX2 (Figure 8). For control we tested the amounts of actin (data

not shown). The unaltered protein levels denoted that these signalling molecules do not interfere with the translational regulation of CAP.

1.1.1 Localization of CAP in the signal transduction mutants

The CAP localization studies were carried out using cell biological and biochemical assays in *aca*⁻, *pia*⁻, HSB101, *gα2*⁻ and *gβ*⁻, *car1*^{1/3}⁻, *pik 1*^{1/2}⁻, and *pka*⁻ cells. The distribution of CAP was studied by double immunofluorescence, using CAP specific monoclonal antibody 230-18-8 and an appropriate Cy3 conjugated secondary antibody. The 230-18-8 mAb is specific for the N-terminal domain of CAP, and was used for most of the localization studies of CAP. The cells were analysed in a Leica confocal laser scan microscope.

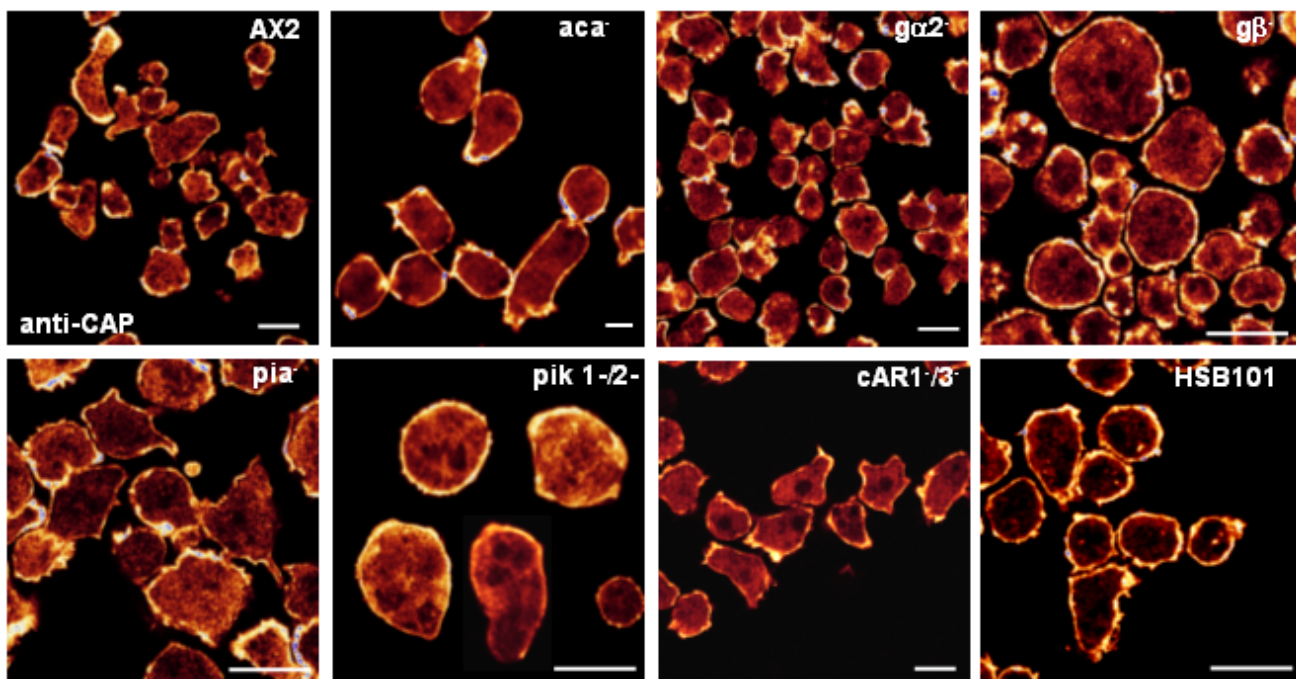


Figure 9: Localization of endogenous CAP in signalling mutants (*t₀* cells). Distribution of endogenous CAP in *aca*⁻, *pia*⁻, HSB101, *gα2*⁻ and *gβ*⁻, *car1*^{1/3}⁻, *pik 1*^{1/2}⁻, and *pka*⁻ cells. CAP was detected using mAb 230-18-8 followed by an appropriate secondary Cy3 coupled antibody. The confocal micrographs show that the protein is present in the cytosol and most prominently close to the membrane and also at the leading fronts. The distribution of CAP seems to be like that in the wild type and is thus unaltered in these mutants. Bar, 10 μm.

In wild type AX2 cells CAP is enriched at the cell cortex and is also found in the cytosol. The *aca*⁻, *pia*⁻, HSB101, *gα2*⁻ and *gβ*⁻, *car1*^{1/3}⁻ cells showed a similar localization of CAP. Overall, the localization of CAP in these signalling mutants, is unaltered as it was similar to the one observed in the wild type AX2. Thus, from these data we conclude that CAP localization in the cell cortex near the plasma membrane is not determined by ACA or its regulator PIA, and neither by signalling molecules further upstream from ACA such as cAR, the cAMP dependent CAR receptor nor the G-proteins and PI3-kinases (Figure 9).

1.1.2 Localization of CAP in *pka*⁻ cells

As upstream components of the cAMP signalling network did not affect CAP localization, we next analysed a downstream effector, the cAMP dependent protein kinase A, PKA, which acts downstream of adenylate cyclase. A wide range of developmental processes in *Dictyostelium* is mediated by PKA as a central component of the cAMP-signalling pathway. Furthermore, PKA plays an essential regulatory role at several stages of development (Mann et al., 1997). Consistent with this it was found that a number of postaggregative genes are not expressed in *pka*⁻ cells, even when they are synergised with wild type cells (Harwood et al., 1992). This holoenzyme in *Dictyostelium* is a heterotetramer comprising of a single regulatory (R) and catalytic (C) subunit, and both proteins increase in concentration during the cellular aggregation. The mutants in the regulatory subunit of the PKA are defective in cAMP binding whereas the cells with an inactive C subunit are defective in cAMP relay, the production of cAMP in response to extracellular cAMP stimulation (Harwood et al., 1992). Since, PKA is a gene required for the proper actin organisation and cell polarity in *Drosophila* (Baum et al., 2000), it was interesting to analyse the localization of CAP in the *pka*⁻ cells. Hence we made use of the *pka*⁻ cells defective in the catalytic domain (PKA-C) and also the *pka*⁻ cells with a mutated regulatory subunit (RM-PKA).

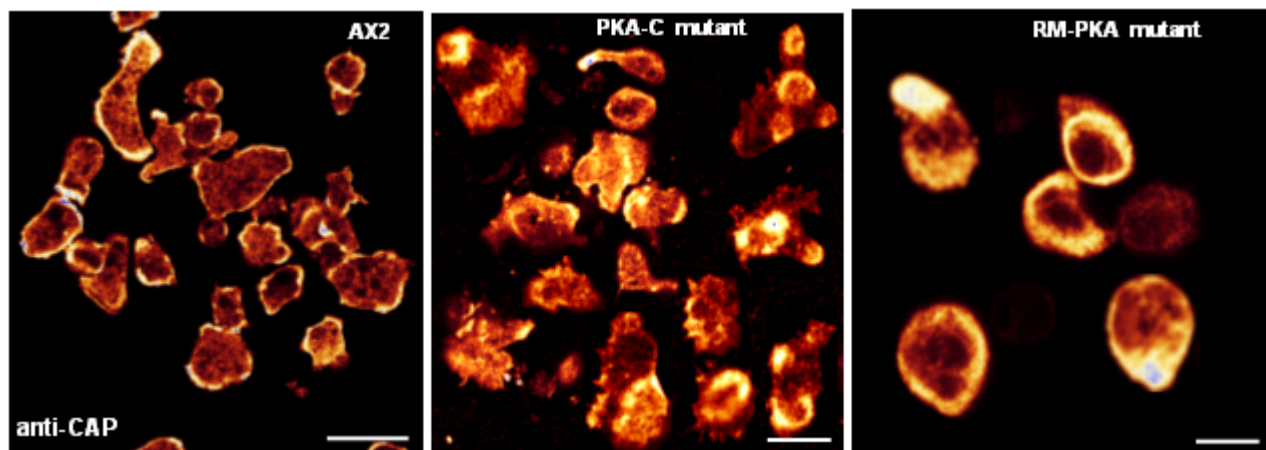


Figure 10: Localization of CAP in the catalytic and regulatory mutants of PKA. The t_0 PKA mutants were immunostained with CAP specific monoclonal antibody followed by staining with Cy3 conjugated goat-anti mouse IgG as the secondary antibody to visualise the endogenous CAP protein. The CAP protein concentrates in circular crowns in the PKA-C mutant, showing an aberrant localization of CAP in comparison to the wild type. The RM-PKA mutants showed an enrichment of CAP in some patches and a thick rim near the cell cortex, suggesting that the localization of CAP is altered and affected in the PKA minus cells and CAP localization seems to be dependent on PKA. Bar, 10 μ m.

It was observed that CAP protein in the PKA-C cells preferentially accumulates in the form of circular rings or crowns in the cytoplasm, where it is very abundant and concentrated in patches and in circular rings near to the cell cortex. These crown structures appeared aberrant and were more numerous in most of the PKA-C cells, indicating that CAP failed to reach the cell cortex as in the wild type AX2 (Figure 10). The distribution of CAP in RM-PKA cells defective in the regulatory

subunit of PKA was more or less comparable to the PKA-C cells, indicating that the localization of CAP is affected by PKA. This distribution of CAP suggests that PKA may be the molecule or may generate the signals for targeting CAP to the cell cortex for its required functioning at the plasma membrane.

The disturbed localization of CAP in pka^- cells was analysed by confocal imaging at different focal planes to visualise the pattern of CAP distribution (Figure 11). The images at the different focal planes were captured at equalised and optimised sections. The CAP protein seems to be abundantly concentrated in the top visible focal plane of the PKA-C cells.

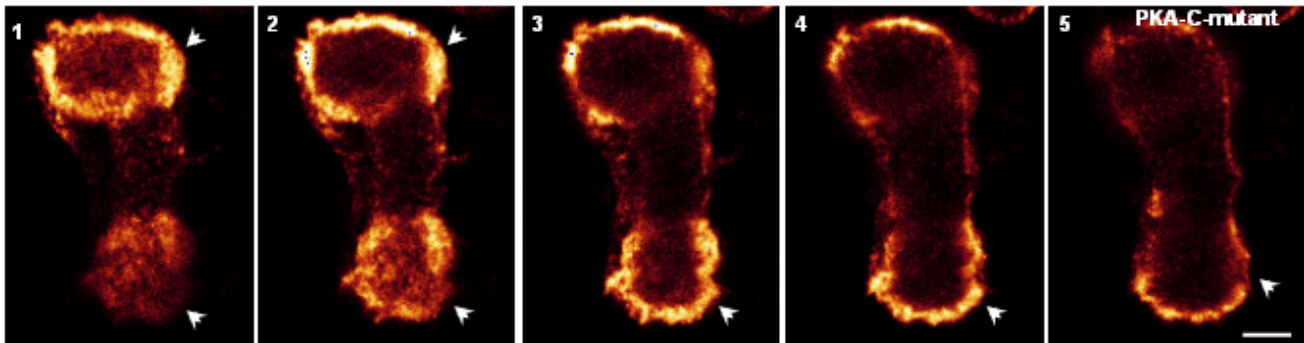


Figure 11: Localization of CAP in the PKA-C mutant at different focal planes. The pka^- cells were fixed with methanol and stained with CAP monoclonal antibody 230-18-8. The cells were visualised with the confocal microscope where the images were taken from the top to the bottom planes at equalised sections to see the protein accumulation at the different focal planes. It was observed that CAP concentrates in circular crowns in PKA-C cells, showing an aberrant localization of CAP seen by the top visible plane. The arrowhead denotes the regions of interest. Bar, 10 μ m.

Based on our previous findings that CAP co-localizes with F-actin, we studied the distribution of actin with the actin specific mAb act 1-7. Similar to CAP the actin distribution was also found to be disturbed. Actin accumulated in concentrated patches in the cytosol and showed an abnormal distribution in comparison to wild type AX2, where actin was primarily found around the cells near the plasma membrane (Figure 12).

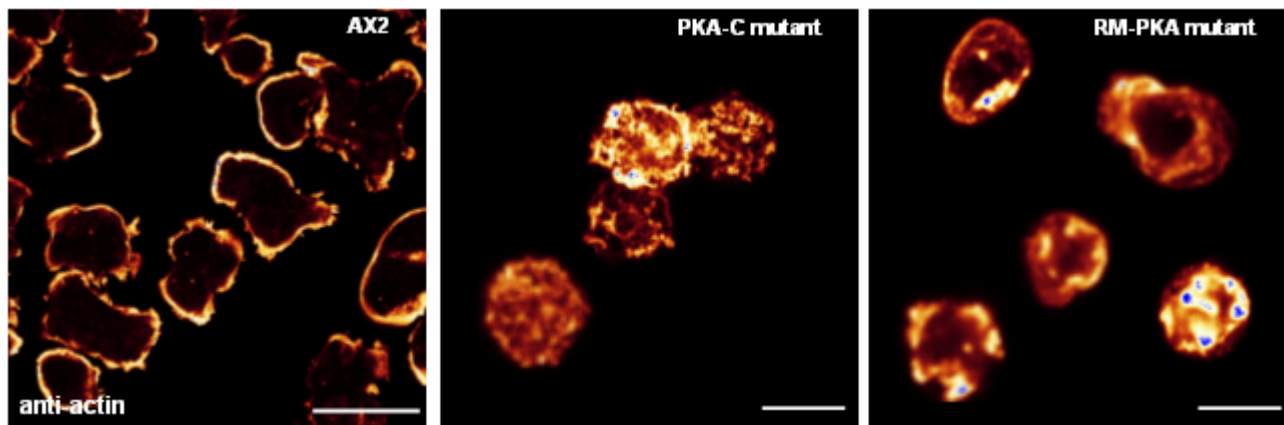


Figure 12: Distribution of actin in the PKA-C and RM-PKA cells. The pka^- cells were immunostained with actin specific mAb Act-1-7 and observed under the confocal microscope. It was seen that actin accumulates richly in the cytosol and concentrates in patches showing a disturbed distribution in the absence of either of the PKA subunits, in AX2 actin staining is primarily at the plasma membrane. Bar, 10 μ m.

1.2 Expression of CAP-GFP fusion protein in the *aca*⁻, *pia*⁻, *gα2*⁻ and *gβ*⁻ and *pik 1/2*⁻ cells

To understand the role of CAP in these signalling mutants we generated GFP fusion proteins of CAP for the *in vivo* studies. The *aca*⁻, *pia*⁻, *gα2*⁻, *gβ*⁻ and *pik1/2*⁻ and AX2 cells were transformed with a vector allowing expression of a full length CAP-GFP fusion protein and stable transformants were obtained which were used for the further analysis. The levels of CAP-GFP in these mutants were detected by western blot analysis using a CAP specific mAb 230-18-8. They were found to be approximately two fold higher in comparison to the endogenous CAP in the mutants and in AX2 (Figure 13a). CAP-GFP was also detected with a GFP specific monoclonal antibody confirming equal levels in comparison to the AX2 cells expressing CAP-GFP (Figure 13b).

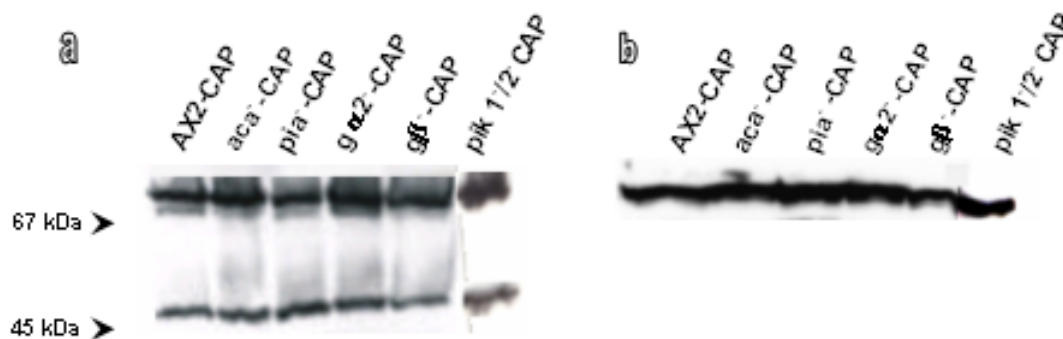


Figure 13: Expression of CAP-GFP and endogenous CAP in *aca*⁻, *pia*⁻, *gα2*⁻, *gβ*⁻ and *pik1/2*⁻ cells. The AX2 cells expressing CAP-GFP fusion protein serve as control. 3×10^5 cells were lysed in SDS sample buffer and the cell homogenates were resolved by SDS-PAGE (12% acrylamide), blotted as before and the blot was labelled with the CAP specific monoclonal antibody 230-18-8 (a) and with the GFP specific monoclonal antibody K3-184-2 (b). The expression of CAP-GFP was found to be two fold more than that of endogenous CAP at 50 kDa (a) in all the mutants.

1.2.1 Localization of CAP-GFP in signalling mutants

To investigate the *in vivo* behaviour of CAP in these mutants an attempt was made to analyse the localization pattern of CAP by using the GFP-tagged version. Stable transformants in the signalling mutants were obtained and were confirmed by visual inspection under a fluorescence microscope. First the wild type and mutants expressing the full length CAP-GFP fusion protein were investigated for the localization of endogenous and CAP-GFP by cell fixation and immunostaining with CAP specific mAb 230-18-8. CAP-GFP localised to the cell borders, where it was enriched, and also to the cytoplasm. The GFP-fusion protein was recognized by the CAP specific monoclonal antibody 230-18-8 and in general a good overlap was observed (Figure 14). The immunoblots were also confirmed by the immunofluorescence studies of CAP-GFP. However, these studies also suggested that localization of endogenous and CAP-GFP is independent of PIA, G-protein ($\alpha 2$ and β subunits), and PI3-kinase in comparison to the AX2 cells expressing CAP-GFP.

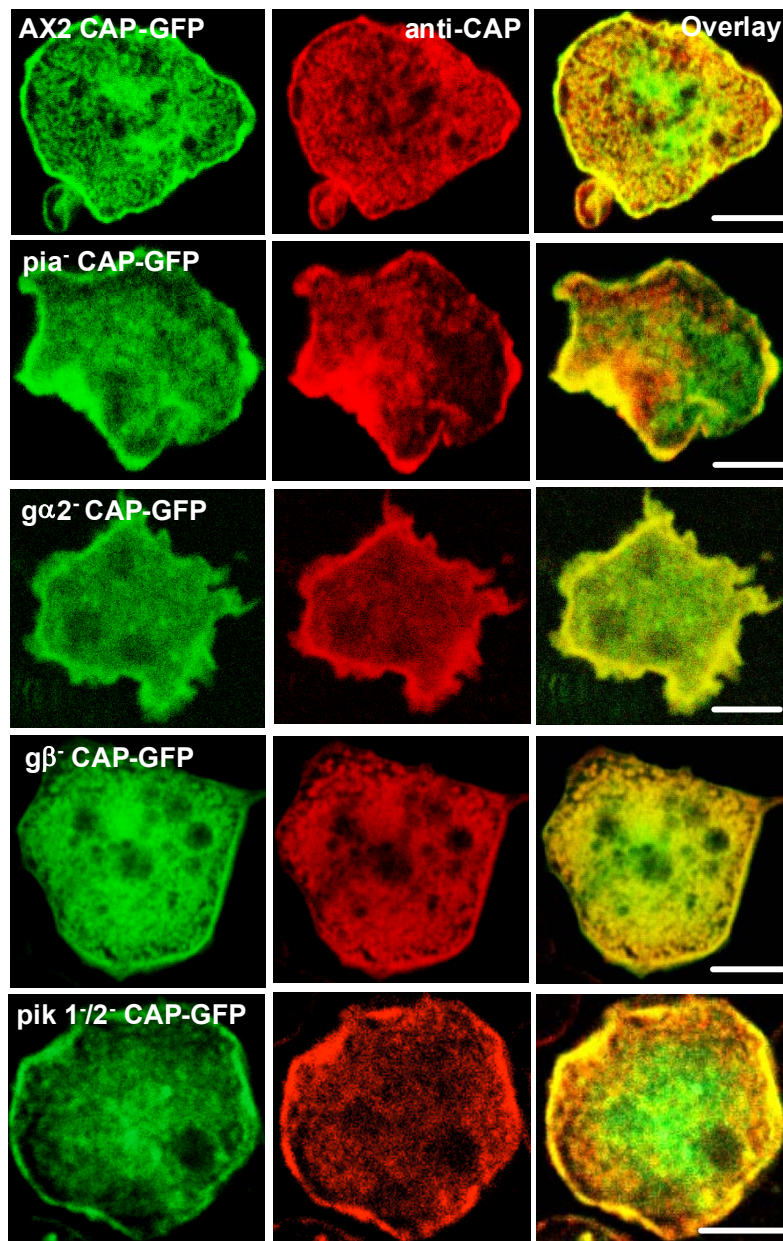


Figure 14: Localization of CAP-GFP in the pia^- , $\text{g}\alpha 2^-$, $\text{g}\beta^-$ and $\text{pik} 1/2^-$. A vector allowing expression of CAP-GFP fusion protein was transformed into these mutants to determine the localization of endogenous CAP and CAP-GFP. The cells were fixed and stained with mAb 230-18-8 to detect the endogenous CAP and CAP-GFP. Both the endogenous and CAP-GFP localise to the cell cortex and also stained the cytosol and the CAP-GFP distribution does not alter the staining of the endogenous CAP. Furthermore, the distribution of CAP-GFP is not affected in the signalling mutants. Bar, 10 μm .

1.3 Re-localization of CAP in aca^- , pia^- , HSB101, $\text{g}\alpha 2^-$, $\text{g}\beta^-$, $\text{cAR} 1/3^-$, $\text{pik} 1/2^-$, and PKA^- during phagocytosis

To study whether the behavior of CAP is affected in the absence of these signalling molecules we analysed events involving the actin cytoskeleton like phagocytosis, pinocytosis and aggregation where the CAP functioning could be dependent on some key regulators, which could be transmitting signals required for a rearrangement of CAP during these actin-dependent processes. Phagocytosis is the engulfment of large particles, including bacteria, yeast and apoptotic cells and is a feature of professional phagocytes, macrophages and neutrophils. The phagocytosis studies were carried out such that the various signalling mutants were incubated with un-labelled yeast cells, fixed and immunolabelled with mAb 230-18-8. The confocal microscopy revealed that CAP accumulates at the

phagocytic cups and phagosomes in the mutants and thus is involved in the process of phagocytosis as in wild type AX2.

The *pik1*^{1/2}⁻ cells are reported to show altered phagocytosis as they were unable to phagocytose autoclaved bacteria and phagocytosis of live bacteria occurred only after a prolonged delay (Zhou et al., 1998). However, the *pik1*^{1/2}⁻ cells did not affect the re-localization of CAP to the phagocytic cups and phagosomes that eventually were formed. AX2 cells expressing dominant negative N17 RacA and HSB101 cells showed a weak staining of CAP at phagocytic cups and phagosomes (Figure 15). Furthermore, the *car1*^{1/3}⁻ and *pka*⁻ cells showed an aberrant accumulation of CAP, where the CAP rich membrane progresses but does not seem to completely surround the yeast particle. There was no CAP seen at the extreme edges and at some regions of the newly forming phagocytic cups as observed for the wild type. Albeit, CAP relocates to the phagocytic cups and phagosomes but the protein seems to fail forming the accumulation in a sharp rim in *car1*^{1/3}⁻ and *pka*⁻ cells in comparison to AX2 (Figure 15). The disturbed localization of CAP in *car1*^{1/3}⁻ could be due to inappropriate signalling at the cell surface. The altered distribution of CAP upon the stimulus in *pka*⁻ could be explained by the requirement of PKA for targeting CAP to the cell cortex.

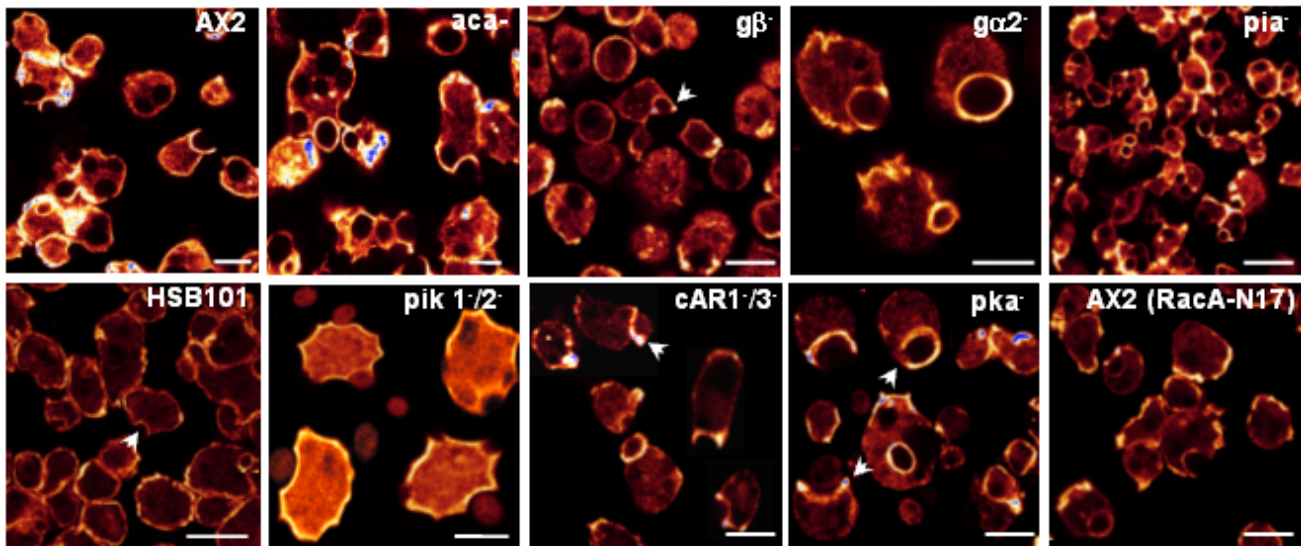


Figure 15: Localization of CAP in signalling mutants during phagocytosis. The cells were allowed to settle with unlabelled yeast cells for 15 minutes, fixed and then labelled with mAb 230-18-8 to detect the localization of the endogenous CAP during this actin driven process of phagocytosis. It was determined that CAP prominently distributes to the phagocytic cups and also the phagosomes. Arrowhead denotes the cells of interest. Bar, 10 μ m.

The *gβ*⁻ cells are impaired in phagocytosis and chemotaxis due to inappropriate regulation of the actin cytoskeleton (Peracino et al., 1998). It was therefore interesting to study the role of CAP during phagocytosis in *gβ*⁻ cells which may give more insight into the role of CAP in the rearrangement of the actin cytoskeleton. The *gβ*⁻ cells were further analysed by immunofluorescence studies with the CAP specific mAb where it was found that most of the cells did not phagocytose, however in a few

cells we observed uptake of particles and found that CAP relocates to the phagocytic cup and phagosomes resembling wild type behaviour (Figure 15). These results indicate that relocalization of CAP is independent of the G β subunit.

1.3.1 Determination of the presence of CAP in phagosomes

To follow the re-localization of CAP to the phagocytic cups and phagosomes also at the biochemical levels we isolated phagosomes (Maniak et al., 1995, with some modifications, Material and methods). The phagosome fractions were then processed to detect CAP. Abundant level of CAP was observed in the phagosome fraction supporting the immunofluorescence studies (Figure 16). For control we tested the distribution of Annexin C1, a protein also found in phagosomes.

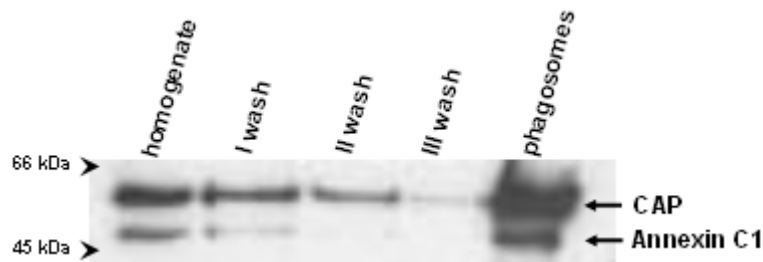


Figure 16: An immunoblot showing the presence of CAP in the phagosomes. 4×10^6 cells/ml were re-suspended in nutrient medium, carboxylated paramagnetic beads of 1-2 μ m diameter were then added in a ratio of 100 beads per cell, phagocytosis was stopped by centrifugation and cells were lysed by subsequent freeze thaw cycles and phagosomes were isolated by magnetic extraction. The phagosome fractions were resolved on SDS-PAGE (12% acrylamide) and immunolabelled with mAb 230-18-8 to show the presence of CAP in homogenates and subsequent washes. Significant amount of CAP was found in the phagosome fractions, Annexin C1 served as control (a kind gift from Marija Marko).

1.3.2 Association of CAP with membrane fractions

The localization studies revealed that CAP localizes to the cell cortex and also stains the cytosol. Hence, an attempt was made to isolate the membrane and cytosol fractions to detect the presence of CAP in these fractions.

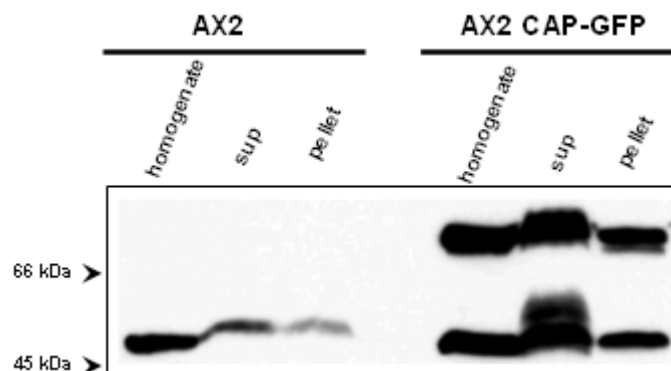


Figure 17: Cell fractionation studies of CAP in AX2 and AX2 cells expressing CAP-GFP. To demonstrate the presence of CAP in membranes, an experiment was designed to isolate the membrane and cytosol fractions. 9×10^8 cells were lysed by sonication, the cells were inspected under a light microscope for complete cell lysis and the lysate was then separated by centrifugation at 100,000 x g for 30 minutes to separate the cytosol from the membrane fraction. The supernatant fraction was collected and the pellet was washed twice with the homogenisation buffer and finally resuspended in the same buffer. The fractions were lysed with 2X sample buffer and resolved on a SDS-PAGE (12%

acrylamide), blotted and probed with mAb 230-18-8 to detect the presence of CAP in the cytosol and membrane fraction of both wild type and wild type expressing the CAP-GFP.

AX2 wild type cells and AX2 transformants stably expressing CAP-GFP fusions were lysed in the homogenisation buffer by sonication and centrifuged to separate the fractions (materials and method). The immunoblot showed that CAP is present at higher amounts in the cytosolic fraction of both AX2 and AX2 CAP-GFP cells. Nevertheless, CAP was also observed in the membrane fraction (Figure 17). These data indicated the association of CAP with membranes and further support the immunofluorescence studies.

1.4 Analysis of CAP and CAP-GFP in the pia^- , $\text{g}\alpha 2^-$, $\text{g}\beta^-$, and $\text{pik } 1/2^-$ cells during phagocytosis

We have made use of mutants expressing CAP-GFP to study the role of CAP during phagocytosis. The mutants expressing CAP-GFP were challenged with labelled or unlabelled yeast cells, fixed and immunostained with mAb 230-18-8.

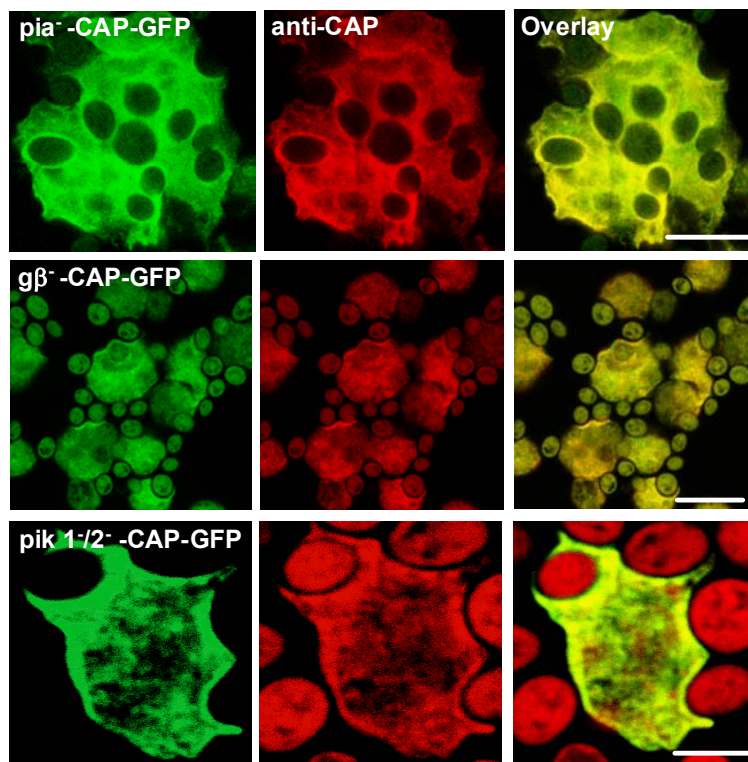


Figure 18: Re-localization of CAP-GFP in pia^- , $\text{g}\beta^-$, and $\text{pik } 1/2^-$ as visualized by confocal microscope. The cells were incubated with the labelled or un-labelled yeast, fixed with cold methanol and immunostained with mAb 230-18-8. CAP-GFP was found at the phagocytic cups and phagosomes during phagocytosis in a similar pattern like the endogenous CAP. Bar, 10 μm

Like endogenous CAP, CAP-GFP also localized to the phagocytic cups and phagosomes where it co-localized with the endogenous CAP. During these studies we found that expression of CAP-GFP enhanced the altered phagocytosis of $\text{pik } 1/2^-$ cells and partially the impaired phagocytosis of the $\text{g}\beta^-$ cells in comparison to the mutant (Figure 18). Furthermore, the immunofixing suggested that the re-localization of endogenous and CAP-GFP during phagocytosis does not depend on these above signalling molecules.

1.4.1 Redistribution of GFP fusion proteins of CAP and its domains in *aca*⁻ cells during phagocytosis

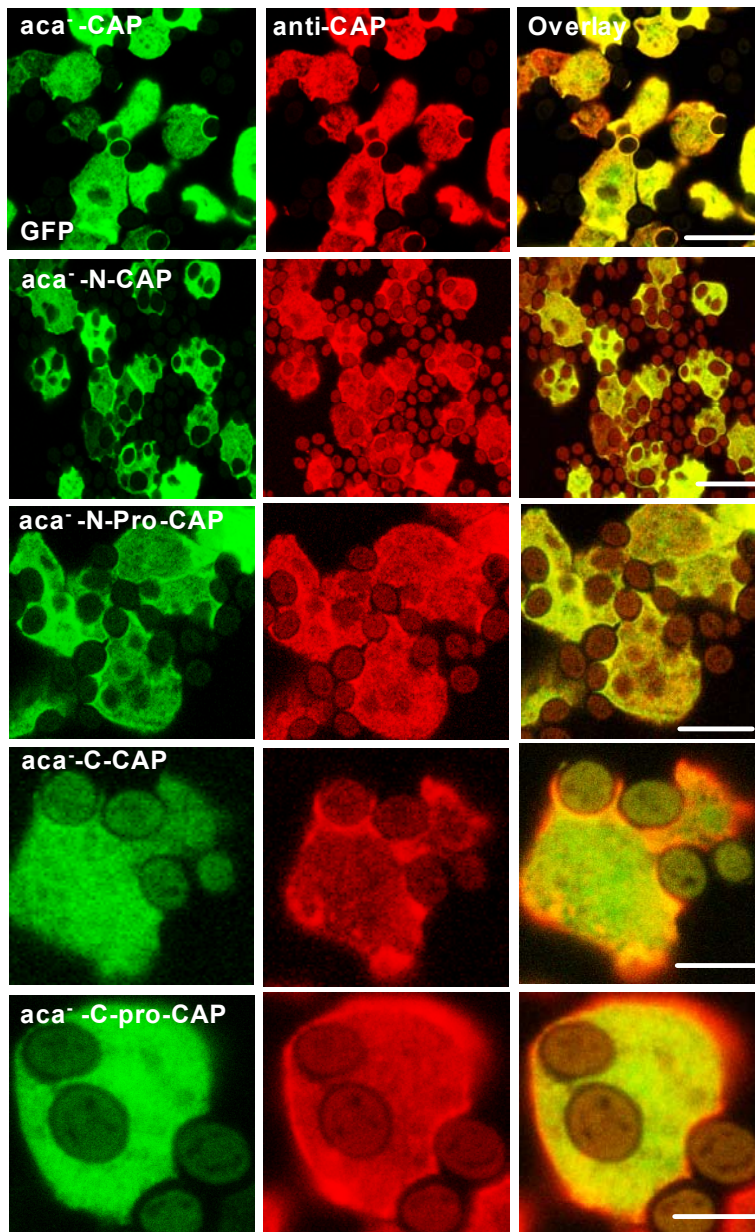


Figure 19: Distribution of GFP fusions of CAP and its domains in *aca*⁻ cells during phagocytosis. The *aca*⁻ transformants expressing the GFP fusions of CAP were allowed to adhere to the coverslip, and treated with unlabelled yeast cells for 15 minutes and stained with mAb 230-18-8 to detect the distribution of these GFP fusions during phagocytosis. CAP-GFP localizes to the phagocytic cups and phagosomes as a thick rim in the membrane rich progressions (top panel). Similar observations were made for the N-terminal domain of CAP with or without proline stretch (second and third panels). In contrast, the C-terminal domain of CAP showed an overall staining in the cytoplasm and was not enriched at the phagocytic cups or phagosomes. The antibody used is specific for the N-terminal domain and does not recognise the C-domain fused to GFP. Bar, 10 μ m

The expression of CAP-GFP and its domains in the *aca*⁻ cells, allowed us to analyse the involvement of the different domains of CAP in phagocytosis in the absence of ACA. CAP-GFP localizes to the sites of yeast engulfment and is also found enriched in the phagosomes. The N-CAP-GFP and N-Pro-CAP-GFP fusions showed a similar behaviour as CAP-GFP, and were present at the phagocytic cups and phagosomes. The C-terminal domain of CAP with or without the proline rich stretch showed a cytoplasmic distribution. Moreover, the GFP-tagged C-domain of CAP did not alter the localization of endogenous CAP to the regions of phagocytic cups and phagosomes as revealed by staining with mAb 230-18-8 (bottom panel) (Figure 19). These data indicate that the localization of CAP is unaffected in the *aca*⁻ cells and CAP functioning during phagocytosis is independent of ACA.

1.4.2 Live imaging visualizing the dynamics of CAP-GFP in *aca*⁻, *pia*⁻, *gα2*⁻, *gβ*⁻, and *pik1*^{1/2}⁻ cells

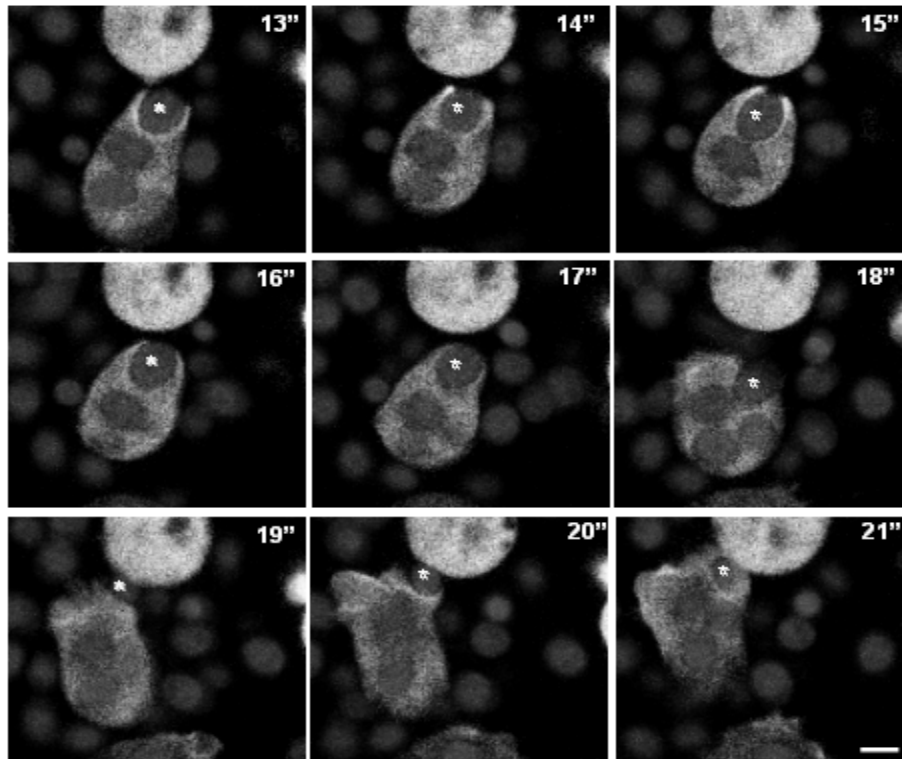


Figure 20: Dynamics of CAP-GFP in AX2 transformants expressing CAP during phagocytosis. AX2 cells expressing CAP-GFP were allowed to adhere to glass coverslips and then the supernatant was replaced by phosphate buffer containing TRITC-labelled yeast. Confocal images were taken at the times indicated. It is noticed that CAP enriches at the cell cortex where it redistributes dynamically in the form of a rim around the phagocytic cup. It is present at the extreme edges of the newly forming phagosome and involved in the engulfment of the yeast particle. The star indicates the yeast cell of interest. Bar, 10 μ m.

The immunostaining studies during phagocytosis in the above mutants showed that CAP was present at the phagocytic cups and phagosomes. It initiated an interest to observe the dynamics of CAP-GFP in *in vivo* conditions by live imaging. Phagocytosis is initiated by adhesion of a particle to the surface of the cell, and a phagocytic cup is formed at the cell surface involving active rearrangements of the actin cytoskeleton and also re-localization of CAP to the phagocytic cup and newly forming phagosome (Figure 20). In an attempt to study and visualize the dynamics of CAP-GFP during phagocytosis, mutants expressing full length CAP-GFP were allowed to settle on a glass coverslip and challenged with TRITC-labelled yeast cells (Materials and method). The dynamics of CAP-GFP redistribution during phagocytosis were captured by confocal Laser scan microscopy. The images were taken in series at equalized parameters to get a sequence of images, which could unravel the dynamics displayed by CAP-GFP. The study of re-localization of CAP-GFP in *aca*⁻, *pia*⁻, *gα2*⁻, *gβ*⁻ and *pik1*^{1/2}⁻ cells by live imaging was performed as done for AX2 cells expressing CAP-GFP. We noted that the *aca*⁻ and *pia*⁻ cells expressing CAP-GFP showed a drastic uptake in yeast particles although the cells were quite sensitive to the Laser light. To avoid damaging the cells upon intense light exposure, the laser intensity was attenuated to 1/50 of its maximal power. Since the yeast particles were strongly labelled, the small fraction of their emission obtained by excitation at 448nm was sufficient to record their fluorescence together with that of GFP. Sequences showing the

dynamics of CAP were assembled where we observe that the CAP-GFP protein does relocalizes within seconds to the site of yeast engulfment and participates dynamically during phagocytosis. The dynamics of CAP-GFP were comparable to the AX2-CAP-GFP cells. It is also clear from the studies that the dynamic re-localization of CAP-GFP is independent of ACA and PIA molecules (data not shown).

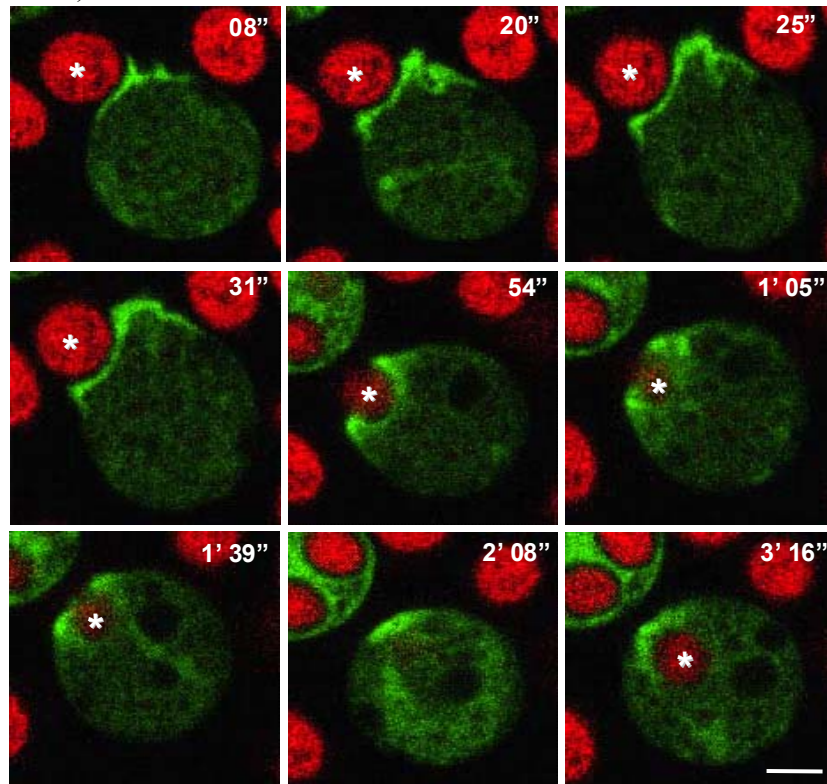


Figure 21: Dynamics of GFP-CAP in the $g\alpha 2^-$ cells during phagocytosis. The $g\alpha 2^-$ cells expressing CAP-GFP were allowed to adhere on glass coverslips and the supernatant was replaced by phosphate buffer containing TRITC-labelled yeast cells. Confocal images were taken at the times indicated. CAP enriches at the cell cortex where it redistributes dynamically in the form of a rim around the phagocytic cup, where it is enriched at the extreme edges of the newly forming phagosome. * represent the yeast cell of interest. Bar, 10 μ m.

The dynamics of CAP-GFP in G-protein mutants (Figure 21, 22) provided more insight into the role of CAP in the absence of the G-proteins $\alpha 2$ and β as G-proteins are required for regulating the actin cytoskeleton during phagocytosis. In $g\alpha 2^-$ cells we observed a dynamic re-localization of CAP to the membranes forming the phagocytic cups and phagosomes. CAP-GFP is relocalizes within seconds to the rim of the phagocytic cup. Cup progression leads to the formation of a coat around the yeast cell that contains CAP-GFP, which further extends around the particle resulting in the internalization of the particle (Figure 21). Moreover we observed that CAP-GFP was moving in the form of waves within the cells from the cortex of the other opposite end of the cell to the site of engulfment (as shown in the seventh panel). This dynamics of CAP-GFP also reveals that the re-localization of CAP is not dependent on signalling by the $G\alpha 2$ subunit.

The G-protein β subunit is an important regulator of the actin dynamics during phagocytosis as the $g\beta^-$ cells are defective in phagocytosis due to an impaired regulation of the actin cytoskeleton. Therefore, it was interesting to study the dynamic role of CAP-GFP in $g\beta^-$ cells as CAP also appears to be a key regulator of actin dynamics. The live imaging of $g\beta^-$ cells expressing CAP-GFP was

carried out in a similar manner as before. CAP-GFP was able to dynamically re-localize to the site of particle engulfment at the cell surface, however an enormous amount of the protein was still assembled at the cortex in contrast to the results obtained in $g\alpha 2^-$ cells (Figure 22).

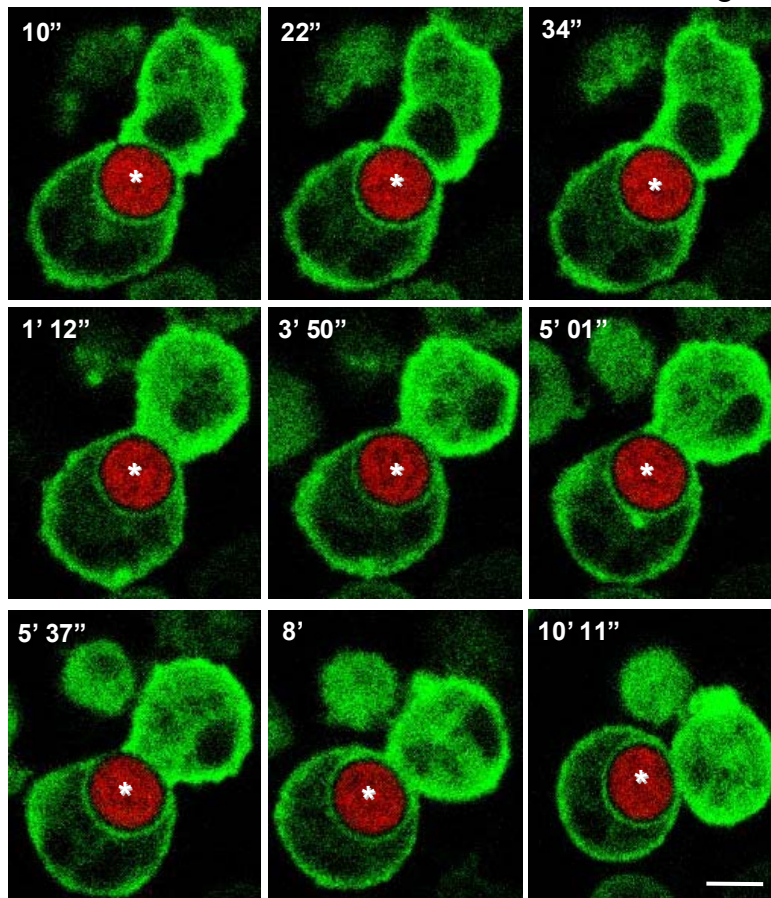


Figure 22: Dynamics of CAP-GFP in the $g\beta^-$ cells. The $g\beta^-$ cells expressing CAP-GFP were investigated for the dynamic re-localization of CAP-GFP by obtaining a series of confocal images at the times indicated. The cells were challenged with labelled yeast and observed under a confocal laser-scanning microscope. The images were taken at intervals of 10 seconds. The CAP-GFP is seen at the region of the yeast particle uptake and also at the cell periphery. * represent the yeast cell of interest. Bar, 10 μ m.

Also even after an extended time the CAP-GFP remained accumulated at the particle ingestion site in comparison to the wild type cells expressing CAP-GFP. However, it was intriguing to see the association of CAP with the actin cortex as the defect in phagocytosis of $g\beta^-$ cells was correlated with an impairment in the regulation of F-actin formation. In $g\beta^-$ cells expressing CAP-GFP and actin were found together at the phagocytic cups and phagosomes and co-localize (Figure 23).

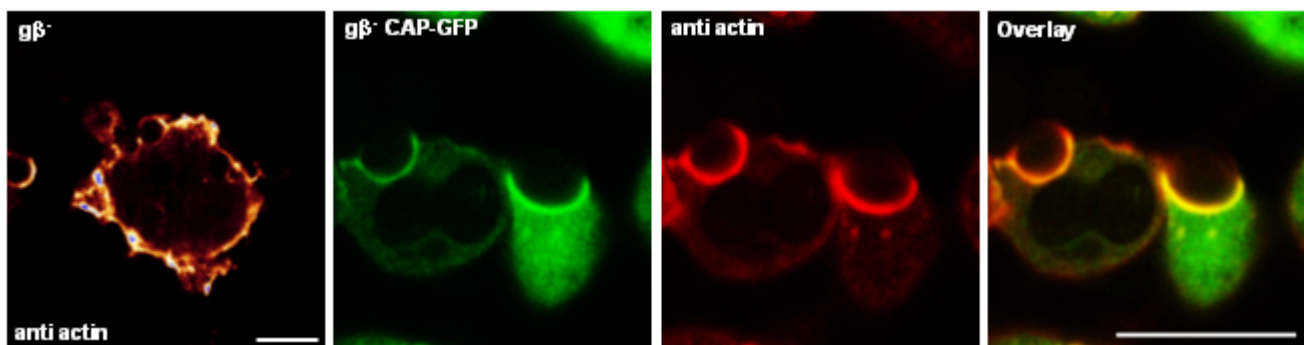


Figure 23: CAP-GFP and actin distribution in the $g\beta^-$ cells during phagocytosis. The $g\beta^-$ cells expressing CAP-GFP were immunostained with actin specific mAb Act-1-7 after fixation with cold methanol and observed under the confocal

microscope to visualize the association of CAP with actin at the phagocytic cups and phagosomes. CAP-GFP relocates to the site of phagocytosis and also co-localized with actin. Bar, 10 μ m.

From our observations we conclude that the re-localization of CAP is not dependent on the G-protein β subunit, however the rearrangements of the cytoskeleton during phagocytosis require G β signalling and cannot be overcome by increased concentrations of CAP.

The *pik1^{-/-}* cells are altered in their phagocytic uptake (Zhou et al., 1998). The phagocytic live microscopy was performed for the *pik1^{-/-}* cells expressing CAP-GFP in a similar way like before with labelled yeast cells. CAP-GFP relocated to the phagocytic cup and phagosomes in the absence of the PI3-kinase correlating with the immunofluorescence results and surprisingly, it was noticed that CAP-GFP enhanced the uptake of yeast particles in the *pik1^{-/-}* cells (Figure 24).

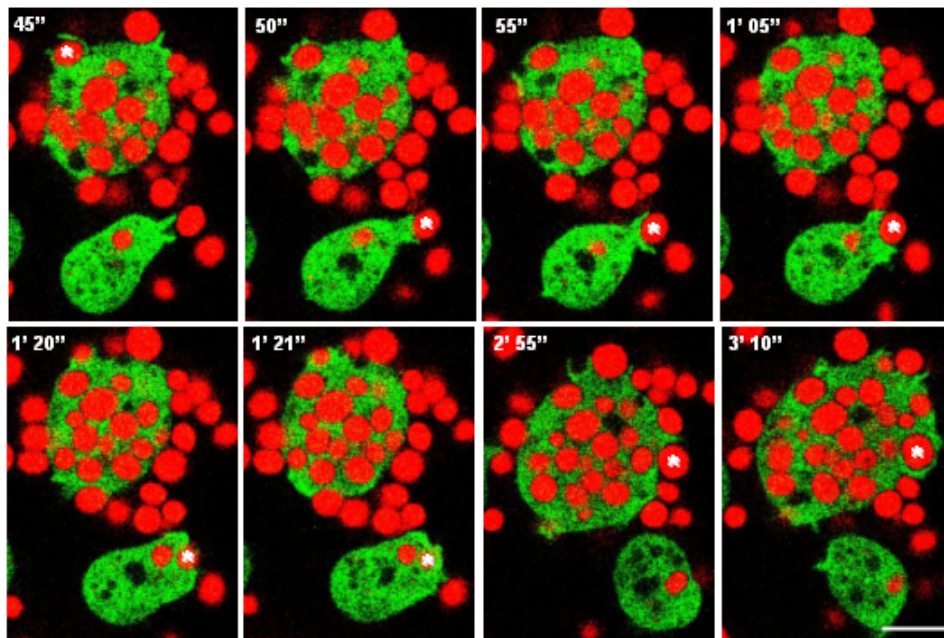


Figure 24: Dynamics of CAP-GFP in *pik1^{-/-}* cells during phagocytosis. The *pik1^{-/-}* cells expressing CAP-GFP were challenged with TRITC-labelled yeast. The confocal serial imaging of living cells revealed that CAP relocated to the site of uptake and CAP expression enhanced the phagocytic uptake. The images were taken at the times indicated. * represent the yeast cell of interest. Bar, 10 μ m.

1.4.3 Quantitative analysis of phagocytosis in the *aca⁻*, *pia⁻*, *ga2⁻* and *g β ⁻* and *pik1^{-/-}* cells

In addition to our phagocytosis experiments showing the localization and dynamics of CAP and CAP-GFP a quantitative analysis was performed for the *aca⁻*, *pia⁻*, *ga2⁻* and *g β ⁻* and *pik1^{-/-}* cells and mutants expressing CAP-GFP. AX2 and AX2 cells expressing CAP-GFP were the experimental controls. The quantitative phagocytosis performed by mixing 2×10^6 cells with a five fold excess TRITC-labeled heat-killed yeast particles. After 15 minutes of incubation, samples were withdrawn and the fluorescence of non-ingested particles was quenched with trypan blue. Fluorescence from internalized yeasts was measured at the designated time points. Data are presented as relative

fluorescence determined at 544/577 nm in the spectrofluorimeter, AX2 being considered 100%. All values are the average of at least three to four independent experiments. In these experiments *aca*⁻ and *pia*⁻ cells showed a pattern of yeast uptake like AX2 (Figure 25a), whereas, the *aca*⁻ and *pia*⁻ cells expressing CAP-GFP showed an enhancement in the uptake of the yeast particles in comparison to AX2. The AX2 cells expressing CAP-GFP also showed a 1.5 fold increase in comparison to wild type. Also the *aca*⁻ cells expressing the CAP-GFP showed an increase of 1.5 when compared to AX2. The *pia*⁻ cells expressing CAP-GFP internalized yeast particles at a rate that was two fold greater than the control AX2 (Figure 25b). These results indicate that CAP overexpression has a positive effect on phagocytosis.

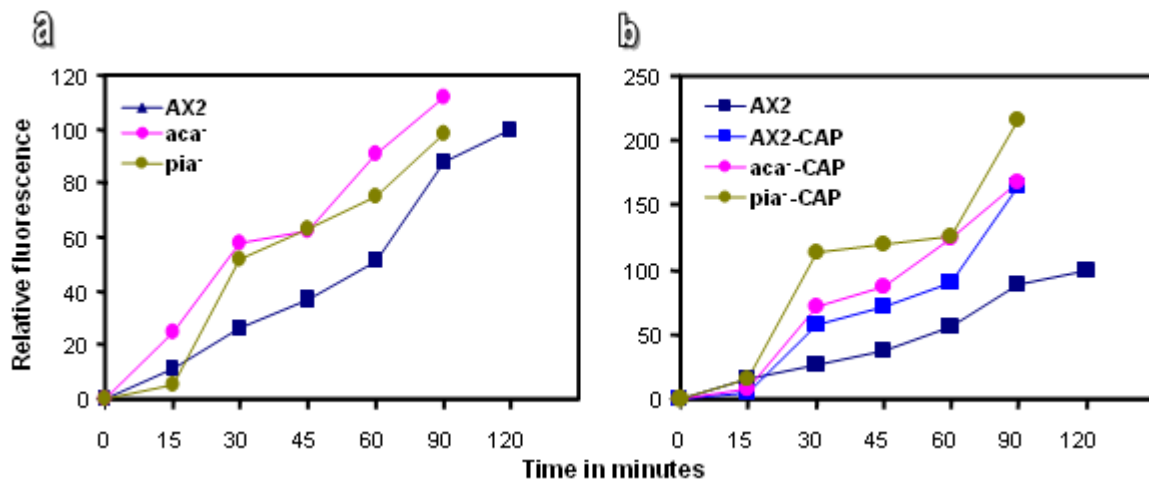


Figure 25: Quantitative analysis of phagocytosis in *aca*⁻, *pia*⁻ cells and mutants expressing CAP-GFP. (a) The quantitative analysis of *aca*⁻ and *pia*⁻ cells and mutants expressing CAP-GFP were the results of three independent experiments. The quantitative uptake of yeast particles by *aca*⁻ and *pia*⁻ cells was comparable to AX2. However, cells expressing CAP-GFP showed an enhancement in the uptake of the yeast particles which was found to be 1.5-2 fold higher when compared to AX2 (b).

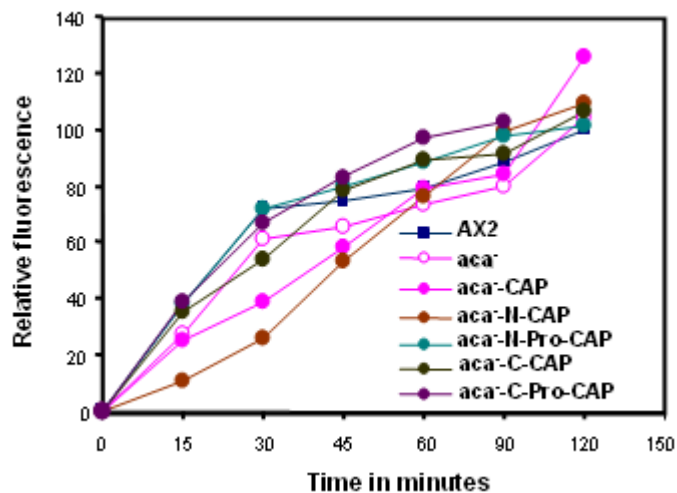


Figure 26: Quantitative analysis of phagocytosis in *aca*⁻ cells and cells expressing GFP fusions of CAP and its domains. The *aca*⁻ cells expressing GFP fusions of CAP and its domains were quantitatively analysed to identify the domain of CAP that plays an important role in the enhancement of phagocytosis. It was found that all domains of CAP influenced the yeast particle uptake which was similar to the control AX2. The data represented are the result of four independent experiments.

To determine which fusions of CAP plays a role in phagocytosis, the *aca*⁻ cells expressing different domains of CAP were further analysed for quantitative phagocytosis. The quantitative results did not

differ much from the control AX2 as, the rate of internalization of yeast particles was quite similar (Figure 26).

The quantitative analysis of phagocytosis by $\alpha 2^-$ cells showed that they internalized the yeast particles at half the rate of the AX2 control, however the β^- cells showed a more severe defect in the internalization of yeast particles which reached 20% in comparison to wild type AX2 (Figure 27a), correlating with the results of our immunofluorescence studies. The $\alpha 2^-$ cells expressing CAP-GFP showed an enhancement in the uptake of yeast particles with a nearly 1.5 fold influx rate when compared to AX2 (Figure 27b). The β^- cells expressing CAP-GFP showed a two fold increase in internalizing of the yeast particles in comparison to β^- cells (compare Figure 27a and b).

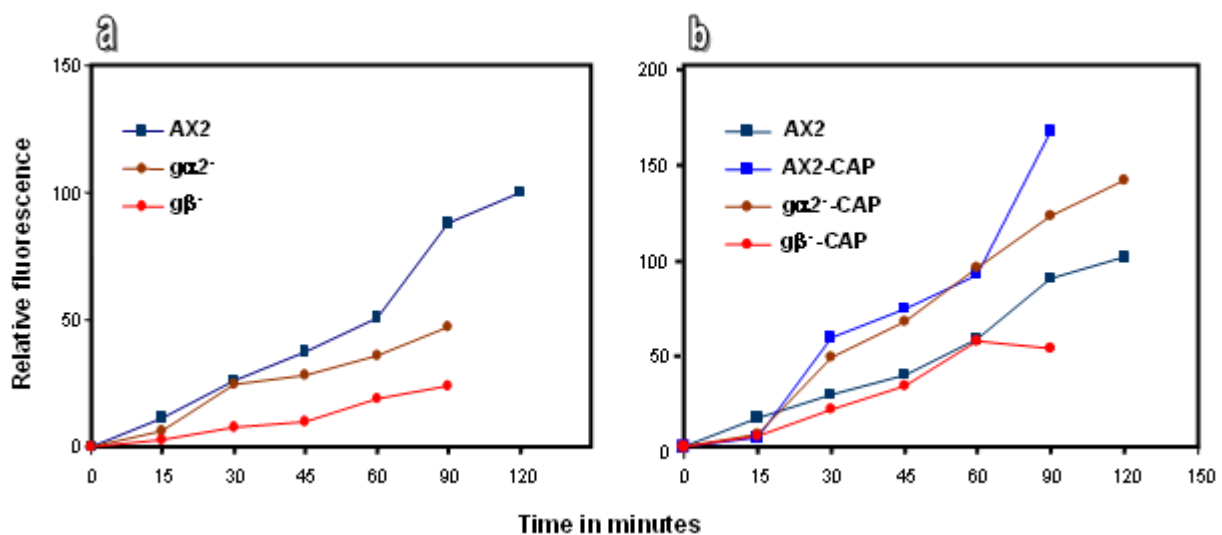


Figure 27: (a) Quantitative phagocytosis of $\alpha 2^-$, β^- , and (b) mutants expressing CAP-GFP. The Data plotted here are the results of four independent experiments. The $\alpha 2^-$ cells are slower in their phagocytic uptake rates however the cells expressing CAP-GFP showed a significant enhancement in the uptake of yeast (1.5 fold higher in comparison to AX2). The β^- cells were severely defective in phagocytosis, however the β^- cells expressing CAP-GFP showed a significant improvement and internalized with a 2 fold higher rate in comparison to the β^- cells.

Consistent with our immunofluorescence and live imaging data it is apparent that expression of CAP-GFP improved the phagocytic uptake of the β^- cells. However expression of CAP-GFP could not rescue the defect of the β^- cells phagocytic defect completely, indicating the primary requirement of G β subunits during phagocytosis.

The $\text{pik } 1/2^-$ cells are altered in their phagocytic uptake, and the ingestion rate of the $\text{pik } 1/2^-$ in our assay was 50% less or slower than in AX2. Upon expression of CAP-GFP $\text{pik } 1/2^-$ cells showed a significant improvement in the internalization of yeast particles in comparison to $\text{pik } 1/2^-$ and the influx rate was comparable to AX2. The data obtained were consistent with our previous immunofluorescence studies that indicated that the phagocytic rates are enhanced in the $\text{pik } 1/2^-$ cells expressing CAP-GFP. Taken together all our results support the notion that the expression of CAP-

GFP rescues the altered phagocytic defect of the *pik 1/2⁻* cells which was comparable to the wild type (Figure 28).

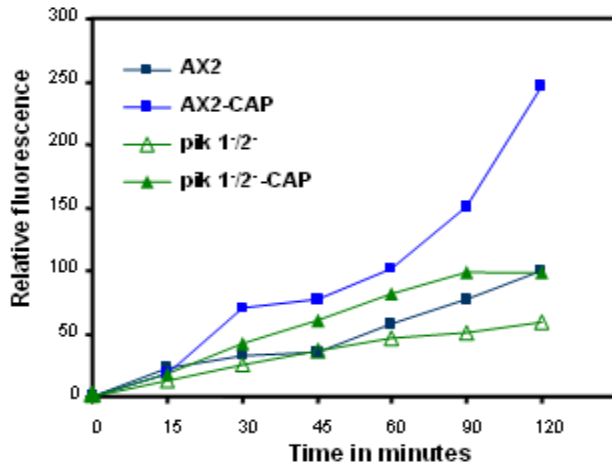


Figure 28: Quantitative phagocytosis analysis of the *pik1/2⁻* cells and cells expressing CAP. The quantitative results were obtained from four individual experiments. Expression of CAP-GFP rescues the altered phagocytic defect of the *pik 1/2⁻* cells which are slower in particle ingestion, and expression of CAP-GFP shows a similar internalization rate as AX2.

1.5 Re-localization of CAP during pinocytosis in the *aca⁻*, *pia⁻*, *gα2⁻*, *gβ⁻* and *pik 1/2⁻* cells

Pinocytosis is the ingestion of dissolved materials by endocytosis, where the cytoplasmic membrane invaginates and pinches off placing small droplets of fluid in a pinocytic vesicle. The liquid content of the vesicle is then slowly released into the cytosol. In general this material will be dissolved in water and thus this process is also referred to as "cellular drinking" to indicate that liquids and material dissolved in liquids are ingested by the cell. This is opposed to the ingestion of large particulate material like bacteria or other cells or cell debris. Observing cell uptake of fluorescent molecules from the medium by live microscopy one can follow pinocytosis. The phenomenon of macropinocytosis accounts for the fluid-phase uptake and depends on the integrity of the actin cytoskeleton and its regulators in *Dictyostelium* (Maniak et al., 1995).

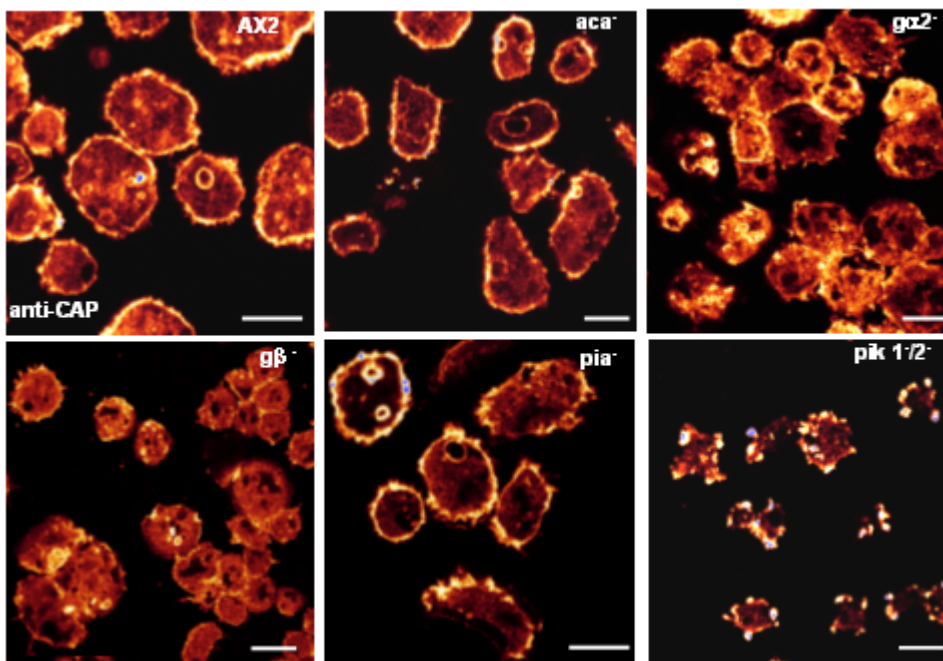


Figure 29: Re-localization of CAP during pinocytosis in *aca⁻*, *pia⁻*, *gα2⁻* and *gβ⁻* and *pik 1/2⁻* cells. The cells were allowed to adhere onto coverslips and replaced with starvation buffer containing TRITC-dextran, cells were immunostained with mAb 230-18-8, after fixation with paraformaldehyde and picric acid. The mutants showed accumulation of CAP at the pinocytic cups and pinosomes. Bar, 10 μm.

A redistribution of CAP is observed during pinocytosis and our previous report indicated that CAP bsr cells are defective in pinocytosis, as in axenic medium CAP bsr cells grew more slowly and did not reach saturation densities as observed for wild type AX2 (Noegel et al., 1999). The immunofluorescence results indicated that CAP relocates to the pinocytic cups and pinosomes and this behaviour did not seem to be dependent on the signal transduction molecules tested (Figure 29). Thus, CAP as a regulator of actin dynamics plays an active role during pinocytosis, where it relocates to the area of high actin turnover and allows the rearrangement of the actin cytoskeleton and appears to be an important regulator of pinocytosis.

1.5.1 Live dynamics of CAP-GFP in the aca^- , pia^- , $ga2^-$ and $g\beta^-$ cells during pinocytosis

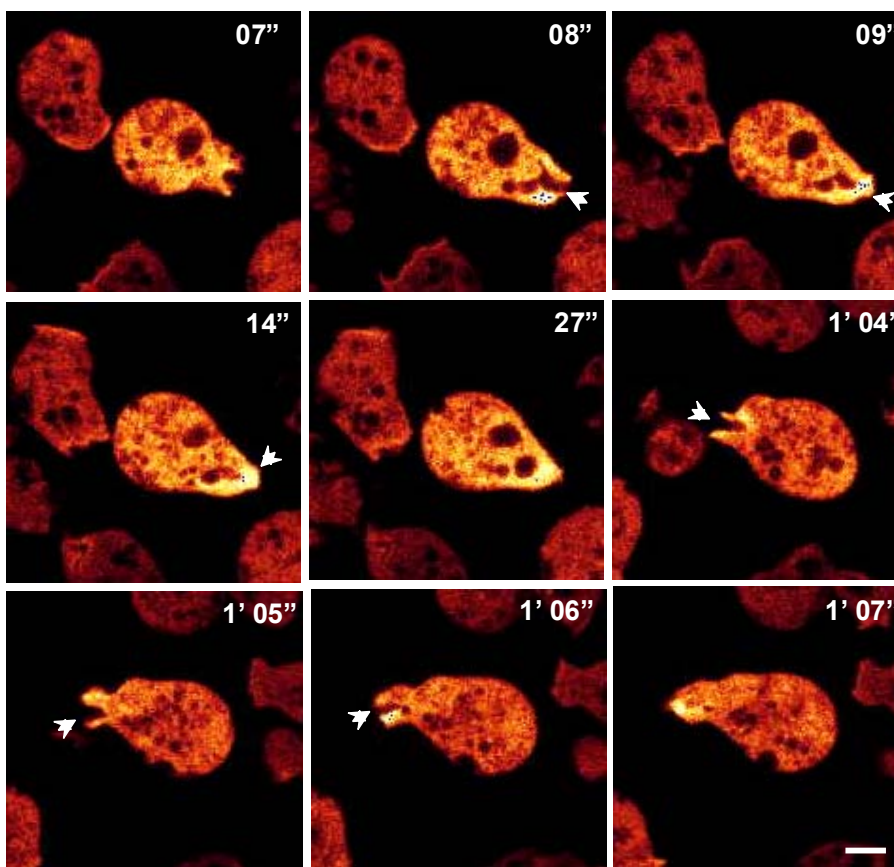


Figure 30: Dynamics of CAP-GFP in AX2 cells during pinocytosis. The cells were allowed to adhere on glass coverslips and challenged with TRITC-dextran. The confocal serial imaging of living cells shows that CAP relocates and enriches to the pinocytic cups and pinosomes during pinocytosis. The images were taken at the times indicated and arrowheads denote the enrichment of the CAP-GFP at the macropinosome. Bar, 10 μ m.

AX2 cells expressing CAP-GFP served as control for all live imaging of pinocytosis. The AX2 cells expressing CAP-GFP showed a prominent re-localization of CAP-GFP to the site of the newly forming pinosome, where it enriches and dissociates within seconds from the macropinosome as revealed by the time series images captured by the confocal microscope (Figure 30). The aca^- cells expressing CAP-GFP gave more insight into the functioning of CAP during pinocytosis. Here the cortical enrichment of CAP-GFP is clearly apparent. The CAP-GFP prominently relocates from the cell cortex and accumulates at the region of the fluid uptake indicating that the relocalization of GFP-CAP during pinocytosis is independent of ACA (Figure 31).

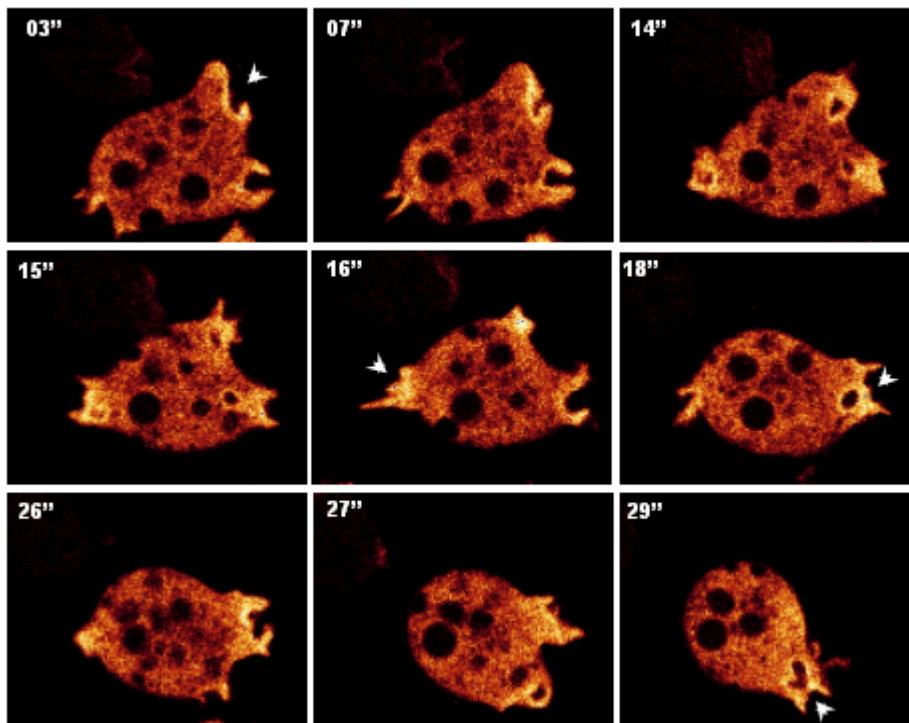


Figure 31: Dynamics of CAP-GFP in *aca*⁻ cells during pinocytosis. The cells were allowed to adhere onto glass coverslips and challenged with TRITC-dextran. The confocal serial imaging the cells shows that CAP-GFP relocates to the pinocytic cups and pinosomes where it enriches and accumulates as the cup progresses to the extreme edge during the formation of the pinosome. The images were taken at the times indicated. The arrowhead denotes the enrichment of the CAP-GFP and the area of interest. Bar, 10 μ m.

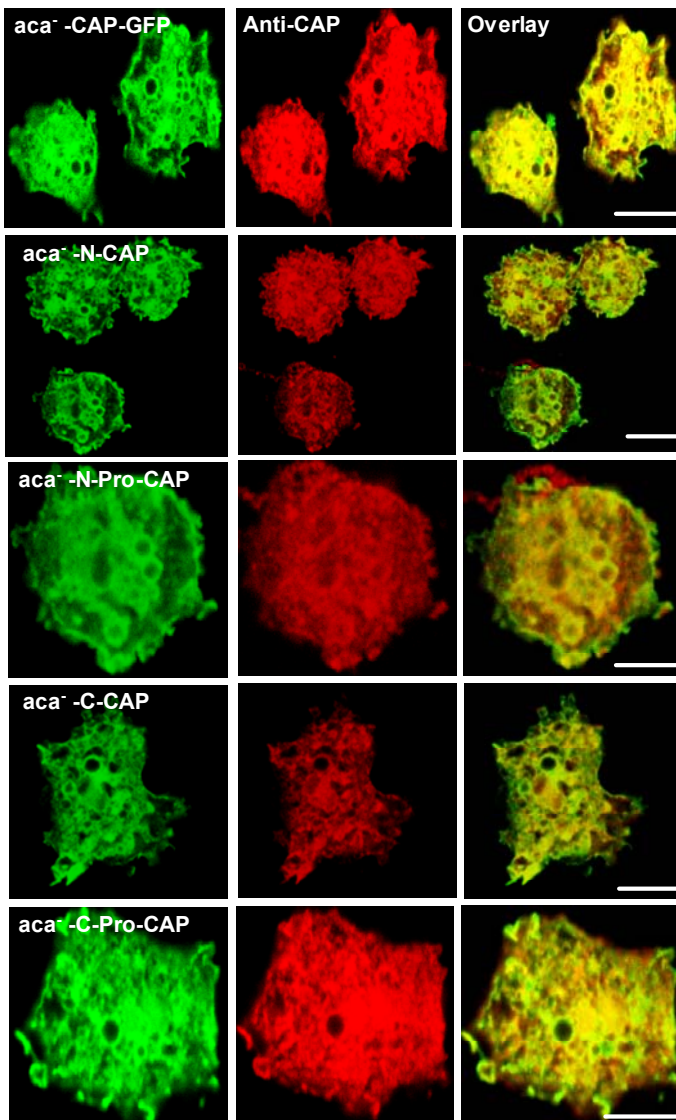


Figure 32: Localization of GFP fusions of CAP and its domains in the *aca*⁻ cells. The cells were fixed with para-formaldehyde and picric acid after treating with TRITC-dextran and then immunolabelled with mAb 230-18-8 to detect the localization of CAP and its domains. It appears that all domains of CAP are required for pinocytosis as they are found around large vesicles and as they co-localize with endogenous CAP. Bar, 10 μ m.

In order to investigate which domain of CAP is the principal determinant in the event of pinocytosis and formation of macropinosomes, we made use of the *aca*⁻ cells expressing GFP fusions of CAP and its domains. From the immunolabelling studies it is clear that all domains of CAP participate in the process of pinocytosis, as we see the enrichment of all fusions at the pinocytic cups and macropinosomes during pinocytosis (Figure 32). However, we cannot rule out the possibility that they associate with endogenous CAP and co-distribute.

In the *pia*⁻, *gα2*⁻ and *gβ*⁻ cells CAP-GFP also relocates and enriches at the protrusions of the membrane forming the macropinosomes (Figure 33), making a notion that the dynamics of CAP-GFP during pinocytosis is independent of the ACA regulator PIA and of G-proteins ($\alpha 2$ and β subunit).

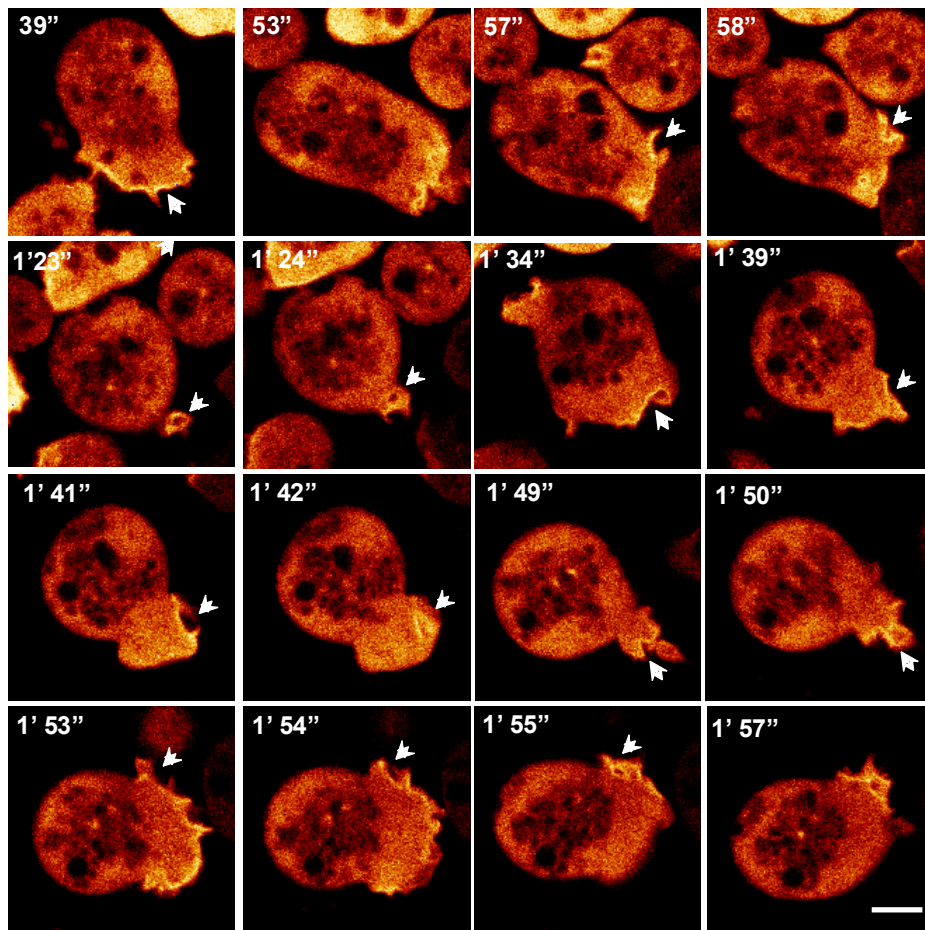


Figure 33: Dynamics of CAP-GFP in *pia*⁻ cells during pinocytosis. The *pia*⁻ cells expressing CAP-GFP were challenged with TRITC-dextran and confocal images showed that CAP-GFP relocates to the pinocytic cups and pinosomes during pinocytosis. The images were taken at the times indicated, and the arrowhead shows that the protein accumulates at the cell cortex during pinocytosis. Bar, 10 μ m.

1.6 Dynamics of CAP-GFP in the *pik 1/2*⁻ cells during pinocytosis

Dictyostelium pik 1/2⁻ cells are severely impaired in pinocytosis and have an altered F-actin distribution (Zhou et al., 1998). The redistribution of CAP-GFP during formation of the macropinosome can be followed at the site of the cell marked with an arrowhead. At the beginning of the sequence a CAP-GFP rich membrane invaginates within a few seconds (time indicated) and the protrusion of the CAP-GFP rich membrane progresses until the edges of the protrusion fuse to form a macropinosome containing CAP-GFP. Thereafter, CAP-GFP gradually disassociates from the

macropinosome within one minute to liberate the pinosome into the cytosol. In the end CAP-GFP does not completely dissociate from the pinosome (Figure 34). This process of CAP-GFP dynamics indicates that CAP is involved in this process, and also denotes that the re-localization and dynamics of CAP-GFP functions independent of PI3-kinase.

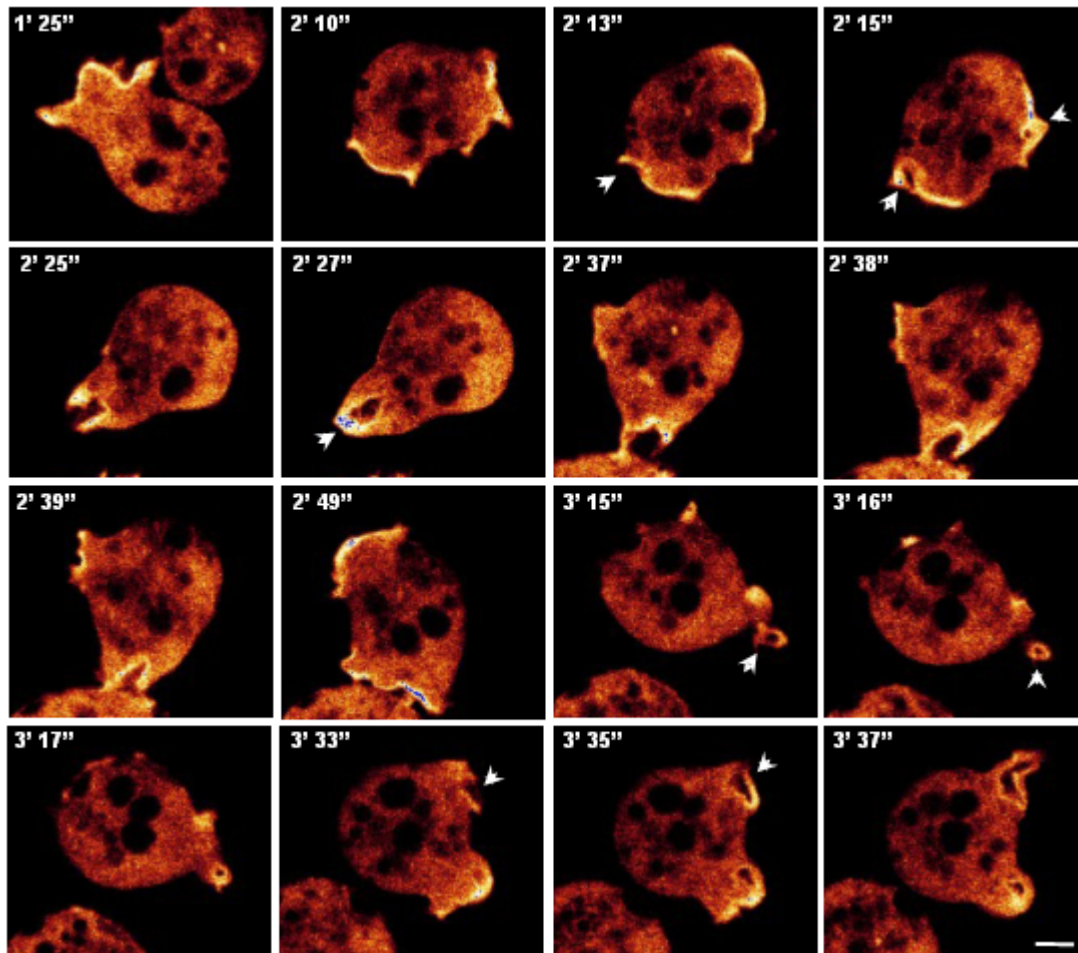


Figure 34: Dynamics of CAP-GFP in pik 1/2⁻ during pinocytosis. The pik 1/2⁻ cells expressing CAP-GFP were carried out for live microscopic imaging by challenging with TRITC-labelled dextran. The confocal serial imaging of living cells expressing CAP-GFP shows that CAP protein enhances the pinocytic uptake and relocalizes to the site of action where it shows enrichment of CAP-GFP. The images were taken at times indicated and the arrowhead denotes the enrichment of CAP-GFP at the forming pinosome and the region of interest. Bar, 10 μ m.

1.6.1 Quantitative analysis of pinocytosis in pik 1/2⁻ cells and cells expressing CAP-GFP

The live imaging and the immunofluorescence studies indicated an active role of CAP in the pinocytic uptake of pik 1/2⁻ cells. To confirm this observation a quantitative analysis of pinocytosis in the pik 1/2⁻ cells and mutants expressing CAP-GFP was performed. Fluid-phase endocytosis was assayed in the presence of TRITC-labelled dextran as a marker. Fluorescence from the internalized marker was measured at selected time points and determined at 544/574 nm in the spectrofluorimeter. The data shown are the average results of four independent experiments, and AX2 and AX2 cells expressing CAP-GFP are our controls.

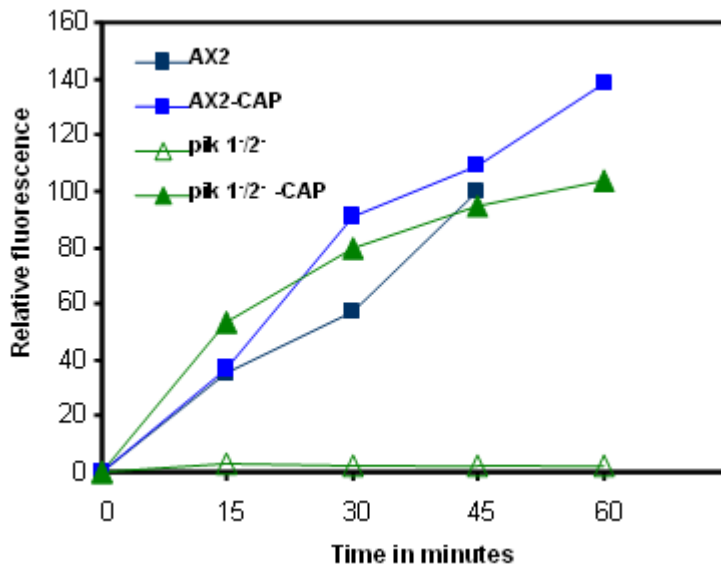


Figure 35: Fluid-phase endocytosis of TRITC-dextran in the pik 1/2⁻ cells and mutant expressing CAP-GFP. Cells were resuspended in fresh axenic medium at 5×10^6 cells/ml in the presence of 2 mg/ml TRITC-dextran. Data are presented as relative fluorescence, AX2 values being considered 100 %. All values are the average of at least four independent experiments. Expression of CAP-GFP in the pik 1/2⁻ cells significantly improved all the pinocytotic parameters for the influx of TRITC-dextran. Moreover it completely rescued the severe impairment in pinocytosis of the pik 1/2⁻ cells.

The AX2 cells expressing CAP-GFP showed a 1.5 fold increase in the uptake of fluid in comparison to the wild type. The quantitative analysis also reveals that all pinocytosis parameters are severely reduced in pik 1/2⁻ which only had 5% of the influx rate. Interestingly, it was observed that the pik 1/2⁻ cells expressing CAP-GFP rescued the severe impairment in the internalisation of fluid marker of pik 1/2⁻ cells, and shows an influx rate significantly comparable to the AX2 control (Figure 35). The data indicated that expression of CAP-GFP enhanced the influx of fluid in the pik 1/2⁻ cells and suggest a role of CAP in the pinocytotic uptake and imply that the dynamics of CAP-GFP are independent of PI3-kinase.

1.6.2 Distribution of F-actin in the pik 1/2⁻ cells expressing CAP-GFP

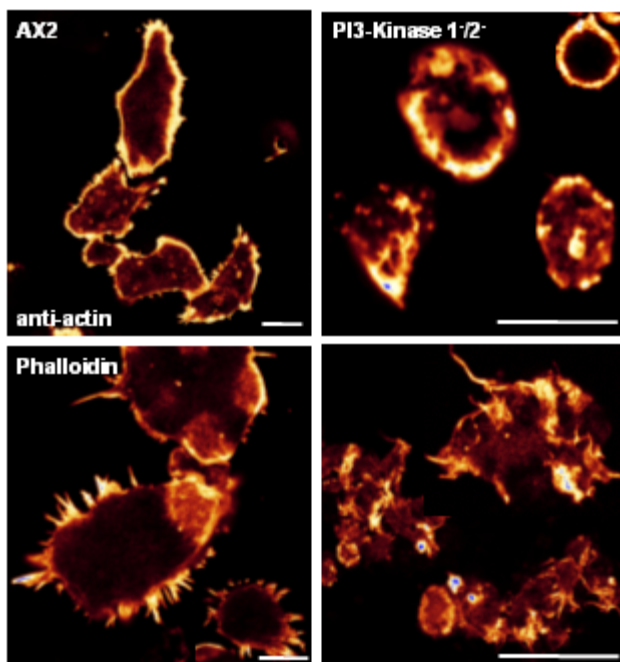


Figure 36: Distribution of actin and filamentous actin in AX2 and pik 1/2⁻ cells. The cells were immunolabelled to detect actin with actin specific mAb Act-1-7 and F-actin using an F-actin specific dye, rhodamine-phalloidin. The images were obtained with a laser scan microscope, which reveals that the mutant shows an altered distribution of actin and F-actin in comparison to the wild type AX2. Bar, 10 μ m.

The results obtained from the analysis of phagocytosis and pinocytosis of $\text{pik} 1^{-/2^{-}}$ cells raised the question about the distribution of actin, which was, visualised with actin specific mAb act 1-7 and rhodamine-phalloidin detecting filamentous actin (F-actin). In wild type AX2 actin was heterogeneous around the cell periphery and concentrated in actin crowns and specialized actin structures, whereas in the $\text{pik} 1^{-/2^{-}}$ cells actin was less evenly distributed around the periphery and showed a patchy distribution (Figure 36). Expression of CAP-GFP in $\text{pik} 1^{-/2^{-}}$ cells changed the altered patterns of the distribution of filamentous actin. The $\text{pik} 1^{-/2^{-}}$ cells showed a more homogenous distribution of actin around the cell periphery and lacked the aberrant structures seen in the mutant. Various phalloidin-staining structures characteristic of macropinosomes could be detected in both wild type AX2 and the $\text{pik} 1^{-/2^{-}}$ cells expressing CAP-GFP but not in the case of $\text{pik} 1^{-/2^{-}}$ cells (Figure 37). Circular protrusions containing swirls of phalloidin-stained F-actin were visible on the apical surface of the AX2 and $\text{pik} 1^{-/2^{-}}$ cells expressing CAP-GFP unlike in $\text{pik} 1^{-/2^{-}}$ cells. These results denoted that expression of CAP-GFP affects and reverted the distribution of actin and F-actin in the $\text{pik} 1^{-/2^{-}}$ cells, which also explain the results of the complete rescue in pinocytosis of the $\text{pik} 1^{-/2^{-}}$ cells.

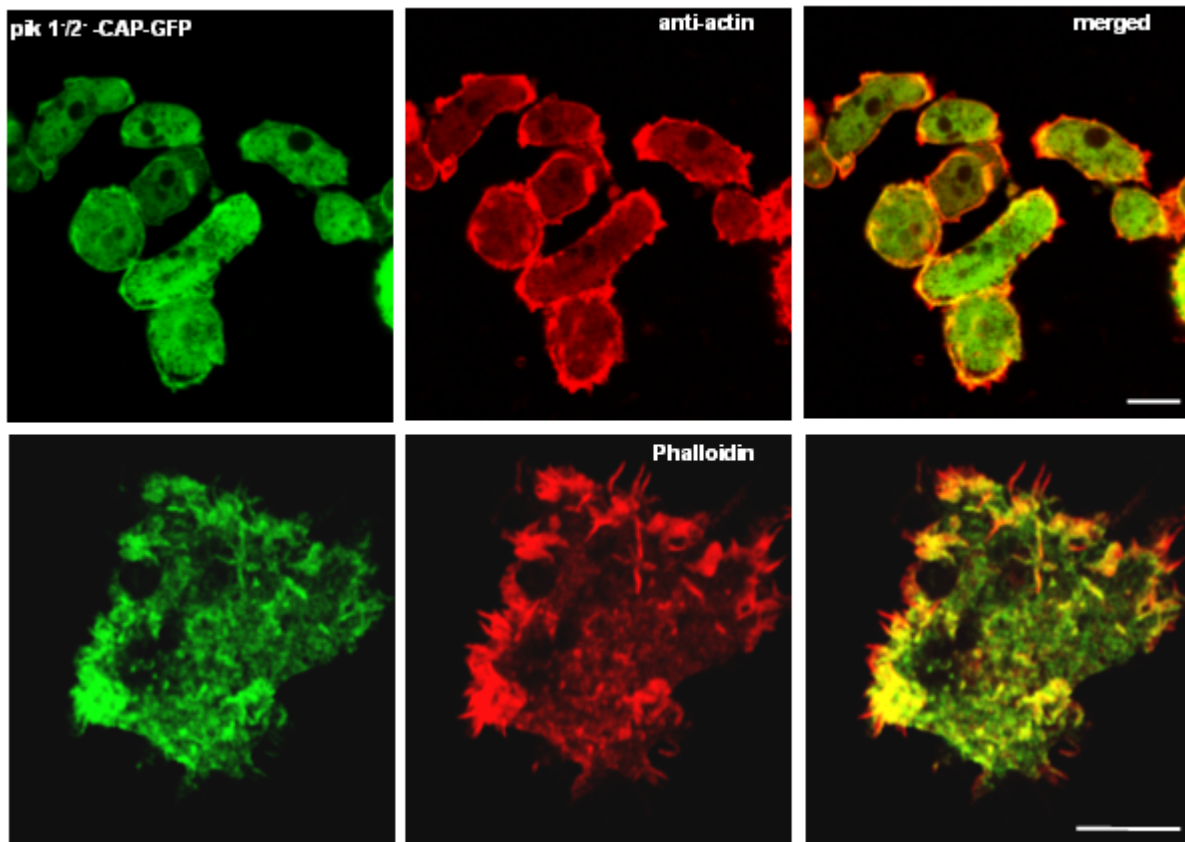


Figure 37: Distribution of actin and F-actin in $\text{pik} 1^{-/2^{-}}$ cells expressing CAP-GFP. To detect actin and F-actin in the $\text{pik} 1^{-/2^{-}}$ cells expressing CAP-GFP actin specific mAb Act-1-7 was used and F-actin was visualized with a F-actin specific dye, rhodamine-phalloidin. The images revealed that CAP-GFP expression corrects the altered distribution of actin and F-actin in the $\text{pik} 1^{-/2^{-}}$ cells comparable to AX2. Bar, 10 μm .

1.7 Role of CAP in the aggregation of $\text{pik} 1^{-}/2^{-}$ cells

The $\text{pik} 1^{-}/2^{-}$ cells have defects in streaming during development. Albeit they are motile they do not form mounds suggesting that aggregation rather than motility was impaired (Zhou et al., 1998). However, there was a fundamental difference in the manner in which the double knockout cells migrated and also in respect to cell polarization the mutants showed a polarity defect. Confocal microscopy revealed that aggregation stage AX2 wild type cells were polarised and CAP was enriched at the cell periphery at the leading fronts and also at the rear ends. The $\text{pik} 1^{-}/2^{-}$ cells were more rounded and had few protrusions (Figure 38).

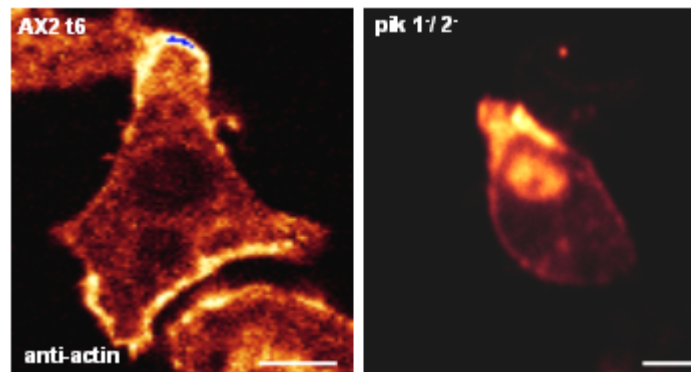


Figure 38: Distribution of CAP in aggregating $\text{pik} 1^{-}/2^{-}$ cells. The wild type and mutant cells were starved for 6 hrs in Soerenson phosphate buffer and fixed with cold methanol and immunolabelled with mAb 230-18-8 to visualise the distribution of CAP. In AX2 CAP accumulates at the leading fronts and rear ends of the cells, the mutant displayed an altered distribution. Bar, 10 μm .

In $\text{pik} 1^{-}/2^{-}$ cells expressing CAP-GFP the polarity appeared to be restored, as the cells were highly polarized and CAP predominantly localised to the leading fronts (Figure 39).

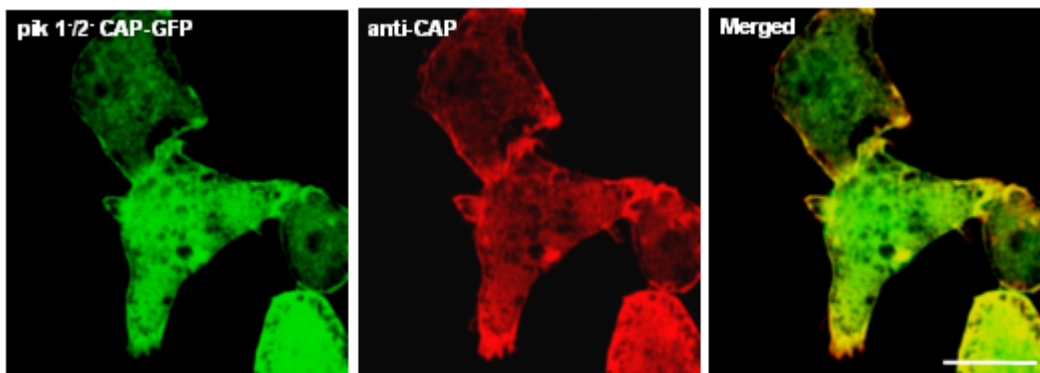


Figure 39: Distribution of CAP-GFP aggregating $\text{pik} 1^{-}/2^{-}$ cells. The $\text{pik} 1^{-}/2^{-}$ cells expressing CAP-GFP were immunostained with mAb 230-18-8 and visualised under the confocal microscope. The cells were polarised and CAP localised to the fronts of the cells. Bar, 10 μm .

1.8 Role of CAP for aggregation competence in $\text{pik} 1^{-}/2^{-}$ cells

To dissect the role of CAP in the $\text{pik} 1^{-}/2^{-}$ cells during aggregation we followed the dynamics of CAP-GFP in live cells responding to a cAMP pulse. Serial confocal images were obtained during the following minutes. AX2 cells expressing CAP-GFP served as control.

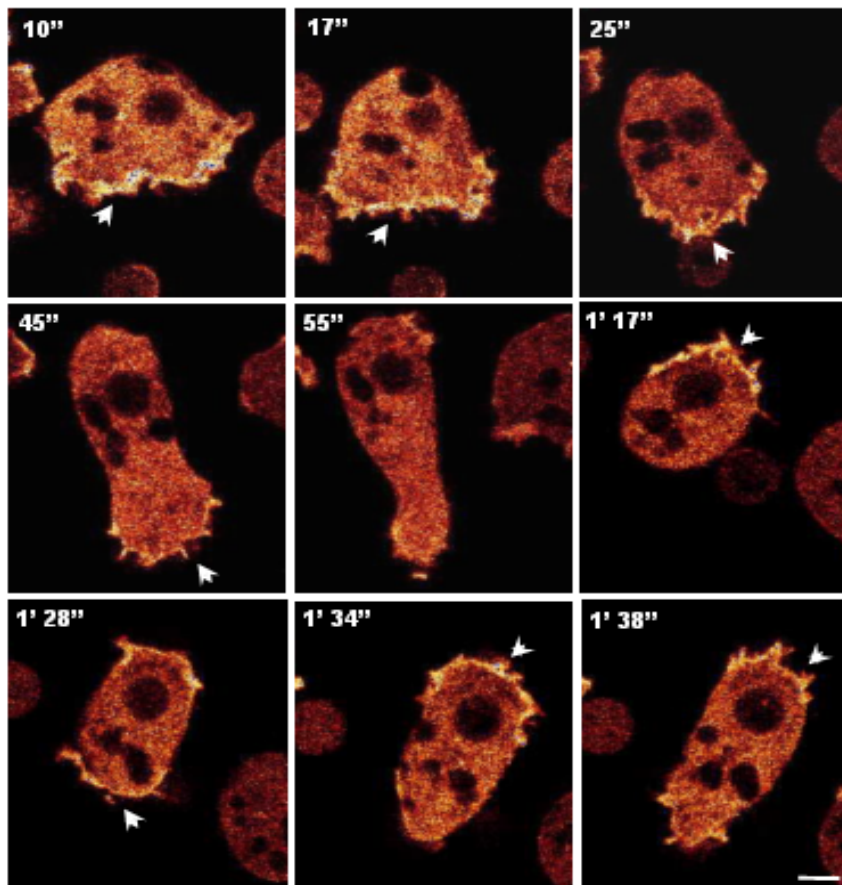


Figure 40: Dynamics of CAP-GFP in aggregation competent AX2 cells expressing CAP-GFP. The cells were transferred to coverslips after 6 hrs of starvation and challenged with a cAMP pulse 10^{-5} μ M and the dynamics of CAP-GFP were recorded using the confocal microscope. In AX2 cells the protein translocated and enriched at the leading fronts and tails. The arrowhead denotes the enrichment of the CAP-GFP at the leading edge, and the region of interest. The images are captured at the times indicated at the top left. Bar, 10 μ m.

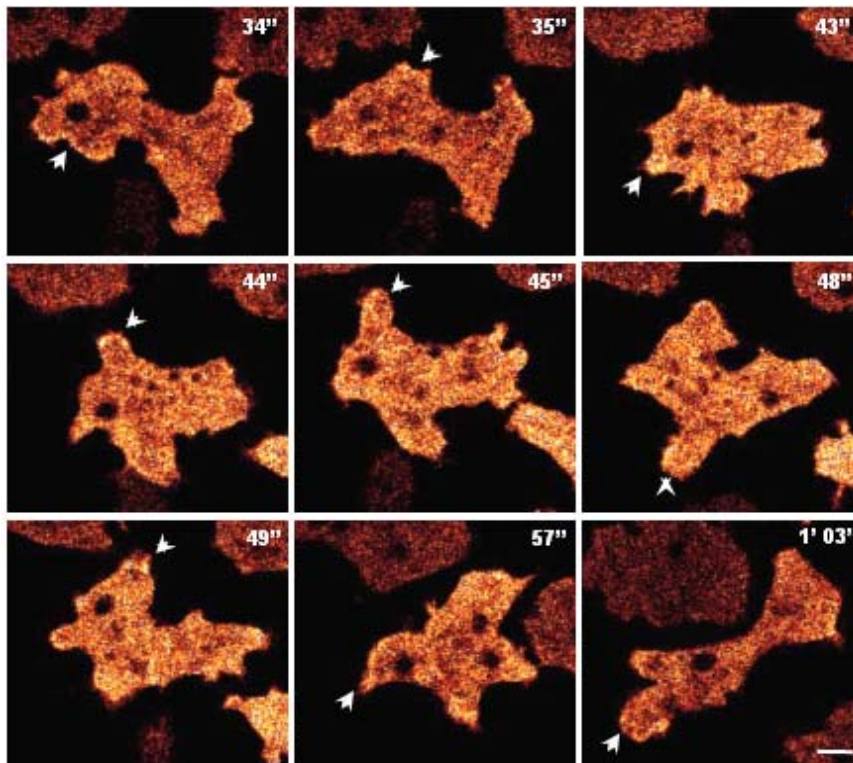


Figure 41: Dynamics of CAP-GFP in aggregation competent pik 1/2 cells expressing CAP-GFP. The cells were starved for 6 hrs to acquire aggregation competence, and given a pulse of 10^{-5} μ M cAMP. CAP-GFP localizes to the cortex at the leading front of the cell and cells were motile and polarised, and CAP-GFP was found to accumulate in the pseudopods. The images are captured at the times indicated, and the arrowhead denotes the enrichment of the CAP-GFP at the leading edge. Bar, 10 μ m.

Aggregation competent AX2 cells expressing CAP-GFP attained a typical elongated shape with a defined front and tail. They were highly motile and moved by extension of the pseudopods in which CAP-GFP was enriched (Figure 40). The pik 1/2 cells expressing CAP-GFP behaved in a similar

way, they were motile and showed the extension of pseudopods rich with CAP-GFP (Figure 41). These results implicate that expression of CAP-GFP leads to a polarisation of $\text{pik} 1/2^-$ cells during aggregation.

1.9 Role of CAP in growth and development of $\text{pik} 1/2^-$ cells

The $\text{pik} 1/2^-$ cells grow more slowly compared to wild type AX2 in axenic growth medium. They do not grow in shaking culture due to defects in pinocytosis. When grown in axenic cultures $\text{pik} 1/2^-$ cells were significantly smaller than wild type cells (Zhou et al., 1998). The $\text{pik} 1/2^-$ cells not only have a growth defect but also show abnormal phenotypes when they aggregate and develop. They form multiple tips that resolve into independent slugs producing very short and thick abnormal fruiting bodies. Interestingly, $\text{pik} 1/2^-$ cells expressing CAP-GFP in addition to improved growth showed more normal developmental phenotypes. The aggregates formed by $\text{pik} 1/2^-$ cells expressing CAP-GFP did no longer exhibit multiple tip formation. Instead they formed independent tips arising singly from the mounds. The images taken at later times indicated that they also developed into individual fruiting bodies like AX2 which had much longer and thin stalks (Figure 42).

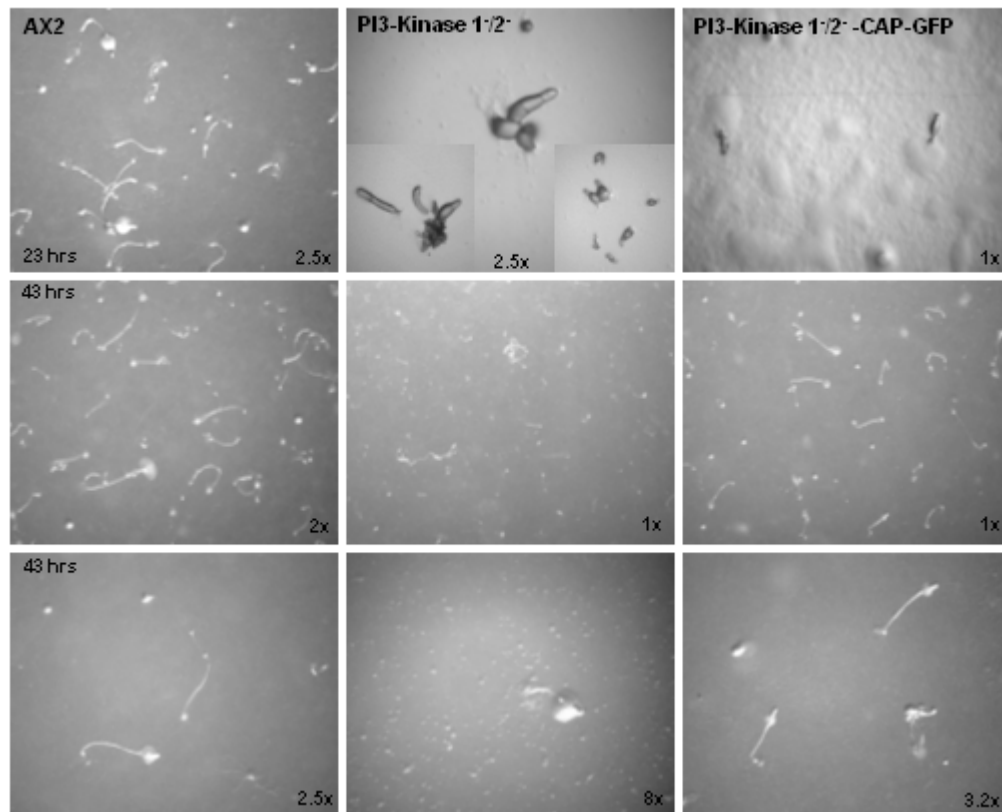


Figure 42: Growth and developmental phenotypes exhibited by $\text{pik} 1/2^-$ cells expressing CAP-GFP. The cells were starved on non-nutrient agar plates and images were obtained at the times indicated using a stereo-microscope. Expression of CAP-GFP improves the abnormal phenotypes shown by the mutant to a great extent. The aggregates do not form multiple tips, and transform into thin, long fruiting bodies like AX2. The sizes are shown in respect to the magnification used while obtaining the images.

Development of the *pik 1⁻2⁻* cells expressing CAP-GFP on agar was delayed when compared with AX2 wild type but noticeably faster than in the mutant. These results also signify the importance of CAP in the developmental programme of *Dictyostelium*.

2.0 Role of CAP in the aggregation and development of aggregation deficient *aca⁻* null cells

During the initial stages of aggregation of the social amoeba *Dictyostelium* amoebae move chemotactically in response to waves of cAMP, which are initiated periodically by aggregation centres and relayed outward by surrounding cells. The cells detect this extracellular cAMP signal via highly specific serpentine seven transmembrane cAMP receptors. Upon binding cAMP these receptors activate a signal transduction cascade resulting in the activation of the aggregation stage adenylyl cyclase (ACA), an enzyme that spans the plasma membrane 12 times and contains two large cytoplasmic domains (designated as C1 and C2) (Devreotes, 1989; Pitt et al., 1992; Parent and Devreotes, 1996). In order to gain more insight into the signalling events involved in cell migration, we studied the mechanisms by which *D. discoideum* amoebae use cAMP to regulate cell migration using two approaches. First we determined the role of CAP in the aggregation and development of the aggregation deficient *aca⁻* cells and secondly we used the GFP technology to study the aspects of cell polarity and regulation of the actin cytoskeleton by expression of GFP fusions of CAP and its domains.

2.1 Expression of GFP fusions of CAP and its domains in *aca⁻* cells

We first investigated the expression levels of GFP fusions of CAP and its domains in the *aca⁻* cells. The schematic representation of the domain fusions is shown below.

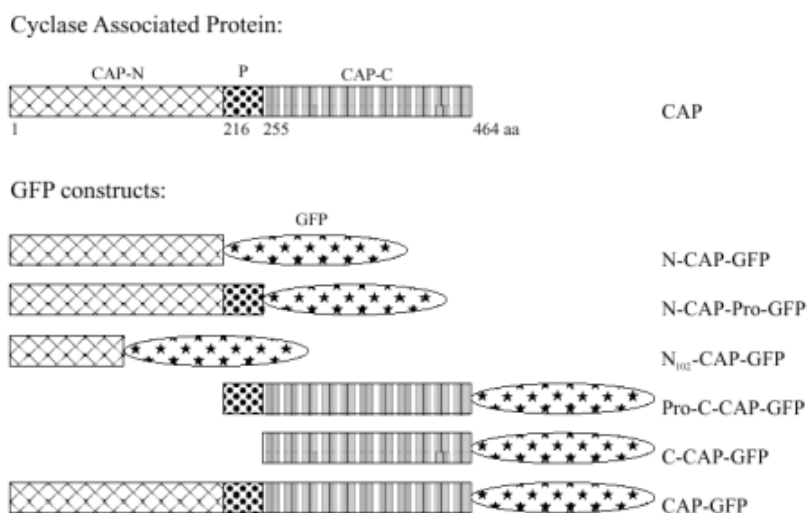


Figure 43: Schematic representation of GFP fusions of CAP and its domains.

For expression of specific domains fused to GFP, we used the N-terminal domain of CAP without (amino acid residues 1 to 215) and with the proline rich region (amino acid 1-254). For the C-terminal domain fusions with (residues 216-464) or without (amino acids 255-464) the proline rich regions were used. The PCR products were cloned in frame into the pDdA15GFP vector giving rise to proteins N-terminally fused to GFP. Transcription of the fusion genes are under the control of the actin 15 promoter allowing expression during growth and development (Noegel et al., 1999).

The expression levels of GFP fusion of CAP and its domains in *aca*⁻ cells were detected by immunoblotting. The immunoblots shown below confirmed the expression of CAP in the *aca*⁻ cells and *aca*⁻ transformants stably expressing CAP-GFP fusion protein.

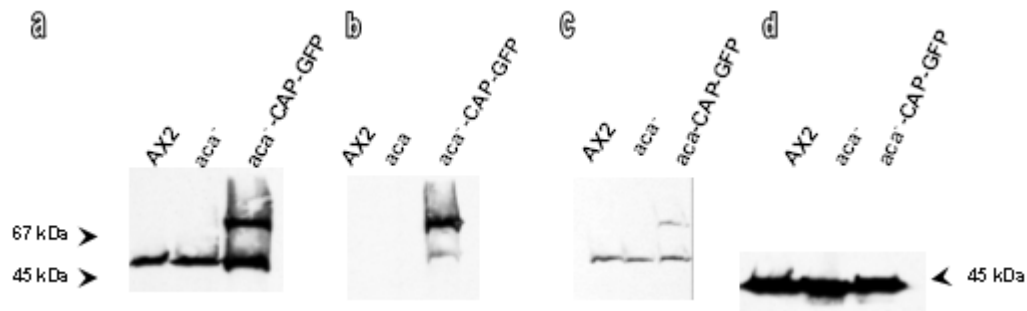


Figure 44: Immunoblots demonstrating the expression of endogenous CAP and CAP-GFP in *aca*⁻ cells. 5×10^5 cells were lysed in 2x sample buffer and separated by SDS-PAGE (12% acrylamide), blotted and probed. Immunoblot (a) is probed with mAb 230-18-8, detecting the endogenous CAP (50 kDa) and the CAP-GFP (~80 kDa). Blot (b) is immunostained with the GFP specific monoclonal antibody K3-184-2 which only picks up the CAP-GFP band, and the blot (c) is stained with C-terminus specific CAP monoclonal antibody 223-445-1 which shows both the endogenous and the CAP-GFP. In (d) actin is detected with mAb act-1-7 serving as loading control.

In *aca*⁻ cells CAP is expressed in amounts comparable to the wild type and the CAP-GFP levels were comparable to the levels of endogenous CAP. The immunoblots also showed that the GFP fusions were stably expressed in the absence of ACA (Figure 44, 45) and their levels were not affected by ACA.

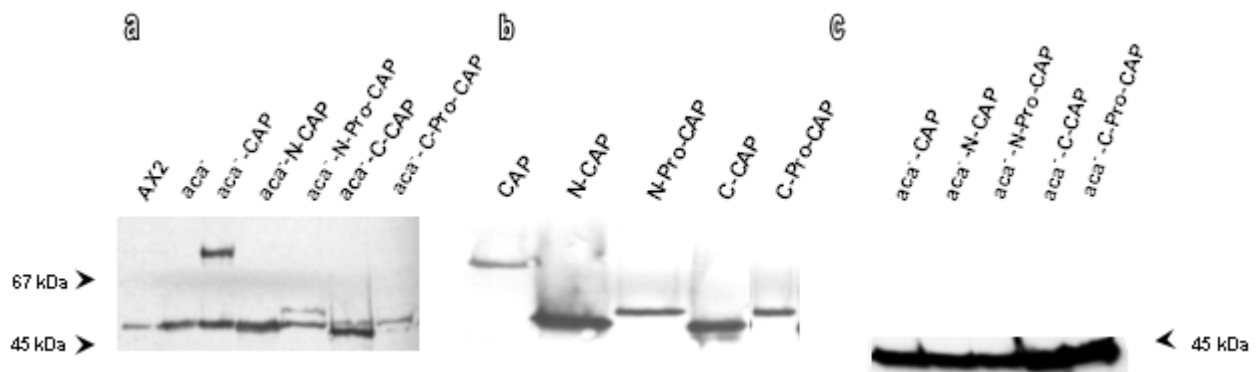


Figure 45: Expression of CAP GFP fusions in *aca*⁻ cells. ACA transformants stably expressing CAP GFP fusions were analysed by western blotting. 5×10^5 cells were lysed and loaded onto SDS-PA gels (12% acrylamide). The blots were then stained with mAb 230-18-8 detecting full-length CAP and N-terminal fusion proteins, which in part were close in molecular mass to CAP (a.). In (b) the blot is probed with GFP specific mAb K3-184-2, showing only the GFP fusions of CAP. In (c) the blot was stained with mAb act-1-7 for control.

2.2 Localization of CAP GFP fusions in *aca*⁻ cells

In AX2 transformants the full length CAP-GFP protein is enriched in the peripheral regions, and the cytoplasm shows a weak overall staining. GFP tagged N-CAP and N-Pro-CAP fusion proteins were present throughout the cytoplasm and also showed an accumulation at the cell periphery. This distribution is nearly identical to the one observed for the full length CAP-GFP. C-CAP-GFP and Pro-C-CAP-GFP fusions were present throughout the cytosol without being enriched at the periphery.

of the cells (Noegel et al., 1999). In the *aca*⁻ cells CAP-GFP and the GFP tagged domains showed a similar distribution. Also, the endogenous CAP was present all over the cytosol and was enriched at the cell cortex and co-localized perfectly with the full length and the N-terminal GFP fusions whereas in case of cells expressing the C-terminal domains fused to GFP co-distribution was observed only in the cytosol in the *aca*⁻ cells. These data indicate that ACA is not required for targeting CAP and its domains to the cell cortex and does not interfere with the distribution of CAP (Figure 46).

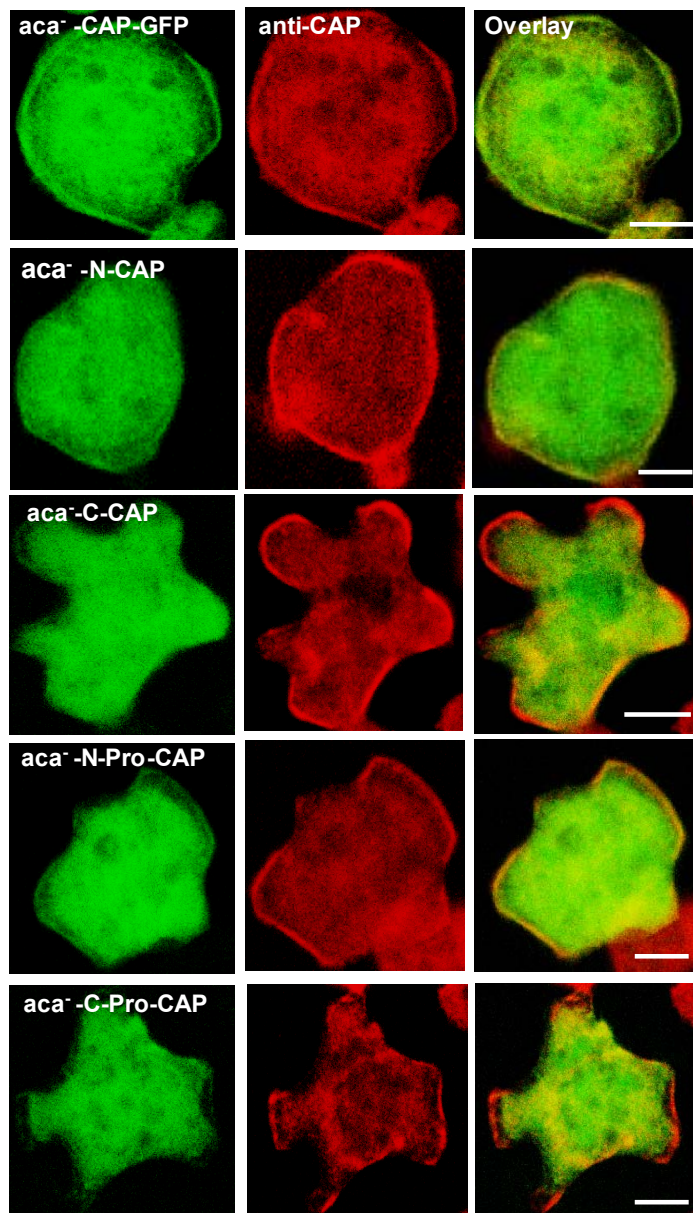


Figure 46: Localization of GFP tagged CAP and its domains in *aca*⁻ visualised by confocal microscopy. The ACA transformants were fixed with methanol and Immunostained with mAb 230-18-8 followed by a specific Cy3 conjugated secondary antibody. In cells expressing CAP-GFP, the fusion protein (top panel) is present in the cytosol and most prominently close to the membrane. The N-domain fusions of CAP-GFP showed that the protein is present throughout the cell and particularly enriched at the cell borders (shown in second and fourth panel). In case of C-domain fusions of CAP with GFP, the protein is present throughout the cell and does not show the enrichment at the membrane (third and the last panel). The endogenous CAP localizes to the cell membrane and also weakly stains the cytosol. Bar, 10 μ m.

2.3 Moderate overexpression of CAP rescues the aggregation defect of *aca*⁻ cells

Cells lacking the aggregation stage specific adenylyl cyclase (ACA) cannot aggregate (Patel et al., 2000). They are however capable of moving up a chemoattractant gradient but are unable to stream as they are deficient for polarity (Kriebel et al., 2003). In order to gain more insight into the role of CAP in the process of aggregation, we made use of the *aca*⁻ and *aca*⁻ cells expressing CAP-GFP. The *aca*⁻

cells expressing CAP-GFP and appropriate control cells were starved for 6 hrs, allowed to adhere onto the glass coverslip and immunolabelled with the CAP specific mAb.

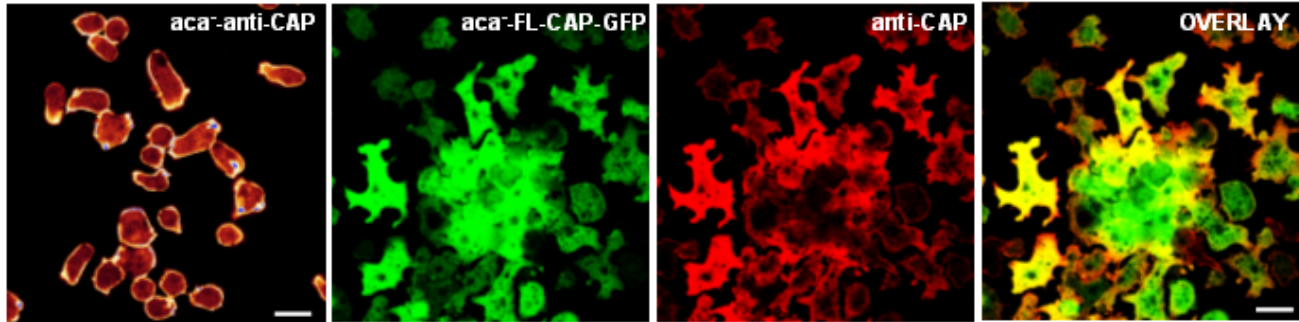


Figure 47: Role of CAP-GFP in aggregation of the *aca*⁻ cells. The *aca*⁻ cells expressing CAP-GFP were starved for aggregation competence for 6 hrs and the cells were fixed and immunolabelled with mAb 230-18-8 to detect the distribution of CAP. CAP-GFP expressing cells form aggregation centres and were polarised indicating that CAP-GFP expression enhances aggregation in *aca*⁻ cells. Bar, 10 μ m.

The *aca*⁻ cells showed an enrichment of endogenous CAP at the cortex of moving cells *in vivo* (data not shown). At t_6 they showed structures similar to aggregation centres or mounds and the cells seemed to be polarized although we did not note stream formation. Furthermore, the generation of cell polarity influenced the cells to develop extensive pseudopods where CAP-GFP was enriched (Figure 47).

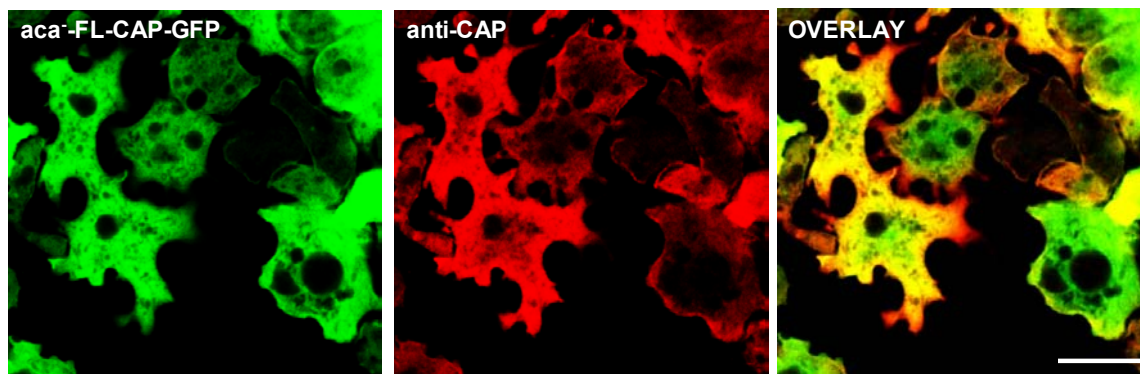


Figure 48: CAP-GFP in individual *aca*⁻ cells during aggregation. The *aca*⁻ cells expressing CAP-GFP were allowed to aggregate and CAP-GFP as well as endogenous CAP distribution was tested. The endogenous CAP was highly enriched at the extreme leading edges and cortex of the aggregating cells. Bar, 10 μ m.

It was also observed that the endogenous CAP accumulated at the cortex and showed a distribution slightly different from the one of CAP-GFP because it was found in peripheral regions where no CAP-GFP was present (Figure 48). However, CAP-GFP dominated the aggregation centres and streaming mounds. The GFP-CAP strongly co-localized with the endogenous protein at the cytosol. Taken together, expression of CAP-GFP enhances the aggregation of the aggregation deficient *aca*⁻ cells and improves the acquisition of the cellular polarity dependent on the actin cytoskeleton and its regulators.

2.3.1 Role of CAP-GFP fusions in the *aca*⁻ cells during aggregation

We next tested which domain of CAP is involved in improving the aggregation of the *aca*⁻ cells. N-Pro-CAP-GFP expressing *aca*⁻ cells behaved in a way similar to cells expressing the full length CAP-GFP in regard to the formation of aggregation centres, where they co-distributed with the endogenous CAP. However, cells expressing the C-terminal domains showed fewer and smaller aggregates in comparison to the full length and the N-terminal fusions. Moreover, a strong antibody staining was observed at the cortex of the cells without accumulation of C-CAP-GFP. It seems that the N-terminal domain of CAP is sufficient to improve aggregation of *aca*⁻ cells (Figure 49).

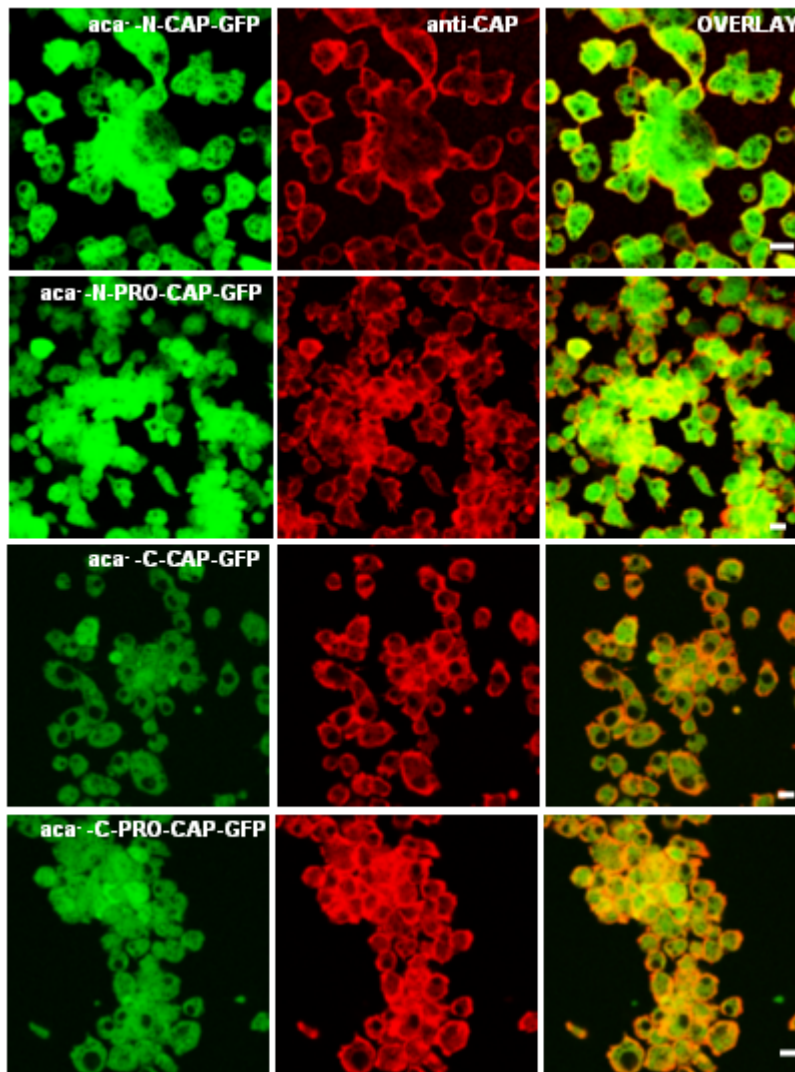


Figure 49: Role of GFP fusions of CAP in the aggregation of the *aca*⁻ cells. The *aca*⁻ cells expressing the GFP fusion of CAP were fixed with methanol and immunostained with the CAP specific antibody 230-18-8 to detect the distribution of the GFP fusions. The confocal microscopy visualises that the N-terminus with proline rich region is the domain of CAP involved in the aggregation of the *aca*⁻ cells. Similar results were obtained with this domain of CAP from the second clone studies. Bar, 10 μ m.

2.4 Agglutination of the *aca*⁻ cells expressing CAP-GFP and N-CAP-Pro-GFP

To substantiate the confocal microscopy data, we obtained the images of the agglutinating *aca*⁻ cells expressing CAP-GFP and N-Pro-CAP-GFP using a phase contrast microscope. The *aca*⁻ cells were kept in the starvation buffer to acquire aggregation competence and images were taken at various

time points to document the formation of the agglutinates. AX2 wild type and AX2 cells expressing CAP-GFP were taken as controls.

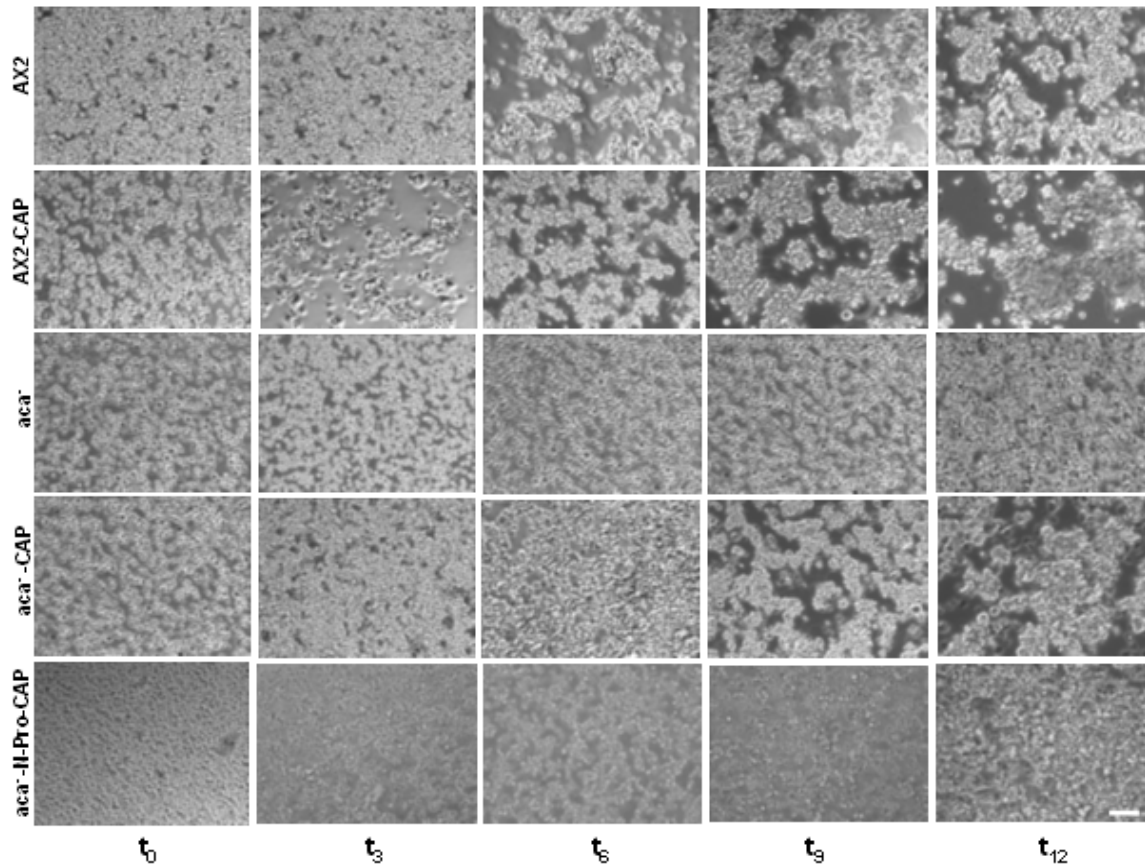


Figure 50: Agglutination of *aca*⁻ cells expressing the CAP-GFP and N-CAP-Pro-GFP. Phase contrast microscopy showing the agglutinating *aca*⁻ cells expressing the CAP-GFP and N-Pro-CAP in suspension. 1×10^7 cells were shaken in Soerenson phosphate buffer, and images were obtained at times indicated using 20x bright field phase contrast microscope (Olympus). AX2 cells and AX2 expressing CAP are our controls. The phase contrast images reveal that the *aca*⁻ cells do not form any aggregates, whereas the null cells expressing the CAP-GFP and N-CAP-Pro-GFP form aggregates. The bar indicates 100 μ m.

The agglutinate formation in the AX2 cells expressing CAP-GFP was noticed to be faster and greater than in the AX2 wild type, as they started agglutinating before the 3 hr of starvation and formed bigger aggregates at later times. The phase contrast microscopy revealed that the *aca*⁻ cells are deficient for aggregation, however expression of the CAP-GFP complements the aggregation defect of the *aca*⁻ cells and agglutinates are formed at time from 4-6 hrs of starvation and increase with time (Figure 50). Moreover, it was also seen that the GFP-N-Pro- CAP allowed the cells to adhere to each other in the absence of ACA, but the agglutinates were smaller and formed at a slower rate compared to the *aca*⁻ cells expressing CAP-GFP (Figure 50). The agglutination of the *aca*⁻ cells expressing CAP-GFP was also quantified. The cells were shaken in suspension under starvation conditions and the optical density at 600 nm was measured at the times indicated using a spectrophotometer. The starting OD was considered to be 100% for each strain. From the quantitative agglutination it was

observed that the AX2 cells expressing CAP-GFP agglutinated more than one fold of AX2 wild type. Also, the *aca*⁻ cells expressing CAP-GFP agglutinated significantly similar to AX2 (Figure 51).

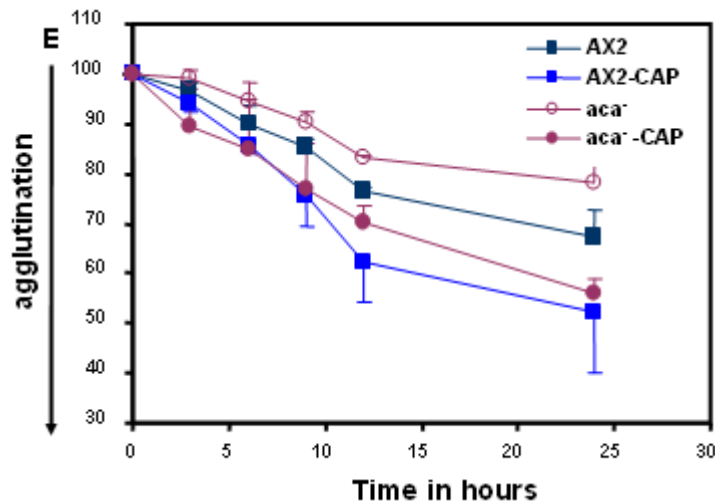


Figure 51: Time course of agglutination of *aca*⁻ cell expressing CAP-GFP. 1×10^7 cells / ml were shaken in Soerenson phosphate buffer, and the OD 600 nm was measured at times 0, 3, 6, 9 and 12 hrs using a spectrophotometer. The *aca*⁻ cells expressing CAP-GFP agglutinated in a similar way to AX2. Each point indicates the mean of three independent experiments. Bars represent the standard deviation.

2.5 Developmental phenotypes of *aca*⁻ cells expressing CAP-GFP

The *Dictyostelium* cells aggregate during starvation under submerged conditions, while post aggregation development and fruiting body formation require a solid substratum. The commonly used substratum in the laboratory to study development is agar. To determine the role of CAP-GFP during the early stages of development, equal amounts of cells were placed on phosphate agar under starvation and the developmental stages were captured using the phase contrast microscope at 20 hrs of development. The developmental phenotypes captured by phase contrast microscopy showed that wild type AX2 cells and AX2 cells expressing CAP-GFP formed fruiting bodies, although the expression of CAP-GFP enhanced the rate of development. The *aca*⁻ cells failed to enter the developmental programme. However *aca*⁻ cells expressing CAP-GFP and N-CAP-Pro-GFP showed an enhancement in the development of the aggregation deficient *aca*⁻ cells, and formed streams of moving cells and aggregates with highly polarised cells reaching the aggregation centres. The data suggest that moderate CAP and N-Pro-CAP expression improves the development of the *aca*⁻ cells but does not allow complete restoration (Figure 52).

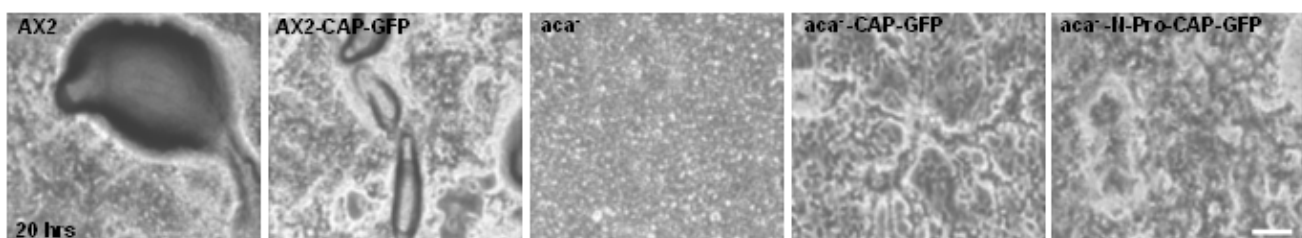


Figure 52: Development in the *aca*⁻ cells expressing CAP-GFP and N-CAP-Pro-GFP. The strains were plated in monolayer on phosphate agar depleted of any nutrients and allowed to undergo development at 21 °C. The images were captured using a 20X bright field phase contrast microscope at 20 hrs of development. Significant differences were seen in the development of the *aca*⁻ cells and mutant expressing CAP-GFP and N-CAP-Pro-GFP, which showed the formation of aggregating mounds albeit they could not develop into fruiting bodies. The bar indicates 100 μ m.

2.6 Cell adhesion mechanism in the *aca*⁻ cells expressing CAP-GFP and N-CAP-Pro-GFP

To address if the CAP mediated aggregation in the *aca*⁻ cells expressing the GFP fusions of CAP is Ca²⁺ dependent, an attempt was made to analyse the mechanism of cell adhesion in *aca*⁻ cells. Soon after the initiation of the developmental cycle of *Dictyostelium*, cells acquire EDTA-sensitive cell-cell contacts mediated by the glycoprotein gp24. Cells at the aggregation stage display a second type of cell adhesion site, the EDTA-resistant cell-cell binding sites, mediated by the glycoprotein gp80 (Desbarats et al., 1994). Cells were shaken in starvation buffer and cultures were drawn from the master flask and shaken in the presence or absence of 10mM EDTA in 24 well plates for an additional hour. Images were taken every 3 hrs using a phase contrast microscope both in the presence or absence of EDTA to visualise the differences in the agglutination of the strains.

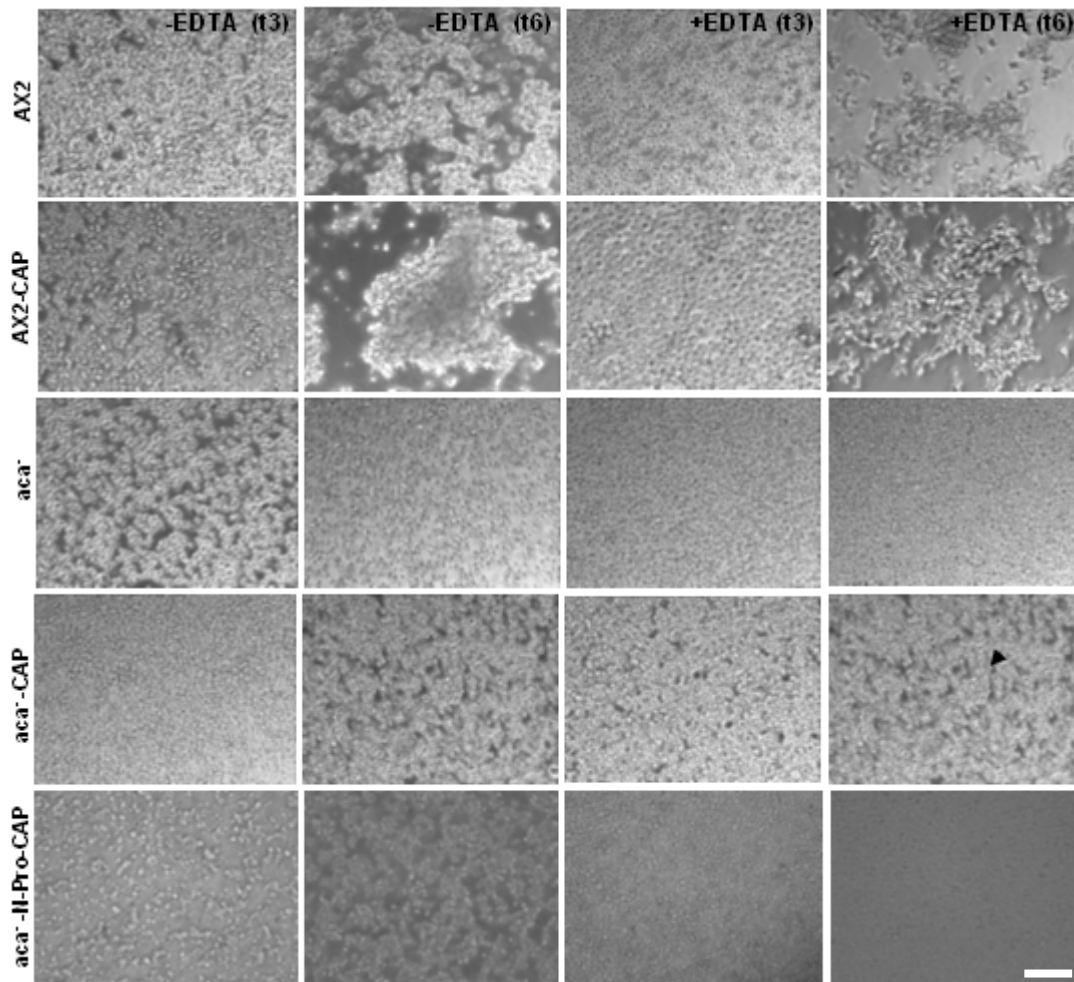


Figure 53: Cell to cell adhesion in the *aca*⁻ cells expressing CAP-GFP and GFP-N-Pro- CAP in the presence or absence of EDTA. 1×10^7 cells washed twice with Soerenson phosphate buffer were shaken in suspension at 21 °C in the same buffer. Samples were withdrawn at the indicated time points and shaken in Nunc well dishes in the presence or absence of 10 mM EDTA. Images were obtained using a 20 X bright field phase contrast microscope. AX2 and AX2 expressing CAP-GFP are the control panels. It was observed that *aca*⁻ cells expressing CAP-GFP and N-CAP-Pro-GFP agglutinate in the absence of EDTA and remain isolated in the presence of EDTA indicating that the cell contacts formed are sensitive to EDTA. Arrow indicates the formation of small agglutinates by *aca*⁻ cells expressing CAP-GFP even in the presence of EDTA. The bar indicates 100 μ m.

The images revealed that AX2 and AX2 cells expressing CAP-GFP starts agglutinating at 3 hrs and develop into large aggregates at 6 hrs, and proceed to form much larger agglutinates at later time points in the absence of EDTA, albeit it was seen that expression of CAP-GFP enhances the aggregation in AX2 as they seem to form much larger aggregates at 6 hrs of starvation in comparison to AX2. Addition of EDTA postponed aggregation for 5-6 hrs of starvation until the EDTA resistant gp80 cell adhesion molecule is expressed. At 6 hrs, the AX2 and AX2-CAP-GFP cells were seen to form EDTA stable aggregates. With the *aca*⁻ cells expressing the CAP-GFP and N-CAP-Pro-GFP we noticed that they developed into aggregates at 6 hrs of starvation in the absence of EDTA. The aggregates were much smaller than in the wild type and remained sensitive to EDTA, although some small aggregates were seen in the *aca*⁻ cells expressing CAP-GFP (shown by arrowhead) even in the presence of EDTA. The results were highly reproducible and also observed in an independent cell line. These results imply that *aca*⁻ cells expressing CAP-GFP were able to form EDTA sensitive cell contacts and develop into mounds. They also show that the cell adhesion mechanism is Ca²⁺ dependent (Figure 53).

2.7 Time course and quantification of cell-cell adhesion in the *aca*⁻ cells expressing CAP-GFP and N-CAP-Pro-GFP

To determine the time course of agglutination rates and the cell cohesion mechanism of *aca*⁻ cells expressing CAP-GFP and N-CAP-Pro-GFP a quantitative analysis of agglutination was carried out in both the presence and absence of 10 mM EDTA. The agglutinating cells in the cultures were optically determined by measuring the cell density at OD 600nm with/without EDTA at every half hour after the start of starvation. This analysis revealed that AX2 and AX2 cells expressing CAP-GFP agglutinated to a faster and greater extent in the absence of EDTA and were agglutinating at slower rates in the presence of EDTA. These results denoted that the cell adhesion in the wild type strains is sensitive to EDTA at a certain period but becomes resistant after 6 hrs as the expression of the *csA* adhesion molecule (gp80) enhances the agglutination even in the presence of the Ca²⁺ chelator and shows the EDTA resistant cell adhesion mechanism. Moreover, it was also observed that AX2 cells expressing CAP-GFP were able to agglutinate at faster rates. The agglutination of the *aca*⁻ cells expressing CAP-GFP showed the formation of agglutinates only in the absence of EDTA, indicating that they were sensitive to EDTA. It was also observed from the agglutinating curves of the *aca*⁻ cells expressing CAP-GFP that the agglutination was 1.5 fold greater in the absence of EDTA when compared to the curves showing the agglutination in the presence of EDTA suggesting that CAP mediating aggregation is EDTA sensitive (Figure 54).

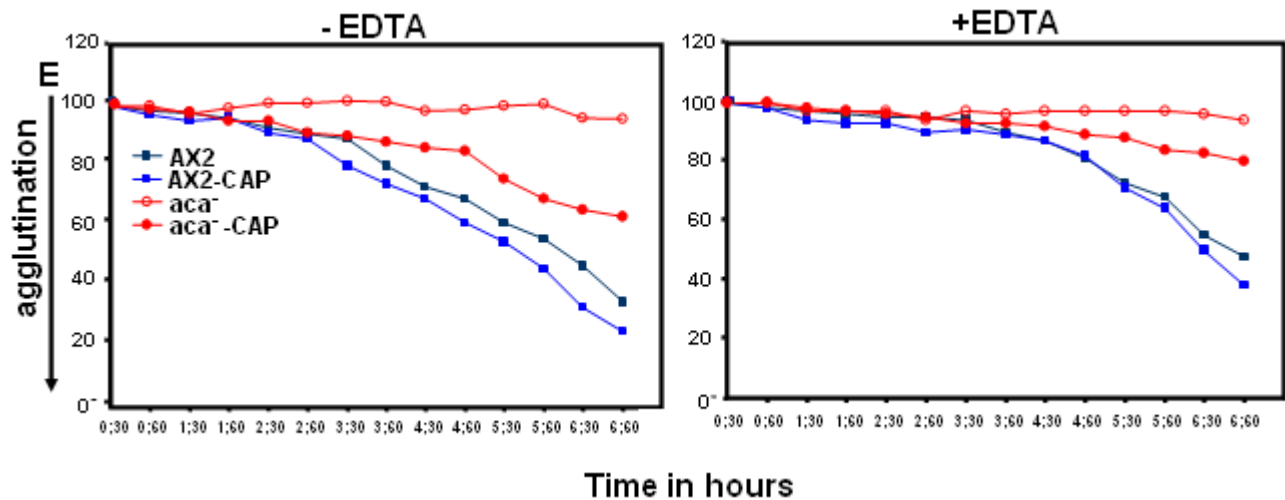


Figure 54: Quantitative agglutination of *aca⁻* cells expressing CAP-GFP. 1×10^7 cells/ml were shaken in starvation buffer in the presence or absence of 10 mM EDTA to detect whether the cell cohesion mechanism is Ca^{2+} dependent or independent. The OD 600 nm was obtained at the times indicated to measure the decrease in individual cell number as agglutination progresses in the presence or absence of EDTA using a spectrophotometer. The results are the mean of at least four independent experiments. The curves show that the *aca⁻* cells expressing CAP-GFP agglutinate in the absence of EDTA, however they were sensitive to EDTA and the rate of agglutination was almost declined. The agglutination was 1.5 fold more seen in the *aca⁻* cells expressing CAP-GFP in the absence of EDTA in comparison to the agglutination in the presence of 10 mM EDTA.

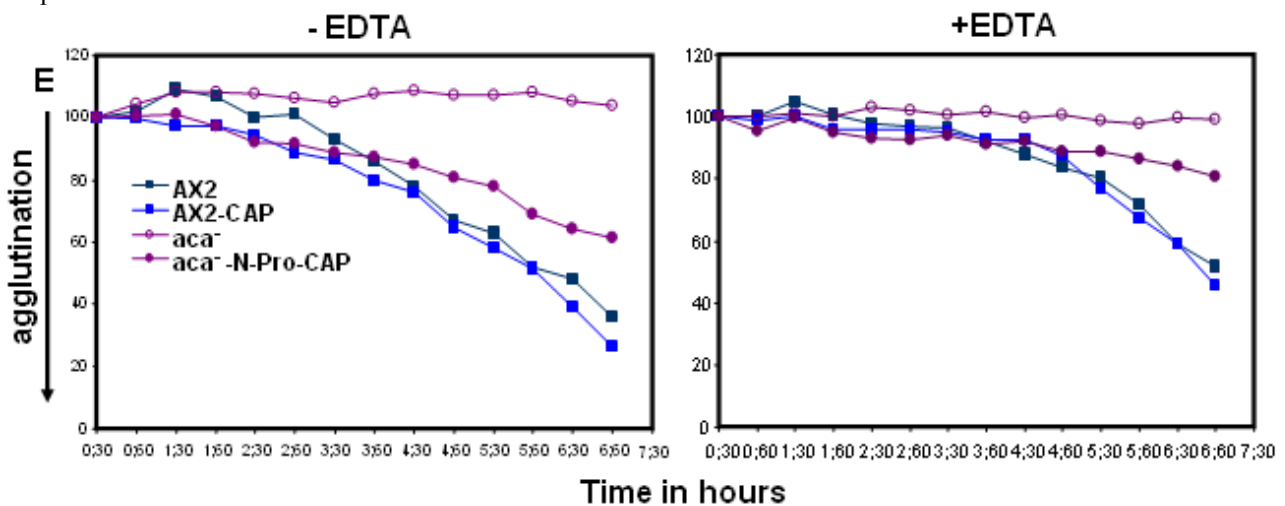


Figure 55: Quantitative agglutination of *aca⁻* cells expressing N-CAP-Pro-GFP. 1×10^7 cells/ml were shaken in starvation buffer in similar conditions described for the CAP-GFP, in the presence or absence of 10 mM EDTA. The OD measurements at 600 nm were obtained using a spectrophotometer. The reading shows agglutination in the presence or absence of EDTA. Data shown represent the results of at least four independent experiments. The curves obtained for the *aca⁻* cells expressing GFP-N-Pro-CAP reveal that they agglutinate in the absence of EDTA however they were sensitive to EDTA.

The *aca⁻* cells expressing the N-CAP-Pro-GFP behaved in a way similar to the full length CAP and agglutinated in the absence of EDTA and remained to be sensitive to EDTA. The rate of agglutination exhibited by the *aca⁻* cells expressing N-CAP-Pro-GFP was 1.5 fold greater in the absence of EDTA and declined in the presence of EDTA. Moreover the rates of agglutination exhibited by both the *aca⁻* cells expressing CAP-GFP and N-CAP-Pro-GFP was 1.5 fold more in the absence of EDTA, which indicates that the cell adhesion mechanism occurring is the same in both the strains. These

quantitative agglutination results also correlated with and confirmed the images obtained in the presence or absence of EDTA, and further indicated that CAP mediated aggregation in *aca*⁻ cells is EDTA sensitive or calcium dependent (Figure 55).

2.8 Expression of cAR1 receptor in the agglutinating *aca*⁻ cells expressing CAP-GFP and N-CAP-Pro-GFP

The *aca*⁻ cell expressing CAP-GFP and its N-CAP-Pro-GFP were analysed for the presence of cAMP receptor 1 (*carA*) mRNA, a marker for early development. The AX2, AX2 cells expressing CAP-GFP and the *aca*⁻ cells are shown in the control panels. The cells were allowed to develop synchronously in shaking suspensions under starvation conditions and total RNA was extracted from each strain. The RNA samples were resolved on agarose gels in the presence of formaldehyde and blotted on nitrocellulose membrane. The cAMP receptor 1 (*carA*) (Klein et al 1988) was detected in all control panels and also in RNA from the *aca*⁻ cells expressing CAP-GFP and N-CAP-Pro-GFP (Figure 56).

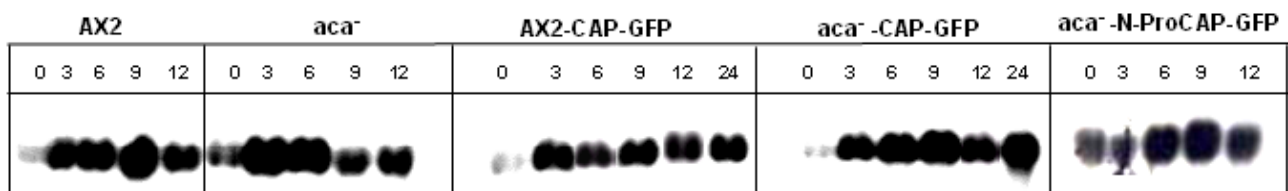


Figure 56: Expression of developmentally regulated gene cAR1 in the *aca*⁻ cells expressing CAP-GFP and N-CAP-Pro. 1×10^7 cells/ml were allowed to develop under starvation conditions and total RNA was isolated from each strain at the times (in hours) indicated. 20 μ g RNA per time point were resolved by gel electrophoresis and transferred to membranes for northern blot analysis using the cAR1 probe. The blot showed the cAR1 message in the *aca*⁻ cells expressing CAP-GFP and N-CAP-Pro-GFP as compared to the controls.

2.9 Expression of cell adhesion molecules in the *aca*⁻ cells expressing CAP-GFP and N-CAP-Pro-GFP

The development of *Dictyostelium* displays many of the features of animal embryogenesis, including regulated cell-cell adhesion. The mechanism governing this process is similar to epithelial sheet sealing in animals. During early development in *Dictyostelium* some of the molecules expressed mediate cell-cell adhesion between amoebae as they form a loosely packed multicellular mass. Soon after the initiation of the developmental cycle of *Dictyostelium*, cells acquire EDTA-sensitive cell-cell contact sites mediated by the glycoprotein gp24. Cells at the aggregation stage display a second type of cell adhesion sites, the EDTA-resistant cell-cell binding sites, mediated by the glycoprotein gp80/csA (Desbarats et al., 1994). We analysed the cell adhesion mechanism occurring in the *aca*⁻ cells expressing CAP-GFP and the N-Pro-CAP-GFP. Furthermore, we determined the expression levels of the cell adhesion molecules csA and DdCAD1 in the *aca*⁻ cells expressing CAP-GFP and N-CAP-Pro-GFP, by western and northern blot analysis. For the western blot analysis cells were starved

and samples were withdrawn at the times indicated and preceded for immunoblotting using a csA specific mAb. AX2 and AX2 cells expressing CAP-GFP were the controls. The csA mAb detected the csA protein at 80 kDa in the control strains however no csA was detected in the *aca*⁻ cells and cells expressing CAP-GFP and N-Pro-CAP-GFP (Figure 57a). We also looked at the CAP level which was found to be unaltered (Figure 57b).

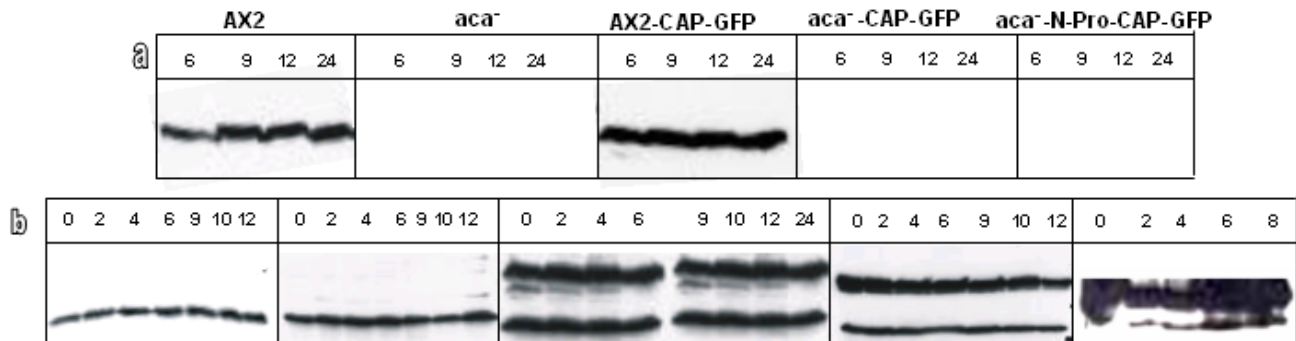


Figure 57: Immunoblot to detect the csA cell adhesion molecule (gp80) in the *aca*⁻ cells expressing CAP-GFP and GFP-N-CAP-Pro. (a) Cells were allowed to develop and 1 ml cultures were withdrawn at the times (in hours) indicated, and lysed in 2X lysis buffer, and the proteins were resolved in SDS-PA gels (10% acrylamide). The immunoblot was labelled with csA specific mAb 33-249-17, followed by a horseradish peroxidase coupled secondary antibody. No csA was detected in the *aca*⁻ cells and cells expressing GFP fusions of CAP. (b) The blots were re-probed with the CAP specific mAb 230-18-8 to see the levels of endogenous CAP (50 kDa) and CAP-GFP (80kDa) and GFP-N-CAP-Pro (55kDa), which were found to be unaltered.

As CAP-GFP expression led to an enhancement in the agglutination we determined the levels of csA in the AX2 and cells expressing CAP-GFP.

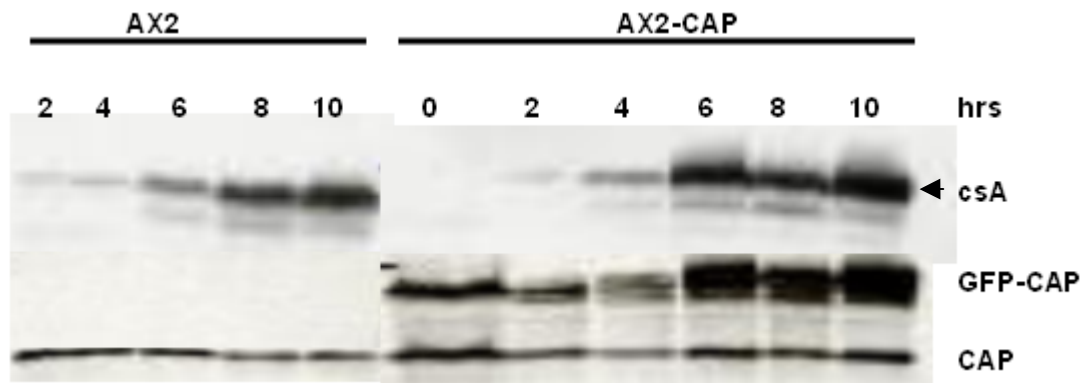


Figure 58: Immunoblot detecting the csA cell adhesion molecule in AX2 and AX2 cells expressing CAP-GFP. 1×10^7 cell/ml were allowed to develop under starvation conditions and 1ml cultures were withdrawn at the times indicated, cells were lysed in 2X lysis buffer, resolved on SDS-PA gels (10% acrylamide). The immunoblot was labelled with csA specific mAb 33-249-17 followed by a horseradish peroxidase coupled secondary antibody. The csA immunoblot showed that csA was expressed more strongly in the AX2 cells expressing GFP in comparison to the AX2 (top panel, the arrow indicates the glycosylated form of the csA glycoprotein, which is 80 kDa) These blots were re-probed with mAb 230-18-8 (lower panel) to see the levels of CAP which were found to be unaltered.

The results of the immunoblots showed that the csA was expressed at an earlier time in AX2, when compared to AX2 cells expressing CAP-GFP (Figure 58). Since in *aca*⁻ cells no csA protein was detected by western blot analysis, we tried to detect the expression of csA at the transcript level. A

northern blot containing RNA from various stages was probed with *csA* cDNA probe, which detected the transcripts in the AX2 wild type and AX2 cells expressing CAP. A faint signal was seen in *aca*⁻ cells expressing the CAP-GFP (Figure 59a). The blots were re-probed with a CAP cDNA for control (Figure 59b).

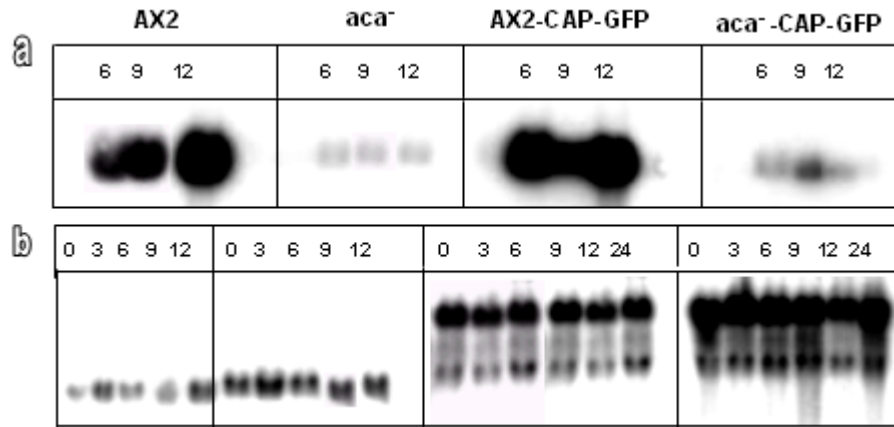


Figure 59: Expression of cell adhesion molecule *csA* in the *aca*⁻ cells expressing CAP-GFP as detected by northern blot analysis. (a) 1×10^7 cells/ml were allowed to develop under starvation conditions and total RNA was isolated using Qiagen RNaseasy kit. 20 μ g RNA per time point were resolved by gel electrophoresis and transferred to nitrocellulose membranes for northern blot analysis and probed with the *csA* probe. The northern blot analysis detected a faint *csA* message in the *aca*⁻ cells expressing CAP-GFP as compared to the AX2 and AX2 cells expressing CAP-GFP control panels. (b) The blot was re-probed with the CAP cDNA to see the CAP expression at the transcript level in the agglutinating cells.

Furthermore, to substantiate the EDTA sensitive cell adhesion mechanism in *aca*⁻ cells expressing CAP-GFP and the N-CAP-Pro-GFP, we investigated the expression of the calcium dependent cell adhesion molecule, DdCAD1 at the mRNA level. Soon after the initiation of *Dictyostelium*, cells acquire EDTA-sensitive cell-cell binding sites mediated by the glycoprotein gp24 (DdCAD1). Cells at the aggregation stage display a second type of cell adhesion site, the EDTA-resistant cell-cell binding site, mediated by the glycoprotein gp80.

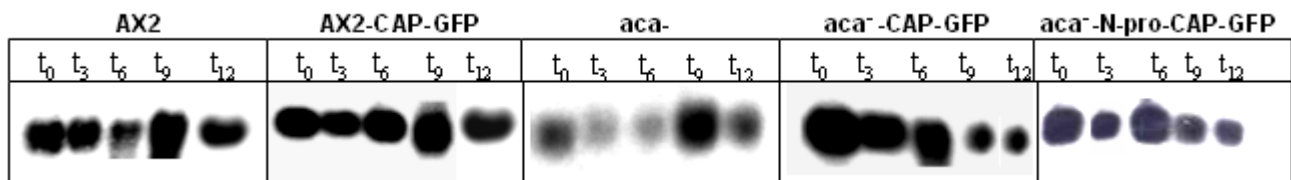


Figure 60: Expression of DdCAD1 cell adhesion molecule in the *aca*⁻ cells expressing CAP-GFP and GFP-N-CAP-Pro by northern blot analysis. 20 μ g total RNA per time point were resolved by gel electrophoresis and transferred to nitrocellulose membranes for northern blot analysis with the gp24/ DdCAD1 probe. The northern blot analysis showed that there is enhancement in the expression of the DdCAD1 cell adhesion molecule in the *aca*⁻ cells expressing CAP-GFP and GFP-N-CAP-Pro in comparison to the *aca*⁻ cells.

The northern blot analysis indeed revealed that the expression of the DdCAD1 is enhanced in the *aca*⁻ cells expressing CAP-GFP and N-CAP-Pro-GFP in comparison to the *aca*⁻ cells (Figure 60). These results also correlated with the enhancement seen in the agglutination of the *aca*⁻ cells expressing

CAP-GFP and N-CAP-Pro-GFP in the absence of EDTA. All these results suggest that the CAP mediated aggregation seen in the absence of ACA is Ca^{2+} dependent, where DdCAD1 could play an important role.

2.10 Distribution of polarity markers in the *aca*⁻ cells and *aca*⁻ cells expressing CAP-GFP and N-CAP-Pro-GFP

The actin based cytoskeleton is comprised of actin, myosin and actin associated proteins, which are the primary regulators of cell shape and movement in the eukaryotic cells. To understand the concept of cell polarity during aggregation, we investigated the distribution of the cell polarity markers like myosin, α -actinin and filamin in the *aca*⁻ cells and null cells expressing GFP fusions of CAP. Myosin is a cell polarity regulator, which distributes to the posterior and lateral surface of the highly polarized cells, α -actinin is primarily a cytosolic protein, which shows abundant distribution in the cytoplasm and enriches at the leading fronts and tails in polarized cells. The actin binding protein filamin accumulates at the front and rear end of the cell and discontinuously along the periphery (Figure 61).

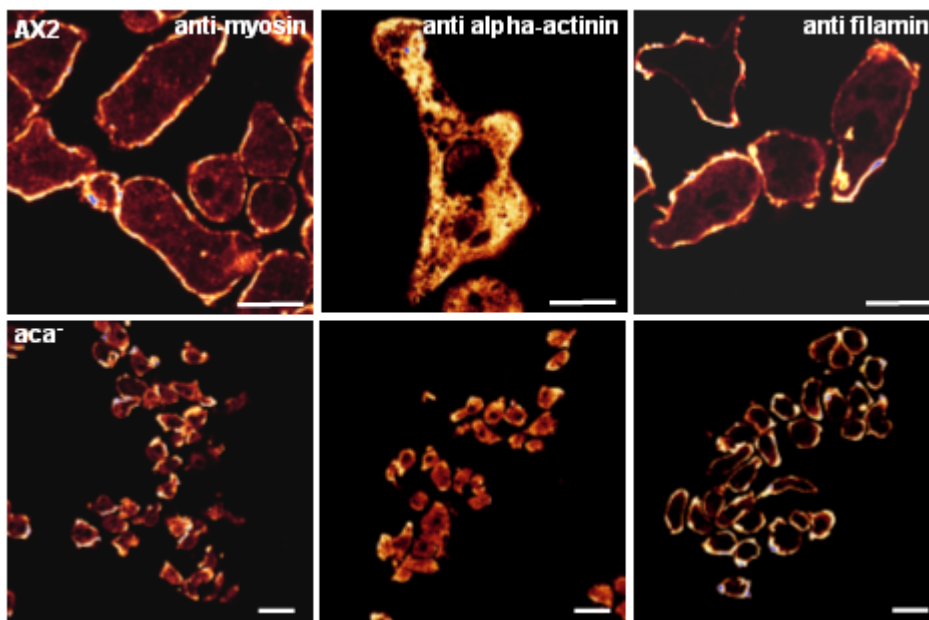


Figure 61: Distribution of cell polarity markers myosin, α -actinin and filamin. The AX2 and *aca*⁻ cells were challenged for aggregation competence, fixed and immunolabelled with the antibodies specific to myosin (56-395-2), α -actinin (47-62-2) and filamin (82-454-12) to detect the distribution of these markers in the *t*₆ cells of AX2 and *aca*⁻ cells. Myosin is seen at the posterior and lateral cell surface, α -actinin seen all over the cells with enrichment at the leading front and filamin was distributed strongly at the posterior end and discontinuously at the cell borders. The AX2 cells were polarised, whereas *aca*⁻ cells showed polarity defects. Bar, 10

To analyse the distribution of myosin, α -actinin and filamin in the *aca*⁻ cells expressing CAP-GFP and N-CAP-Pro-GFP, we performed immunofluorescence studies using cells after 6 hrs of starvation. The AX2 wild type and AX2 cells expressing CAP-GFP served as controls. In AX2 wild type cells the myosin distributed to the rear ends and also to the lateral sides. This distribution is thought to compress the formation of the lateral pseudopods during cell migration. The α -actinin was localised all over the cytosol with some enrichment at the leading edges of the cells, and filamin was distributed prominently at the posterior and discontinuously around the cell borders. The *aca*⁻ cells are

small and exhibit a polarity defect. Nevertheless it was observed that the *aca*⁻ cells show a similar pattern of distribution of these markers (Figure 61).

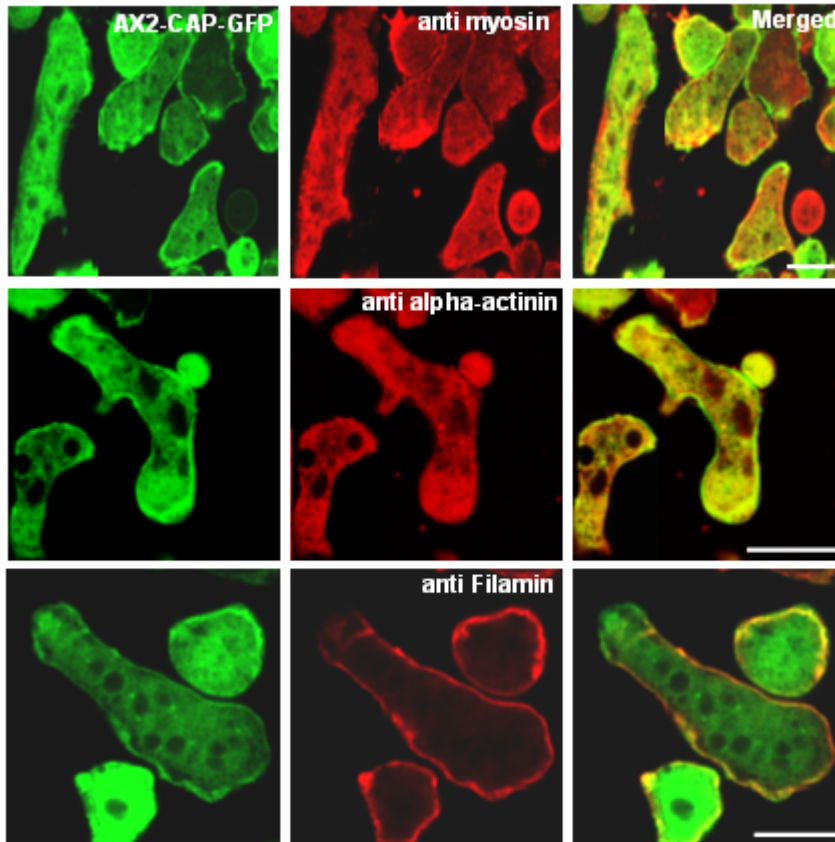


Figure 62: Distribution of cell polarity markers myosin, α -actinin and filamin in AX2 cells expressing CAP-GFP. The cells were starved for 6 hrs fixed and immunolabelled with the antibodies specific to myosin (56-395-2), α -actinin (47-62-2) and filamin (82-454-12) to detect the distribution of these markers. Confocal microscopy showed that myosin is present at the posterior end and lateral sides of the cells where it co-localizes with CAP-GFP at the posterior of the cell, α -actinin localizes all over the cell but is enriched at the leading front of the cell along with CAP-GFP and filamin was distributed strongly at the posterior like in AX2. The AX2 cells expressing CAP-GFP were highly polarised indicating that CAP-GFP rescues cell polarity. Bar, 10 μ m.

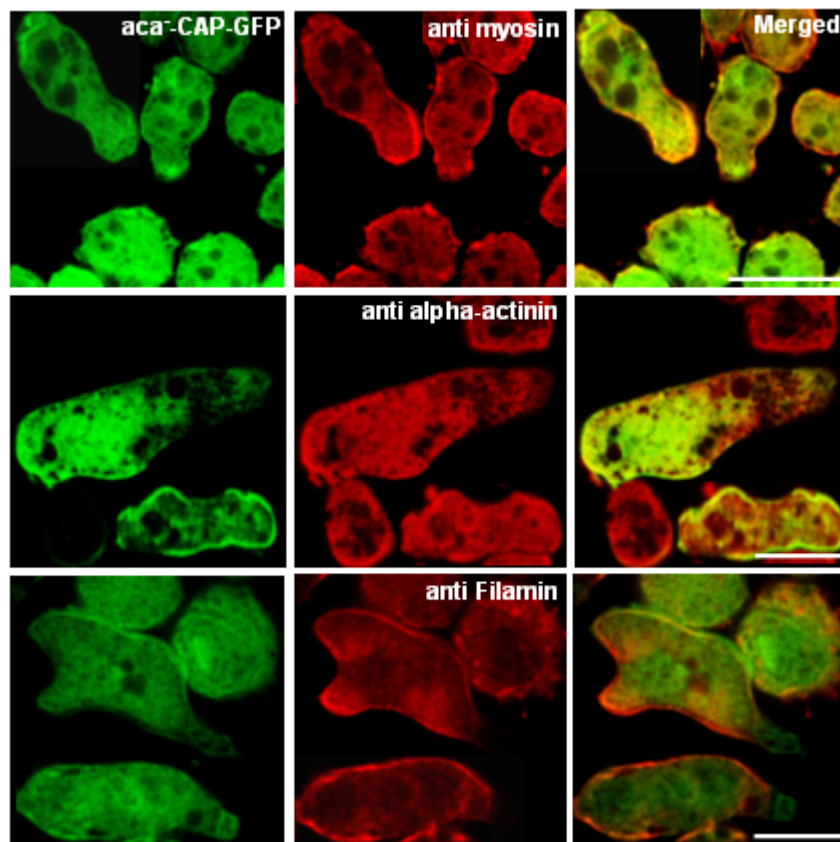


Figure 63: Distribution of cell polarity markers, myosin, α -actinin and filamin in the *aca*⁻ cells expressing CAP-GFP. The cells were starved for 6 hrs and immunostained with monoclonal antibodies specific to the polarity markers myosin (56-395-2), α -actinin (47-62-2) and filamin (82-454-12) to detect the distribution of these markers. Confocal microscopy showed myosin at the posterior and lateral sides of the cells where it co-localizes with CAP-GFP at the posterior, α -actinin was found to be all over the cell but enriched at the leading front as CAP-GFP and filamin was distributed strongly at the posterior like in AX2. The *aca*⁻ cells expressing CAP-GFP were polarised indicating that CAP-GFP restores cell polarity in the polarity deficient *aca*⁻ cells. Bar, 10 μ m.

AX2 cells expressing CAP-GFP (Figure 62), and *aca*⁻ cells expressing CAP-GFP (Figure 63) showed a very similar staining for the distribution of these polarity markers as in AX2. α -Actinin was at the posterior end of the cells where it co-localised with CAP-GFP, myosin was predominant at the lateral sides, allowing for a highly polarised cell shape and compressing the formation of lateral pseudopods to maintain the correct directionality of the cell. The CAP-GFP was co-localising with α -actinin at the leading fronts and all over the cell in both AX2 and *aca*⁻ cells expressing CAP-GFP. The distribution of filamin was also comparable to the one in wild type, where it was highly enriched at the posterior and discontinuously at the cell cortex, CAP-GFP seems to be co-localising with filamin at the posterior end and in some filamin rich membrane areas (Figure 63). The *aca*⁻ cells expressing N-CAP-Pro-GFP showed myosin at the lateral and posterior sides of the cells, the N-CAP fusion protein was distributed all over the cell with enrichments at the cell cortex. α -Actinin was enriched at the leading fronts and all over the cell and co-localised with N-CAP-Pro-GFP at some parts. The cells showed a clear and prominent distribution of filamin that was highly enriched at the rear end of the cells and did not seem to merge with the N-CAP-Pro-GFP in the *aca*⁻ cells (Figure 64). Overall, the polarity markers were distributed normally in absence of ACA, which was comparable to AX2 however, expression of CAP-GFP and N-CAP-Pro-GFP attained cell polarity in the polarity deficient *aca*⁻ cells.

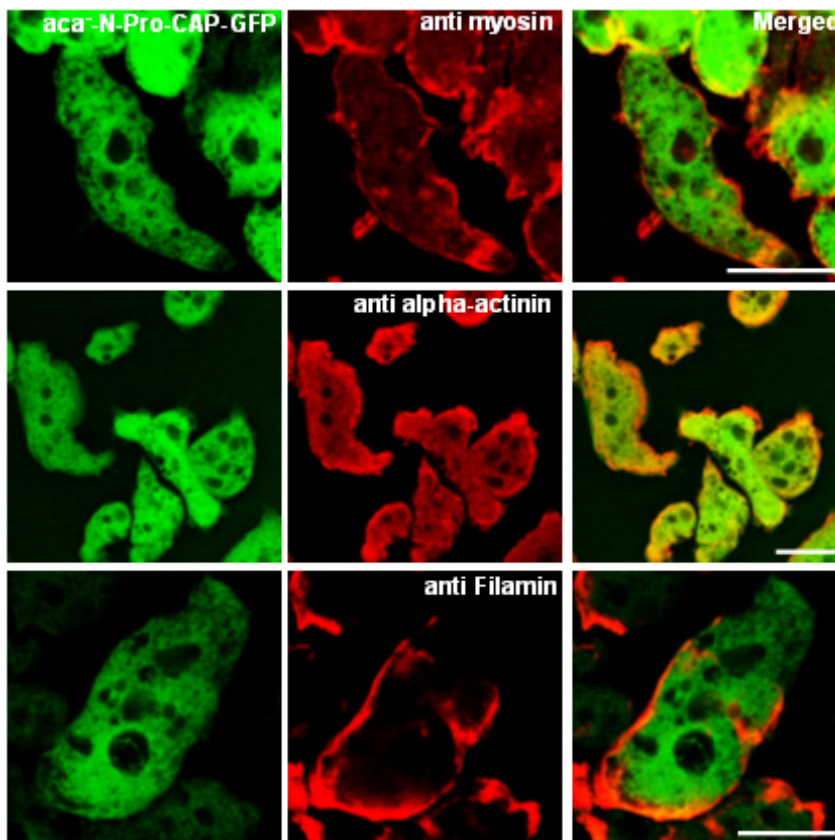


Figure 64: Distribution of myosin, α -actinin and filamin in the *aca*⁻ cells expressing N-CAP-Pro-GFP. The *aca*⁻ cells expressing N-Pro-CAP-GFP were stained with the monoclonal antibodies specific to the polarity markers myosin (56-395-2), α -actinin (47-62-2) and filamin (82-454-12). Myosin is at the posterior and lateral sides of the cells, α -actinin was seen to fill the cytosol but was enriched at the leading front of the cell and filamin was distributed strongly at the posterior like in AX2 wild type. The *aca*⁻ cells expressing N-CAP-Pro-GFP did not show any co-localization with these polarity markers, but the cells were polarised indicating that N-CAP-Pro-GFP plays a role in the cell polarity of the *aca*⁻ cells. Bar, 10 μ m.

3.0 Role of CAP in AX2 cells expressing constitutively active and dominant negative RacA and in LimD⁻ cells

3.1 Localization of CAP in AX2 cells expressing constitutively active and dominant negative RacA

Since the localization of CAP at the cell cortex was not determined by the upstream signalling molecules G-protein coupled cAR receptor, adenylyl cyclase or its regulator Pianissimo, G-proteins ($\alpha 2$ and β subunit) and also PI3-kinase we next tested small GTPases, which act as molecular switches cycling between an active GTP-bound state and an inactive GDP-bound state. The Rac GTPases are key regulators of the actin cytoskeleton, chemotaxis, cell motility, cytokinesis and endocytosis (Dumontier et al., 2000). As no knockout mutants are available we made use of the constitutively active RacA (RacA-V12) and the dominant negative RacA (RacA-N17) cells generated by F. Rivero. Mutation of Gly-12 to valine (V12) renders the Rac protein constitutively active, whereas mutation of Thr-17 to asparagine (N17) results in a dominant negative protein. For overexpression of constitutively active and dominant negative variants a tetracycline-controlled inducible system was used, which was recently adapted for *Dictyostelium* (Blaauw et al., 2000).

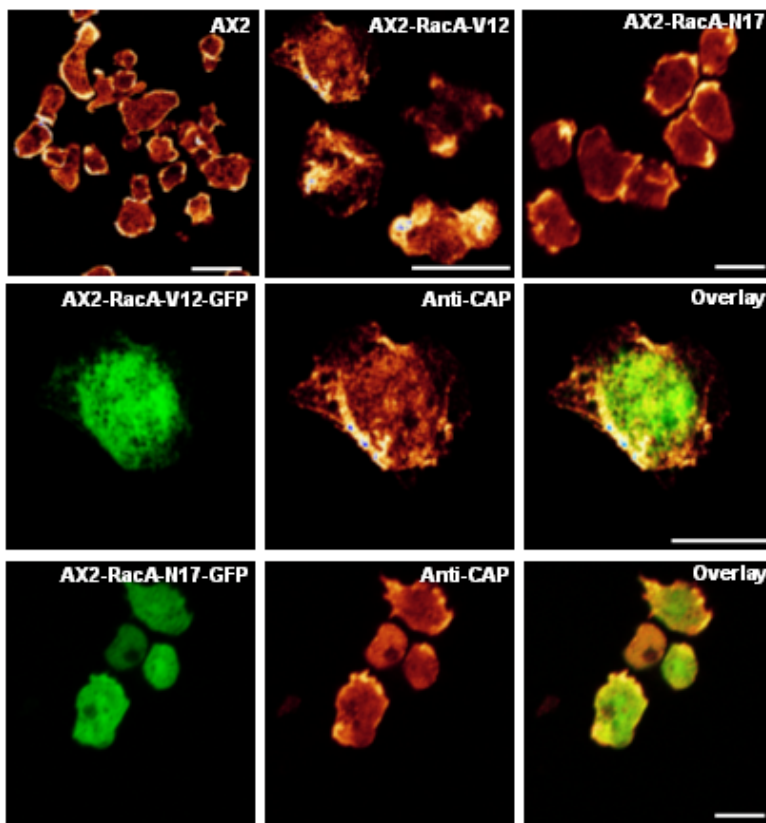


Figure 65: Localization of CAP in AX2-RacA cells. CAP enriches in the cell cortex and shows a cytoplasmic staining in wild type cells (top left panel). Cells were fixed with methanol and immunolabelled with the mAb 230-18-8. Cells expressing RacA V12-GFP (Both top and middle panel) showed an altered distribution of CAP. The dominant negative RacA N17 cells showed a weak localization of CAP at the cell cortex and in the cytoplasm (top right and also lower panel). Bar, 10 μ m.

The CAP localization in the AX2 -RacA V12 cells appears to be quite different in comparison to the wild type AX2. CAP accumulated at some regions and also the filopodia were enriched with CAP. AX2 cells expressing dominant negative RacA protein (N17) showed a CAP labelling at the cell

borders and a weak staining in the cytosol. Thus, the distribution of CAP differed in cells expressing RacA V12 and N17 GFP fusions from the one in AX2 (Figure 65).

3.2 Localization of CAP in *LimD*⁻ cells

LIM domain proteins are key players in the organisation of the actin cytoskeleton and in a number of fundamental pathways controlling the cell proliferation and differentiation. *LimD*⁻ cells have a polarisation defect. The localization of CAP in vegetative *LimD*⁻ cells seems to be unaffected and the protein was enriched at the periphery and was also present in the cytosol. However, in starving cells (*t*₆) *LimD*⁻ cells showed a disturbed localization of CAP (Figure 66). The protein was seen in forming crowns, but was not present in cell protrusions. From these data one could conclude that the proper localization of CAP in the starving amoebae depends on this protein or can depend on polarity. The disturbed localization of CAP in aggregation competent *LimD* cells (at 6 hours of starvation) was analysed by confocal imaging at different focal planes to visualise the accumulation of CAP in crowns at different planes (Figure 67). This revealed that CAP is abundantly enriched in the top visible plane of the *LimD*⁻ cells.

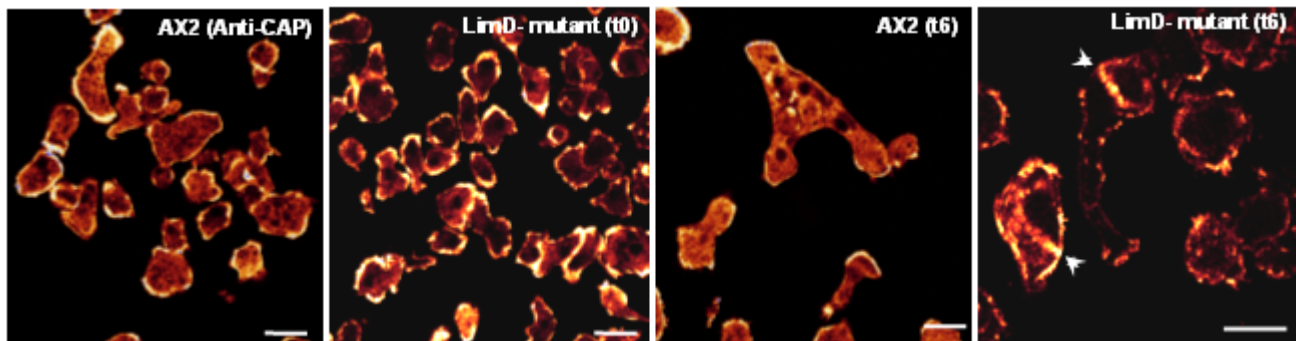


Figure 66: Localization of CAP in vegetative and starving *LimD*⁻ cells. The CAP protein localizes to the cell periphery and cytoplasm in wild type cells when immunolabelled with mAb 230-18-8. The localization of CAP seems to be unaffected in vegetative *LimD*⁻ cells whereas the localization is disturbed in starving *LimD*⁻ cells where it was present in crowns as shown by arrowheads. Bar, 10 μ m.

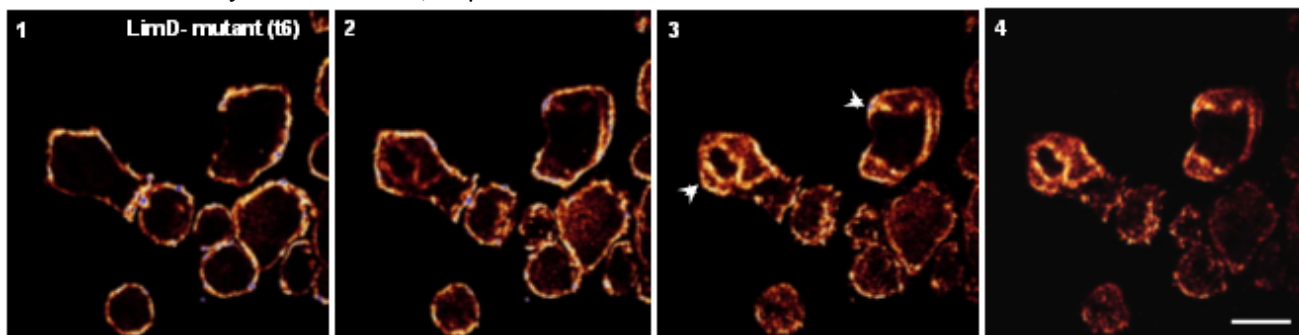


Figure 67: Localization of CAP in starving *LimD*⁻ cells (*t*₆) at different focal planes. The cells were shaken in suspension in Soerenson phosphate starvation buffer, and the starved cells were fixed with methanol and stained with mAb 230-18-8. The cells were inspected by confocal microscopy and the images were taken from the bottom to the top planes at equalised sections to see the protein distribution at different planes as denoted by the arrowheads. CAP was enriched in the cytosol at some places in the form of crowns at the top visible plane. Bar, 10 μ m.

3.3 Complementation analysis of CAP bsr by GFP-LimD

CAP bsr, the *Dictyostelium* mutant in which the CAP gene has been inactivated by homologous recombination is defective in several aspects of growth and development. The mutant cells are heterogeneous with regard to cell size and are often multinucleated indicating a cytokinesis defect. In shaking suspension the mutant cells grew more slowly and did not reach saturation densities as observed for wild type cells. This was paralleled by a reduction in fluid phase endocytosis. Recently, we reported that CAP is required for cell polarization and cAMP relay as CAP bsr cells are defective in polarity and chemotaxis (Noegel et al., 2004). All these multiple defects suggest that CAP is a multifunctional protein and we were interested to find if any other molecule with an important role in endocytosis, polarity and chemotaxis could complement these defects in CAP bsr. Hence, we tested whether LimD, a molecule with important regulatory roles during all events of cell polarity and chemotaxis could support those functions in CAP bsr cells (Khurana et al., 2002).

3.4 Dynamics of GFP-LimD in CAP bsr during endocytosis

As mentioned before, macropinocytosis accounts for most of the fluid phase uptake in *Dictyostelium* and depends on the integrity of the actin cytoskeleton. We studied the dynamics of GFP-LimD in CAP bsr during fluid phase endocytosis with an appropriate control of AX2 cells expressing GFP-LimD.

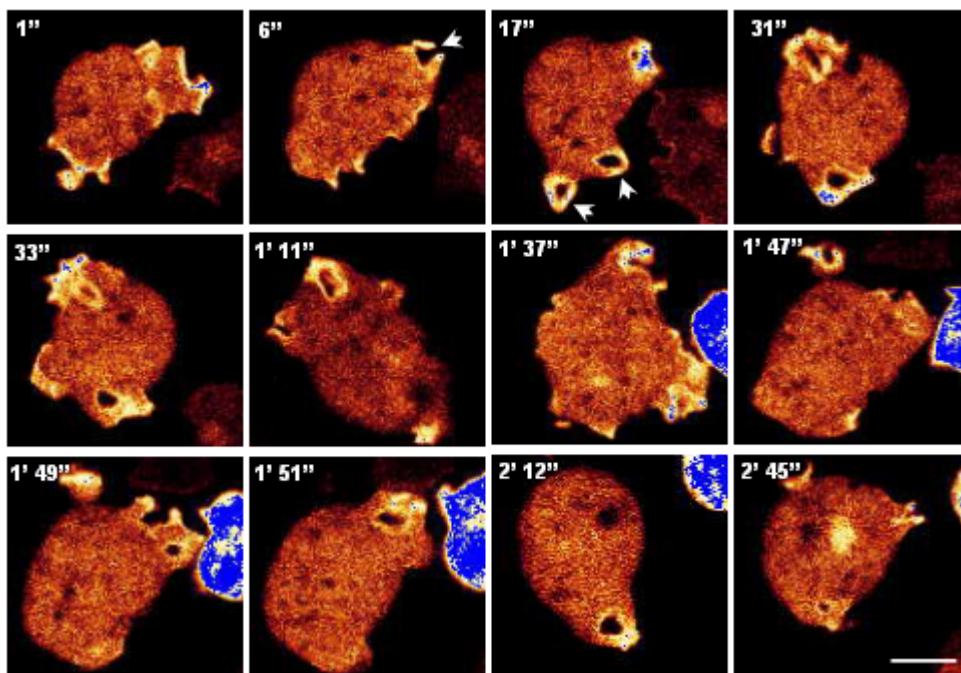


Figure 68: Dynamics of GFP-LimD in AX2 cells during live pinocytosis. AX2 cells expressing GFP-LimD were allowed to settle on glass coverslips and challenged with TRITC-dextran. The confocal images were taken at the times indicated. It was observed that GFP-LimD strongly enriches at the cell cortex forming macropinosomes and reveals the redistribution of GFP-LimD during the formation of the pinocytic vesicle. The arrowhead denotes the enrichment of GFP-LimD at the site of macropinocytosis. Bar,

In AX2 cells the cortical enrichment of GFP-LimD is clearly apparent, showing the redistribution of GFP-LimD during the formation of a macropinosome (Figure 68). At the beginning of the sequence a GFP-LimD rich membrane invaginates (6 seconds) and the protrusion of GFP-LimD rich membrane

progresses until the edge of the protrusions fuse to form a macropinosome containing a portion of the surrounding liquid coated by GFP-LimD. Thereafter, GFP-LimD gradually dissociates from the macropinosome to liberate the macropinosome into the cytosol. This process is highly suggestive of an involvement of GFP-LimD at early stages of endocytosis.

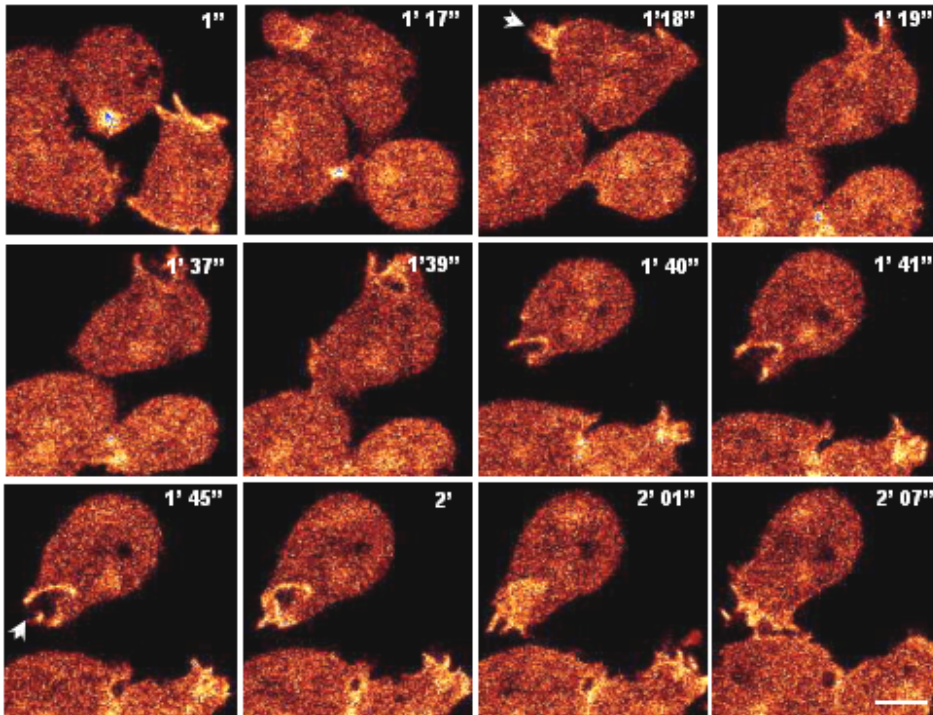


Figure 69: Dynamics of GFP-LimD in CAP bsr during pinocytosis. CAP bsr cells expressing GFP-LimD were challenged with TRITC-dextran and images were obtained at the times indicated. GFP-LimD was found to redistribute to the pinocytic cups and pinosomes and enriches at the cell cortex. Bar, 10 μ m.

The dynamics of GFP-LimD in CAP bsr cells during pinocytosis was similar to AX2 (Figure 69). GFP-LimD rescued the pinocytic defect of CAP bsr cells (see below), and relocated to macropinosomes and accumulated at the cell cortex during pinocytosis.

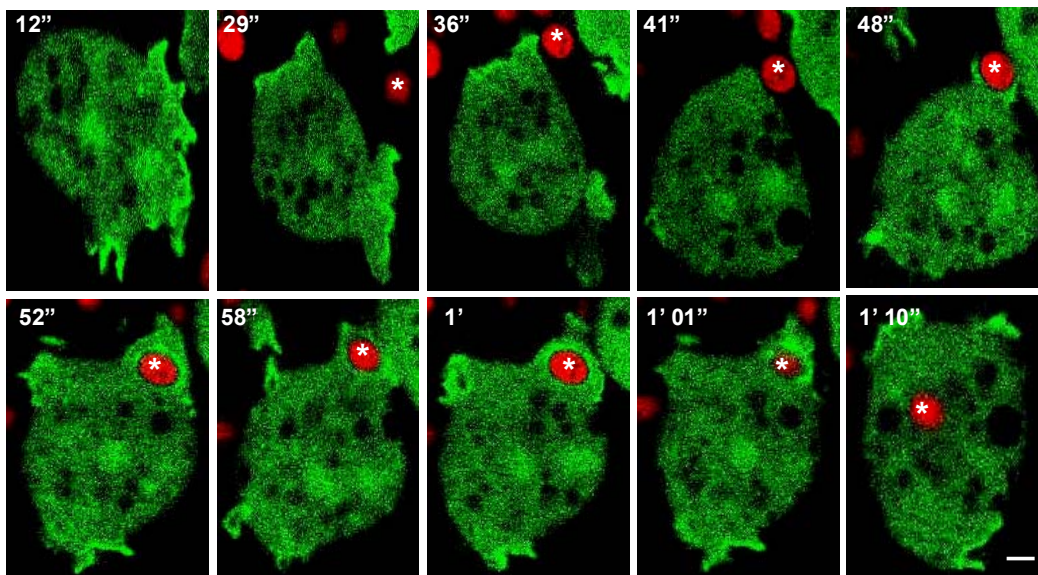


Figure 70: Dynamics of GFP-LimD in CAP bsr during phagocytosis. CAP bsr cells expressing GFP-LimD were allowed to settle on glass coverslip and challenged with TRITC labelled yeast. The confocal images were taken at the times indicated. It was noted that GFP-LimD strongly enriches at the cell cortex where the phagocytic cup is formed. * denotes the yeast cell of interest. Bar, 10 μ m.

To further confirm the dynamics of GFP-LimD in CAP bsr, we performed live imaging of GFP-LimD during phagocytosis of yeast cells. In the sequence shown (Figure 70) GFP-LimD accumulated at the phagocytic cup, and the cup progression led to the formation of a coat around the yeast cell that was enriched in GFP-LimD, followed by the engulfment of the yeast cell. It was also observed that GFP-LimD gradually dissociated from the phagosome after the yeast particle was successfully ingested (Figure 70). These results showed a dynamic re-localization of GFP-LimD in the absence of CAP.

3.5 Expression of GFP-LimD restores pinocytosis in CAP bsr cells

The dynamics of GFP-LimD in CAP bsr during pinocytosis suggested that expression of GFP-LimD plays a role in enhancement of the pinocytic uptake in CAP bsr. Therefore, we analysed the rate of fluid uptake in the CAP bsr expressing GFP-LimD by quantitative fluid-phase endocytosis.

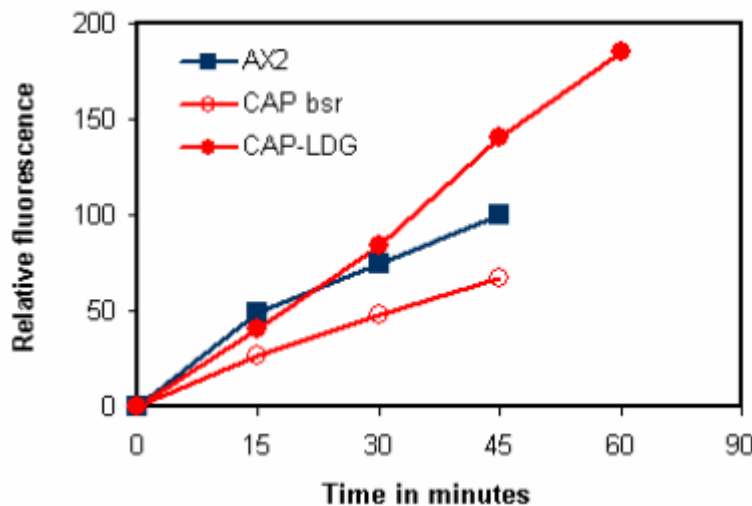


Figure 71: Quantitative pinocytosis of CAP bsr cells expressing GFP-LimD.

Cells were resuspended in fresh axenic medium at 5×10^6 cells/ml in the presence of 2 mg/ml TRITC-dextran. Data are presented as relative fluorescence, AX2 being considered 100%. All values are the average of at least four independent experiments. Expression of GFP-LimD improved the pinocytic influx of TRITC-dextran, moreover it completely rescued the pinocytosis defect of CAP bsr cells. LDG stands for GFP-LimD.

The quantitative uptake was assayed in the presence of TRITC-labelled dextran as a marker and fluorescence from the internalized marker was measured at selected time points and determined at 544/574 nm in the spectrofluorimeter. AX2 and CAP bsr are the experimental controls. The quantitative data indicated that expression of GFP-LimD enhances the rate of influx upto 3 fold more in CAP bsr cells when compared to the mutant (Figure 71) and suggest that GFP-LimD rescues the pinocytic uptake of CAP bsr.

3.6 Role of CAP in cAMP signalling

Dictyostelium is unique in its ability to utilize cAMP for initiation and progression through development, and we showed that CAP is required for cAMP relay (Noegel et al., 2004). To unravel the cross talk of CAP with other signalling molecules during cAMP signalling we made use of CAP

bsr cells expressing GFP-LimD and analysed the role of LimD after a cAMP pulse. AX2 cells expressing GFP-LimD represent the control cells.

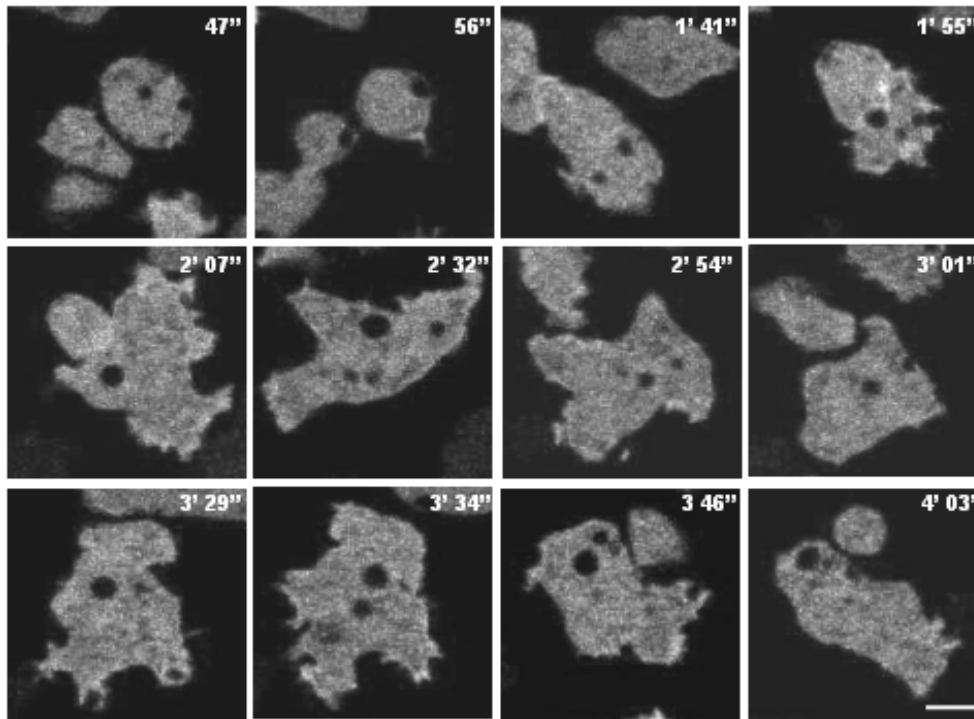


Figure 72a: Dynamics of GFP-LimD in the aggregation competent AX2 cells. The cells were adhered on glass coverslips after 6 hrs of starvation and a cAMP pulse (10^{-5} μ M) was given and the re-localization of GFP-LimD followed at the times denoted using the confocal microscope. GFP-LimD was found to re-localize to the leading fronts. Bar, 10 μ m.

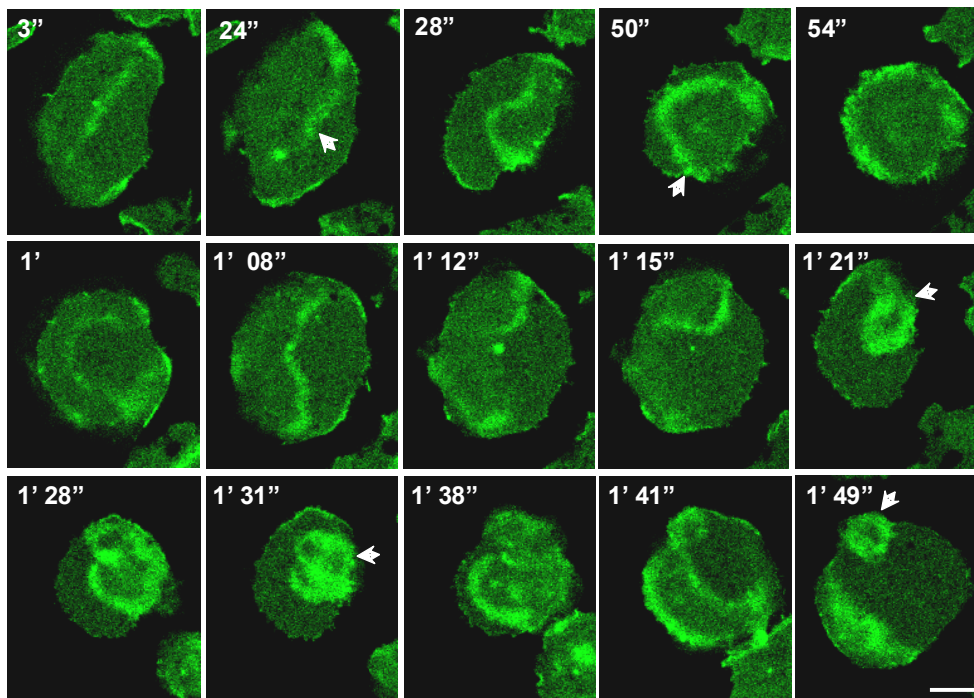


Figure 72b: GFP-LimD in aggregation competent CAP bsr cells expressing GFP-LimD. The cells were starved for 6 hrs and challenged with a cAMP pulse 10^{-5} μ M. Serial confocal sections were taken at the indicated times. CAP bsr expressing GFP-LimD were flat and the protein accumulated in wave like structures that moved from the cytosol to the cell cortex. The arrowhead denotes the region of interest. Bar, 10 μ m.

GFP-LimD in AX2 cells showed a highly dynamic behaviour and was found in newly formed cell protrusions of these active cells (Figure 72a). CAP bsr cells expressing GFP-LimD were studied in a similar manner however the serial confocal microscopy images showed a different behaviour of the protein response to cAMP. Also, CAP bsr cells expressing GFP-LimD were more flat and round and were not as motile as AX2 cells. GFP-LimD was present in a large wave like structure that enlarged

and moved from the cell centre to the cortex in half circles, and finally was present in crown structures (Figure 72b). These results indicate a requirement for CAP during aggregation and suggest an involvement of CAP during cAMP signalling.

4.0 Identification of binding partners for *Dictyostelium* CAP

A number of proteins associated with the actin cytoskeleton contain SH3 domains, which may provide the physical basis for functional interactions with structural and regulatory proteins in the actin cytoskeleton. CAP contains domains involved in actin binding, adenylyl cyclase association in yeast, SH3 domain binding, and oligomerization (Hubberstey et al., 2002), suggesting that CAP may interact with a wide range of molecules involved in the reorganisation of the actin cytoskeleton and signalling. Therefore, we carried out a search for binding partners by both genetic and biochemical approaches.

4.1 Does CAP physically interact with aggregation specific adenylyl cyclase (ACA)?

In yeast, CAP binds to adenylyl cyclase and has been implicated in adenylyl cyclase activation *in vivo*. The interaction domain in CAP was localised to a short N-terminal stretch (amino acids 1-168) that is highly conserved in CAP from other species. In *Dictyostelium* CAP (Figure 73), it shows 39% identity and 61% similarity to the *S. cerevisiae*, and human CAP (Field et al., 1988). In adenylyl cyclase the binding site is located at the C-terminus (amino acids 1768-2026) (Mintzer et al., 1994).

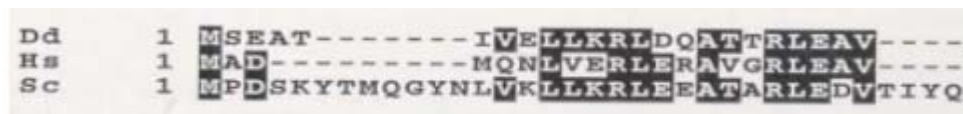


Figure 73: Conserved amino acids in the N-termini of *Dictyostelium*, human and yeast CAP. The identical amino acids are boxed. This sequence is localized in *Saccharomyces cerevisiae* at positions 19-21 and 26-28 and has the potential to form an amphipathic helix, which has been implicated in protein-protein interactions. This region has been suggested to function as adenylyl cyclase binding motif.

To study the possible interaction of CAP with ACA we amplified the full length CAP cDNA and the C-terminus of adenylyl cyclase (C-ACA) from the genomic DNA of *Dictyostelium*, and cloned the full length CAP into the DNA binding domain expression vector (Figure 74) (Harper et al., 1993) and the 419 base pair fragment corresponding to the C-terminus of the *Dictyostelium* adenylyl cyclase (position 4394-4813) of the published sequence; (Pitt et al., 1992) into the activation domain expression vector (Figure 74) to detect a direct interaction of CAP with C-ACA by the yeast two hybrid assay (refer materials and methods for primers and cloning).

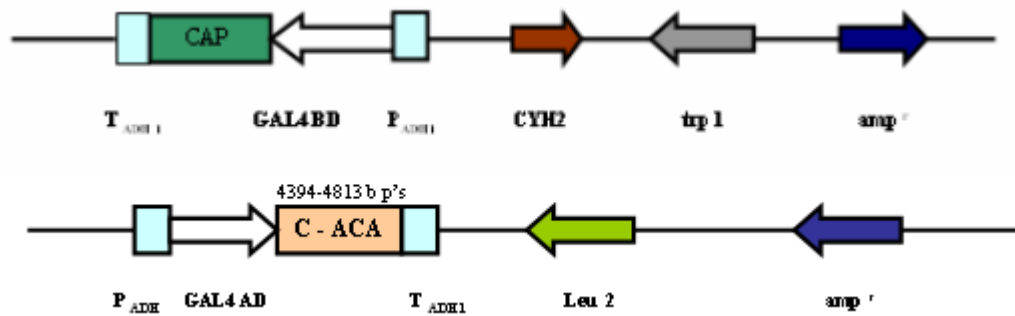


Figure 74: Cloning of CAP in the pAS2 and C-ACA in the pACT2 vector. (a) The full length CAP (~1.5 kb) was cloned into the pAS2 containing the GAL4₍₁₋₁₄₇₎ DNA-binding domain, tryptophan nutritional marker (TRP1), and ampicillin resistance. (b) The C-terminal fragment of ACA (4394-4813) was cloned into pACT2 containing the GAL4₍₇₆₈₋₈₈₁₎ activation domain, leucine nutritional marker (LEU2), ampicillin resistance and HA epitope tag.

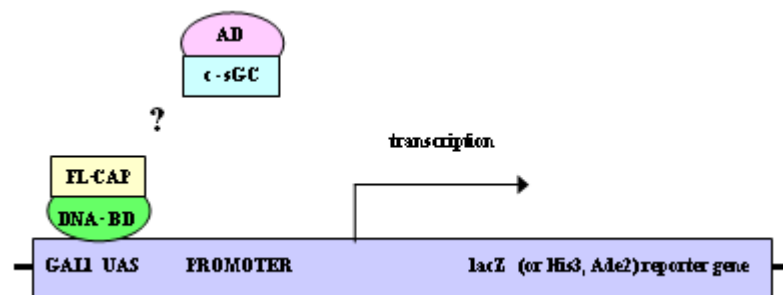
Furthermore, different domains of CAP were cloned into the pAS2 vector and analysed for the detection of any possible direct interaction of the individual domains of CAP with the C-terminus of ACA (Table 1). The co-transformants were obtained in the following yeast strains Y187, Y190 and PJ69-4A on the respective minimal media plates, SD/-Leu/-Trp/-His, SD/-Leu/-Trp and SD/-Leu/-Trp/-His/-Ade based on the strain backgrounds by incubation of the plates for 4-6 days at 30°C. However, when assayed for β -galactosidase activity (*lacZ* expression) by filter lift assay we could not detect any direct interaction of N- or C-terminal domains of CAP with the C-terminus of ACA (see Materials and methods). The yeast two-hybrid assay results are indicated in Table 1.

Yeast two hybrid Experiments	-Trp, -Leu	-Trp,-leu, -His	-Trp,-Leu, -His + 25mM 3AT	-Trp,-leu,-Ade	Filter lift β -gal test
Strain Y187, Y190 & PJ-69	-	-	-	-	-
pAS2+pACT2 (vector controls)	+	-	-	-	-
pAS2+pCL1 (positive control)	+	+	+	+	+
CAP+C-ACA	+	-	-	-	-
N-CAP+C-ACA	+	+	-	-	-
C-CAP+C-ACA	+	+	-	-	-

Table 1: Yeast two hybrid assay results of CAP and C-ACA interaction. Data indicated are the phenotypes observed when assayed for the direct interaction of CAP and its domains with the C-ACA in regard to growth on the minimal selection and *lacZ* expression by β -gal filter lift assay. + indicates the growth on minimal media /colonies turning blue. The co-transformants were obtained rarely in the Y187 strains, and the co-transformants assayed for the β -gal activity showed negative results where the colonies did not turn blue at 7-8 hrs or overnight incubation of the β -gal filters at 30°C when compared to the positive control. However it was observed that the co-transformants turned blue after 14-16 hrs or mostly by 1-2 days of incubation at room temperatures. The experiment also showed that CAP and C-ACA and N-CAP and C-ACA co-transformants were able to grow on the triple selection plates of tryptophan, leucine and histidine, when compared with the growth of C-CAP and C-ACA co-transformants. The data did not provide evidence for an interaction between CAP and the C-terminus of ACA

4.2 Does CAP interact with guanylyl cyclase?

Adenylyl cyclases (ACs) and guanylyl cyclases (GCs) in *Dictyostelium* have a high degree of amino acid sequence identity and are expected to have a similar structure of their catalytic sites. Guanylyl cyclase A (GCA) and soluble guanylyl cyclase (sGC) encode GCs in *Dictyostelium* and have a topology similar to 12 transmembrane domain and soluble adenylyl cyclase, respectively (Roelofs et al., 2002). The C-terminus of sGC shares approximately 41% of amino acid identity with the C-terminus of ACA. sGC predicts a 2843 amino acid protein with a molecular weight of 315 kDa. We amplified the C-terminal fragment of sGC (2.4 kb) showing a high degree of identity to the C-terminus of ACA and cloned it into the activation domain vector to investigate any possible direct interaction of CAP with sGC by the yeast two hybrid assay (as schematically represented below). The co-transformants were obtained on all minimal selection plates and in β -gal test the co-transformants of CAP and C-terminus of sGC turned blue similar to the experimental positive control (Table 2), indicating that CAP and C-terminus of sGC seem to interact in *in vivo* conditions. To further confirm the yeast two hybrid results, experiments were designed to show the interaction at the biochemical level in GST pull down assays, and the C-terminal fragment of sGC was cloned into a GST fusion vector and expressed in *E. coli* to perform pull down assays. These experiments are in progress.



Yeast two hybrid Experiments	-Trp, -Leu	-Trp,-leu, -His	-Trp,-Leu, -His + 25mM 3AT	-Trp,-leu,-Ade	Filter lift β -gal test
Strain (PJ-69)	-	-	-	-	-
pGBKT7+pGADT7	+	-	-	-	-
pGBKT7+c-sGC	+	-	-	-	-
pGADT7+CAP	+	-	-	-	-
pGBKT7+pCL (positive control)	+	+	+	+	+
CAP+c-sGC (Experiment)	+	+	+	+	+

Table 2: Interaction of CAP with the C-terminus of sGC. The yeast two hybrid assay results are summarized in the table above, which indicate the phenotypes observed when assayed for detecting the direct interaction of CAP with the C-sGC. Co-transformants grown on the minimal selection and lacZ expression by β -gal filter assay is shown. The results of the yeast two hybrid assays denoted a direct interaction of CAP with the C-terminus of sGC. + indicates the growth on minimal media /colonies turning blue.

4.3 Interaction of CAP with ARP2/3 complex subunits

To identify proteins interacting with CAP immunoprecipitations were performed with whole cell lysate of AX2 cells expressing CAP-GFP and CAP bsr cells expressing GFP fusions of CAP. CAP and associated proteins were immunoprecipitated with the GFP specific mAb bound to protein A sepharose beads and analysed by matrix associated laser desorption-ionization mass spectrometry, MALDI-MS (Materials and methods). These experiments with appropriate controls like AX2 wild type and CAP bsr resulted in the identification of several proteins (ranging in mass from 190-20 kDa). The protein that was repeatedly obtained is the cyclase-associated protein CAP, supporting the notion that the protein dimerizes or form a multimeric complex. We were able to co-immunoprecipitate the 34-kDa subunit (P34-ARC) and 21-kDa subunit (P21-ARC) of the Arp2/3 complex, the actin nucleation machinery. Arp2/3 is a complex of seven protein subunits including two actin-related proteins (Arp2 and Arp3) and five novel proteins. This complex binds to the sides of actin filaments and is concentrated at the leading edges of motile cells, localizes to regions of actin assembly such as macropinocytic cups, the actin comet tails of the intracellular pathogen *Listeria monocytogenes* and motile actin patches associated with the plasma membrane of budding yeast (Mullins et al., 1998).

Yeast two hybrid Experiments	-Trp, -Leu	-Trp,-leu,-His	-Trp,-Leu,-His+25mM 3AT	-Trp,-leu,-Ade	Filter lift β -gal test
Strain (P.J-69)	-	-	-	-	-
pGBKT7+pGADT7	+	-	-	-	-
pGBKT7+p34-ARC	+	***	-	-	***
pGADT7+CAP	+	-	-	-	-
pGBKT7+pCL1 (Positive control)	+	+	+	+	+
CAP+ Arp2/3 (P34-ARC Subunit) Experiment	+	+	-	-	+

Table 3: Interaction of CAP with the P34-ARC subunit. The table represents the yeast two hybrid results, indicating the phenotypes observed. The results show a possible direct interaction of CAP with the P34-ARC, but could not be confirmed as the P34-ARC subunit showed auto-activation with the pGBKT7 vector. + indicates growth on minimal media /colonies turning blue and *** indicates auto-activation.

To confirm the immunoprecipitation results we investigated the possible direct interaction of CAP with the P34-ARC subunit. We amplified the ARPE (P34-ARC) gene (956 base pairs) from the genomic DNA using the ARPE specific primers (Materials and methods) and cloned it into the activation domain vector to test the direct interaction of this Arp2/3 subunit with CAP by the yeast two hybrid assay. Co-transformants were obtained on the -Trp,-Leu,-His minus plates and turned blue on the β -gal filters like the positive control. However, the P34-ARC when tested for auto-activation

was able to auto-activate resulting in positive LacZ results (Table 3). Further experiments need to be done to confirm this interaction.

4.4 Interaction of CAP with the vacuolar H⁺-ATPases (V-ATPases) complex

A role of CAP in endocytosis and vesicle trafficking is suggested by data from yeast where CAP was shown to interact indirectly or directly with many key components of the endocytic and actin regulatory network (e.g., Sla1p, Abp1p, Rvs167p, Act1p and Aip1p) and that suggested an involvement of CAP in large regulatory complexes linking elements of the actin polymerization and disassembly network with molecules essential for endocytosis and vesicle movement (Hubberstey and Mottillo, 2002). We also identified the vacuolar ATP synthase subunit d in our immunoprecipitation studies. The vacuolar ATP synthase d subunit of the integral membrane V₀ complex of V-ATPases is a 41 kDa accessory protein designated as DVA41 in *Dictyostelium*. Vacuolar H⁺-ATPases (V-ATPases) are highly conserved proton pumps that couple hydrolysis of cytosolic ATP to proton transport out of the cytosol. They are required for energizing and acidifying the intracellular compartments of the vacuolar system in eukaryotic cells (Lu et al., 2002). In further immunoprecipitation experiments we precipitated also the V-ATPase B subunit (32 kDa, three different experiments), and p59, an endocytic vesicle protein (four independent experiments). To test the interaction between the d subunit and CAP we amplified the d subunit of V-ATPases (1071 base pairs) and cloned the DVA41 gene into an activation domain vector. The yeast two hybrid assays were done in a similar way as before (also refer Materials and method).

Yeast two hybrid Experiments	-Trp, -Leu	-Trp,-leu,-His	-Trp,-Leu,-His+25mM 3AT	-Trp,-leu,-Ade	Filter lift β-gal test
Strain (PJ-69)	-	-	-	-	-
pGBKT7+pGADT7	+	-	-	-	-
pGBKT7+V-ATPase (d subunit)	+	-	-	-	-
pGADT7+CAP	+	-	-	-	-
pGBKT7+pCL1 (Positive control)	+	+	+	+	+
CAP+V-ATPase (d subunit) Experiment	+	+	-	-	+

Table 4: Summary of the interaction of CAP with V-ATPase d subunit. The yeast two hybrid assay results are denoted in the table above, showing the phenotypes observed under the different assay conditions. The transformants grew on the minimal selection plates (-Trp,-Leu,-His). However they could not grow on the stringent selection plates in the absence of Adenine. The *lacZ* expression was positive for the colonies obtained on the -Trp,-Leu,-His plates. The results of the yeast two hybrid assays denoted a direct interaction of CAP with the V-ATPase d subunit. + indicates growth on minimal media /colonies turning blue.

However, the results were not very conclusive, as growth was not observed under all conditions assayed (Table 4). For further analysis we have cloned the DVA41 into a GST vector. The availability of reagents specific for several v-ATPase components allowed us to investigate the interaction with CAP by immunofluorescence studies. The AX2 cells expressing CAP-GFP were fixed and immunostained with antibodies specific for the contractile vacuole system (vacuolar ATPases A subunit, Vata) revealing an association of CAP-GFP with vacuoles and showing an apparent co-localization with the vacuolar marker (Figure 75).

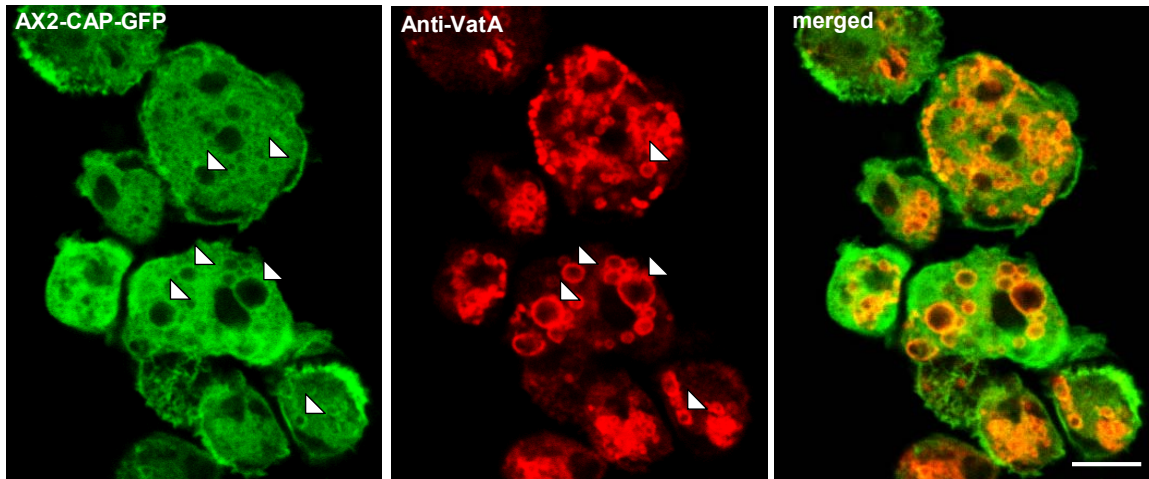


Figure 75: Association of CAP with internal vacuolar membranes. AX2 cells expressing the CAP-GFP were allowed to adhere on glass coverslip, fixed as before and immunolabelled with the Vata specific mAb 221-35-2 (which is a marker for the contractile system) to visualize the association of CAP-GFP with the vacuolar membranes. It was observed that CAP-GFP associates and colocalize with the vacuolar marker. Arrowheads indicate association of CAP-GFP with vacuoles. Bar, 10 μ m.

These results indicated that CAP-GFP associates with and enriches at vacuolar membranes. To further confirm the association of CAP-GFP with vacuoles, AX2 cells expressing GFP-Nramp1 were stained with the CAP specific mAb to see if CAP also associates with Nramp1 enriched vacuoles.

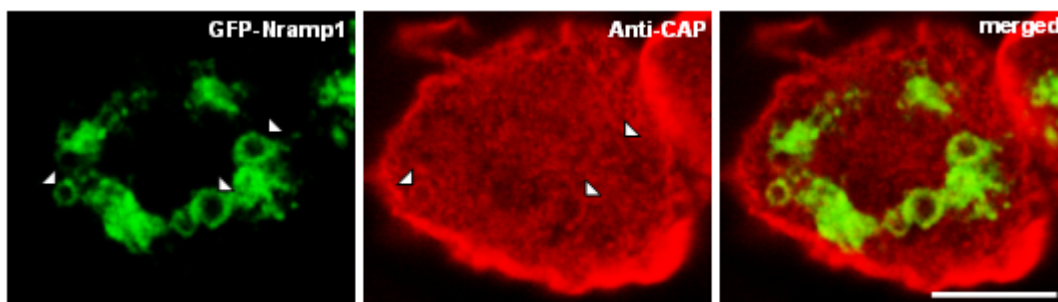


Figure 76: CAP is not present on all Nramp1 decorated vacuoles. The AX2-GFP-Nramp1 cells were fixed and stained with CAP specific mAb 230-18-8 and visualized by confocal microscopy. CAP is found only on some Nramp1 enriched vacuoles. Arrowhead denotes the vacuoles of interest. Bar, 10 μ m.

Natural resistance to infection with intracellular parasites such as *Mycobacteria*, *Salmonella* and *Leishmania* is controlled by a gene that encodes a membrane protein designated as Natural Resistance-Associated Macrophage Protein (Nramp1). In macrophages after phagocytosis, Nramp1 is

targeted to the membrane of the microbe-containing phagosome, where it may modify the intra-phagosomal milieu to affect microbial infection (Gruenheid et al., 1999). *Dictyostelium* also harbors a Nramp1 homolog. We examined AX2 cells expressing GFP-Nramp1 by confocal microscopy and found that CAP is present on some but not all GFP-Nramp1 decorated vacuoles (Figure 76).

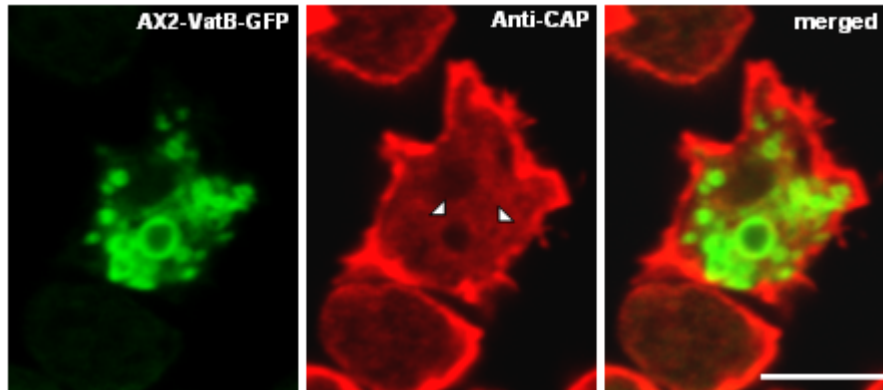


Figure 77: CAP weakly associate with VatB. The GFP-VatB cells were fixed and immunolabelled with the CAP specific mAb 230-18-8 to see if CAP codistribute with this Vacuolar B subunit. The confocal microscopy showed that the VatB-GFP did not show a strong staining of the vacuoles like VatA, and we found that CAP found on some VatB rich vacuoles shown by the arrowheads. Bar, 10 μ m.

Furthermore, we analysed the association of CAP with the VatB subunit, and immunostained AX2 cells expressing GFP-VatB with the CAP mAb to detect a co-localization of CAP with GFP-VatB. The confocal microscopy revealed that VatB-GFP is diffusely distributed and found at some vacuoles, and overlaps with CAP at some spots (Figure 77, shown by arrowheads).

4.5 The vacuolar network is disturbed in the absence of CAP

To explore the role of CAP in the vacuolar ATPases vacuolar system further we investigated the distribution of the V-type ATPase complex in CAP bsr cells, proposing that absence of CAP may affect the V-ATPases network. The CAP bsr cells were fixed and stained for the VataA subunit.

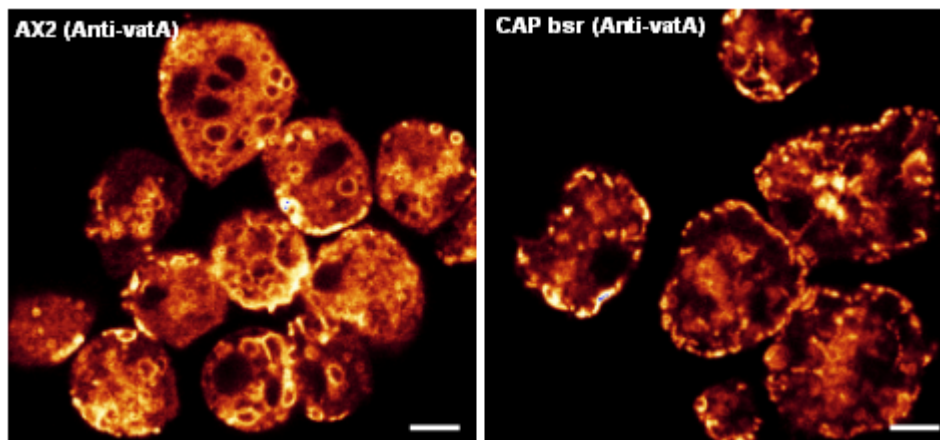


Figure 78: Distribution of the contractile vacuole system revealed by VatA labeling in CAP bsr. The CAP bsr cells were fixed with cold methanol and immunolabelled with a marker specific for the vacuolar ATPase A subunit (mAb 221-35-2) to visualize the distribution of VatA in the absence of CAP. The confocal microscopy revealed that the VatA

staining is diffused, disturbed and weak. Also the vacuoles are quite small in comparison to the wild type AX2. Bar, 10 μm .

The AX2 wild type cells showed a strong and profound staining of vacuoles throughout the cytosol as well as a predominant cytosolic and vacuolar membrane staining. Interestingly, in the absence of CAP the Vata staining was diffused and disturbed, the vacuoles were not intact and numerous and the strong cytoplasmic and vacuolar staining in the cytoplasm was not observed like in AX2 cells (Figure 78).

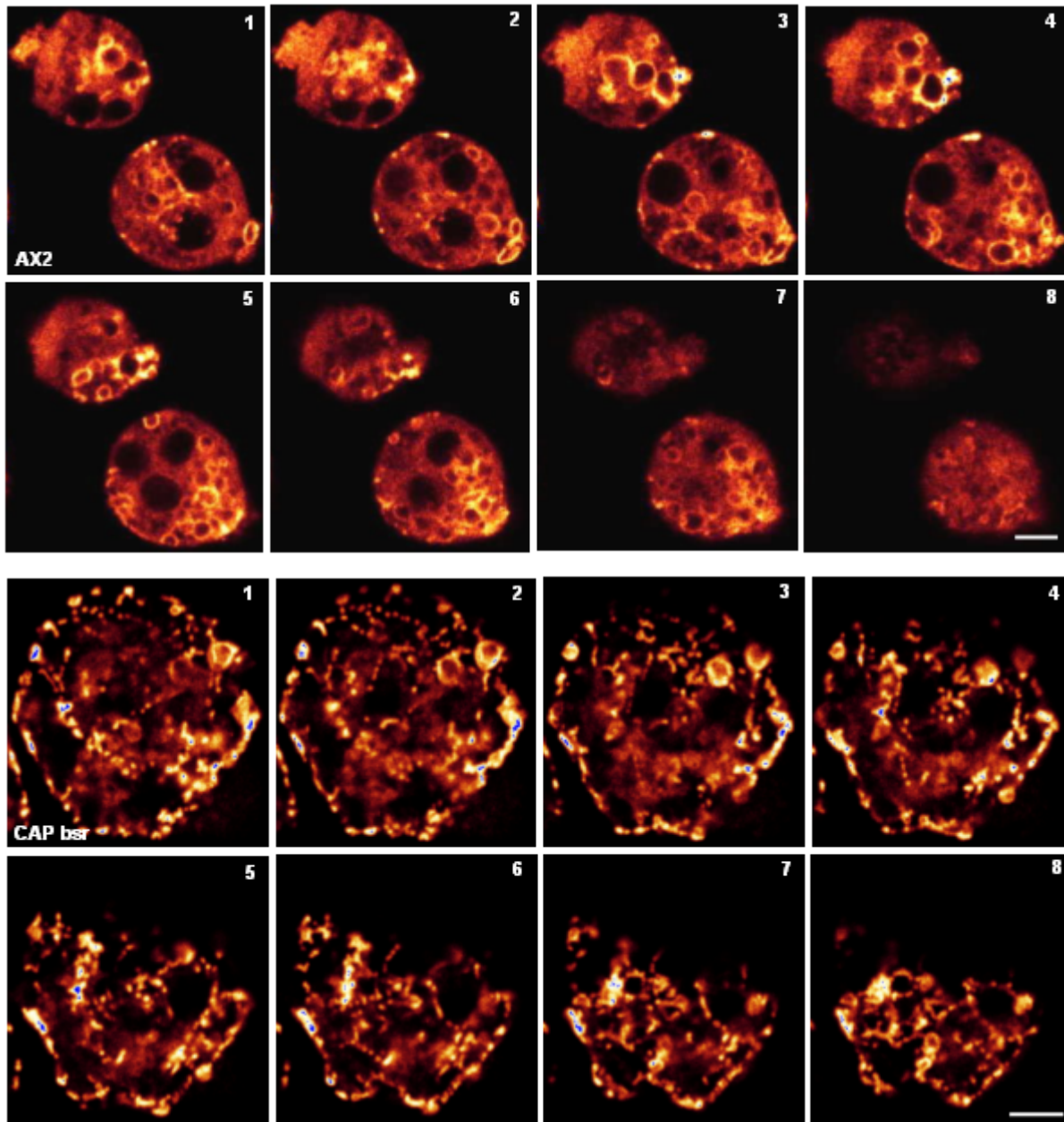


Figure 79: Distribution of the contractile vacuole system revealed by VataA labeling in CAP bsr in comparison to AX2 at different focal planes. The AX2 wild type and CAP bsr cells were fixed and immunostained with the VataA specific mAb 221-35-2 to visualize the distribution of VataA. The confocal microscopy obtained by equalized and optimized different focal planes revealed that the VataA staining is diffused, disturbed and weak, and also the vacuoles are quite small and do not appear at different sections in comparison to the wild type AX2. Bar, 10 μm .

Since the vacuolar system had a different appearance in CAP bsr cells with smaller vacuoles that were mostly seen at the cell periphery, we analysed the distribution of vacuoles at different focal planes by confocal microscopy and confirmed that the VatA containing structures were distributed throughout the cell. Furthermore, the cytosolic staining appeared to be absent (Figure 79). In contrast in AX2 the VatA antibody richly labelled the vacuolar membranes and intact vacuoles are visible when sections are assembled from top to bottom planes. The results were further confirmed by testing the expression levels of VatA in the wild type AX2, AX2 cells expressing CAP-GFP and CAP bsr cells. The immunoblot revealed that VatA levels were significantly reduced in CAP bsr showing a faint band of VatA in comparison to the wild type cells (Figure 80).

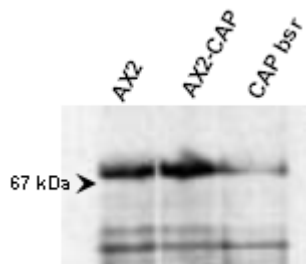


Figure 80: Immunoblot showing the expression levels of VatA in CAP bsr. The cells were axenically grown and 2×10^5 cells/ml were lysed with 2x sample buffer, the proteins resolved on SDS-PAGE gels (10% acrylamide) and immunoblotted with VatA specific mAb 221-35-2, followed by enhanced chemiluminescence. The blot shows that VatA is expressed at two fold higher level in AX2 and AX2 cells expressing CAP-GFP in comparison to CAP bsr.

4.6 Expression of CAP GFP fusion protein restores the disturbed vacuolar system in CAP bsr

Above, we presented results suggesting that CAP-GFP associates and co-distributes with vacuolar membranes stained with VatA in AX2 wild type cells and we also showed that the vacuolar network was disturbed and VatA staining is altered in the absence of CAP. These findings triggered further studies of CAP interaction with the vacuolar system. Previously, we showed that expression of full length CAP restored all defects in CAP bsr.

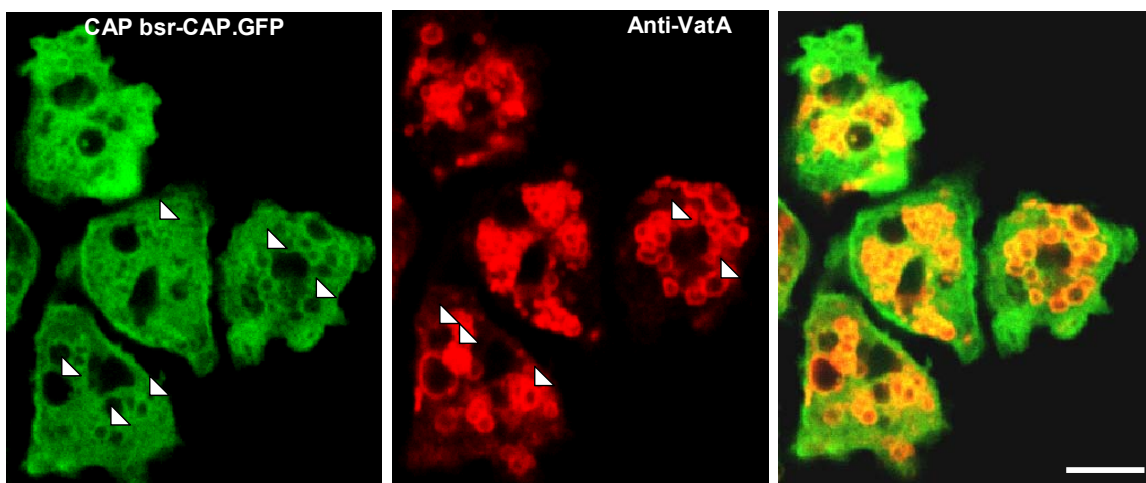


Figure 81: Restoration of vacuolar membrane distribution in CAP bsr expressing CAP-GFP. The CAP bsr cells expressing CAP-GFP were fixed and immunostained with the VatA specific mAb 221-35-2 to visualize the distribution of VatA. The confocal microscopy revealed that the VatA staining is completely restored by the expression of CAP-GFP, the VatA showed a strong staining distributed preferentially on the vacuolar network. The vacuoles formed were numerous, and furthermore CAP-GFP co-distributed with VatA. Bar, 10 μ m.

Here we made use of CAP bsr transformants expressing CAP-GFP and individual domains of CAP and proved that the altered distribution of the vacuolar network is completely restored by the expression of CAP-GFP (Figure 81)

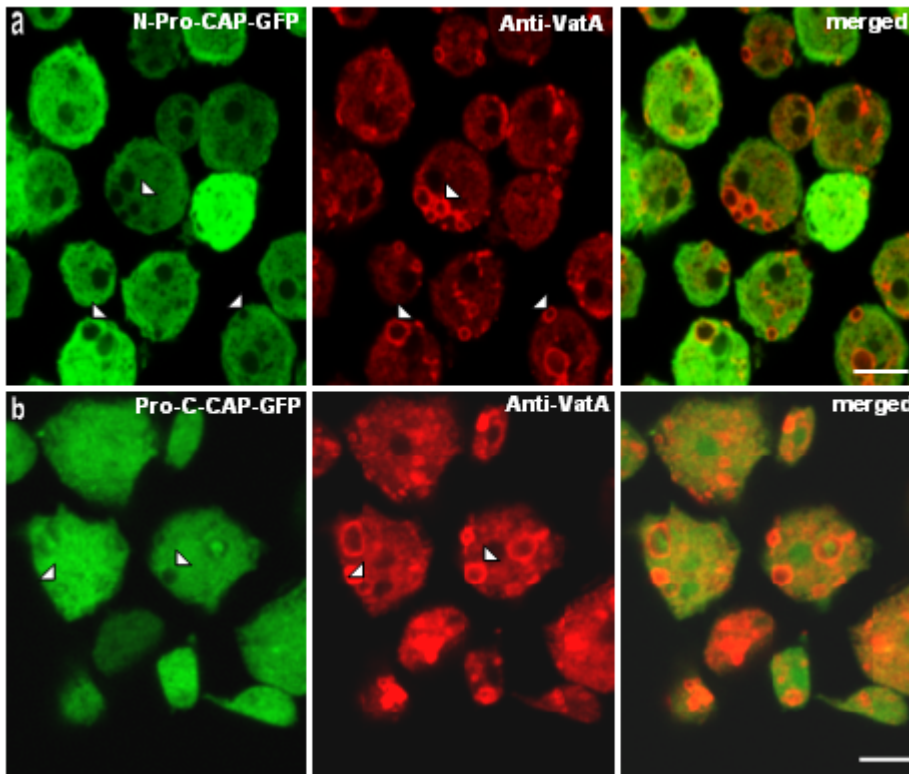


Figure 82: Partial restoration of the vacuolar distribution in CAP bsr expressing GFP fusions of CAP domains. CAP bsr expressing N-Pro-CAP-GFP and C-Pro-CAP-GFP were fixed and immunostained with the VatA specific mAb 221-35-2. The VatA staining is restored partially with the expression of N-CAP-Pro-GFP, and generated larger and intact vacuoles (a). C-Pro-CAP-GFP expression also restored the vacuolar network to some extent, however fewer vacuoles were detected by VatA staining, but the vacuoles formed were intact and showed strong accumulation of VatA (b). Bar, 10 μ m.

The VatA stained vacuolar membranes also showed an enrichment of CAP-GFP. The vacuoles were large, distributed all over the cytosol (Figure 81). We found that expression of the N-Pro-CAP-GFP also restored the disturbed vacuolar network in CAP bsr, but to a partial extent. The number of vacuoles appeared to be reduced when compared to the CAP-GFP expressing CAP bsr cells. However they were strongly stained large and at some regions N-Pro-CAP-GFP co-localized with VatA (Figure 82a). Furthermore, we also observed that expression of C-Pro-CAP-GFP rescued the diffused vacuolar network to some extent and the cytosolic VatA staining in CAP bsr cells (Figure 82b).

5.0 Transcriptional analysis of CAP bsr using DNA microarrays

The availability of the *Dictyostelium* genome sequence resulted in the generation of microarrays. This allowed us to study the global expression of genes in CAP bsr cells. The *Dictyostelium discoideum* microarray 6000 carries 6000 unique sequences that represent expressed sequence tags (EST, which cover 50% of the *Dictyostelium* genome), partial gene sequences (PGS, these are fragments of known sequences), as well as positive and negative controls (which are selected partial gene sequences from *Dictyostelium*) and commercial controls (SpotReport). To analyse the transcripts total RNA was

isolated from vegetatively growing AX2 wild type and CAP bsr cells and reverse transcribed. Four independent experiments were performed, where each experiment had two different batches of the wild type and mutant RNA. Totally, eight slides were probed with different combinations of the labelled cDNA from the four batches of RNA prepared in duplicates. The respective cDNAs were labelled with Cy3 and Cy5 fluorescent dyes and the mixture was used for the assay and the spotted chips were hybridized, washed and scanned. The scanned arrays were processed for the data analysis using the ScanArray software (Perkin Elmer). The microarray analysis revealed that 554 genes are significantly regulated in the absence of CAP with a delta value of ± 1.646 . The delta value is a tuning parameter used to determine the cut off significance based on the false positive rate (0.53416) as shown by the SAM plot (significant analysis of microarrays) (Figure 83). It was analysed that out of 554 significant genes 214 of them were up regulated and 340 genes were down regulated.

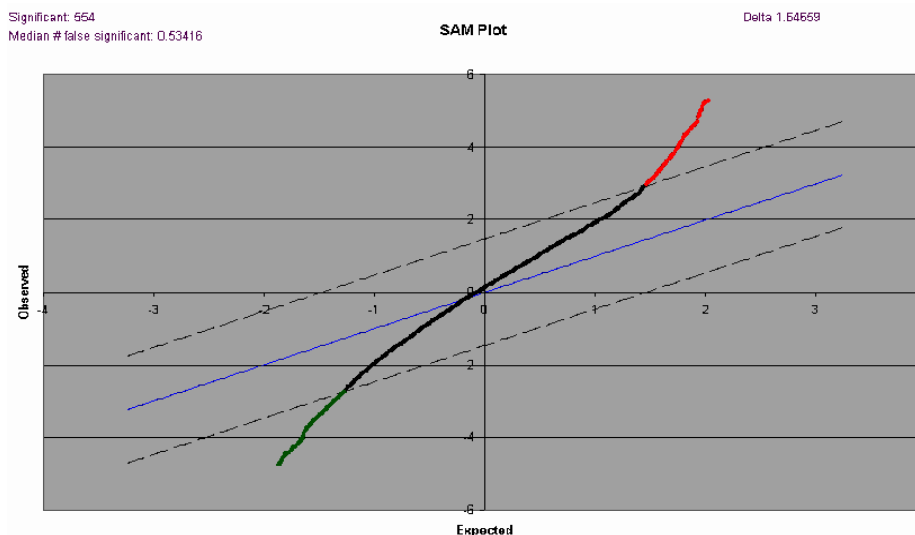


Figure 83: SAM plot showing the results of the CAP bsr microarray analysis. The CAP bsr microarray results reveal that 214 genes are induced as indicated by the cluster of genes shown in red in the top right panel of the plot, and 340 genes were significantly down-regulated which are represented by the cluster of genes in green towards the left bottom panel. The significant cut off rate indicated by the dashed lines is 1.64 with a least false positive rate of 0.5 for the 554 genes.

Out of the 214 up-regulated genes, 9 belong to the group of partial gene sequences PGS (represented by the first 9 genes of table 5). Most of the genes up regulated were categorized in the signal transduction category. An interesting gene induced was RegA, which encodes the phosphodiesterase enzyme PDE known to negatively regulate the cAMP dependent protein kinase A (PKA). The extracellular regulated MAP kinase (ERK1), p21 activated kinase (pakA), intracellular signalling kinase (statA), tyrosine protein kinase-2 (splB), hybrid histidine kinase (dhkB) and protein kinase C activator (sgkA) in the list of up-regulated genes showed a fold increase of 1.3-1.7. The dynein heavy chain is a cytoskeletal protein in the up-regulated list. The growth and developmental genes like vegetative stage specific gene H5 showed a great fold increase in the CAP bsr. Furthermore, it was noticed that sapA, tipC and small aggregate formation protein are involved in multicellular organization and cyto-differentiation. 12 genes were grouped under transport facilitation and protein

destination, in which the intriguing candidate was vacuolinA. The remaining genes were mostly hypothetical proteins and uncertain/unclassified genes (Table 5).

Gene ID	Gene Name	Score(d)	Ratio	function
AJ005398	regA	3.466903	1.33	cAMP phosphodiesterase; regA
U48706	smlA	3.7887415	1.33	small aggregate formation (smlA)
U61984	pgmA	3.9002363	1.23	phosphoglucomutase A
X15387	H5	24.316565	4.76	H5 gene
X52465	D2	4.4516637	1.46	crystal protein
Z15124	cdyn-hc	3.499835	1.51	cytoplasmic dynein heavy chain
X54452	spiA	3.6514973	1.48	sporulation-specific prespore
L36205	CP5	5.2287084	1.30	cysteine proteinase CP5
J01284	disc-1c	4.3566888	3.24	discoidin-1c gene
SLA374	vacA1	9.2114522	1.91	vacuolin A, endocytosis
SLA843	hypothetical protein	6.1822025	1.40	unknown
SLB759	statA	4.1507212	1.36	intracellular signaling cascade
SLD691	abcG21	6.5488797	1.71	ABC transporter, transport facilitation
SLG787	sgkA	3.9375535	1.48	protein kinase C activation
SLH488	pakA	3.6552153	1.41	cytokinesis and the regulation of the cytoskeleton
SLI754	camBP46	4.4603337	1.58	Putative calmodulin-binding protein
SSB370	hypothetical protein	4.4056509	1.68	unknown
SSB785	rsc11	3.5538068	1.19	random slug cDNA-11
SSC268	sp1B/pyKB/dpyk2	3.6394036	1.60	Tyrosine-protein kinase 2
SSC331	erk1	3.5316625	1.71	extracellular signal-regulated kinase
SSC656	H5	14.078754	4.13	Vegetative specific protein H5
SSC802	npc1	3.3919631	1.71	cholesterol homeostasis
SSD557	apg9	4.8185156	1.65	Multicellular Development
SSE894	cbp9	4.1341716	1.39	Calcium binding protein CBP9
SSG451	tipC	4.3312575	1.40	early development
SSH169	abcG3	3.9430002	1.42	ABC transporter, transport facilitation
SSJ163	dhkB	6.8486116	1.60	Hybrid histidine kinase DHKB
SSK432	sapA	3.5982656	1.30	Cellular biogenesis: peroxisome and lysosome
SSL850	dscC	7.4646858	2.44	Discoidin I, Multicellular organization
VSE791	smlA	4.7110207	1.27	Small aggregate formation protein
VSG467	hypothetical protein	4.6340654	1.37	unknown
VSI416	hypothetical protein	3.4186903	1.18	unknown
VSI349	hypothetical protein	5.9380519	1.53	unknown

Table 5: Genes up-regulated in the absence of CAP. The gene ID and gene name are shown in the first column, the middle columns denotes the fold expression and the score given by SAM plot. The last column indicates the role of the candidates in cellular processes. Interesting candidates up-regulated are mostly the signalling kinases.

The genes down regulated are in higher number when compared to the genes induced (Table 6). We observed that the candidates repressed were mostly cytoskeletal components, growth and developmental factors transport facilitation components and transcription/translational genes and some of them were signalling molecules. The cytoskeletal genes repressed significantly are profilin I, profilin II, villidin, beta-tubulin, dynacortin, coactosin and myosin. The signalling genes were NDP kinase, Gip17, Rho GDP-disassociation inhibitor (rdiA), and Rab1a GTPase. Gip17 and NDP kinase are both members of the NDP kinase family, where Gip17 encodes the cytosolic nucleoside

diphosphate (NDP) kinase, and NDP kinase (guk) defines a nuclear-encoded mitochondrial NDP kinase.

Gene ID	Gene Name	Score(d)	Ratio	Gene function
AB007025	DdEF1b	-3.173360923	0.79	elongation factor 1b
AF020409	docA	-3.285225588	0.71	disruption causes morphological defect
A32505	NDPk	-4.489937864	0.77	NDP kinase
AF025951	hsc70	-3.149693036	0.88	heat-shock cognate protein 70
AF030823	bt	-3.570809146	0.80	beta tubulin gene, microtubule dynamics
AF222688	det	-3.034080349	0.74	Dynactin, cytokinesis, cell shape
AJ000063	arf1	-4.17322761	0.79	ADP-ribosylation factor 1
D50338	rpl27a	-7.007106635	0.64	ribosomal protein
J05457	Gip17	-4.434835724	0.72	nucleoside diphosphate kinase
L27657	rpl19	-5.598949403	0.66	ribosomal calmodulin-binding protein
L35173	rps17	-3.204839597	0.74	ribosomal protein
M19337	myo-1c	-3.027607835	0.73	myosin light chain mRNA
M26017	ef2	-3.467341096	0.72	elongation factor 2
M96668	por	-3.496833356	0.79	channel protein; porin
U27536	cysbs	-4.205385645	0.74	cystathionine beta synthase
U27539	S24	-3.373231594	0.74	40S ribosomal protein
U61988	prtD	-3.22290643	0.75	similar to proteasome
X14909	rpl7	-3.618738169	0.69	ribosomal protein
X14970	elf-4D	-4.357191545	0.71	translation initiation factor
X15382	V18	-6.193739561	0.71	ribosomal protein
X15383	V14	-9.721219879	0.67	vegetative specific gene
X55672	cox6	-4.653475822	0.75	cytochrome c oxidase subunit VI
X56192	rapP2	-4.023227995	0.74	ribosomal acidic phosphoprotein P2.
X61580	prof2	-4.380408923	0.69	Profilin II, G-actin binding protein
X61581	prof1	-7.632305101	0.74	Profilin I, G-actin binding protein
X61797	coaA	-3.544823629	0.84	Coactosin, F-actin binding protein
X69484	s31	-3.680421933	0.71	ribosomal protein S31
X74287	prv	-4.115351338	0.68	S.ciliosum chloroplast intergenic spacer DNA
X95896	cox1	-7.046580942	0.38	cytochrome c oxidase I.
Y00145	UDPGP	-3.035867532	0.85	UDP glucose pyrophosphorylase gene
Z11691	cmf	-4.990721808	0.63	density-sensing factor
SLA566	tipD	-3.031059863	0.53	Multicellular organization, Morphogenesis
SLE690	tipA	-3.447101481	0.80	Multicellular organization, Morphogenesis
SLE796	villidin	-4.930401157	0.52	linker between membranes and cytoskeleton
SLK151	ribosomal protein	-4.193836858	0.63	translation
SSD706	rdiA	-3.546261937	0.8	Rho GDP-dissociation inhibitor
SSF195	rab1a	-3.428891601	0.71	Ras-related protein, vesicular trafficking
SSH277	em1C	-4.403869071	0.82	myosin essential light chain
SSH379	tranlocase	-5.915113534	0.58	ADP/ATP translocase, transport facilitation

Table 6: Genes down-regulated in the CAP bsr cells. The gene ID and gene name are in the first two columns and the fold decrease is shown in the fourth column. The score obtained from the SAM plot is shown in the middle panel. The interesting candidates down regulated are Profilin I & II, villidin, and NDP kinases.

The growth and developmental genes repressed were vegetative stage specific genes like V14 and V18, elongation factors (ef1b and ef2, elf-4D), cell density factors (cmf) and tipA and tipD genes involved in multicellular development. The majority of the genes are the ribosomal proteins rp27a, rp19, rps17 and rpl7, some of them also fall under the mitochondrial components like porin and

cytochrome oxidase subunits. The rest of the genes repressed are the hypothetical proteins and others fall in uncertain and unclassified groups (Table 6).

The repression of profilin, ubiquitous G-actin sequestering proteins was further supported by immunoblotting with profilin I and II mAb with which we estimated the amounts of profilin I and II in AX2 and CAP bsr. The immunoblot revealed that both profilin I and II were reduced to two fold in CAP bsr when compared to the wild type (Figure 84).

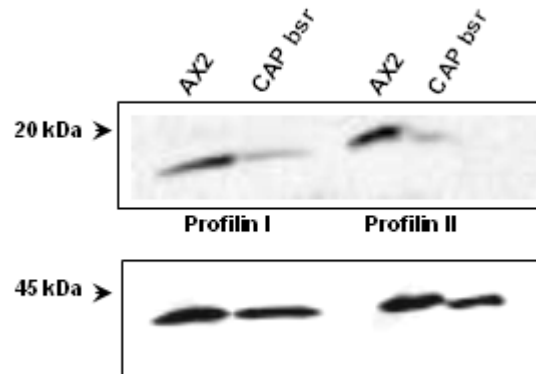


Figure 84: Immunoblot showing reduced amounts of Profilin I and II in CAP bsr in comparison to AX2. 2×10^5 cells were lysed with 2x sample buffer and resolved on SDS-PA gels (15% acrylamide). They were blotted onto nitrocellulose and probed with the respective profilin I (153-245-10) and profilin II (174-336-12) mAb followed by enhanced chemiluminescence. It was observed that the profilin levels are comparably less in CAP bsr when compared to AX2. The blot was analysed for the loading controls by re-probing for actin.

It was also noticed that some of the immuno-precipitation products appeared in the microarray lists of up or down regulated genes and correlated with the association and functioning of CAP. The most important candidates obtained in both the immuno-precipitation experiments and microarray analysis were p21 activated protein kinase (pakA) which is involved in the regulation of actin and cytokinesis, small aggregate formation protein (smlA) and D2 crystal protein, which are required for early aggregation stage, G-protein activator NDP kinase, tipD, a gene required for multicellular development, s24 ribosomal protein and mitochondrial components like porin and cytochrome oxidase subunits (refer to tables 5 and 6).

Discussion

The link between signal transduction and subsequent alterations in the cytoskeleton is a central theme in cytoskeleton research. A protein that may provide this link is the Cyclase-associated protein CAP, first found in *S. cerevisiae* (Field et al., 1988). CAPs are highly conserved, ubiquitous, bifunctional proteins that modulate the actin-based cytoskeleton and play a role in Ras signalling (Hubberstey and Mottillo, 2002; Field et al., 1990; Freeman et al., 1995). The CAP homologue of *Dictyostelium discoideum* is involved in microfilament reorganisation at anterior and posterior plasma membrane regions during directed cell movement. It exhibits approximately 39% identity and 61% similarity to CAPs from human and yeast respectively, and possesses the CAP characteristic length and domain organisation (Gottwald et al., 1996). Our studies show that CAP determines cell polarity and affects development. We have provided evidence that it plays an important role in cellular processes requiring high actin turnover and remodulation of the actin cytoskeleton. We also determined that moderate overexpression of CAP in an adenylyl cyclase mutant led to induction of a developmental stage where they formed mounds suggesting a role for CAP in growth and development of *Dictyostelium*.

1.0 Localization and dynamics of CAP in signalling mutants

S. cerevisiae has provided the most detailed analysis of CAP localization. In yeast, CAP is localized through its poly-proline domain to the cortical actin patches, where active actin turnover takes place (Freeman et al., 1996). In mammalian cells, CAP is diffusely distributed throughout the cytoplasm and can concentrate at the cell membrane and lamellipodia of migrating fibroblasts (Freeman et al., 2000). In higher eukaryotes, CAP is a cytoplasmic protein, but its precise localization can vary (Hubberstey and Mottillo, 2002). The CAP homologue of *Dictyostelium* is a PIP₂ regulated G-actin sequestering protein which is present in the cytosol and shows enrichment in the cell cortex near the plasma membrane and targeting of CAP to the cell cortex is mediated by its N-terminal domain (Noegel et al., 1999). To understand the precise localization of CAP in *Dictyostelium*, and to address the question which signals are required to recruit the protein to the cell cortex we performed localization studies of CAP in a series of mutants with defects in signal transduction pathways.

The aggregation stage specific adenylyl cyclase ACA of *Dictyostelium* is homologous to the G-protein regulated mammalian adenylyl cyclase. In the budding yeast *Saccharomyces cerevisiae* it has been established that adenylyl cyclase (CYR1, which catalyzes the production of cAMP) is a major downstream effector of RAS1 and RAS2, which are structural, functional and biochemical homologues of mammalian Ras. The yeast adenylyl cyclase forms a complex with the 70 kDa adenylyl cyclase-associated protein (CAP) (Shima et al., 2000). The direct association of yeast

CAP/Srv2 with adenylyl cyclase prompted us to investigate the localization of CAP in *aca*⁻ cells of *Dictyostelium*. However, the expression of CAP and its localization as well as the dynamic behaviour of various GFP-fusion proteins were as in wild type. These results suggested that localization of CAP and its domain is not determined by ACA, and is also not required for the correct expression level of CAP. Also, the localization and expression of CAP in *piaA*⁻ and in a temperature sensitive mutant for *piaA* that in addition lacked *acaA* and *acrA* was found to be unaffected and unaltered in comparison to the wild type. Likewise, G-protein $\alpha 2$ and β deficient cells showed a correct expression levels and targeting of CAP to the cell cortex, and similar observations were also made in *cAR1*⁻ and *cAR3*⁻ cells and in cells lacking PI3-kinases 1 and 2 which are located further downstream in the signalling cascade. Taken together, the localization of CAP to the cell cortex was found to be independent of the known fundamental signalling molecules anchored at the cell membrane.

The further downstream effector PKA is a central player in cAMP signal transduction. Interestingly, we observed that localization of *Dictyostelium* CAP is altered in mutants in the regulatory subunit mutant of PKA (RM-PKA) and severely affected in a mutant carrying an inactive catalytic subunit of PKA (PKA-C). CAP preferentially accumulated in the form of circular rings or crowns in the cytoplasm, where it concentrated abundantly and appeared as ectopic structures showing an aberrant localization of CAP. Moreover, in RM-PKA mutants CAP was abundantly concentrated in patches near the cell cortex. Further microscopic studies revealed that these aberrant structures appeared at the top visible focal plane. Actin accumulated also in patches and distributed abnormally in the PKA mutant in comparison to the wild type. CAP expression is however unaltered in PKA-C mutants when compared to the wild type. Our data are further supported by the recent reports from *Drosophila* where in a screen to identify the mutations perturbing the proper organization of the actin cytoskeleton and acolyte polarity in *Drosophila* a homologue of CAP was identified as well as a mutation in the catalytic subunit of PKA (Baum et al., 2000). The defects were dramatically enhanced in the double mutants exhibiting an exaggerated phenotype. This implies a related function for CAP and PKA in the germline and suggests that PKA and CAP functionally cooperate in the germline to control actin organization and that they may be elements of a conserved signal transduction pathway (Baum et al., 2000). Our findings that CAP localization at the cell cortex depends on PKA led us to speculate that CAP may play a key role in the PKA/cAMP signalling pathway in the cell and functionally co-operate to control the actin organization in order to bring about coordinated cell polarity events requiring remodeling of the actin cytoskeleton.

2.0 CAP is a general regulator of phagocytosis

Particle ingestion or phagocytosis is a very active process in *Dictyostelium*. It involves rearrangements of the actin cytoskeleton, which actively and characterized. Also, the phenomenon of phagocytosis exhibited by macrophages resembles the professional phagocyte *Dictyostelium* in several aspects. When the particle attaches to the membrane of *Dictyostelium* cells phagocytosis is induced and a phagocytic cup is formed by the invagination and fusion of the plasma membrane. The actin cortex, actin binding proteins and signal transduction molecules are further essential component for this process. The role of many cytoskeletal components during phagocytosis has been well studied. Coronin, myosin IB, myosin VII, ABP120/gelation factor/Ddfilamin, Lim domain containing proteins, a 34 kDa F-actin bundling protein and actin interacting protein (DAip1) are some of the known proteins that take part in phagocytosis and localize with actin at the phagocytic cup during early stages of phagocytosis (Cox et al., 1996; Rivero et al., 1996a; Konzok et al., 1999; Titus, 1999, Khurana et al., 2001). Our studies showed that CAP plays a dynamic role during phagocytosis, where it predominantly relocates to the cell cortex and enriches at the site of membrane invagination during the ingestion of the particle. The GFP-CAP live revealed that CAP plays an efficacious role during phagocytosis. These findings were further supported by the presence of higher amounts of CAP in the phagosome fraction. Furthermore, the data suggested that CAP is involved in the early stages of phagocytosis. The redistribution of CAP strongly resembled the one observed for cells expressing GFP-actin suggesting a role for CAP in remodeling of the actin cytoskeleton. Mutant analysis showed that phagocytosis also requires proper cell signalling for a remodeling of the actin cytoskeleton. We therefore investigated if the signalling molecules ACA, ACA regulator Pianissimo (PIA), ACA in combinations with ACR and Pianissimo, the heterotrimeric G-proteins $\alpha 2$ and β subunits, cAMP receptors CAR 1 and 3, PI3-kinase 1 and 2, and PKA have any role in the re-localization of endogenous CAP upon a stimulus. Our microscopic data revealed that the dynamic redistribution of CAP from the cell cortex to the phagocytic cups and phagosomes was unaffected and unaltered in the mutants of ACA, PIA, cAR1⁻/3⁻, G α 2 and PI3-kinases. The G β ⁻ cells are severely impaired in phagocytosis due to inappropriate regulation of the actin cytoskeleton failing to rearrange the actin cytoskeleton in the form of a phagocytic cup and phagosomes (Peracino et al., 1998). The G β deficiency did not affect the property of CAP to redistribute to the phagocytic cups in those few cells which showed phagocytosis, suggesting that re-localization of CAP to the phagocytic cup and phagosome is not dependent on the G β subunit and also reveal the primarily involvement of G β subunit signalling during phagocytosis. In contrast, in PKA-C mutant CAP accumulation at the

phagocytic cups was uneven, discontinuous and did not accumulate sharply at the phagocytic cup, which indicates the PKA-C requirement of to target CAP to the cell cortex during the stimulus. AX2 cells expressing dominant negative RacA showed a slightly weaker association of CAP at the site of phagocytosis. Although, imaging data showed that GFP-CAP in *pik1⁻/2⁻* cells relocalized dynamically and accumulated at the phagocytic cups and phagosomes and the expression of GFP-CAP improved the altered phagocytosis of *pik1⁻/2⁻*. The imaging of GFP-CAP in the G β subunit showed CAP redistributes to the site of phagocytosis. However GFP-CAP remained at the same site from 10 seconds to even 10 minutes, suggesting a defect in cytoskeletal dynamics. The quantitative analysis of phagocytosis supported the live imaging where the AX2-GFP-CAP cells internalized 1.5 fold more than wild type. A drastic enhancement of 1-2 folds in the yeast uptake in *aca⁻*, *pia⁻*, *g α 2⁻* and *pik1⁻/2⁻* expressing GFP-CAP was observed in comparison to wild type. Expression of GFP-CAP partially improved the phagocytic defect of *g β ⁻* with a two folds increase in comparison to the mutant. The *aca⁻* cells expressing GFP fusions of CAP and its domains were more or less comparable to the wild type AX2. All our phagocytosis studies suggest the involvement and functioning of CAP at the cortex during phagocytosis and implicate CAP to be a general regulator of phagocytosis in *Dictyostelium*, although the CAP mutant (CAP bsr) did not show impairment in phagocytosis.

3.0 Dynamics of CAP during pinocytosis

Dictyostelium cells take up fluid by macropinocytosis, which depends on the integrity and on rearrangements of the actin cytoskeleton. Many actin-associated proteins are involved in the process of macropinocytosis, but so far *in vivo* dynamics studies are available only for Coronin, DAip1, RacF, LimC and LimD (Hacker et al., 1997; Konzok et al., 1999; Rivero et al., 1999, Khurana et al 2001). The analysis of CAP bsr cells showed a slower growth and reduced saturation densities. This was paralleled by a reduction in fluid phase endocytosis (Noegel et al., 1999). The CAP redistribution during pinocytosis in the various signalling mutants did however not show alterations as compared to wild type and from our studies we can conclude that these signalling components are also not regulating CAP during pinocytosis.

3.1 CAP rescues the impaired pinocytosis of *pik1⁻/2⁻* cells

The PI3-kinase PIK 1 and 2 possibly through modulations of the levels of PIP₃ and PIP₂ regulate the organization of actin filaments necessary for circular ruffling during macropinocytosis and the *pik1⁻/2⁻* cells is severely impaired in pinocytosis (Zhou et al., 1998). Expression of GFP-CAP rescued the severe pinocytic defect of the *pik1⁻/2⁻* cells as revealed from our live imaging and quantitative

analysis. The confocal microscopy visualized that GFP-CAP dynamically remobilizes from the actin cortex to the areas of membrane ruffles forming the macropinosome, and CAP persists around the vesicle ingesting the fluid and protrudes, progresses and circularizes surrounding the liquid in the form of the vesicle and disassociates from the pinched vesicle within few seconds. However, it was observed that CAP moves around the vesicle rapidly indicating its role even during late endocytosis. We also observed that the cells pinocytose very frequently and at a higher rate of internalization in $\text{pik1}^{-/2^{-}}$ cells expressing GFP-CAP. The quantitative data supported this as all the pinocytosis parameters that were severely reduced in $\text{pik1}^{-/2^{-}}$ cells (which only had 5% influx rate) were found to be improved by the expression of GFP-CAP at an influx rate of 100%, which was comparable to the wild type. Another observation made with the growing cells was a correction in the cell size. From being highly variable in the $\text{pik1}^{-/2^{-}}$ cells CAP expression led to a more regular cell size and thereby may have increased the cell surface for the improved uptake of fluid. Alternatively, the actin rearrangements in areas participating in pinocytosis may occur in a more efficient way upon overexpression of CAP. As CAP overexpression could overcome the pinocytosis and cell shape defects of the $\text{pik1}^{-/2^{-}}$ cells, suggest that CAP should perform a role downstream of PI3-kinases.

3.2 CAP restores the altered distribution of actin and filamentous actin in $\text{pik1}^{-/2^{-}}$ cells

The altered phagocytosis and the severe impairment in pinocytosis of $\text{pik1}^{-/2^{-}}$ cells are reported to be due to the observed altered distribution of the filamentous actin (Zhou et al 1998). The abnormalities in these processes in the double knockouts prompted us to examine the distribution of the filamentous actin and the correction brought about by the expression of the GFP-CAP. Our results confirmed that expression of GFP-CAP restored the distribution of actin and F-actin in the $\text{pik1}^{-/2^{-}}$ cells. The GFP-CAP transfected mutant and the wild type cells were polarized and exhibited an actin staining which was heterogeneous and concentrated in actin crowns and specialized structures, while the mutants were predominantly rounded with few protrusions and the actin staining was more homogeneous and evenly distributed around the periphery. Various phalloidin-staining structures characteristic of macropinocytosis were detected at the apical surface of both wild type and mutant expressing GFP-CAP, which appeared as circular membrane ruffles with enrichment of GFP-CAP which overlapped with the filamentous actin. In contrast, short actin spikes forming smaller crowns were visible in the $\text{pik1}^{-/2^{-}}$ cells. These results explain the role and complementation of the GFP-CAP in the $\text{pik1}^{-/2^{-}}$ cells endocytosis and indicate that CAP overexpression can overcome the PI3-kinase deficiencies.

4.0 Developmental regulation of CAP in *pik1⁻/2⁻* cells

To gain insight into the potential role of CAP in regulating *Dictyostelium* development we again made use of the *pik1⁻/2⁻* cells, which have severe defects in development. The mutants are reported to exhibit abnormal growth and developmental phenotype, as they took 1 to 2 days longer to initiate development once the bacteria were depleted, and only a small fraction of the mutant cells within plaques aggregated. They did not form aggregation streams and lacked mound formation, which resulted in multiple tips that resolved into independent slugs producing abnormal fruiting bodies (Zhou et al., 1995; 1998). Our microscopic results revealed that endogenous CAP was enriched at the front of the cell and did not appear at the posterior region of the cell, in comparison to the AX2 wild type where CAP distributed to the leading fronts and tail. However this distribution due to the lack of morphological complexity in the *pik1⁻/2⁻* cells was complemented with the expression of GFP-CAP. We found in live imaging analysis where we exposed the cells to cAMP, that GFP-CAP corrected the polarity and streaming defects in the aggregation competent cells. Also, mutants expressing GFP-CAP initiated development comparable to the wild type, and exhibited aggregation streams and mounds that formed single tips resolving into independent slugs and producing normal and individual fruiting bodies which were thin and long unlike the mutant. The data imply that CAP functions as regulator of development. It is reported that disruption of *Dictyostelium* PI3K genes 1 and 2 reduces the PIP₂ and PIP₃ levels and thereby alters the F-actin distribution leading into defects in the processes involving the actin cytoskeleton (Zhou et al., 1998). The corrections in *pik1⁻/2⁻* cells expressing GFP-CAP could be explained by the role of PI3-kinase involvement in modulating the PIP₂ levels, and it could be speculated that in the absence of PI3-kinases PIP₂ inhibition of CAP is reduced and expression of GFP-CAP may compete with the reduced PIP₂ molecules and may affect the distribution of F-actin and the rearrangement of the actin cytoskeleton.

5.0 Role of CAP in aggregation and early development of *aca⁻* cells

Describing *Dictyostelium* development is essentially a panegyric to the regulatory potential of cAMP. Starving *Dictyostelium* amoebae survive adverse conditions by gathering into communities that provide optimal conditions for spore formation and dispersal. During development cAMP is used as chemoattractant or hormone, as morphogen, and as intracellular messenger. The *Dictyostelium* system has developed a remarkably versatile mechanism for pulsatile synthesis and secretion of cAMP that is the backbone of its capacity for self-organization. So far, a direct link between CAP and adenylyl cyclase ACA from organisms other than yeast has not been made. We have performed a

series of experiments that were designed to unravel a cross talk between both proteins. First we did cAMP relay experiments and found that the cAMP relay was altered in the CAP bsr, and that the relay response is much lower and considerably slower in the CAP bsr in comparison to the wild type AX2. We also found that CAP bsr had normal levels of ACA at the protein level and stimulation of ACA activity in cellular extracts of CAP bsr is normal (Noegel et al., 2004). To gain more insight into the role of CAP during aggregation and development of *aca*⁻ cells, we made use of the *aca* null cells expressing GFP-CAP to unravel the exertive role of CAP in the absence of ACA. The confocal microscopy approved the rescuing role of CAP in *aca*⁻ cells expressing GFP-CAP and showed that these cells were highly polarised and were able to stream and aggregate and form mounds. Moreover, the morphological alterations were paralleled by the expression of proteins thought to be responsible for these events. The region required for this CAP activity was found to reside in the N-terminus of CAP and we also found that the proline rich stretch with N-terminus enhanced the aggregation of *aca*⁻ cells.

5.1 Moderate CAP overexpression improves the development of *aca*⁻ cells but does not allow complete restoration

Aca⁻ cells fail to develop, whereas GFP-CAP or N-Pro-CAP expression leads to stream and mound formation, which might be due to the rescue of the polarity defect. The step of mound formation could be explained by the enhancement seen in the expression of DdCAD1 molecule, an EDTA sensitive adhesion molecule. The CAP mediated aggregation in *aca*⁻ cells could be because of the possibility that the moderate CAP expression could be triggering other adenylyl cyclases to undergo aggregation and mound formation in *aca*⁻ cells. It is known that ACA is not required to provide intracellular cAMP for PKA activation but is essential to produce extracellular cAMP for co-ordination of cell movement during all steps of development and for induction of developmental gene expression (Pitt et al., 1993). It has been suggested that all intracellular signalling by cAMP during development of *Dictyostelium* is mediated by the cAMP dependent protein kinase, PKA, since cells carrying null mutations in the *acaA* gene can develop so as to form fruiting bodies under some conditions if PKA is constitutively active by overexpressing the catalytic subunit (Anjard et al., 2001). It was also reported that cells lacking both adenylyl cyclases *acaA* and *acrA* develop and form mounds at higher cell densities, express cell specific genes at reduced levels and secrete cellulose coats but do not form fruiting bodies when PKA is constitutive (Anjard et al., 2001). Our results point to a role of CAP in the cAMP signalling pathway together with other molecules to restore the developmental defects noticed in *aca*⁻ cells. However, it is unclear which are the other components involved in CAP mediated aggregation and which signalling systems involve CAP.

6.0 An overview of the significance of CAP in the signalling mutants

The studies undertaken in the signalling mutants, strongly suggests that CAP function is integrated in the growth and development as CAP overexpression can overcome defects in cell polarity, phagocytosis, macropinocytosis and aggregation. In most cases CAP rescued defects involving the rearrangement of the actin cytoskeleton (Table 1).

	AX2	aca ⁻	pia ⁻	Gα2 ⁻	Gβ ⁻	pik 1 ^{1/2} ⁻	AX2-GFP-CAP	aca-GFP-CAP	pia-GFP-CAP	Gα2 ⁻ -GFP-CAP	Gβγ ⁻ -GFP-CAP	pik 1 ^{1/2} -GFP-CAP
Phagocytosis	+	+*	+*	(+)	-	(+)	++	++*	++*	+	(±)	++
Pinocytosis	+	+	+	(+)	+	-	++	++	++	++	++	++
Aggregation	+	-	-	-	-	(+)	++	(+)	nd	nd	nd	+

Table 1: An Overview of the CAP dynamics studied in various signalling mutants. + indicates positive activity like AX2, (+) lesser activity, +* enhanced positive activity, ++ two fold higher activity, ++* enhancement in the two fold higher activity, - defect in activity. nd represents not determined.

7.0 Localization of CAP depends on LimD and is modulated by RacA

Lim domain containing proteins act as an adapter molecule mediating interactions between actin filaments and cytoskeleton-associated proteins at the cortical cytoskeleton. Our results showed that localization of CAP in the limD⁻ is unaltered in the growing cells, where it was enriched at the cell borders and also stained the cytosol. However, starving limD⁻ cells showed a different pattern of CAP distribution where it was found in the form of crowns near the cortex unable to reach the membrane or the leading fronts of the migrating cells in comparison to wild type. The confocal microscopy of limD⁻ also suggested that CAP accumulation in the enriched crown structure is at the distinct sections. These results can be interpreted that CAP localization during cell movement requires the cytoskeleton adapter LimD.

Since the localization of CAP was not determined by the upstream molecule are anchored at the plasma membrane, we studied the role of the small GTPases in targeting CAP to the cell cortex. In *Dictyostelium* the Rho family comprises 15 members, some of them (Rac1a/b/c, RacF1/F2, RacB) are the members of the Rac subfamily, another, RacA belongs to the RhoBTB subfamily. *Dictyostelium* Rho GTPases regulate actin polymerization, cell morphology, endocytosis, cytokinesis, cell polarity and chemotaxis (Rivero and Somesh, 2002). The localization studies of CAP in AX2 cells expressing

constitutively active or dominant negative RacA suggested that the constitutive expression of RacA alters the distribution of CAP, where it was distributed unevenly in large patches near the cell cortex and showed enrichments in the filopodia. The dominant negative RacA cells did not show such altered distribution pattern of CAP however, the CAP staining was weak in both the cytosol and the cell cortex. We thus have identified two potential regulators of CAP LimD and RacA.

8.0 LimD expression restores the defect in endocytosis of CAP bsr

Khurana et al. reported previously that the Lim domain containing protein LimD of *Dictyostelium* binds in vitro to F-actin and is important for cellular polarity. We studied the role of GFP-LimD in the absence of CAP during endocytosis and our live imaging revealed that expression of LimD rescued the endocytic defect of CAP bsr, and plays a dynamic role during the fluid uptake where it redistributes to macropinosomes and is involved in the actin associated process of endocytosis. The live microscopic sequence revealed that a GFP-LimD rich membrane invaginates and the protrusion of the membrane progresses until the edge and fuses to form a macropinosome, thus relaying the dynamics of LimD in the CAP bsr which was comparable to the wild type cells expressing GFP-LimD. These results of redistribution of GFP-LimD were further corroborated by live imaging studies of phagocytosis. Quantitative analysis of pinocytosis indicated that the influx rate of CAP bsr expressing GFP-LimD was 3 fold higher in comparison to CAP bsr. It appears that the two proteins have roles in similar cellular processes (i.e. generation of cell polarity) and can substitute each other. As their activity as actin-associated proteins appears to differ, LimD is an F-actin binding protein and CAP primarily interacts with G-actin, which must evoke a different mechanism.

9.0 CAP is required for cAMP signalling

CAP is required for cell polarization, chemotaxis and cAMP relay and we were interested to investigate the role of CAP in these aspects by complementation analysis with GFP-LimD in CAP bsr. LimD⁻ cells are also reported to be defective for cell polarization and chemotaxis (Khurana et al., 2002). Our cAMP pulse assay in CAP bsr expressing GFP-LimD by live microscopy revealed that the CAP bsr expressing GFP-LimD have severe defects in the distribution of GFP-LimD in response to extracellular cAMP. The live imaging revealed that the CAP bsr cells expressing GFP-LimD were flattened and roundish, where GFP-LimD accumulated in larger granular structures, which enlarged and extended from the cell centre to the periphery and crawled in the form of waves failing to reach the cell cortex. After some seconds the GFP-LimD was found enriched in circular crown structures

and was concentrated in thick circular spheres in comparison to the AX2 cells expressing GFP-LimD. These observations suggest that the absence of CAP could be responsible for the altered distribution of GFP-LimD in response to a cAMP pulse. Furthermore, the observations lead us to speculate that the cell polarization defect in CAP bsr expressing GFP-LimD could be due to the altered signalling for the proper cAMP relay in the absence of CAP, thus suggesting the requirement of CAP in the cAMP signalling.

10.0 Does CAP interact with cyclases?

In yeast, a physical interaction had been shown between adenylyl cyclase and CAP via a CAP binding domain at the C-terminus of the adenylyl cyclase (Nishida et al., 1998), the interaction domain in CAP was localised to a short N-terminal stretch that is highly conserved in CAP from other species. It has been suggested that the short N-terminal stretch contains the potential to form an amphipathic helix, a structure implicated in protein-protein interactions. This sequence is localised in *Saccharomyces cerevisiae* at positions 19-21 and 26-28 and we found that this sequence is also highly conserved in *Dictyostelium* CAP suggesting a physical interaction of CAP with adenylyl cyclase in *Dictyostelium*. Although the C-terminal part of *Dictyostelium* ACA shares 31% identity with that of yeast adenylyl cyclase we could not detect a direct interaction of CAP or its I domains with ACA when we performed a yeast two hybrid assay. Nevertheless, we found that the co-transformants were growing in the required minimal media but did not result in positive β -gal test (Table 1). This might leave a remote possibility of an interaction of *Dictyostelium* CAP with ACA, which could not be detected in the yeast system under the strong selection pressure of the assay.

Recently it was reported that the *Dictyostelium* guanylyl cyclase A (GCA) and soluble guanylyl cyclase (sGC) exhibit a high degree of amino acid sequence identity with ACA and can be converted into an adenylyl cyclase by a mutation in the catalytic sites (Roelofs et al., 2002). Moreover, the C-terminus of sGC shares 41% identity with the C-terminus of ACA, the putative site of interaction with CAP. sGC predicts a 2843 amino acid protein and we detected a possible direct interaction of CAP with the C-terminus of sGC a 2.4 kb fragment by yeast two hybrid experiments. These results require further support by different methods, which is in progress. The possible interaction of CAP with sGC leads us to speculate that CAP may play a role in the GC pathway correlating with our previous findings that the cAMP-induced cGMP response is altered in the CAP mutant (Noegel et al., 2004).

11.0 Does CAP interact with the Arp2/3 complex?

The Arp2/3 complex is a ubiquitous and important regulator of the actin cytoskeleton, involved in the nucleation mechanism, a mechanism essential for filament formation, and appears to involve stabilization of polymerization intermediates. It binds to the sides of actin filaments and is concentrated at the leading edges of motile cells (Mullins et al., 1998). In the highly motile cells of *Dictyostelium* the Arp2/3 complex is rapidly re-distributed to the cytoskeleton in response to external stimuli during phagocytosis, macropinocytosis, and chemotaxis (Insall et al., 2001). The Arp2/3 complex promotes the branched or dendritic nucleation of new actin filaments from pre-existing ones by the generation of new fast growing (barbed) ends (Amann and Pollard, 2001). These branched structures are the major component of the lamellipodia of migrating cells (Svitkina and Borisy, 1999), suggesting that the Arp2/3 complex is a physiologically important nucleator of actin polymerisation.

The Arp2/3 complex is composed of seven subunits, including the actin-related proteins Arp2 and Arp3 and five other proteins, p41-Arc, p34-Arc, p21-Arc, p20-Arc and p16-Arc. In *Dictyostelium* the predicted sequences of the subunits show a strong homology to the members of the mammalian complex, with the larger subunits generally better conserved than the smaller ones. It appears that these proteins are well conserved in evolution and play an essential role in initiating new actin filaments in a variety of cell types (Machesky and Insall, 1999).

Our immunoprecipitation experiments of CAP from *Dictyostelium* AX2 cells expressing GFP-CAP resulted in co-precipitation of the p34-Arc subunit and p21-Arc subunit of the Arp2/3 complex. The potential CAP interaction with the Arp2/3 subunits further affirms a role for CAP in the actin polymerisation. Unfortunately, the yeast two hybrid experiments to detect the direct interaction of CAP with the p34-Arc subunit failed as the p34-Arc subunit was auto-activating.

12.0 Interaction of CAP with the Vacuolar H⁺ ATPases complex

All eukaryotic cells contain a highly conserved multi-subunit enzyme, the vacuolar H⁺ ATPase, which uses the energy from ATP hydrolysis to transport protons across biological membranes. The V-type ATPases or V-ATPases also called as proton pumps have a very complex structure consisting of an integral (transmembrane) V₀ domain composed of 5 subunits (subunits a-d), that serves as a proton channel and a peripheral V₁ domain that contains the ATP binding site, is involved in ATPase activity and is composed of 8 subunits (subunits A-H) (Figure 85). The V-type ATPases are related in structure and probably in mechanism to the F-type ATPases, which are appropriately called as ATP

synthases. For V-ATPases ATP hydrolysis by the peripheral V_1 domain drives the protons through the V_0 integral domain from the cytoplasm to the lumen. In contrast, the F-type ATPases normally function in opposite direction that is in ATP synthesis. The V-type ATPases are responsible for the acidification of lysosomes, endosomes, the Golgi complex, and secretory vesicles in animal cells, and function in processes such as receptor mediated endocytosis, intracellular targeting of lysosomal enzymes, protein processing and degradation, the coupled transport of small molecules and pump protons across the plasma membrane of various cell types (Nishi and Forgac 2002). Recent reports have further shown the importance of V-ATPases in many other aspects. V-ATPases have been proposed to have roles in tumour metastasis as they have been found in the plasma membrane of certain tumour cells. In macrophages and neutrophils, plasma membrane V-ATPases are involved in cytoplasmic pH homeostasis, bone resorption and also function in renal acidification. A possible link between V-ATPases and the cytoskeleton has been suggested by the observation that mutations of the yeast VMA4 gene that encodes subunit E cause changes in cell morphology, aberrant bud formation and changes in the cytoskeleton (Zhang et al., 1998).

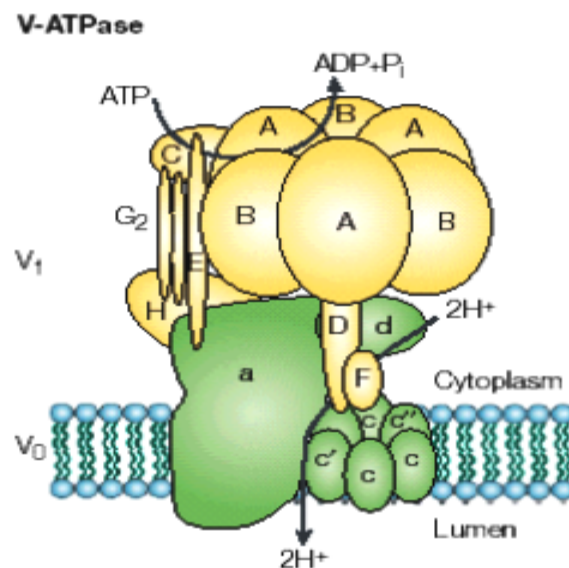


Figure 85: Structural composition of the V-ATPases. For the V-ATPases ATP hydrolysis by the peripheral V_1 domain (shown in yellow) drives proton transport through the integral V_0 domain (shown in green) from the cytoplasm to the lumen (taken from Nishi and Forgac 2002).

Our attempts to identify binding partners of CAP resulted in the isolation of the vacuolar ATP synthase subunit d of the integral membrane V_0 complex of the V-ATPases, also known as DVA41 (Figure 85). Subsequent experiments resulted repeatedly in the isolation of the vacuolar ATPase B subunit. Interestingly, our yeast two hybrid assay showed a possible direct interaction of CAP with DVA41, however the interaction could be transient or weak as the co-transformants could not grow upon the omission of adenine a stringent nutritional marker (Table 4). Such an interaction was further

confirmed by the association of GFP-CAP with the vacuolar marker for the vacuolar ATPases A subunit (Figure 75), where CAP co-localised with VatA and showed a strong association with enrichments in the vacuolar network. We also found that CAP associated vacuoles weakly overlap with GFP-N-ramp1 vacuoles. Furthermore, we observed a restricted co-localization of CAP with VatB, the vacuolar ATPase B subunit. The results are evident for the association of CAP with the vacuolar ATPase which was further supported by the finding that the vacuolar network is disturbed and is mostly absent in CAP bsr visualised by the vacuolar marker VatA. This goes along with a reduced expression of VatA in CAP bsr in comparison to the wild type AX2 and AX2 cells expressing GFP-CAP. Inspection of subsequent focal plane images revealed that the vacuoles are distributed in all different planes in the wild type. In contrast, CAP bsr had few vacuoles near the plasma membrane and the image slices showed the absence of the vacuoles. We also found that expression of GFP-CAP restored the disturbed vacuolar system in CAP bsr showing the importance of CAP in the localization and distribution of the vacuolar system, where GFP-CAP co-localised with the VatA marker and rescued the diffused and disturbed staining of VatA, and the vacuoles were observed to be intact and large and showed a strong staining of the vacuolar marker.

To further attain which domain may be involved in the restoration of the altered distribution of vacuolar network we carried out further studies and found that the N-terminus with the proline stretch restored the disturbed vacuolar network in CAP bsr to a partial extent. The expression of GFP-N-Pro-CAP showed lower number of vacuoles in comparison to the full length CAP restoration but the vacuoles were intact and large. It was also found that the C-Pro-CAP-GFP also restored the distribution of the vacuolar network to some extent. This was not comparable to GFP-CAP, but the vacuoles formed were quite large and intact. Taken together these results suggest a strong interaction and association of CAP with the vacuolar system where CAP may be involved in functional aspects of V-ATPases.

The immuno-precipitation experiments resulted in a series of molecules, which will need to be further analysed in detail. Further molecules obtained were the Ras related Rab-GTPases Rab4, Rab11, RabA and RabB. Our preliminary results showed that CAP associates with the Rab-GTPases, and shows a similar granular distribution as Rab-GTPases. Interestingly, Rab4 and Rab4 like GTPase (RabD) in *Dictyostelium* co-localize with V-H⁺ ATPases in the reticular membranes of the contractile vacuole complex (Bush et al., 1994). These studies suggested an interaction of CAP with V-ATPases and Rab-GTPases, which together could be components of the endocytic pathway in *Dictyostelium*. Furthermore, the IP experiments revealed CAP as binding partner, the cytoskeletal components dynamin and cortexillin, and signalling molecules such as pkaA, protein kinase 2, NDP kinase and

histidine kinase (*dokA*, *dhkC*), GTP binding protein (*SAS1*), PDI, cAMP inducible D7 and D2 protein. Other molecules were *tipD*, porin, cytochrome oxidase (1/2), vacuolin B and small aggregate formation protein (Table 5). The significance of these interactions needs to be determined.

13.0 Microarray analysis signifies CAP as a regulator of signal transduction, multi-cellular development and cytoskeleton

The DNA microarray technology can generate a large amount of data describing the pattern of gene expression. These data when properly interpreted can yield a great deal of information concerning differential gene expression. Using microarray analysis we performed a genome wide determination of expression patterns in vegetative CAP bsr to understand the importance of CAP in the regulation of genes. Four independent experiments with duplicate batches resulted in 554 significant genes with a finest tuning delta value of +/- 1.646 and a lowest false positive rate of 0.534. Out of 554 significant candidates, 214 were upregulated and 314 were down regulated as suggested by the SAM plot (Figure 83). The most interesting molecule in the up-regulated category is *RegA*, (which is 1.33 fold expressed) a gene coding for cAMP phosphodiesterase (PDE), homologous to the mammalian cyclic nucleotide phosphodiesterase. It is a class I cAMP PDE, which functions within the cell and is analogous to a class II phosphodiesterase (*psdA*) that functions extracellularly. The *RegA* transcript, which is prominently present in pre-stalk and pre-spore cells, is expressed at a low level in vegetative cells, and is induced rapidly during aggregation, remaining present throughout development (Shaulsky et al., 1996). *RegA* activity is detectable at early stages of development and even in immunoprecipitates from growing cells. *RegA* functions at an intersection between cAMP and two component signal transduction systems, combining in itself domains characteristic of both systems.

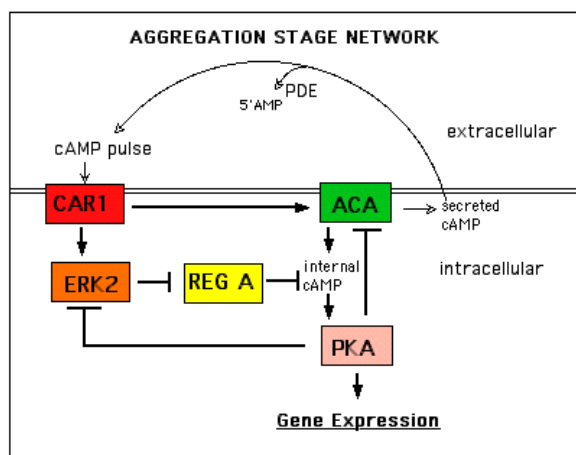


Figure 86: The aggregation circuit. Pulses of cAMP are produced when ACA is activated after the binding of extracellular cAMP to the surface receptor CAR1. Ligand-bound CAR1 activates the protein kinase ERK2 that may transmit the signal to ACA. An alternate circuit in which the activation of ACA by ligand-bound CAR1 is independent of ERK2 has the same properties as our standard circuit. When cAMP accumulates internally, it activates the protein kinase PKA by binding to the regulatory subunit of PKA. ERK2 is inactivated by PKA and no longer inhibits the cAMP phosphodiesterase *RegA* by phosphorylating it. A protein phosphatase activates *RegA* such that *RegA* can hydrolyze internal cAMP. Either directly or indirectly, CAR1 is phosphorylated when PKA is activated, leading to loss-of-ligand binding. When the internal cAMP is hydrolyzed by *RegA*, PKA activity is inhibited by its regulatory subunit and protein phosphatase(s) returns CAR1 to its high-affinity state. Secreted cAMP diffuses between cells before being degraded by the secreted phosphodiesterase PDE. The double horizontal line represents the membrane surface of a cell (Laub and Loomis, 1998).

The up-regulation of RegA gives an explanation for the developmental delay of CAP bsr cells as RegA is known to negatively regulate the cAMP dependent protein kinase A (PKA) by inhibiting cAMP (Figure 86) which in turn may result in developmental delay and altered cAMP relay in CAP bsr. The CAP mediated aggregation in *aca*⁻ could also give a hint that expression of CAP may negatively regulate RegA, which in turn may lead to the constitutive expression of PKA, probably the PKA-C and may influence the enhancement of agglutination of the *aca*⁻ expressing GFP-CAP thus, suggesting a role of CAP in the cAMP signalling pathway.

Another important signalling molecule was the extracellular regulated MAP kinase (ERK1). The MAP kinase cascade is a universal signalling unit used by a wide number of eukaryotic signalling pathways. Typically it is composed of members of MEK kinase (MAP kinase kinase kinase, MEKK), MEK (MAP kinase kinase) and MAP kinase (or ERK) families (Chung and Firtel 2002). Two MAP kinases, ERK1 and ERK2 have been identified in *Dictyostelium*. The function of ERK1 is not clear, but it may belong to a MAP kinase pathway including MEK1 and proposed to activate guanylyl cyclase (GCA). PAKa was also transcriptionally upregulated in the CAP bsr microarray analysis. The PAK family of serine/threonine kinases comprises at least four isoforms that are differentially expressed in mammalian tissue (Knaus and Bokoch, 1998). PAKs have been implicated in the morphological changes resulting from the alterations of the cytoskeleton associated with Rac and Cdc42 that direct signal transduction from the plasma membrane to the cytoskeleton by phosphorylating actin-binding proteins. PAKa is required for cytokinesis and regulation of the actin and myosin cytoskeleton (Chung and Firtel 2002). Another kinase induced is STATa an intracellular signalling kinase required for tyrosine phosphorylation (Briscoe et al., 2001). Histidine kinase (*dhkB*), Tyrosine protein kinase-2 (*splB*) and protein kinase activator (*sgkA*) were found to be 1.3-1.7 fold up regulated in the CAP bsr. The results from these transcriptional studies pointed to a role of CAP in the signal transduction cascade involving the kinases.

Dynein is a cytoskeletal component induced which is known to play a significant role during cytokinesis and regulation of the actin cytoskeleton, it is known to nucleate microtubules to organize them into radial arrays in vivo (Malikov et al 2004). Taken together, a great majority of genes belonging to the category of multicellular organisation were induced, and cytodifferentiation factors like *sapA*, *tipC* and small aggregate formation protein were up regulated (refer Table 6 of results). The microarray further showed that the cytoskeletal machinery was significantly repressed in the absence of CAP, implicating an important role of CAP in the cytoskeleton of *Dictyostelium* (refer Table 7). Both Profilin I and II were 0.75 fold down regulated and these results were further confirmed by our immunoblots also showing a decrease of both Profilin I and II in CAP bsr. Profilins are ubiquitously

G-actin sequestering proteins and are suggested to be sister proteins for CAP which also interact with G-actin. The regulation of Profilin is also controlled by membrane phospholipids like PIP₂ or its precursor PIP. Furthermore, they are the binding partners for WASP and play an important role in the actin polymerisation, thereby inducing the reorganisation of the cytoskeleton (Stewart et al., 1999). Lack of both profilin isoforms result in impairment in cytokinesis and forms multinucleated cells and exhibit arrest in development and led to an increased concentration of F-actin and decrease in motility (Haugwitz et al., 1991). We also noted increased levels of CAP in the profilins I/II minus mutant (Gottwald et al., 1996). These data and our microarray data further support the link between CAP and profilins and suggest them to be components of the same machinery and also explain the cytokinesis and developmental defects of CAP bsr.

Intriguingly, it was found that villidin is repressed to 0.52 fold less in CAP bsr in comparison to the wild type. Villidin is a novel WD repeat and villin related protein associated with membranes and cytoskeleton and is involved in cell motility, endocytosis and phototaxis (Gloss et al., 2003). The other cytoskeletal elements repressed were coactosin, beta-tubulin, dynacortin, myosin essential and light chains. Many of the growth and developmental genes were repressed in their expression. These were vegetative specific genes V14 and V18, elongation factors (ef1b, ef2 and elf-4D), and genes required for multicellular development like tipA and tipD. The data suggest a role of CAP in growth and development. The majority of molecules down regulated fall under the transcriptional/translational group, and were mostly ribosomal proteins (rp27a, rp19, rps17 and rp17) and the other sub-division was transport facilitation involving mostly hypothetical genes. These molecules implicated the influence of CAP on the transcription and cargo machinery of the cell. Also, the mitochondrial components like porin and cytochrome oxidase subunits were repressed in the CAP bsr microarray analysis.

Interestingly, the repressed signalling molecules were of the NDP kinase family (guk and Gip17) both encoding a nucleoside diphosphate kinase NDPK which were 0.8 fold down regulated in CAP bsr. Interest in this enzyme is increasing as a result of its possible involvement in cell proliferation and development. NDP kinase is one of the major sources of GTP in *Dictyostelium* cells and it is been suggested that the effects of an altered NDP kinase activity on cellular processes might be the result of altered transmembrane signal transduction via guanine nucleotide binding proteins (G-proteins). It has been also reported that part of the NDP kinase is associated with the membrane and stimulated by cell surface receptors. The GTP produced by the action of NDP kinase is capable of activating G-proteins as monitored by altered G-protein-receptor activations and the activation of the effector enzyme phospholipase C (Bominaar et al., 1993). NDP kinase is reported to be involved in

modulating the contraction of the *Dictyostelium* cytoskeleton and proposed to be in physical contact with the cytoskeleton, by channelling ATP to the myosin molecule and play a direct role in regulating cytoskeletal contraction or facilitating contraction when intracellular ATP concentrations are low (Aguado-Velasco et al., 1996). The *Dictyostelium* NDP kinase is highly homologous to Nm23 and Awd proteins involved in mammalian tumor metastasis and *Drosophila* development (Wallet et al., 1990).

We also found that Rho GDP disassociation inhibitor (*rdiA*) and *Rab1a* was 0.7-0.8 fold reduced in CAP bsr. Rho GDI modulates the cycling of the Rho GTPases between active GTP bound and inactive GDP bound states and the cells deficient in Rho GDI show defects in cytokinesis, actin reorganisation and the contractile vacuoles (Rivero et al., 2002). These results create a possible link of CAP with the important regulators of the cytoskeleton like Rho GDI. This correlates with defects of CAP bsr in cytokinesis, actin remodelling and the diffused and altered vacuolar network. Interestingly, it was found that some of the molecules up/down regulated were also the molecules obtained in the immuno-precipitation (IP) studies like PAKa (p21 activated protein kinase), *smlA* (small aggregate formation protein) and D2 crystal protein. As the down regulated molecules we observed G-protein activator NDP kinase, a multicellular developmental gene *tipD*, *s24* ribosomal protein and mitochondrial components like porin and cytochrome oxidase subunits (also refer tables 5, 6, 7).

The microarray data need to be further substantiated by northern and western blot analysis and also by real time PCR. The transcriptional studies suggest the significance of CAP in both signal transduction pathways and the cytoskeleton in *Dictyostelium* and it raises the possibility of CAP to be a global regulator of most events occurring within the cell. It is hoped that, when the complete genome sequence is available, the current studies can be expanded to a genome-wide survey, which will undoubtedly uncover the roles of other genes that clustered into the hypothetical and uncertain/unclassified category and enlighten the significance of CAP in the global regulation. The transcriptional studies gave more insight into CAP multifunction at both molecular and cellular levels and suggested CAP to be a linker molecule in the cytoskeleton and signalling.

14.0 Outlook

Taken together, our results emphasize that CAP is a component of the cAMP signalling pathway and in remodelling of the actin cytoskeleton. We speculate that CAP could be assigned a position downstream of PI3-kinases because of its role in rescuing the defects in pinocytosis, F-actin distribution and development of the *pik1^{-/-}* cells. Our data of PKA requirement for targeting CAP to

Summary/zusammenfassung

Dictyostelium discoideum amoebae offer great opportunities to elucidate the signalling pathways involved in the generation of cell polarity. They constantly change their shape and form new ends in response to a plethora of environmental signals. This process requires distinct signalling molecules, the chemotactic machinery and components of the cytoskeleton such as CAP, which in *Dictyostelium* is involved in actin cytoskeleton rearrangements. *Dictyostelium* cells deficient for CAP show a defect in cell polarization during development and an altered cAMP relay response. In this work we wanted to study the position of CAP in the signalling network and made use of mutants defective in components of cAMP signalling (ACA, cAR1/3, G α 2, G β , PI3-kinase, Pianissimo and PKA) in which we studied CAP and CAP associated responses.

Our studies revealed that CAP functions independent of ACA, cAR1/3, G α 2, G β , PI3-kinase and Pianissimo whereas the cAMP dependent protein kinase A (PKA) is necessary for targeting CAP to the sites of its cellular action. The localization data suggest that CAP and PKA may functionally co-operate to control actin organization and cell polarity. We further observed that CAP functions downstream of PI3-kinases or in parallel pathways because overexpression of CAP rescued the severe impairment in pinocytosis in the pik1⁻/2⁻ cells, their altered distribution of F-actin and also the abnormal developmental phenotypes. In line with this proposal CAP could partially rescue the phagocytosis defect of the g β ⁻ cells. CAP expression also improved the development of aggregation deficient aca⁻ cells but did not lead to complete restoration. The cell polarity and streaming defects of aca⁻ cells were also rescued by the moderate expression of CAP making CAP a molecule downstream in the hierarchy of the signal transduction cascade. On the other hand, CAP regulates LimD, a component of the actin cytoskeleton which in *Dictyostelium* is involved in generation of cell polarity as shown by an altered behaviour of GFP-LimD in CAP bsr cells in comparison to wild type. To gain more insight into the *in vivo* functioning of CAP, we performed a search for binding partners which suggested that CAP associates and interacts with the vacuolar ATPases complex, and that the absence of CAP disrupts the vacuolar network. This underlines the findings obtained in the PI3-kinase mutants that CAP is a general regulator of endocytosis. We also identified ARP2/3 complex p34-ARC subunit, Rab4, Rab11 and porin as potential interacting partners of CAP by biochemical methods. The significance of this interaction is under investigation. Finally, our microarray analysis suggested that in the absence of CAP the actin cytoskeleton and signalling machinery is strongly affected. The up-regulation of regA (negative regulator of intracellular cAMP), and kinases like erk1, statA and pakA might be of relevance for the altered cAMP relay of CAP bsr cells. The repression of the expression of cytoskeletal components like profilins I and II, villidin, coactosin, myosin and signalling molecules like NDP kinases, RhoGDI suggest CAP to be a global regulator. Taken together our data support a function for CAP as adapter molecule linking the actin cytoskeleton and signalling.

CAP in *Dictyostelium discoideum* ist in die Regulation des Zytoskeletts und in Signaltransduktionsprozesse involviert. Ein Verlust des Proteins führt zu Defekten in Wachstum und Entwicklung und einem Verlust der Zellpolarität. Zellpolarität ist ein herausragendes Merkmal der cAMP-abhängigen Chemotaxis in *Dictyostelium*. Das Vorhandensein einer Reihe von definierten Mutanten mit Defekten in der Chemotaxis, hat es erlaubt, in dieser Arbeit die Einordnung von CAP in die cAMP Signaltransduktionskaskade zu untersuchen. Zur Verfügung standen Mutanten für den cAMP Rezeptor, die assoziierten G-Proteine, für die Adenylatzyklase, PI3-Kinasen und die cAMP-abhängige Proteinkinase A, die für die intrazelluläre Wirkung des cAMP notwendig ist. Untersucht wurden die Lokalisation von CAP und die Umverteilung von CAP während Aktin-abhängiger Prozesse. Dies hat gezeigt, dass CAP unabhängig von diesen Molekülen funktioniert. Im Gegenteil, es wurde beobachtet, dass CAP-Überexpression bestimmte Defekte wie den Endozytosedefekt in der PI3-Kinase Mutante oder den Entwicklungsdefekt in der ACA-Mutante zum Teil aufheben kann. CAP liegt also weiter stromaufwärts in der cAMP Signaltransduktionskette.

Für LimD, eine Komponente des Aktinnetzwerks, deren Ausfall in *Dictyostelium* zu einem Polaritätsverlust führt, wurde beobachtet, dass CAP essentiell für seine korrekte Lokalisation und Umverlagerung in der Zelle ist. Ähnlich abhängig von CAP sind Komponenten der vakuolären ATPase, einem Proteinkomplex von endozytotischen und vakuolären Membranen in *Dictyostelium*. Immunpräzipitationsexperimente belegen eine direkte Verbindung mit der v-ATPase. Weitere Bindeproteine von CAP sind Komponenten des Zytoskeletts. Diese Ergebnisse werden auch durch unsere Microarray-Analysen unterstützt, die in der CAP-Mutante Veränderungen bei Signalmolekülen und in Zytoskelettkomponenten zeigen.

Bibliography

Bibliography

- Aguado-Velasco, C., Veron, M., Rambow, J. A., and Kuczmariski, E. R. (1996). NDP kinase can modulate contraction of *Dictyostelium* cytoskeletons. *Cell Motil Cytoskeleton* *34*, 194-205.
- Amann, K. J., and Pollard, T. D. (2001). Direct real-time observation of actin filament branching mediated by Arp2/3 complex using total internal reflection fluorescence microscopy. *Proc Natl Acad Sci U S A* *98*, 15009-15013.
- Andre, E., Brink, M., Gerisch, G., Isenberg, G., Noegel, A., Schleicher, M., Segall, J. E., and Wallraff, E. (1989). A *Dictyostelium* mutant deficient in severin, an F-actin fragmenting protein, shows normal motility and chemotaxis. *J Cell Biol* *108*, 985-995.
- Anjard, C., Soderbom, F., and Loomis, W. F. (2001). Requirements for the adenylyl cyclases in the development of *Dictyostelium*. *Development* *128*, 3649-3654.
- Aubry, L., Klein, G., Martiel, J.-L. and Satre, M. Kinetics of endosomal pH evolution in *Dictyostelium discoideum* amoebae. Study by fluorescence spectroscopy.(1994). *J. Cell Sci.* *105*, 861-866
- Baldauf, S. L., Roger, A. J., Wenk-Siefert, I., and Doolittle, W. F. (2000). A kingdom-level phylogeny of eukaryotes based on combined protein data. *Science* *290*, 972-977.
- Baum, B., Li, W., and Perrimon, N. (2000). A cyclase-associated protein regulates actin and cell polarity during *Drosophila* oogenesis and in yeast. *Curr Biol* *10*, 964-973.
- Benlali, A., Draskovic, I., Hazelett, D. J., and Treisman, J. E. (2000). act up controls actin polymerization to alter cell shape and restrict Hedgehog signalling in the *Drosophila* eye disc. *Cell* *101*, 271-281.
- Bertholdt, G., Stadler, J., Bozzaro, S., Fichtner, B., and Gerisch, G. (1985). Carbohydrate and other epitopes of the contact site A glycoprotein of *Dictyostelium discoideum* as characterized by monoclonal antibodies. *Cell Differ* *16*, 187-202.
- Blaauw, M., Linskens, M. H., and van Haastert, P. J. (2000). Efficient control of gene expression by a tetracycline-dependent transactivator in single *Dictyostelium discoideum* cells. *Gene* *252*, 71-82.
- Bominaar, A. A., Molijn, A. C., Pestel, M., Veron, M., and Van Haastert, P. J. (1993). Activation of G-proteins by receptor-stimulated nucleoside diphosphate kinase in *Dictyostelium*. *Embo J* *12*, 2275-2279.
- Bominaar, A. A., and Van Haastert, P. J. (1994). Phospholipase C in *Dictyostelium discoideum*. Identification of stimulatory and inhibitory surface receptors and G-proteins. *Biochem J* *297 (Pt 1)*, 189-193.
- Bonner J, Evidence for the formation of cell aggregates by chemotaxis in development of the slime mold *Dictyostelium discoideum*.(1947). *J. Exp. Zool.* *106* 1-26
- Bretscher, A. (2003). Polarized growth and organelle segregation in yeast: the tracks, motors, and receptors. *J Cell Biol* *160*, 811-816.

Bibliography

- Briscoe, C., Moniakis, J., Kim, J. Y., Brown, J. M., Hereld, D., Devreotes, P. N., and Firtel, R. A. (2001). The phosphorylated C-terminus of cAR1 plays a role in cell-type-specific gene expression and STATA tyrosine phosphorylation. *Dev Biol* 233, 225-236.
- Bullock W, Fernandez J and Short J (1987). XL1-blue: A high efficiency plasmid transforming *recA Escherichia coli* strain with beta-galactosidase selection. *BioTechniques*. 5, 376-378.
- Bush, J., Nolta, K., Rodriguez-Paris, J., Kaufmann, N., O'Halloran, T., Ruscetti, T., Temesvari, L., Steck, T., and Cardelli, J. (1994). A Rab4-like GTPase in *Dictyostelium discoideum* colocalizes with V-H(+)-ATPases in reticular membranes of the contractile vacuole complex and in lysosomes. *J Cell Sci* 107 (Pt 10), 2801-2812.
- Carraway, K. L., and Carraway, C. A. (1995). Signalling, mitogenesis and the cytoskeleton: where the action is. *Bioessays* 17, 171-175.
- Chen, M. Y., Long, Y., and Devreotes, P. N. (1997). A novel cytosolic regulator, Pianissimo, is required for chemoattractant receptor and G protein-mediated activation of the 12 transmembrane domain adenylyl cyclase in *Dictyostelium*. *Genes Dev* 11, 3218-3231.
- Chung, C. Y., and Firtel, R. A. (1999). PAKa, a putative PAK family member, is required for cytokinesis and the regulation of the cytoskeleton in *Dictyostelium discoideum* cells during chemotaxis. *J Cell Biol* 147, 559-76.
- Chung, C.Y., and Firtel, R.A. (2001). *Principles of molecular regulations*. Human press.
- Chung, C. Y., and Firtel, R. A. (2002). Signalling pathways at the leading edge of chemotaxing cells. *J Muscle Res Cell Motil* 23, 773-9.
- Claviez M, Pagh K, Maruta H, Baltus W, Fisher P and Gerisch G (1982). Electron microscopic mapping of monoclonal antibodies on the tail region of *Dictyostelium* myosin. *EMBO J*. 1. 1017-1022.
- Coates, J. C., and Harwood, A. J. (2001). Cell-cell adhesion and signal transduction during *Dictyostelium* development. *J Cell Sci* 114, 4349-4358.
- Cox, D., Wessels, D., Soll, D. R., Hartwig, J., and Condeelis, J. (1996). Re-expression of ABP-120 rescues cytoskeletal, motility, and phagocytosis defects of ABP-120- *Dictyostelium* mutants. *Mol Biol Cell* 7, 803-823.
- de Hostos, E. L., Rehfuess, C., Bradtke, B., Waddell, D. R., Albrecht, R., Murphy, J., and Gerisch, G. (1993). *Dictyostelium* mutants lacking the cytoskeletal protein coronin are defective in cytokinesis and cell motility. *J Cell Biol* 120, 163-173.
- Desbarats, L., Brar, S. K., and Siu, C. H. (1994). Involvement of cell-cell adhesion in the expression of the cell cohesion molecule gp80 in *Dictyostelium discoideum*. *J Cell Sci* 107 (Pt 6), 1705-1712.
- Devreotes, P. (1989). Cell-cell interactions in *Dictyostelium* development. *Trends Genet* 5, 242-245.
- Devreotes, P. N. (1994). G protein-linked signalling pathways control the developmental program of *Dictyostelium*. *Neuron* 12, 235-241.

- Ding, J., Vlahos, C. J., Liu, R., Brown, R. F., and Badwey, J. A. (1995). Antagonists of phosphatidylinositol 3-kinase block activation of several novel protein kinases in neutrophils. *J Biol Chem* *270*, 11684-11691.
- Dumontier, M., Hocht, P., Mintert, U., and Faix, J. (2000). Rac1 GTPases control filopodia formation, cell motility, endocytosis, cytokinesis and development in *Dictyostelium*. *J Cell Sci* *113* (Pt 12), 2253-2265.
- Field, J., Nikawa, J., Broek, D., MacDonald, B., Rodgers, L., Wilson, I. A., Lerner, R. A., and Wigler, M. (1988). Purification of a RAS-responsive adenylyl cyclase complex from *Saccharomyces cerevisiae* by use of an epitope addition method. *Mol Cell Biol* *8*, 2159-2165.
- Field, J., Vojtek, A., Ballester, R., Bolger, G., Colicelli, J., Ferguson, K., Gerst, J., Kataoka, T., Michaeli, T., Powers, S., and et al. (1990). Cloning and characterization of CAP, the *S. cerevisiae* gene encoding the 70 kd adenylyl cyclase-associated protein. *Cell* *61*, 319-327.
- Firtel, R. A., and Chung, C. Y. (2000). The molecular genetics of chemotaxis: sensing and responding to chemoattractant gradients. *Bioessays* *22*, 603-615.
- Firtel, R. A., and Meili, R. (2000). *Dictyostelium*: a model for regulated cell movement during morphogenesis. *Curr Opin Genet Dev* *10*, 421-427.
- Flick JS, and Johnson M, Two systems of glucose repression of the *Gall* promotor in *Saccharomyces cerevisiae* (1990). *Mol. Cell Biol.* *10* 4757-4769.
- Freeman, N. L., Chen, Z., Horenstein, J., Weber, A., and Field, J. (1995). An actin monomer binding activity localizes to the carboxyl-terminal half of the *Saccharomyces cerevisiae* cyclase-associated protein. *J Biol Chem* *270*, 5680-5685.
- Freeman, N. L., and Field, J. (2000). Mammalian homolog of the yeast cyclase associated protein, CAP/Srv2p, regulates actin filament assembly. *Cell Motil Cytoskeleton* *45*, 106-120.
- Freeman, N. L., Lila, T., Mintzer, K. A., Chen, Z., Pahk, A. J., Ren, R., Drubin, D. G., and Field, J. (1996). A conserved proline-rich region of the *Saccharomyces cerevisiae* cyclase-associated protein binds SH3 domains and modulates cytoskeletal localization. *Mol Cell Biol* *16*, 548-556.
- Geitz, H., Handt, S., and Zwingenberger, K. (1996). Thalidomide selectively modulates the density of cell surface molecules involved in the adhesion cascade. *Immunopharmacology* *31*, 213-221.
- Gerst, J. E., Ferguson, K., Vojtek, A., Wigler, M., and Field, J. (1991). CAP is a bifunctional component of the *Saccharomyces cerevisiae* adenylyl cyclase complex. *Mol Cell Biol* *11*, 1248-1257.
- Gieselmann, R., and Mann, K. (1992). ASP-56, a new actin sequestering protein from pig platelets with homology to CAP, an adenylate cyclase-associated protein from yeast. *FEBS Lett* *298*, 149-153.
- Gloss, A., Rivero, F., Khaire, N., Muller, R., Loomis, W. F., Schleicher, M., and Noegel, A. A. (2003). Villidin, a novel WD-repeat and villin-related protein from *Dictyostelium*, is associated with membranes and the cytoskeleton. *Mol Biol Cell* *14*, 2716-2727.

Bibliography

- Gottwald, U., Brokamp, R., Karakesisoglou, I., Schleicher, M., and Noegel, A. A. (1996). Identification of a cyclase-associated protein (CAP) homologue in *Dictyostelium discoideum* and characterization of its interaction with actin. *Mol Biol Cell* 7, 261-272.
- Gruenheid, S., Canonne-Hergaux, F., Gauthier, S., Hackam, D. J., Grinstein, S., and Gros, P. (1999). The iron transport protein NRAMP2 is an integral membrane glycoprotein that colocalizes with transferrin in recycling endosomes. *J Exp Med* 189, 831-841.
- Hacker, U., Albrecht, R., and Maniak, M. (1997). Fluid-phase uptake by macropinocytosis in *Dictyostelium*. *J Cell Sci* 110 (Pt 2), 105-112.
- Hanahan, D. (1983). Studies on transformation of *Escherichia coli* with plasmids. *J Mol Biol* 166, 557-580.
- Harper J, Adami G, Wei N, Keyomarski K and Elledge S (1993). The p21 Cdk-interacting protein Cip1 is a potent inhibitor of G 1 cyclin-dependent kinases. *Cell*. 75, 805-816.
- Harwood, A. J., Hopper, N. A., Simon, M. N., Bouzid, S., Veron, M., and Williams, J. G. (1992). Multiple roles for cAMP-dependent protein kinase during *Dictyostelium* development. *Dev Biol* 149, 90-99.
- Haugwitz, M., Noegel, A. A., Rieger, D., Lottspeich, F., and Schleicher, M. (1991). *Dictyostelium discoideum* contains two profilin isoforms that differ in structure and function. *J Cell Sci* 100 (Pt 3), 481-489.
- Hiroak I, Hiroshi N. and Hiroto O, High efficiency transformation of *Escherichia coli* with Plasmids (1990). *Gene.*, 96, 23-28.
- Hofmann, A., Hess, S., Noegel, A. A., Schleicher, M., and Wlodawer, A. (2002). Crystallization of cyclase-associated protein from *Dictyostelium discoideum*. *Acta Crystallogr D Biol Crystallogr* 58, 1858-1861.
- Hoffmann C. and Winston F (1987). A ten-minute DNA preparation from yeast efficiently releases autonomous plasmids for transformation of *Escherichia coli*. *Gene*. 57, 267-272.
- Holmes, D. S., and Quigley, M. (1981). A rapid boiling method for the preparation of bacterial plasmids. *Anal Biochem* 114, 193-197.
- Hubberstey, A. V., and Mottillo, E. P. (2002). Cyclase-associated proteins: CAPacity for linking signal transduction and actin polymerization. *Faseb J* 16, 487-499.
- Insall, R., Muller-Taubenberger, A., Machesky, L., Kohler, J., Simmeth, E., Atkinson, S. J., Weber, I., and Gerisch, G. (2001). Dynamics of the *Dictyostelium* Arp2/3 complex in endocytosis, cytokinesis, and chemotaxis. *Cell Motil Cytoskeleton* 50, 115-128.
- James, P., Halladay, J., and Craig, E. A. (1996). Genomic libraries and a host strain designed for highly efficient two-hybrid selection in yeast. *Genetics* 144, 1425-1436.
- Jenne, N., Rauchenberger, R., Hacker, U., Kast, T., and Maniak, M. (1998). Targeted gene disruption reveals a role for vacuolin B in late endocytic pathway and exocytosis. *J Cell Sci* 111 (Pt 1), 61-70.

Bibliography

Khurana, B., Khurana, T., Khaire, N., and Noegel, A. A. (2002). Functions of LIM proteins in cell polarity and chemotactic motility. *Embo J* 21, 5331-5342.

Kim, H. J., Chang, W. T., Meima, M., Gross, J. D., and Schaap, P. (1998). A novel adenylyl cyclase detected in rapidly developing mutants of *Dictyostelium*. *J Biol Chem* 273, 30859-30862.

Kim, J. Y., Caterina, M. J., Milne, J. L., Lin, K. C., Borleis, J. A., and Devreotes, P. N. (1997). Random mutagenesis of the cAMP chemoattractant receptor, cAR1, of *Dictyostelium*. Mutant classes that cause discrete shifts in agonist affinity and lock the receptor in a novel activational intermediate. *J Biol Chem* 272, 2060-2068.

Kimura, K., Hattori, S., Kabuyama, Y., Shizawa, Y., Takayanagi, J., Nakamura, S., Toki, S., Matsuda, Y., Onodera, K., and Fukui, Y. (1994). Neurite outgrowth of PC12 cells is suppressed by wortmannin, a specific inhibitor of phosphatidylinositol 3-kinase. *J Biol Chem* 269, 18961-18967.

Klein, P. S., Sun, T. J., Saxe, C. L., 3rd, Kimmel, A. R., Johnson, R. L., and Devreotes, P. N. (1988). A chemoattractant receptor controls development in *Dictyostelium discoideum*. *Science* 241, 1467-1472.

Knaus, U. G., and Bokoch, G. M. (1998). The p21Rac/Cdc42-activated kinases (PAKs). *Int J Biochem Cell Biol* 30, 857-862.

Konzok, A., Weber, I., Simmeth, E., Hacker, U., Maniak, M., and Muller-Taubenberger, A. (1999). DAip1, a *Dictyostelium* homologue of the yeast actin-interacting protein 1, is involved in endocytosis, cytokinesis, and motility. *J Cell Biol* 146, 453-464.

Kotani, K., Hara, K., Yonezawa, K., and Kasuga, M. (1995). Phosphoinositide 3-kinase as an upstream regulator of the small GTP-binding protein Rac in the insulin signalling of membrane ruffling. *Biochem Biophys Res Commun* 208, 985-990.

Kotani, K., Yonezawa, K., Hara, K., Ueda, H., Kitamura, Y., Sakaue, H., Ando, A., Chavanieu, A., Calas, B., Grigorescu, F., and et al. (1994). Involvement of phosphoinositide 3-kinase in insulin- or IGF-1-induced membrane ruffling. *Embo J* 13, 2313-2321.

Kriebel, P. W., Barr, V. A., and Parent, C. A. (2003). Adenylyl cyclase localization regulates streaming during chemotaxis. *Cell* 112, 549-560.

Kreis, T., and Vale, R., (1993). *Guidebook to the cytoskeletal and motor proteins.*, Oxford University press, 276.

Ksiazek, D., Brandstetter, H., Israel, L., Bourenkov, G. P., Katchalova, G., Janssen, K. P., Bartunik, H. D., Noegel, A. A., Schleicher, M., and Holak, T. A. (2003). Structure of the N-terminal domain of the adenylyl cyclase-associated protein (CAP) from *Dictyostelium discoideum*. *Structure (Camb)* 11, 1171-1178.

Laemmli, U. K. (1970). Cleavage of structural proteins during the assembly of the head of bacteriophage T4. *Nature* 227, 680-685.

Laub, M. T., and Loomis, W. F. (1998). A molecular network that produces spontaneous oscillations in excitable cells of *Dictyostelium*. *Mol Biol Cell* 9, 3521-3532.

Bibliography

- Lehrach, H., Diamond, D., Wozney, J. M., and Boedtker, H. (1977). RNA molecular weight determinations by gel electrophoresis under denaturing conditions, a critical reexamination. *Biochemistry* 16, 4743-4751.
- Lilly, P., Wu, L., Welker, D. L., and Devreotes, P. N. (1993). A G-protein beta-subunit is essential for *Dictyostelium* development. *Genes Dev* 7, 986-995.
- Liu, G., and Newell, P. C. (1993). Role of cyclic GMP in signal transduction to cytoskeletal myosin. *Symp Soc Exp Biol* 47, 283-295.
- Lu, M., Vergara, S., Zhang, L., Holliday, L. S., Aris, J., and Gluck, S. L. (2002). The amino-terminal domain of the E subunit of vacuolar H(+)-ATPase (V-ATPase) interacts with the H subunit and is required for V-ATPase function. *J Biol Chem* 277, 38409-38415.
- Machesky, L. M., and Insall, R. H. (1999). Signalling to actin dynamics. *J Cell Biol* 146, 267-272.
- Malchow, D., Nagele, B., Schwarz, H., and Gerisch, G. (1972). Membrane-bound cyclic AMP phosphodiesterase in chemotactically responding cells of *Dictyostelium discoideum*. *Eur J Biochem* 28, 136-142.
- Malikov, V., Kashina, A., and Rodionov, V. (2004). Cytoplasmic dynein nucleates microtubules to organize them into radial arrays in vivo. *Mol Biol Cell*.
- Maniak, M., Rauchenberger, R., Albrecht, R., Murphy, J., and Gerisch, G. (1995). Coronin involved in phagocytosis: dynamics of particle-induced relocalization visualized by a green fluorescent protein Tag. *Cell* 83, 915-924.
- Mann, S. K., Brown, J. M., Briscoe, C., Parent, C., Pitt, G., Devreotes, P. N., and Firtel, R. A. (1997). Role of cAMP-dependent protein kinase in controlling aggregation and postaggregative development in *Dictyostelium*. *Dev Biol* 183, 208-221.
- Mann, S. K., Brown, J. M., Briscoe, C., Parent, C., Pitt, G., Devreotes, P. N., and Firtel, R. A. (1997). Role of cAMP-dependent protein kinase in controlling aggregation and postaggregative development in *Dictyostelium*. *Dev Biol* 183, 208-221.
- Mavoungou, C., Israel, L., Rehm, T., Ksiazek, D., Krajewski, M., Popowicz, G., Noegel, A. A., Schleicher, M., and Holak, T. A. (2004). NMR structural characterization of the N-terminal domain of the adenylyl cyclase-associated protein (CAP) from *Dictyostelium discoideum*. *J Biomol NMR* 29, 73-84.
- Mintzer, K. A., and Field, J. (1994). Interactions between adenylyl cyclase, CAP and RAS from *Saccharomyces cerevisiae*. *Cell Signal* 6, 681-694.
- Morio, T., Urushihara, H., Saito, T., Ugawa, Y., Mizuno, H., Yoshida, M., Yoshino, R., Mitra, B. N., Pi, M., Sato, T., *et al.* (1998). The *Dictyostelium* developmental cDNA project: generation and analysis of expressed sequence tags from the first-finger stage of development. *DNA Res* 5, 335-340.
- Mullins, R. D., Heuser, J. A., and Pollard, T. D. (1998). The interaction of Arp2/3 complex with actin: nucleation, high affinity pointed end capping, and formation of branching networks of filaments. *Proc Natl Acad Sci U S A* 95, 6181-6186.

Bibliography

- Nellen, W., Datta, S., Reymond, C., Sivertsen, A., Mann, S., Crowley, T., and Firtel, R. A. (1987). Molecular biology in *Dictyostelium*: tools and applications. *Methods Cell Biol* 28, 67-100.
- Nelson, W. J. (2003). Adaptation of core mechanisms to generate cell polarity. *Nature* 422, 766-774.
- Neujahr, R., Heizer, C., Albrecht, R., Ecke, M., Schwartz, J. M., Weber, I., and Gerisch, G. (1997). Three-dimensional patterns and redistribution of myosin II and actin in mitotic *Dictyostelium* cells. *J Cell Biol* 139, 1793-1804.
- Nishi, T., and Forgac, M. (2002). The vacuolar (H⁺)-ATPases--nature's most versatile proton pumps. *Nat Rev Mol Cell Biol* 3, 94-103.
- Nishida, Y., Shima, F., Sen, H., Tanaka, Y., Yanagihara, C., Yamawaki-Kataoka, Y., Kariya, K., and Kataoka, T. (1998). Coiled-coil interaction of N-terminal 36 residues of cyclase-associated protein with adenylyl cyclase is sufficient for its function in *Saccharomyces cerevisiae* ras pathway. *J Biol Chem* 273, 28019-28024.
- Noegel, A. A., Blau-Wasser, R., Sultana, H., Muller, R., Israel, L., Schleicher, M., Patel, H., and Weijer, C. J. (2004). The cyclase-associated protein CAP as regulator of cell polarity and cAMP signalling in *Dictyostelium*. *Mol Biol Cell* 15, 934-945.
- Noegel, A. A., Rivero, F., Albrecht, R., Janssen, K. P., Kohler, J., Parent, C. A., and Schleicher, M. (1999). Assessing the role of the ASP56/CAP homologue of *Dictyostelium discoideum* and the requirements for subcellular localization. *J Cell Sci* 112 (Pt 19), 3195-3203.
- Okaichi, K., Cubitt, A. B., Pitt, G. S., and Firtel, R. A. (1992). Amino acid substitutions in the *Dictyostelium* G alpha subunit G alpha 2 produce dominant negative phenotypes and inhibit the activation of adenylyl cyclase, guanylyl cyclase, and phospholipase C. *Mol Biol Cell* 3, 735-747.
- Pagh, K., and Gerisch, G. (1986). Monoclonal antibodies binding to the tail of *Dictyostelium discoideum* myosin: their effects on antiparallel and parallel assembly and actin-activated ATPase activity. *J Cell Biol* 103, 1527-38.
- Parent, C. A., and Devreotes, P. N. (1996). Constitutively active adenylyl cyclase mutant requires neither G proteins nor cytosolic regulators. *J Biol Chem* 271, 18333-18336.
- Patel, H., Guo, K., Parent, C., Gross, J., Devreotes, P. N., and Weijer, C. J. (2000). A temperature-sensitive adenylyl cyclase mutant of *Dictyostelium*. *Embo J* 19, 2247-2256.
- Peracino, B., Borleis, J., Jin, T., Westphal, M., Schwartz, J. M., Wu, L., Bracco, E., Gerisch, G., Devreotes, P., and Bozzaro, S. (1998). G protein beta subunit-null mutants are impaired in phagocytosis and chemotaxis due to inappropriate regulation of the actin cytoskeleton. *J Cell Biol* 141, 1529-1537.
- Pergolizzi, B., Peracino, B., Silverman, J., Ceccarelli, A., Noegel, A., Devreotes, P., and Bozzaro, S. (2002). Temperature-sensitive inhibition of development in *Dictyostelium* due to a point mutation in the piaA gene. *Dev Biol* 251, 18-26.
- Pitt, G. S., Brandt, R., Lin, K. C., Devreotes, P. N., and Schaap, P. (1993). Extracellular cAMP is sufficient to restore developmental gene expression and morphogenesis in *Dictyostelium* cells lacking the aggregation adenylyl cyclase (ACA). *Genes Dev* 7, 2172-2180.

Bibliography

- Pitt, G. S., Milona, N., Borleis, J., Lin, K. C., Reed, R. R., and Devreotes, P. N. (1992). Structurally distinct and stage-specific adenylyl cyclase genes play different roles in *Dictyostelium* development. *Cell* 69, 305-315.
- Raper KB (1935). *Dictyostelium discoideum*, a new species of slime mould from decaying forest leaves. *J. Agr. Res.* 50, 135-147
- Rauchenberger, R., Hacker, U., Murphy, J., Niewohner, J., and Maniak, M. (1997). Coronin and vacuolin identify consecutive stages of a late, actin-coated endocytic compartment in *Dictyostelium*. *Curr Biol* 7, 215-218.
- Ren, R., Mayer, B. J., Cicchetti, P., and Baltimore, D. (1993). Identification of a ten-amino acid proline-rich SH3 binding site. *Science* 259, 1157-1161.
- Rivero, F., Albrecht, R., Dislich, H., Bracco, E., Graciotti, L., Bozzaro, S., and Noegel, A. A. (1999). RacF1, a novel member of the Rho protein family in *Dictyostelium discoideum*, associates transiently with cell contact areas, macropinosomes, and phagosomes. *Mol Biol Cell* 10, 1205-1219.
- Rivero, F., Furukawa, R., Noegel, A. A., and Fechheimer, M. (1996). *Dictyostelium discoideum* cells lacking the 34,000-dalton actin-binding protein can grow, locomote, and develop, but exhibit defects in regulation of cell structure and movement: a case of partial redundancy. *J Cell Biol* 135, 965-980.
- Rivero, F., Illenberger, D., Somesh, B. P., Dislich, H., Adam, N., and Meyer, A. K. (2002). Defects in cytokinesis, actin reorganization and the contractile vacuole in cells deficient in RhoGDI. *Embo J* 21, 4539-4549.
- Rivero, F., and Somesh, B. P. (2002). Signal transduction pathways regulated by Rho GTPases in *Dictyostelium*. *J Muscle Res Cell Motil* 23, 737-749.
- Roelofs, J., Meima, M., Schaap, P., and Van Haastert, P. J. (2001). The *Dictyostelium* homologue of mammalian soluble adenylyl cyclase encodes a guanylyl cyclase. *Embo J* 20, 4341-4348.
- Roelofs, J., and Van Haastert, P. J. (2002). Characterization of two unusual guanylyl cyclases from *dictyostelium*. *J Biol Chem* 277, 9167-9174.
- Sambrook J, Fritsch EF, and Maniatis T (1989). *Molecular Cloning: A Laboratory Manual*. 2nd ed. Cold Spring Harbor Laboratory Press, Cold Spring Harbor, New York.
- Schleicher M, Gerisch G. and Isenberg G (1984). New actin binding proteins from *Dictyostelium discoideum*. *EMBO J.* 3, 2095-2100.
- Schneider, S., Buchert, M., and Hovens, C. M. (1996). An in vitro assay of beta-galactosidase from yeast. *Biotechniques* 20, 960-962.
- Shaulsky, G., Escalante, R., and Loomis, W. F. (1996). Developmental signal transduction pathways uncovered by genetic suppressors. *Proc Natl Acad Sci U S A* 93, 15260-15265.
- Shaulsky, G., Fuller, D., and Loomis, W. F. (1998). A cAMP-phosphodiesterase controls PKA-dependent differentiation. *Development* 125, 691-699.

Bibliography

- Shima, F., Okada, T., Kido, M., Sen, H., Tanaka, Y., Tamada, M., Hu, C. D., Yamawaki-Kataoka, Y., Kariya, K., and Kataoka, T. (2000). Association of yeast adenylyl cyclase with cyclase-associated protein CAP forms a second Ras-binding site which mediates its Ras-dependent activation. *Mol Cell Biol* 20, 26-33.
- Simpson, P. A., Spudich, J. A., and Parham, P. (1984). Monoclonal antibodies prepared against *Dictyostelium* actin: characterization and interactions with actin. *J Cell Biol* 99, 287-295.
- Soderbom, F., Anjard, C., Iranfar, N., Fuller, D., and Loomis, W. F. (1999). An adenylyl cyclase that functions during late development of *Dictyostelium*. *Development* 126, 5463-5471.
- Stewart, D. M., Tian, L., and Nelson, D. L. (1999). Mutations that cause the Wiskott-Aldrich syndrome impair the interaction of Wiskott-Aldrich syndrome protein (WASP) with WASP interacting protein. *J Immunol* 162, 5019-5024.
- Sussman M, The origin of cellular heterogeneity in the slime molds, *Dictyosteliaceae* (1951). *J. Exp. Zool.* 118, 407-417.
- Sutoh, K. (1993). A transformation vector for *Dictyostelium discoideum* with a new selectable marker bsr. *Plasmid* 30, 150-4.
- Svitkina, T. M., and Borisy, G. G. (1999). Arp2/3 complex and actin depolymerizing factor/cofilin in dendritic organization and treadmilling of actin filament array in lamellipodia. *J Cell Biol* 145, 1009-1026.
- Temesvari, L., Rodriguez-Paris, J., Bush, J., Steck, T. L., and Cardelli, J. (1994). Characterization of lysosomal membrane proteins of *Dictyostelium discoideum*. A complex population of acidic integral membrane glycoproteins, Rab GTP-binding proteins and vacuolar ATPase subunits. *J Biol Chem* 269, 25719-25727.
- Titus, M. A. (1999). A class VII unconventional myosin is required for phagocytosis. *Curr Biol* 9, 1297-1303.
- Towbin, H., Staehelin, T., and Gordon, J. (1979). Electrophoretic transfer of proteins from polyacrylamide gels to nitrocellulose sheets: procedure and some applications. *Proc Natl Acad Sci U S A* 76, 4350-4354.
- Vieira, J., and Messing, J. (1982). The pUC plasmids, an M13mp7-derived system for insertion mutagenesis and sequencing with synthetic universal primers. *Gene* 19, 259-268.
- Wallet, V., Mutzel, R., Troll, H., Barzu, O., Wurster, B., Veron, M., and Lacombe, M. L. (1990). *Dictyostelium* nucleoside diphosphate kinase highly homologous to Nm23 and Awd proteins involved in mammalian tumor metastasis and *Drosophila* development. *J Natl Cancer Inst* 82, 1199-1202.
- Weiner, O. H., Murphy, J., Griffiths, G., Schleicher, M., and Noegel, A. A. (1993). The actin-binding protein comitin (p24) is a component of the Golgi apparatus. *J Cell Biol* 123, 23-34.
- Wennstrom, S., Siegbahn, A., Yokote, K., Arvidsson, A. K., Heldin, C. H., Mori, S., and Claesson-Welsh, L. (1994). Membrane ruffling and chemotaxis transduced by the PDGF beta-receptor require the binding site for phosphatidylinositol 3' kinase. *Oncogene* 9, 651-660.

Bibliography

Westphal, C. H., and Leder, P. (1997). Transposon-generated 'knock-out' and 'knock-in' gene-targeting constructs for use in mice. *Curr Biol* 7, 530-533.

Williams, K. L., and Newell, P. C. (1976). A genetic study of aggregation in the cellular slime mould *Dictyostelium discoideum* using complementation analysis. *Genetics* 82, 287-307.

Wong, E. F., Brar, S. K., Sesaki, H., Yang, C., and Siu, C. H. (1996). Molecular cloning and characterization of DdCAD-1, a Ca²⁺-dependent cell-cell adhesion molecule, in *Dictyostelium discoideum*. *J Biol Chem* 271, 16399-16408.

Wu, L., Hansen, D., Franke, J., Kessin, R. H., and Podgorski, G. J. (1995). Regulation of *Dictyostelium* early development genes in signal transduction mutants. *Dev Biol* 171, 149-158.

Wu, L., Valkema, R., Van Haastert, P. J., and Devreotes, P. N. (1995). The G protein beta subunit is essential for multiple responses to chemoattractants in *Dictyostelium*. *J Cell Biol* 129, 1667-1675.

Yao, J., Harvath, L., Gilbert, D. L., and Colton, C. A. (1990). Chemotaxis by a CNS macrophage, the microglia. *J Neurosci Res* 27, 36-42.

Zhang, J. W., Parra, K. J., Liu, J., and Kane, P. M. (1998). Characterization of a temperature-sensitive yeast vacuolar ATPase mutant with defects in actin distribution and bud morphology. *J Biol Chem* 273, 18470-18480.

Zhou, K., Pandol, S., Bokoch, G., and Traynor-Kaplan, A. E. (1998). Disruption of *Dictyostelium* PI3K genes reduces [32P] phosphatidylinositol 3,4 bisphosphate and [32P]phosphatidylinositol trisphosphate levels, alters F-actin distribution and impairs pinocytosis. *J Cell Sci* 111 (Pt 2), 283-294.

Zhou, K., Takegawa, K., Emr, S. D., and Firtel, R. A. (1995). A phosphatidylinositol (PI) kinase gene family in *Dictyostelium discoideum*: biological roles of putative mammalian p110 and yeast Vps34p PI 3-kinase homologs during growth and development. *Mol Cell Biol* 15, 5645-5656.

Erklärung

Ich versichere, dass ich die von mir vorgelegte Dissertation selbständig angefertigt, die benutzten Quellen und Hilfsmittel vollständig angegeben und die Stellen der Arbeit- einschließlich Tabellen und Abbildungen-, die anderen Werke im Wortlaut oder dem Sinn nach entnommen sind, in jedem Einzelfall als Entlehnung kenntlich gemacht habe; dass diese Dissertation noch keiner anderen Fakultät oder Universität zur Prüfung vorgelegen hat; dass sie - abgesehen von unten angegebenen beantragten Teilpublikationen- noch nicht veröffentlicht ist, sowie, dass ich eine Veröffentlichung vor Abschluss des Promotionsverfahrens nicht vornehmen werde. Die Bestimmungen dieser Promotionsordnung sind mir bekannt. Die von mir vorgelegte Dissertation ist von Frau Prof. Dr. Angelika A. Noegel betreut worden.

Köln, den

Hameeda Sultana

Teilpublikationen:

Noegel AA, Blau-Wasser R, **Sultana H**, Müller R, Israel L, Schleicher M, Patel H, Weijer CJ. (2004). The cyclase-associated protein CAP as regulator of cell polarity and cAMP signalling in *Dictyostelium*. **Mol Biol Cell**. 15:934-945.

Curriculum vitae

Name Hameeda Sultana

Date of Birth 19.08.1976

Place of Birth Bangalore, India.

Nationality Indian

Contact details Institute for Biochemistry I,
Medical faculty,
Joseph Stelzmann Strasse, 52,
50931, Cologne,
Germany
Email: hameeda.sultana@uni-koeln.de
ake57@uni-koeln.de
Telephone: +49-0221-478 6930

Academic profile

Pre-University studies: 1992-1994

NMKRV college for women, Bangalore, India

University studies: 1994-1997

Bachelor of Science (BSc) in Chemistry, Botany & Zoology,
Bangalore University, Bangalore, India

1997-1999

Master of Science (MSc) in Applied Genetics,
Bangalore University, Bangalore, India

Dissertation title: Biochemical studies on insecticide resistance to Deltamethrin on *Culex pipiens quinquefasciatus*- a Filarial mosquito

Advisor: Prof. N.J. Shetty, Centre for Applied Genetics,
Bangalore University, Bangalore, India

Doctoral Study: June 2001-July 2004

Thesis title: Cyclase associated protein CAP in the regulation of the actin cytoskeleton and cell polarity in *Dictyostelium discoideum*

Advisor: Prof. Dr. Angelika A. Noegel,
Institute for Biochemistry I, Medical faculty,
University of Cologne, Cologne, Germany

Lebenslauf

Name Hameeda Sultana

Geburtsdatum 19.08.1976

Geburtsort Bangalore, Indien

Staatsangehörigkeit Indisch

Anschrift Institut für Biochemie I, Medizinische Fakultät
Joseph-Stelzmann Str., 52, 50931, Köln,
Deutschland
Email: hameeda.sultana@uni-koeln.de
ake57@uni-koeln.de
Telefon: +49-0221-478 6930

Voruniversität

1992-1994 NMKRV college, Bangalore, Indien

Studium

1994-1997 Studium der Biologie (*Bachelor of Sciences*),
Bangalore University, Bangalore, Indien

1997-1999 Diploma studium der angewandte Genetik (*Master of Sciences, Applied Genetics*), Bangalore university, Bangalore, Indien

Titel der Diplomarbeit: Biochemical studies on insecticide resistance to Deltamethrin on *Culex pipens quinquefasiatus*- a Filaria mosquito

Promotion studium

Juni 2001-Juli 2004 Institut für Biochemie I,
Medizinische Fakultät der Universität zu Köln

Betreuerin: Frau Prof. Dr. Angelika A. Noegel

Thema: 'A Cyclase associated protein CAP in the regulation of actin cytoskeleton and cell polarity in *Dictyostelium discoideum*'